Technical Report
TR-19-21
December 2019

The sub-Cambrian unconformity in Västergötland, Sweden

Reference surface for Pleistocene glacial erosion of basement

Adrian M Hall
Maarten Krabbendam
Mikis van Boeckel
Clas Hättestrand
Karin Ebert
Jakob Heyman

SVENSK KÄRNBRÄNSLEHANTERING AB

SWEDISH NUCLEAR FUEL
AND WASTE MANAGEMENT CO

Box 3091, SE-169 03 Solna
Phone +46 8 459 84 00
skb.se

SVENSK KÄRNBRÄNSLEHANTERING

ISSN 1404-0344
SKB TR-19-21
ID 1872064

December 2019

The sub-Cambrian unconformity in Västergötland, Sweden

Reference surface for Pleistocene glacial erosion of basement

Adrian M Hall[1], Maarten Krabbendam[2], Mikis van Boeckel[1], Clas Hättestrand[1], Karin Ebert[3], Jakob Heyman[4]

1 Department of Physical Geography, Stockholm University
2 British Geological Survey
3 Natural Sciences, Technology and Environmental Studies, Södertörn University
4 Department of Earth Sciences, University of Gothenburg

Keywords: Cambrian, Unconformity, Baltica, Gneiss, Glacial erosion, Geomorphology, Cosmogenic nuclide.

Preface

A comprehensive study on glacial erosion, denudation and long-term development of bedrock morphology/stability was conducted between 2015 and 2019 at the Forsmark site and in the surrounding Uppland province, Sweden (Hall et al. 2019). The present report describes a study that emanated from that work, investigating one of the main assumptions used in the Forsmark study. To this end, the overall aim of the present study is to explore the use of an ancient low-relief bedrock denudation surface (the sub-Cambrian unconformity) as a reference surface for estimating depths of Quaternary glacial erosion of crystalline basement rock. This is done by studying a key area for this mega-landform in the Trollhättan region, Västergötland province, Sweden. In addition to the present report, another supporting report (Goodfellow et al. 2019), with a similar overall objective and using the same study area as the present study, but using a different scientific starting point regarding the view of the genesis of the sub-Cambrian unconformity, also emerged from the main study. Preferably, the main report of the glacial erosion and denudation study (Hall et al. 2019) should be read in light of both supporting reports.

In order to evaluate the potential use of the sub-Cambrian unconformity as a reference surface for Pleistocene glacial erosion of basement rock, the question is approached in a broad methodological manner. The present study also includes a comprehensive summary of previous relevant geological and geomorphological research. It makes use of new high resolution digital elevation data, cosmogenic nuclide exposure age calculations and glacial erosion simulations. The erosion and burial history of the unconformity is explored, along with the processes that led to its formation. Particular attention is given to establishing the morphology of the unconformity and the pattern of block faulting, using field mapping, digital elevation models, topographical bedrock profiles and summit envelope surfaces. The progressive glacial modification of the unconformity after exhumation is examined across landscapes and landforms using geomorphological evidence. Depths of basement glacial erosion are derived by comparing the present rock surface to models of the unconformity based on summit envelope surfaces. Rates of glacial erosion in the basement over the last 100 ka and 1 Ma are estimated from measurements and scenario modelling of ^{10}Be and ^{26}Al cosmogenic nuclide inventories at four locations. The cosmogenic data used in the present report, as well as supplementary cosmogenic data, are found in Goodfellow et al. (2019).

The glacial erosion study, of which the present work is a part, was initiated by Jens-Ove Näslund (SKB) and jointly designed by Jens-Ove Näslund, Adrian Hall (Stockholm University), Karin Ebert (Södertörn University), Bradley Goodfellow (Stockholm University, Swedish Geological Survey), Clas Hättestrand (Stockholm University), Jakob Heyman (University of Gothenburg), and Arjen Stroeven (Stockholm University).

Adrian Hall coordinated the scientific work within the study, and also conducted field and desk-based studies on long-term burial and erosion history and glacial erosion. Maarten Krabbendam (British Geological Survey) contributed ideas throughout the report and mapped landforms associated with the unconformity and shaped by glacial erosion. Mikis van Boeckel (Stockholm University) analysed fracture patterns and glacial landforms and produced many of geological and geomorphological maps in the report using digital elevation model data from Lantmäteriet and SGU. Karin Ebert developed digital elevation models of the unconformity and derived the glacial erosion estimates from summit erosion surfaces. Clas Hättestrand (Stockholm University) developed geomorphological maps of the unconformity and of glacial bedforms. Sample site selection and cosmogenic nuclide sample collection was carried out by Adrian Hall, Bradley Goodfellow (SGU), Arjen Stroeven (Stockholm University), Marc Caffee and Jakob Heyman. Jakob Heyman conducted the modelling of cosmogenic nuclide erosion and burial histories. Reporting of methods and results for cosmogenic nuclide analysis was led by Jakob Heyman, with contributions by Arjen Stroeven and Bradley Goodfellow. Discussion of the results was written by all authors, led by Adrian Hall. The study includes an important contribution by Marc Caffee (Purdue University) who was responsible for all cosmogenic isotope laboratory analyses.

The results of the present report will be used, together with results of Hall et al. (2019), Goodfellow et al. (2019) and other published scientific information, for constructing future scenarios of climate and climate-related processes in SKB's work on assessing long-term safety of nuclear waste repositories in Sweden. The safety assessments performed for the planned repository for spent nuclear fuel in Forsmark, Sweden, cover a total time span of one million years. Since this time span covers the timescales relevant for glacial cycles, the effect of future glacial erosion needs to be analysed in the safety assessments. In this context, the three reports emerged from the glacial erosion study provide important results on the potential amount of glacial erosion that may be expected in the topographical, geological, and glaciological setting of the Forsmark site.

The report manuscript was externally reviewed by Prof. Paul Bishop (School of Geographical and Earth Sciences, University of Glasgow), Assoc. Prof. Henriette Linge (Dept. of Earth Science, University of Bergen), and Assoc. Prof. Mats Olvmo (Dept. of Earth Sciences, University of Gothenburg). Input to an earlier version of the manuscript was provided by Jens-Ove Näslund (SKB) and Christina Truedsson (Tintra consult).

Stockholm, December 2019

Jens-Ove Näslund
Coordinator Climate Research Programme SKB

Summary

The main aim of the study is to evaluate the potential use of the sub-Cambrian unconformity (U2) in Västergötland as a reference surface for Pleistocene glacial erosion of the basement. U2 is found across large parts of Baltica as a near planar unconformity surface, as shown by evidence of its flatness from outcrops, along strike sections and from other geological evidence, such as the overlying stratigraphy. U2 developed after three phases of erosion: (i) through an initial phase of denudation in southern Sweden that removed basement and Visingsö Group sedimentary cover after ~730 Ma, (ii) extensive levelling of the basement in Västergötland by subaerial weathering and erosion over a period of 36–50 Ma in the Ediacaran when this part of the craton remained stable and (iii) final grading during marine transgression. During flooding from the Late Ediacaran onwards, parts of the rock shelf on Baltica were subjected to shoreline erosion during multiple sea level high stands of < 20–70 m amplitude, leading to formation of basement ultiplains and peneplains. U2 is overlain by thin but laterally continuous Cambrian to Ordovician strata which remain remarkably consistent in facies over very wide geographical areas due to the near planar form of the unconformity. Over large parts of lowland Sweden, U2 occurs close to the present-day surface. The re-exposed and modified unconformity has been commonly referred to as the *sub-Cambrian peneplain*.

In Västergötland, the relief on U2, where still buried, is < 5 m over 6–10 km-long stretches along the flanks of Halleberg and Hunneberg and at Kinnekulle. The exposed basement surface around Early Palaeozoic outliers in the Trollhättan region is modelled by projection of maximum rock summit elevations in DEMs across circles of 0.25 and 1 km radius. The summit envelope surfaces revealed are nearly planar. Hills on the exposed basement are low (5–15 m), broad (with wavelengths of 1–2 km), and widely spaced (over several km). Basement summits remain accordant within an elevation range of 5–10 m at distances of > 11 km from the edge of the buried unconformity. Gneiss summits exposed adjacent to Halleberg and Hunneberg stand at elevations only 2 to 6 m below planar projections of the buried unconformity, a height difference that constrains summit erosion since exhumation. The buried unconformity dips at 0.25–0.4 % towards the north. Beds in overlying Early Palaeozoic sedimentary rocks along the flanks of Halleberg and Hunneberg dip northward at ~0.3 %. Individual planar flats are inclined northward at 0.25–0.4 %. Summit envelope surface inclinations of 0.2–0.4 % match these inclinations. Consistent dips between overlying sedimentary beds, the buried unconformity surface and the present basement surface provide strong support for the view that the present basement surface represents the little modified, re-exposed, slightly tilted and near planar sub-Cambrian unconformity.

U2 is not primarily a structurally controlled surface because it is cut across inclined fractures and variably spaced vertical fractures of Proterozoic age. Planar flats (‘slättbergen’) are smooth, bare bedrock surfaces with relief of < 1–2 m over distances of 0.1–0.9 km flanked by steep rock slopes. Planar flats are found around Trollhättan only on coarse-grained and porphyritic granite gneisses, with vertical fracture spacings up to 10 m wide. Planar flats conform at a few localities, notably at Nordkroken, to near surface horizontal sheet fractures but elsewhere crosscut sub-horizontal fractures or have developed in the absence of long, continuous, horizontal fractures. On the lake shoreline at Kinnekulle, planar flats are overlain by horizontal beds of basal Cambrian pebble conglomerate and sandstone. Planar flats can be interpreted to represent inherited facets of U2, re-exposed but little modified by later glacial erosion.

U2, the overlying Early Palaeozoic cover and Early Permian sills are dislocated by minor (10–60 m vertical throw) faulting of likely Permian age. Profiles derived from LiDAR elevation data support patterns of dislocation and tilting for km-scale fault blocks identified previously. Additional small (< 10 m) vertical displacements are recognised within several large fault blocks. Similar fault block mosaics are identified on U2 around Early Palaeozoic outliers in Närke and Östergötland.

The present basement surface around Trollhättan retains unweathered Cambrian sandstone dykes and Palaeozoic calcite fracture fills, evidence that is consistent with late re-exposure of U2. Large numbers of Cambrian sandstone, Ordovician limestone and Kinnekulle dolerite clasts sourced from Västergötland are found in tills in Jutland, Denmark. The disparity between the small source areas for these rocks around present outliers in Västergötland and the large sink area in Denmark suggests

that these cover and cap rocks remained more extensive than today in Västergötland into the Middle Pleistocene. Re-exposure of the basement unconformity across wide areas of Västergötland for the first time since the Early Cambrian was likely a result of a step-change in erosion by the Fenno-scandian Ice Sheet after 1.1 Ma. Thicknesses of at least a few tens of metres of Early Palaeozoic sedimentary rock likely have been removed from around present-day outliers and wider areas of Västergötland since 1.1. Ma.

Glacial erosion of the re-exposed sub-Cambrian unconformity in Västergötland has lowered its surface and increased its roughness, based on observations along the buried unconformity and on the exposed basement around outliers. Estimated depths of erosion derived from the average height difference between the summit envelope surfaces and the present-day basement surface for the Trollhättan region (14 m) are identical to NE Uppland (14 m). Unlike in Uppland, on the flanks of Halleberg and Hunneberg the additional lowering of the summit envelope can be well constrained to 2–6 m using elevation differences between the buried U2 and adjacent summits on the exposed basement. Further away from the present-day cover rocks, this additional lowering could potentially be larger. Over wide areas, however, less than 5–10 m of basement has been removed from below summit envelope surfaces. Limited depths of glacial erosion, together with late re-exposure from beneath Early Palaeozoic cover, have here allowed the original morphology of the sub-Cambrian unconformity to persist in the present basement landscape at the regional and local scales. The largest volumes of basement rock removed by glacial erosion are represented by the excavation of 10–40 m deep depressions and valleys often located in zones with closely fractured gneisses. The impact of glacial erosion on U2 has been highest in the Sjuntorp area, with average depths of erosion below summit envelope surfaces of 19.4 m. Here the basement surface shows high roughness and is characterized by box hills, roches moutonnées, trenches and star- and box-basins; features that are typical of cnoc and lochain terrain developed after Pleistocene glacial erosion of shields. Hence, landforms typical of glaciated shields have developed after limited lowering of the original U2 surface by glacial erosion.

Cosmogenic nuclide inventories show little or no nuclide inheritance at two localities that stand 5–6 m below U2 close to the flanks of the Halleberg and Hunneberg table mountains. Erosion over the last 100 ka was > 2–3 m and erosion over the last 1 Ma was > 20 m and may have exceeded 40 m. At these locations, results are consistent with re-exposure of U2 from beneath cover rocks in recent glacial cycles by scarp retreat around the hill flanks. Erosion depths on planar flats in Trollhättan town are spatially variable. Under scenarios of constant glacial erosion rate (abrasion) over the last 0.5 or 1 Ma, interpreted as a best fit for the erosion history, a 0.5–2–2 m depth of rock was removed from the top surface of the planar flat at Hjortmossen in the last 100 ka and < 18 m of rock in the last 1 Ma. The preservation of the planar flats is due to the high resistance of hard, massive granite gneisses to glacial erosion and likely also to late re-exposure of these rock surfaces from beneath cover rocks. The range of estimated depths of glacial erosion based on cosmogenic nuclide inventories at Trollhättan is similar to that seen in a larger cosmogenic nuclide dataset at Forsmark.

Whilst the Proterozoic to Early Palaeozoic erosion and burial histories show some differences between Västergötland and Uppland, there are many similarities in the development of the bedrock terrains in these areas through the Phanerozoic. These include the flatness of the sub-Cambrian unconformity, its minor dislocation as seen in tilted fault blocks and the lack of evidence for re-exposure of the basement to Mesozoic to Cenozoic deep weathering. Similar landforms of glacial erosion are seen across different scales around Trollhättan and Forsmark. The processes of glacial erosion operating on low relief, hard, variably fractured basement surfaces in both areas are directly comparable. Modelling of the Early Cambrian unconformity in the Trollhättan region provides a reference surface for identifying the pattern and estimating the average depth of glacial erosion of basement, a technique that can be applied also at Forsmark. The Trollhättan region provides a valuable analogue for understanding past and future glacial erosion on the sub-Cambrian unconformity at and around the proposed spent nuclear fuel repository site at Forsmark.

Sammanfattning

I denna studie analyseras möjligheten att använda den subkambriska inkonformiteten (U2) som en referensyta mot vilken den glaciala erosionen av urberget under pleistocen kan uppskattas. U2 återfinns över stora delar av Baltica som en platt eller nästan platt urbergsyta. Inkonformiteten är tydlig i skärningar, t ex på bergkullar med plana överytor (de västgötska s.k. slättbergen), samt genom stratigrafin, där den är överlagrad av yngre sedimentbergarter. U2 bildades som ett resultat av tre faser av erosion: 1) en initial fas av denudation över södra Sverige, någon gång efter ~730 miljoner år sedan (Ma), som eroderade delar av urberget och Visingsögruppens sedimentära bergarter, 2) vidsträckt utjämning av urbergsytan i Västergötland genom subaeril vittring och erosion under en tidsperiod på 36–50 miljoner år, under ediacara, när denna del av kratonen var relativt stabil, och 3) slutlig avplaning under marin transgression. I samband med transgression från sen ediacara och framåt, med högvattenstånd med upp till 20–70 m amplitud, utsattes berggrundsytan för stranderosion och planades av ytterligare till ett ultiplan och peneplan. U2 överlagras av tunna kambriska och ordoviciska strata som är anmärkningsvärt uthålliga i facies över vidsträckta områden, något som kan kopplas till den nästan helt plana inkonformiteten. Över stora delar av Sveriges lågland befinner sig U2 nära dagens markyta. Den återexponerade och modifierade inkonformiteten kallas allmänt för det *subkambriska peneplanet*.

I Västergötland har U2, där den fortfarande är täckt av sedimentära bergarter längs kanterna av Halleberg, Hunneberg och Kinnekulle, en relief på < 5 m över sträckor på 6–10 km. Där den exponerade urbergsytan i Trollhättanområdet är täckt av sedimentbergarter från tidig paleozoikum kan denna användas som utgångspunkt (i en höjdmodell från Lidardata) för extrapolering av den regionala ursprungliga berggrundsytan. En extrapolation av den maximala höjden på bergytor i ett fönster på 0,25 km respektive 1 km radie över området söder och väster om Halleberg och Hunneberg resulterar i en yta som är nästintill helt plan. De kullar som förekommer på urbergsytan är låga (5–15 m), breda (med våglängder på 1–2 km) och glesa (med flera kilometers avstånd). Urbergskullarnas överytor varierar i höjdled med 5–10 m över sträckor på > 11 km från de platser där inkonformiteten fortfarande är täckt av sedimentbergarter. Exponerade överytor i gnejsberggrunden intill Hallberg och Hunneberg är belägna endast 2–6 m under den rekonstruerade inkonformiteten, vilket därmed kan tas som ett mått på hur mycket dessa överytor eroderats sedan täckbergarterna försvunnit. Den sedimenttäckta inkonformiteten lutar 0,25–0,4 % mot norr. Lagren i de överlagrade tidigpaleozoiska sedimentbergarterna som är exponerade längs kanterna på Halleberg och Hunneberg lutar ca 0,3 % mot norr. Slättbergens överytor lutar även de mot norr med 0,25–0,4 %. Detta stämmer också överens med lutningen 0,2–0,4 % på den yta som länkar samman slättbergens överytor. Att 1) sedimentära bergartslager, 2) den berggrundsyta dessa vilar på, 3) slättbergens överytor, samt 4) den yta som länkar samman slättbergens överytor, alla har en lutning som är mycket lik både i storlek och riktning är en stark indikation på att dagens berggrundsyta i området representerar den nästan plana subkambriska inkonformiteten i återexponerad, svagt modifierad och något lutad form.

U2 skär tvärs över proterozoiska sprickor i berggrunden, oavsett vilken lutning eller vertikala avstånd dessa har. Detta indikerar att U2 inte primärt strukturellt är kontrollerad. Slättbergens överytor utgörs av exponerade berggrundsytor som är mycket jämna, med en relief på < 1–2 m över 100–900 m, och de avgränsas av branter runtom. Plana överytor återfinns enbart på bergkullar av grovkornig porfyritisk granitgnejs med glest avstånd mellan vertikala sprickor (< 10 m). I några områden överensstämmer den plana överytan med horisontella spricker i berggrunden, exempelvis i Nordkroken, medan de plana överytorna på andra slättberg skär tvärs över subhorisontella sprickor, och åter andra slättberg saknar uthålliga subhorisontella sprickor helt. Längs strandlinjen väster om Kinnekulle är den plana urbergsytan överlagrad av horisontella lager av kambrisk sandsten och konglomerat. Slättbergen tolkas därför som återexponerade och glacialt svagt modifierade rester av U2.

Såväl U2 som överliggande tidigpaleozoiska lager och tidigpermiska intrusioner har utsatts för mindre förkastningar (10–60 m vertikal förskjutning), troligen under perm. I höjdmodeller från Lidar-data kan tidigare beskrivna förkastningsmönster och lutningar på bergblock i kilometerskalan bekräftas. Dessutom har ytterligare mindre vertikala förskjutningar (< 10 m) inom de större bergblocken identifieras. Liknande mönster av förkastningsblock i U2 återfinns också runt förekomster av tidigpaleozoiska sedimentbergarter i Närke och Östergötland.

Den nutida urbergsytan kring Trollhättan innehåller ovittrade kambriska sandstensgångar och paleozoiska sprickfyllnader av kalcit. Detta tyder på att U2 återexponerats i relativt sen tid. Stora mängder bergartsfragment av kambrisk sandsten, ordovicisk kalksten och diabas från de västgötska platåbergen har hittats i morän från mellersta och sen pleistocen så långt söderut som Jylland i Danmark. Det begränsade ursprungsområdet för dessa bergarter, i förhållande till det utbredda depositionsområdet i Danmark, indikerar att täckbergarterna i Västergötland var mer utbredda än idag ända in i mellersta pleistocen. Återexponeringen av inkonformiteten över stora delar av Västergötland, för första gången sedan tidig kambrium, var troligen resultatet av en intensifiering i glacialerosion av de fennoskandiska inlandsisarna efter 1,1 Ma. Åtminstone några tiotals meter sedimentberggrund uppskattas ha eroderats i områdena runt de västgötska platåbergen som ett resultat av de kvartära nedisningarna.

Den glacial erosionen av den återexponerade inkonformiteten i Västergötland har resulterat i att urbergsytan har sänkts och reliefen har förstärkts. I genomsnitt är det uppskattade medeldjupet på erosionen 14 m, baserat på avståndet från den yta som går igenom de högsta topparna ner till dagens berggrundsyta. Detta är samma medeldjup som likadana undersökningar i nordöstra Uppland visat (14 m). Till skillnad från i Uppland, går det på flankerna Halleberg och Hunneberg att bestämma även skillnaden mellan U2 och den nuvarande ytan som går genom de högsta topparna. Detta genom att höjdskillnaden mellan U2, där den kan ses under överlagrande sedimentbergarter, och höjden på närliggande bergytor är ca 2–6 m. Längre bort från dagens täckberg kan denna ytterligare sänkning potentiellt vara större. Över stora områden har dock endast 5–10 m eroderats från den yta som sammanbinder bergkullarnas överytor. Den sena återexponeringen av inkonformiteten och den begränsade glaciala erosionen har medfört att delar av den ursprungliga plana urbergsmorfologin här har bevarats, på både regional och lokal skala. Den volymmässigt största glaciala påverkan har skett i sänkor och i dalgångar, särskilt i zoner med uppsprucken gnejs, där upp till 10–40 m berg har eroderats. Allra störst har den glaciala påverkan varit i området kring Sjuntorp där medeldjupet på erosionen är 19,4 m från den yta som går igenom de högsta topparna. Urbergsytan har här hög lokal relief och karakteriseras av rektangulärt avgränsade bergkullar, rundhällar, djupa dalgångar och stjärnformade depressioner; former som är karakteristiska för så kallad *cnoc and lochain*-terräng på sköldområden som utsatts för pleistocen glaciala erosion. De glaciala erosionsformerna i Trollhättanregionen har således utvecklats genom relativt måttlig glacial erosion av den ursprungliga U2-ytan.

Analys av halten kosmogena nuklider från berghällar nära flankerna av Halleberg och Hunneberg visar på ingen eller en mycket ringa tidigare exponering av berggrundsytorna. Erosionen under de senaste 100 ka var > 2–3 m och erosionen under den senaste 1 Ma var åtminstone 20 m, men kan ha varit så mycket som > 40 m. På dessa lokaler är resultaten kompatibla med en utveckling där U2 har exhumerats genom glacial erosion under de senaste glaciala cyklerna genom sluttningsreträtt vid bergsbranterna. Storleken på den glaciala erosionen i området kring Trollhättan varierar dock rumsligt. Under antagande att erosionshastigheten varit konstant (genom t ex glacial abrasion) under de senaste 0,5 eller 1 Ma, indikerar resultaten från kosmogenmätningarna att 0,5–2 m berg har eroderats vid Hjortmossen under de senaste 100 ka, och < 18 m berg under de senaste 1 Ma. Bevarandet av slättbergen kan kopplas till den höga motståndskraften mot glacial erosion hos den hårda, massiva granitgnejsen i området, och sannolikt också den relativt sena återexponeringen av dessa urbergsytor efter att täckbergarterna försvunnit. Storleken av den glaciala erosionen i Trollhättan uppskattad från de kosmogena nukliderna är jämförbar med den uppskattade erosionen som motsvarande undersökningar i Forsmarksområdet, baserat på ett större dataset av kosmogena isotopanalyser, tidigare visat.

Även om det finns skillnader mellan Västergötland och Uppland vad gäller erosions- och sedimentationshistoria under proterozoikum och tidigpaleozoikum, finns många likheter i berggrundsterrängens senare utveckling i de båda områdena, under fanerozoikum. Sådana likheter inkluderar den plana subkambriska inkonformiteten, den ringa tektoniska förskjutningen av bergblock, och bristen på bevis för återexponering av urberget för djupvittring under mesozoikum och kenozoikum. Likartade glaciala erosionsformer i olika skalor återfinns både i Trollhättan och runt Forsmark. De glaciala erosionsprocesserna, som varit verksamma på hårda berggrundsytor med låg relief och varierat sprickmönster, är direkt jämförbara mellan de båda områdena. Rekonstruktionen av den tidigkambriska inkonformiteten i Trollhättanområdet ger en referensyta mot vilken den glaciala erosionens mönster och omfattning kan bestämmas, en teknik som kan tillämpas även i Forsmarksområdet. Trollhättanområdet kan därmed utgöra ett värdefullt referensområde för att förstå den glaciala erosionen av den subkambriska inkonformiteten i och omkring det föreslagna området för slutförvar av utbränt kärnbränsle i Forsmark.

Contents

1 Introduction

Vast expanses of several of the Earth's cratons, including Laurentia (Dawes 2009, Peters and Gaines 2012, Parnell et al. 2014), Baltica (Gabrielsen et al. 2015) and Arabia-Nubia (Angerer et al. 2011), were reduced to very low relief in the latest Neoproterozoic and later flooded and buried during marine transgressions from the Ediacaran onwards. The top-basement erosion surface on Laurentia has been termed the *Great Unconformity* (Derby et al. 2012, Keller et al. 2019). On Baltica, another great unconformity emerges from below Late Ediacaran to Early Cambrian sedimentary cover rocks in Estonia (Liivamägi et al. 2014), Sweden (Elvhage and Lidmar-Bergström 1987, Lidmar-Bergström 1988), southern Norway (Gabrielsen et al. 2015) and western and southern Finland (Söderman 1985, Slater and Willman 2019). The distinctive low relief basement topography that extends away from cover rocks has been widely interpreted as inherited from the sub-Cambrian unconformity and has been generally referred to as the *Sub-Cambrian Peneplain* (SCP) (Figure 1-1).

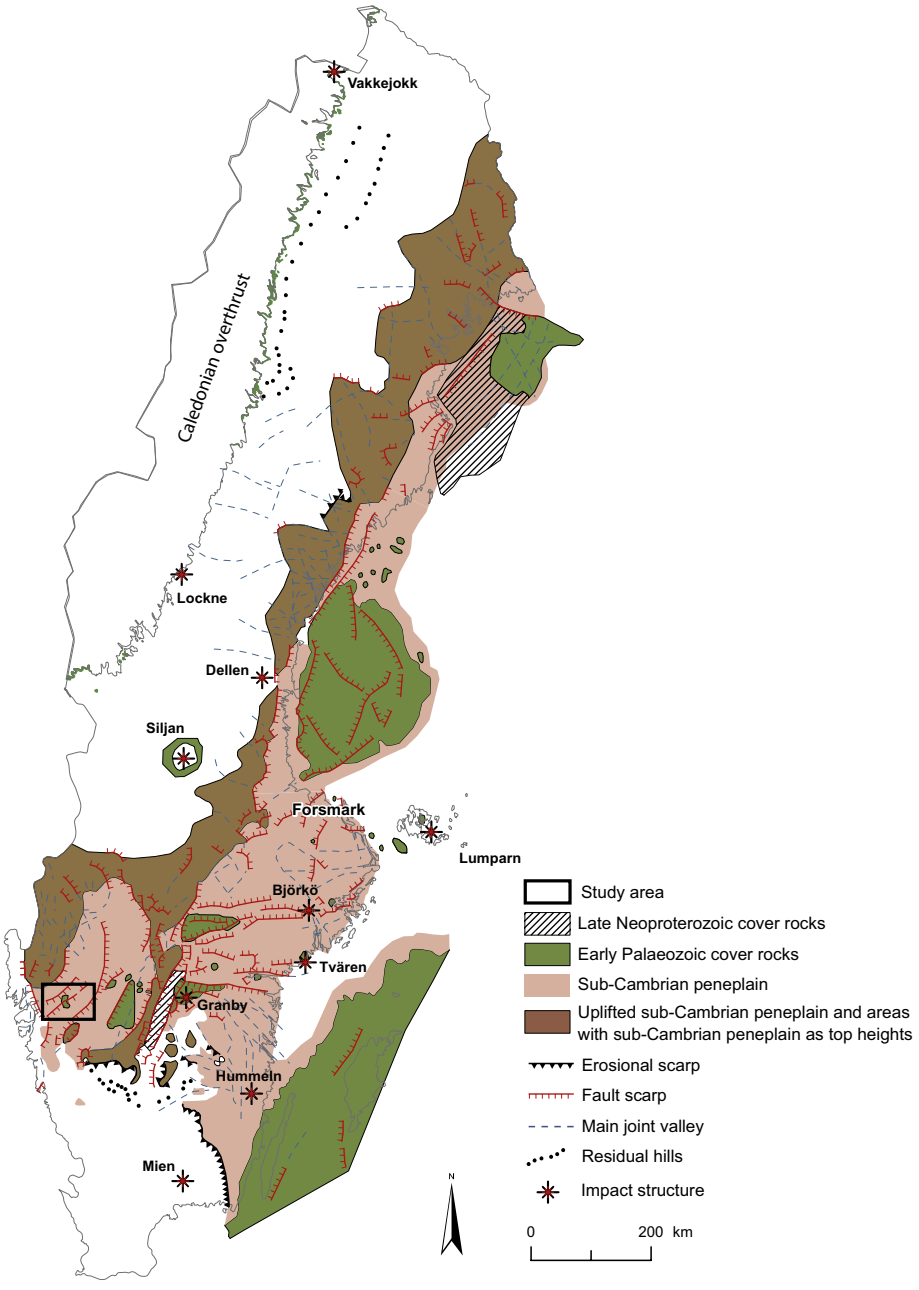

Figure 1-1. *Mapped extent of the SCP in Sweden (modified from Lidmar-Bergström and Olvmo 2015). Only major tectonic lineaments are shown. Study area location in Västergötland is indicated by the box.*

Västergötland in SW Sweden (Figure 1-2) is a type area for the study of the SCP (Rudberg 1970, Lidmar-Bergström 1991, Johansson et al. 2001b). Here, the sub-Cambrian unconformity, the contact between the Proterozoic basement gneisses and the overlying Early Palaeozoic cover, is locally exposed around several outliers of Early Palaeozoic sedimentary rocks (Figure 1-1) that are preserved beneath Early Permian dolerite sills. The exposed basement gneisses maintain similar elevations over wide areas (Figure 1-3). Early Cambrian sandstone dykes are widespread in vertical fractures in the basement (Mattsson 1959), indicating that the former unconformity was close to the present basement surface. The juxtaposition of cover rocks, the buried unconformity and widely exposed basement offers potential for detailed reconstruction of the original form of the SCP and its dislocation by Phanerozoic tectonics (Johansson et al. 1999).

In this report, we explore the potential use of the sub-Cambrian unconformity around Trollhättan as a reference surface for estimating depths of Pleistocene glacial erosion in basement. We first review the erosion and burial history of Västergötland, and the terminology used previously in descriptions of its basement erosion surfaces. Next, the elevation and form of the preserved unconformity is examined where it remains buried beneath Early Palaeozoic cover rocks around Halleberg and Hunneberg, near Trollhättan, and also further N at Kinnekulle (Figure 1-3). The elevation and form of the buried unconformity is then compared to that on the presently exposed basement surface. Summit envelope surfaces are constructed using 3D-models and topographic profiles based on 2 m resolution LiDAR data. Surfaces are constructed for the entire study area and for four study areas where bedrock is widely exposed at distances of 0–15 km from the edges of the preserved Early Palaeozoic unconformity around Halleberg and Hunneberg. Where the summit envelope surfaces maintain slightly lower elevations but similar form to the buried unconformity then the present basement surface is interpreted to be largely inherited from the earlier unconformity surface. At such locations, the summit envelope surfaces can be used as reference surfaces for identifying patterns of Phanerozoic block faulting and for estimation of depths of glacial erosion below the re-exposed sub-Cambrian unconformity. Reconstruction of the sub-Cambrian unconformity around Trollhättan allows comparisons to be made with the equivalent unconformity in Uppland where the exposed basement is of similar morphology and history (Rudberg 1970, Röshoff 1988) but where sedimentary outliers are submerged. The likely origins of the sub-Cambrian unconformity surface in Västergötland are briefly examined.

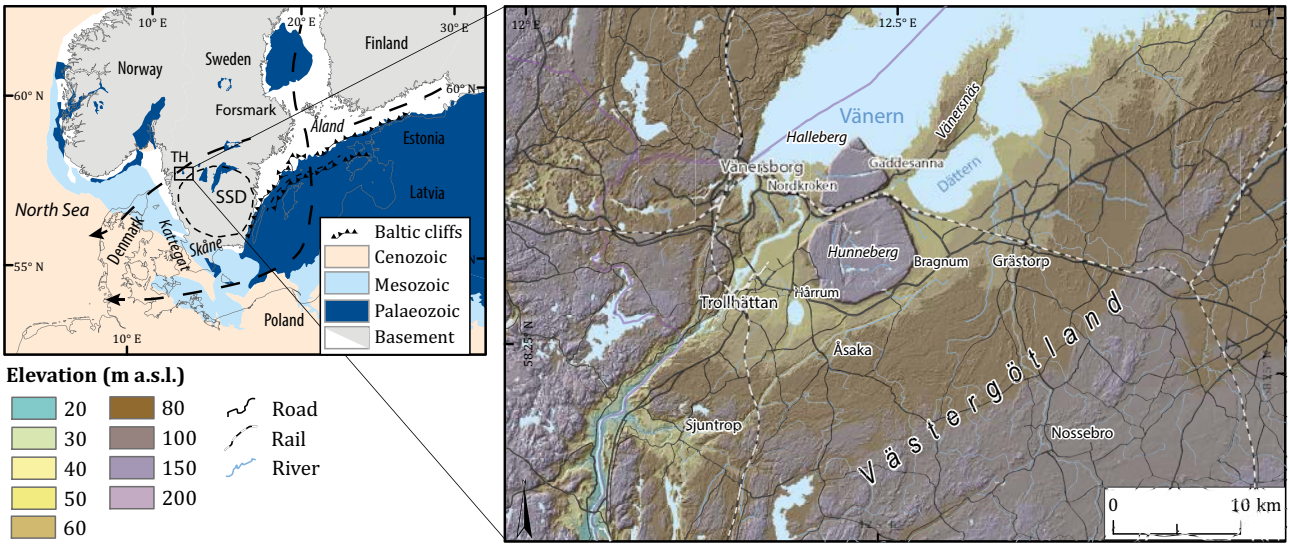

Figure 1-2. *Location of the Trollhättan region. Inset shows the location of Trollhättan (TH) relative to the South Swedish Dome (SSD) and to Forsmark. Dashed black lines are former drainage lines of the Pliocene Baltic River system (Overeem et al. 2001, Lidmar-Bergström et al. 2017). Geological data from Bundesanstalt für Geowissenschaften und Rohstoffe (BGR). Elevation data from Lantmäteriet.*

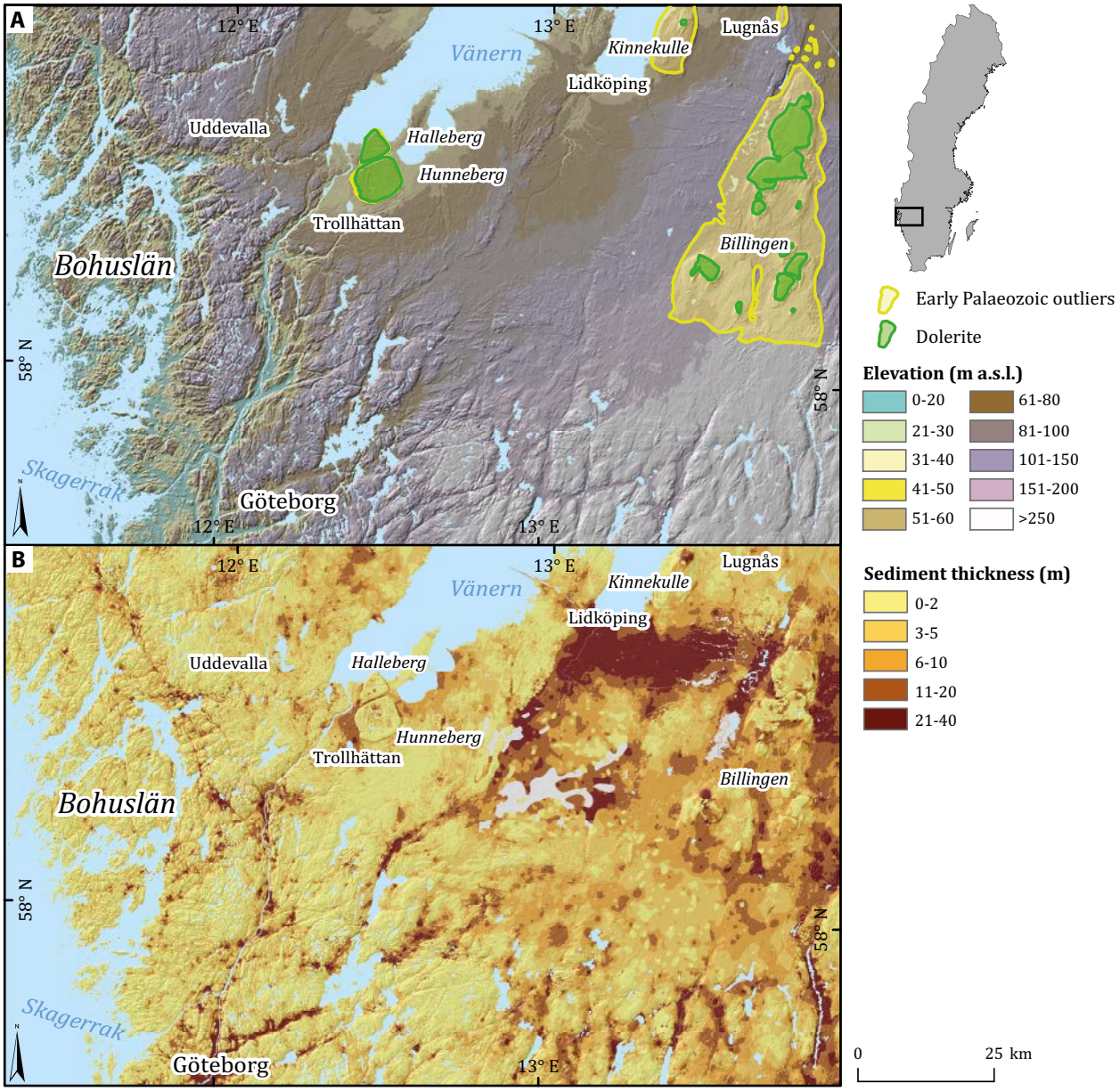

Figure 1-3. *Digital elevation models of relief (Lantmäteriet data) and Quaternary sediment thickness (SGU data) in SW Sweden.*

1.1 Basement geology

The continental crust in southwestern Sweden first formed at ~1.75 Ga but was finally established and stabilised only after the end of the Sveconorwegian orogeny at ~0.9 Ga, the last orogeny to affect southern Sweden. The Sveconorwegian Province comprises crustal segments, separated by N–S trending zones of ductile deformation (Johansson et al. 1993). The Trollhättan area lies within the Median Segment of this Province, bounded to the west by the Göta Älv Shear Zone (Figure 1-4), In the Median Segment, 1.6–1.5 Ga red and grey granite and granodiorite gneisses are widespread, with amphibolite dykes and frequent quartz veins, aplites and pegmatites (Figure 1-5). A metamorphosed dolerite dyke swarm at the southern end of Lake Vänern is dated to 1.3 Ga (Söderlund et al. 2005b).

Regional strike of foliation in the gneiss is NNE-SSW (Samuelsson and Lundqvist 1988), swinging towards NE-SW in the south, with dip to the NW and W. The main faults and fracture zones show a preferred orientation parallel or perpendicular to the foliation of the gneisses (Ahlin 1987). Other fracture trends are also apparent in Digital Elevation Models (DEMs), large quarries and at the local scale (Section 3.4.1).

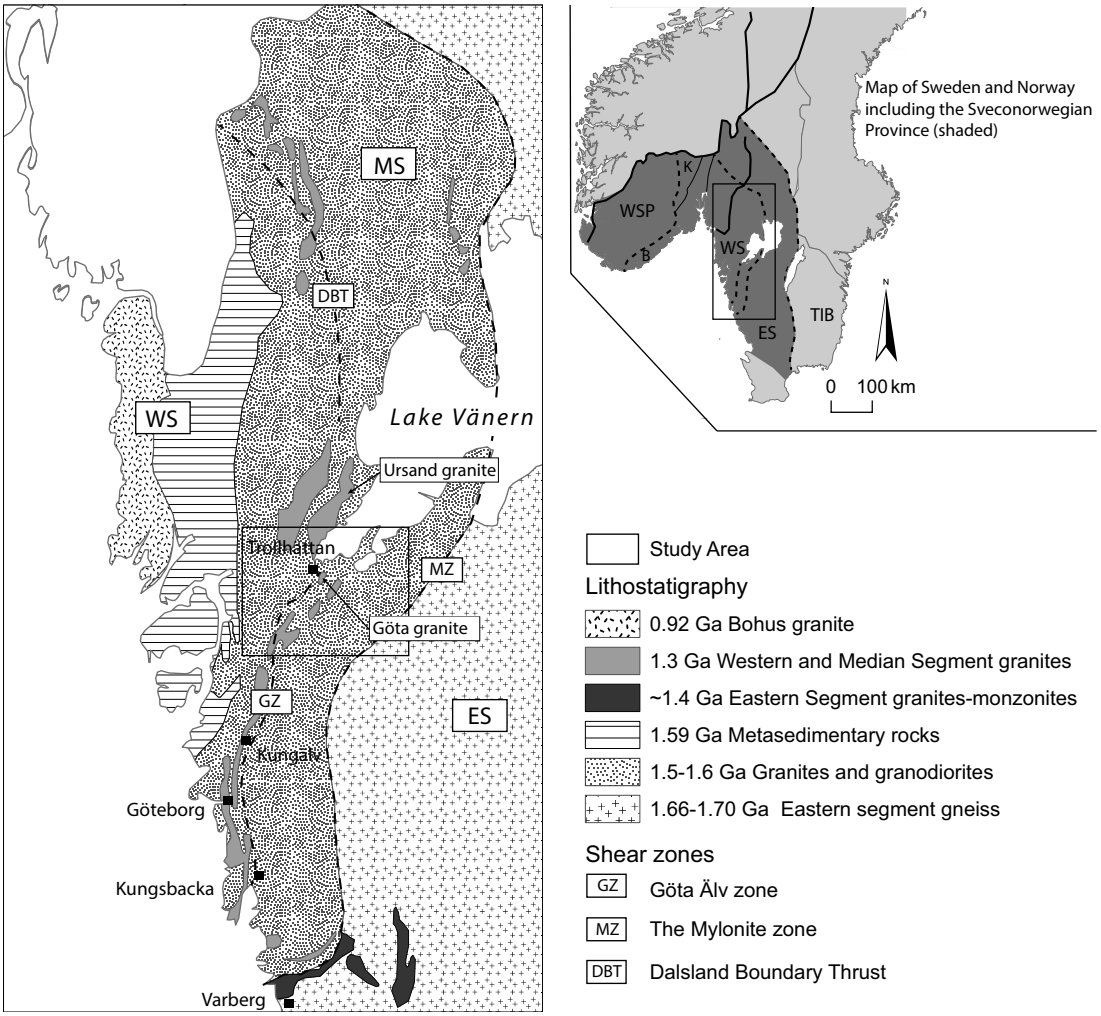

Figure 1-4. *Geological map of SW Sweden Inset map showing the Sveconorwegian Province: ES – Eastern Segment, MS – Median Segment, WS – Western Segment, K – Kongsberg Region, B – Bamble Region, WSP – Western Sub-province, TIB – Trans-Scandinavian Igneous Belt. Adapted from Hegardt et al. (2007).*

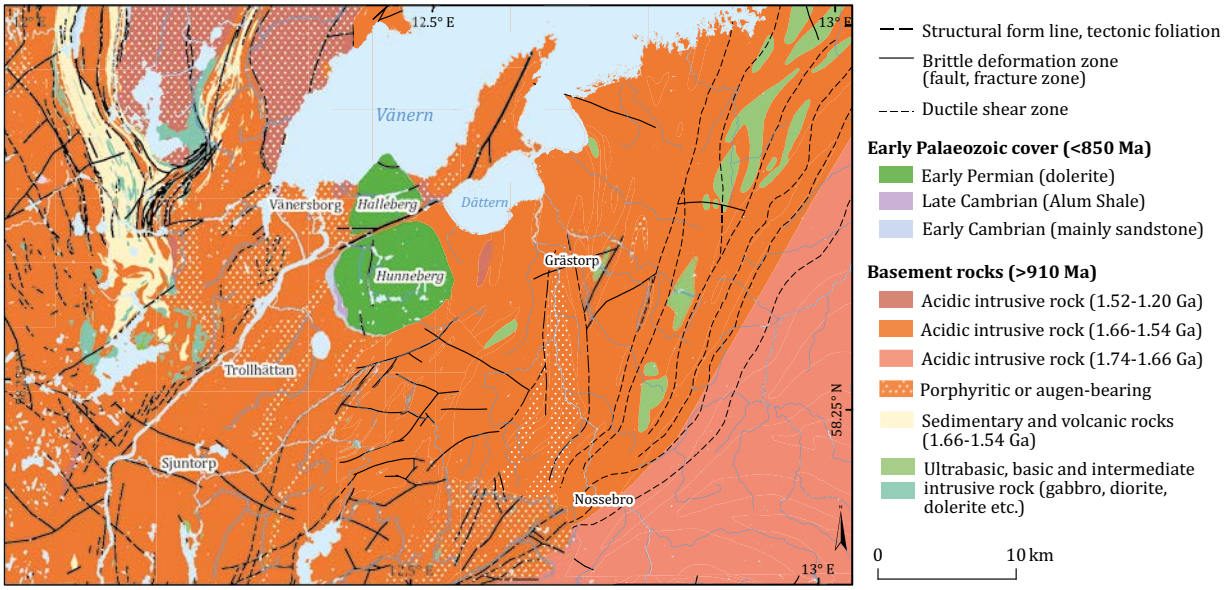

Figure 1-5. *SGU solid geology bedrock map for the Trollhättan region. SGU data for the Vänersborg area is inconsistent and shown here as undifferentiated acid intrusive rock (1.66–1.54 Ga).*

1.2 Neoproterozoic and Phanerozoic erosion and burial

The present basement topography of Västergötland was largely shaped before the Palaeozoic and has been re-exposed only in geologically-recent times. The origins of the basement unconformity that lies beneath Early Palaeozoic cover are viewed in terms of three phases of denudation: (i) deep erosion of this region of Baltica through the Neoproterozoic, (ii) planation of the stable craton surface under subaerial environments and (iii) final grading of rock shelves during Early Cambrian marine transgression.

1.2.1 Neoproterozoic erosion

At the end of the Sveconorwegian orogeny, post-orogenic collapse and km-scale erosion led to crustal cooling by 900 Ma (Viola et al. 2011). Post-orogenic sediments are preserved in the Lake Vättern half-graben that holds the middle Neoproterozoic Visingsö Group (Wickström and Stephens 2020), a 1.4 km thick sequence of sandstones, mudstones and limestones that is constrained in age by isotopic and bio-chronologic ages to between ≤886 and 740 Ma (Moczydłowska et al. 2018) or ~780 and 706 Ma (Pulsipher and Dehler 2019). It is likely that low relief became extensive on that part of Baltica now found in southern Norway and Sweden by 750–700 Ma (Gabrielsen et al. 2015, Moczydłowska et al. 2018). Small sandstone outliers around the Lake Vättern basin indicate that the basement topography buried beneath the Visingsö Group was flat (Wikström and Karis 1993) to hilly (Månsson 1996). Evidence is lacking for the erosional level and surface relief on the basement in Västergötland at this time.

Varangian tillites in western and northern Norway likely record a final phase of Neoproterozoic glaciation on Baltica at ~630 Ma (Nystuen et al. 2008) or ~580 Ma (Jensen et al. 2018). Marginal and intra-cratonic tectonics (Nystuen et al. 2008) ceased after ~584 Ma (Bingen et al. 1998), around 36–50 Ma before the onset of Late Ediacaran-Early Cambrian transgression of Baltica (Nielsen and Schovsbo 2011). Prior to this, detritus from the craton in present day southern Finland was shed south-eastwards to basins in Byelorussia (Paszkowski et al. 2019). Formation of Ediacaran (635–541 Ma) weathering profiles in Estonia, up to 150 m thick in fault zones, is constrained to the period between ~600 and 560 Ma (Liivamägi et al. 2015). Prolonged subaerial erosion operating across the stable craton produced vast areas of exceptionally low relief across Baltica that allowed subsequent flooding of almost the entire craton (Puura et al. 1996, Nielsen and Schovsbo 2011). The extent of Cambrian transgression as indicated by the wide distribution of Cambrian outliers around the present edges of the shield and across its surface (Figure 1-6).

1.2.2 Early Palaeozoic marine transgressions

By the start of the Cambrian at ~541 Ma, Baltica was situated at 35° to 60°S (Torsvik and Cocks 2013), with a warm temperate to moderately humid climate (Dreyer 1988). Baltica was gradually transgressed as sea-level rose through the latest Ediacaran (Nielsen and Schovsbo 2011). A long-term (>50 Ma) trend for sea level rise of ~200 m total through the Cambrian (541–485 Ma) and Early Ordovician (485–470 Ma) was superimposed on short-term high-stands and low-stands of 20–70 m amplitude (Haq and Schutter 2008). Rising sea-level led to flooding across Sweden in the Early Cambrian and deposition of thin, horizontally-bedded sandstones, siltstones and limestones that were continuous for hundreds of kilometres (Nielsen and Schovsbo 2006).

An hiatus, the Hawke Bay unconformity, is widely recorded within Cambrian sequences late in the Early Cambrian (Nielsen and Schovsbo 2015), with non-deposition and erosion across large areas of southern Sweden, Estonia and the St Petersburg region (Artyushkov et al. 2000). This hiatus is a result of combined minor (<40 m) epeirogenic uplift and ≥100 m sea level fall (Artyushkov et al. 2000 Nielsen and Schovsbo 2015). From the early Middle Cambrian, the Alum Shale was deposited in a large, shallow epicontinental sea that covered substantial parts of Baltica (Schovsbo 2002). The Ordovician epicontinental basin of Baltica continued to be characterized by an extremely low average rate of sediment accumulation, rarely exceeding 1–3 mm per 1 000 years, a flat bottom topography, and a long-term tectonic stability (Dronov and Holmer 1999). The carbonate-dominated depositional sequences each have a thickness of only 1.5 to 20 m, or even less, and para-sequences of about 0.2–0.3 m are common, allowing basin-wide recognition of third-order eustatic sea level fluctuations (Dronov and Holmer 1999). The sediment supply to the epicontinental sea gradually decreased during the Early Palaeozoic transgression, due to shrinking of the source land areas and an increased distance from the coastline (Nielsen and Schovsbo 2015). Exposed basement was confined to higher ground in what is now western Norway (Figure 1-7).

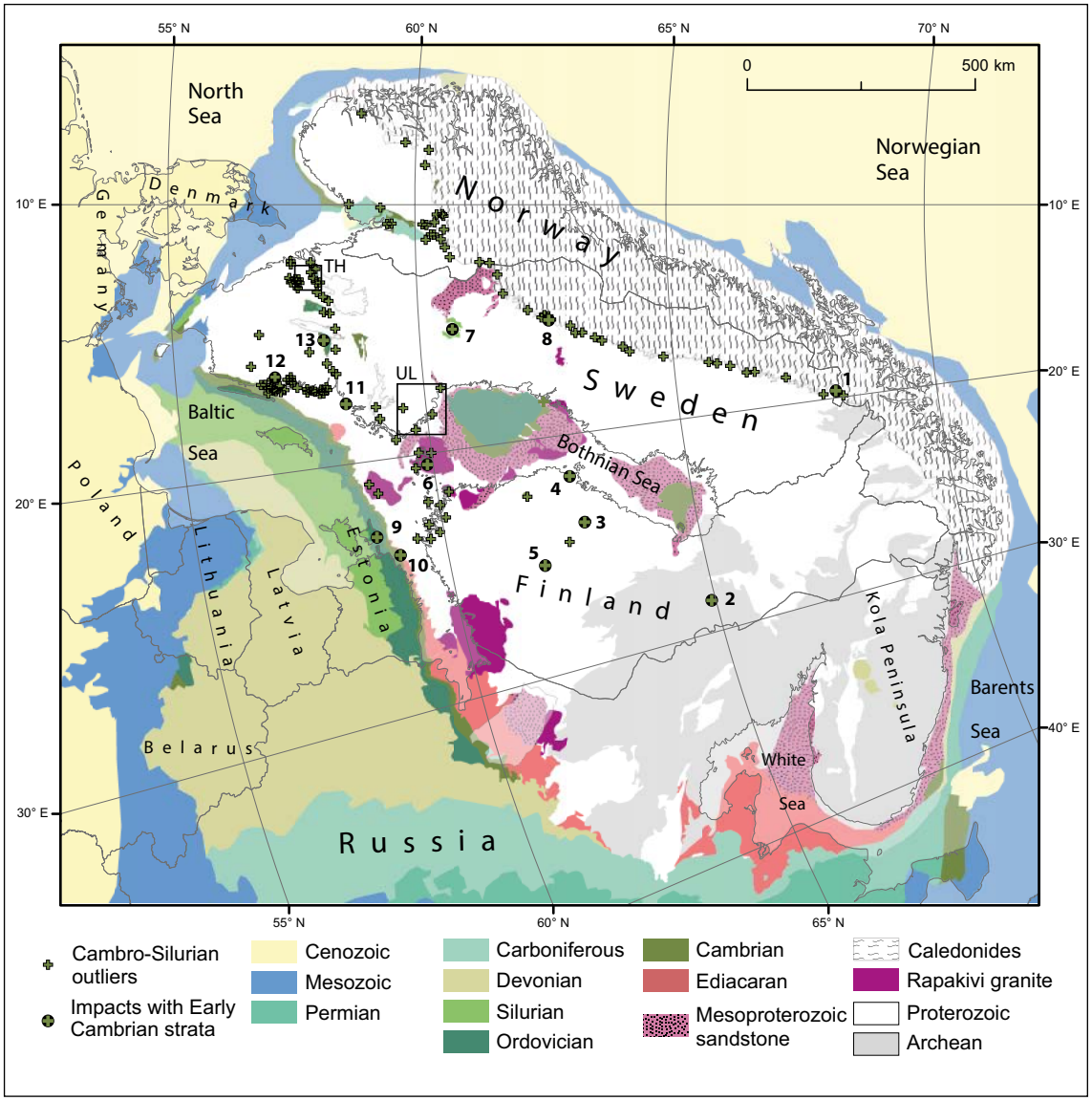

Figure 1-6. *Geology of the Fennoscandian shield and East European platform. In order to emphasises the onlap of Ediacaran-Ordovician sedimentary rocks onto the shield surface below 60° N, the map is rotated with North directed to the right. Cambro-Silurian outliers in Norway and western Sweden pass below the Caledonide nappes. Cambro-Silurian remnants on the exposed shield surface include outliers, Cambrian sandstone dykes and sedimentary rocks preserved in impact structures. 1. Vakkejokk (Ormö et al. 2017). 2. Saarijärvi (Öhman 2007). 3. Lappajärvi (Schmieder and Jourdan 2013). 4. Söderfjärden (Öhman 2007). 5. Karikkoselkä (Uutela 2001). 6. Lumparn (Abels et al. 1998). 7. Siljan (Juhlin et al. 2012). 8. Lockne (Sturkell and Lindström 2004). 9. Kärdla (Puura and Suuroja 1992). 10. Neugrund (Suuroja and Suuroja 2006). 11. Tvären Bay (Lindström et al. 1994) 12. Hummeln (Alwmark et al. 2015). 13. Granby (Alwmark 2009). TH Trollhättan. UL Uppland.*

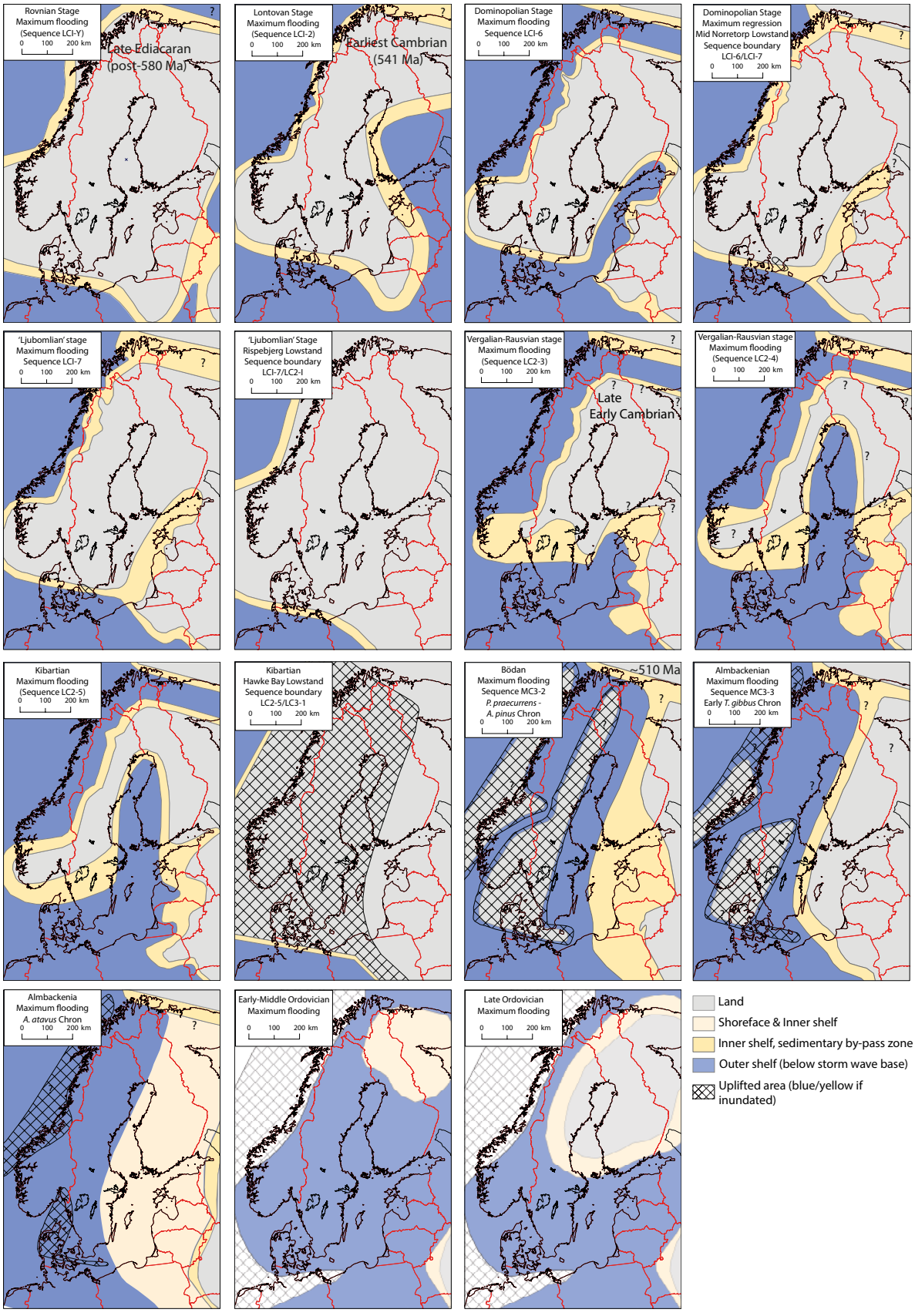

Figure 1-7. *Early Palaeozoic marine transgression across Fennoscandia. Palaeographic maps are assembled from three sources: Early Cambrian (Nielsen and Schovsbo 2011), late Early to Late Cambrian (Nielsen and Schovsbo 2015) and Ordovician (Nikishin et al. 1996). The palaeogeographic maps of Nielsen and Schovsbo are based on information from all known outliers in Fennoscandia. The reconstruction for the early Cambrian Lontovan stage is modified after Slater and Willman (2019). As Cambrian rocks almost certainly extended more widely prior to erosion, the maps are conservative reconstructions of the extent of transgression in each period.*

The flatness of the sub-Cambrian basement surface at the time of transgression is evident from several lines of geological evidence:

- The large area of Baltica that was flooded during sea level high stands (Figure 1-7).
- Thin, condensed Cambrian sequences which are nevertheless remarkably laterally extensive and often traceable over wide geographical areas (Jensen 1997, Tuuling et al. 1997, Nielsen and Schovsbo 2011).
- The low erosional impact and extent of the Hawke Bay Event.

The stratigraphy of Baltica through the Cambrian and Ordovician has been reconstructed in detail, allowing palaeogeographic maps to be made for key periods (Figure 1-7). The maps show that the shield surface was subjected to multiple transgression-retrogression cycles over a period of tens of millions of years (Figure 1-7). The extent of transgression indicates that topography on the shelf was less than the 20–70 m amplitude of Cambrian sea level fluctuations. No deep (> 15 m) channel incision associated with low sea-levels has been reported from any Cambrian succession in Baltoscandia indicating that the underlying rock shelf slope was flat (Artyushkov et al. 2000, Nielsen and Schovsbo 2011).

The basement unconformity in south-central Sweden is overlain by the Early Cambrian File Haidar Formation (Nielsen and Schovsbo 2011). The Formation varies in thickness between 16 and 38 m (with most values between 22 and 26 m) in sections and boreholes in an area stretching from Kinnekulle, including the Vänern and Vättern area towards boreholes in the southern Bothnian Sea (Nielsen and Schovsbo 2011) (Figure 1-8). In south-central Sweden, all available sections and boreholes suggest that the File Haidar Formation was of very uniform thickness over a very wide area (Nielsen and Schovsbo 2011). The great lateral extent of thin, condensed sequences (Slater and Willman 2019) and the lack of lateral facies variations require that the underlying basement unconformity surface was generally flat.

During the ≤6 Ma long Hawke Bay regression at the Early-Middle Cambrian boundary, sea level fell by ≥100 m. The associated disconformity is recorded over a very wide area, stretching from Skåne to Uppland ((Figure 1-8). Typical regional gradients on the disconformity surface are estimated at 0.5–1 m per km (Nielsen and Schovsbo 2015). Only a maximum of 5–10 m of Cambrian strata were removed by erosion during the regressive phase (Nielsen and Schovsbo 2015). The extent of the Hawke Bay Event disconformity, its flatness and the low erosional impact of this regression together indicate that the underlying basement unconformity surface was flat.

1.2.3 Early Palaeozoic cover sequence in Västergötland

The sub-Cambrian unconformity in Västergötland is overlain by the Mickwitzia Sandstone, part of the Early Cambrian File Haidar Formation (Nielsen and Schovsbo 2011). In the Halleberg and Hunneberg sequences, the Mickwitzia Sandstone comprises a discontinuous, thin, basal quartz pebble conglomerate and overlying quartz sandstone (24 m thick) (Lindström 1887). Similar rocks are seen at Kinnekulle, where thin quartz pebble conglomerate layers are overlain by up to 10 m of well-sorted, mature quartz sandstones that form the Mickwitzia Sandstone. Biostratigraphic correlation places the Mickwitzia Sandstone in the upper part of the Early Cambrian (Jensen 1997), potentially > 10 Ma after the start of the Cambrian Period. Deposition took place in a storm dominated, shallow (less than 10 m depth) water environment (Artyushkov et al. 2000, Nielsen and Schovsbo 2011). These Early Cambrian basal pebble gravels and sands were laid down on an almost flat basement surface (Jensen 1997).

At Halleberg and Hunneberg, Early Cambrian sandstone is overlain by early Middle to Late Cambrian Alum Shale (24 m thick), and Early Ordovician limestone (12–14 m thick) (Maletz et al. 1996). The beds dip at 0.3 % to the N (Figure 1-9). Sedimentation continued into the Early Silurian across Västergötland (Bergström and Bergström 1996) but younger rocks are not preserved at Halleberg and Hunneberg. The Early Palaeozoic sequences in Västergötland have been preserved from erosion by Early Permian dolerite sills (Priem et al. 1968, Timmerman et al. 2009) which have acted as cap rocks (Figure 1-10).

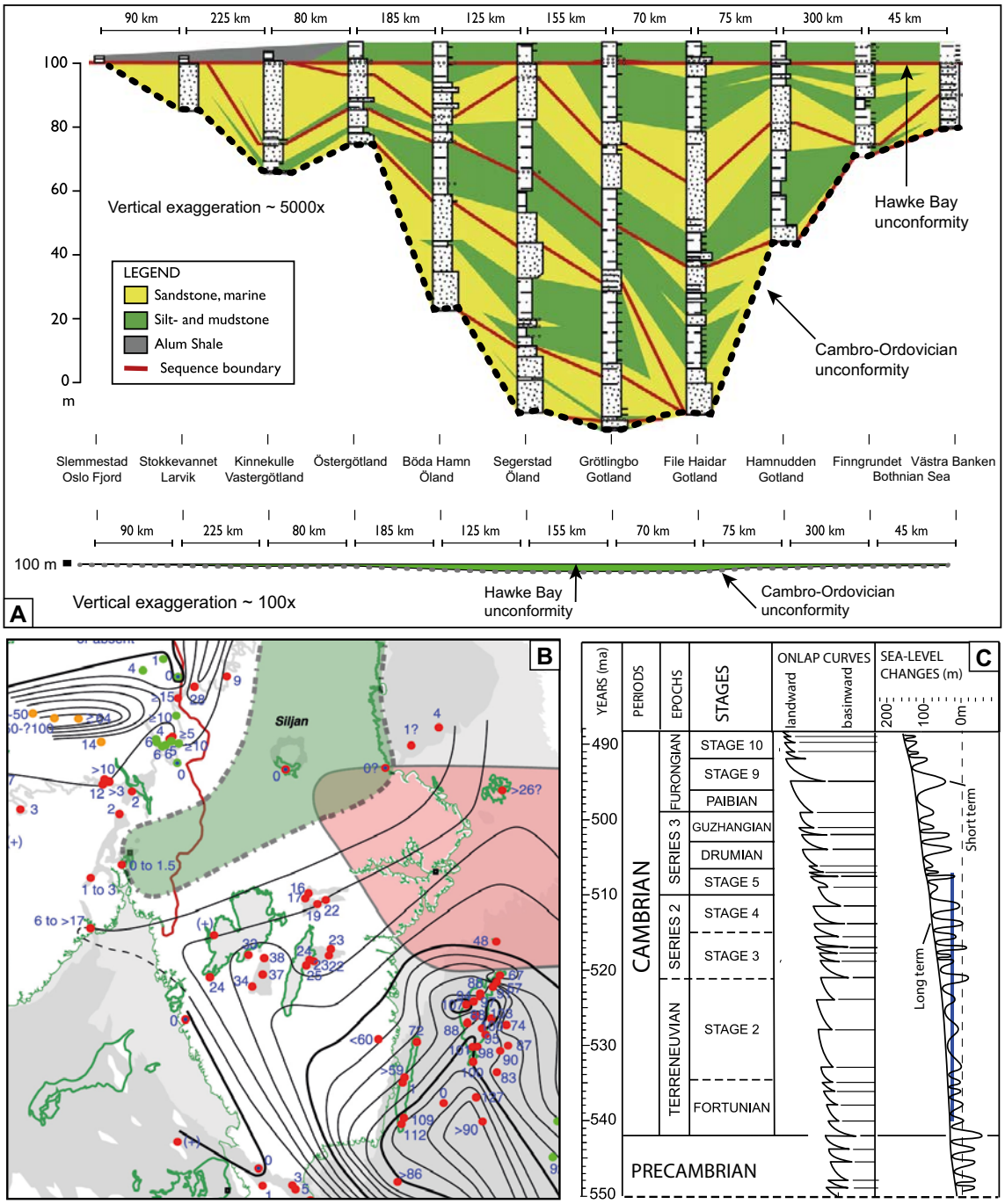

Figure 1-8. *Early Cambrian transgression in southern Sweden and neighbouring areas. A. Correlation diagram (sequence stratigraphy correlations) of the File Haidar Formation between the sub-Cambrian unconformity and the Hawke Bay intra-basinal unconformity. The section extends from the Oslo region, across Västergötland, Öland-Gotland and south-central Sweden to the Bothnian Sea. Top diagram with 5 000 × vertical exaggeration; bottom diagram with 100 × vertical exaggeration. Modified after Nielsen and Schovsbo (2011). B. Isopach map (5 m contours) and measured thickness in sections and boreholes (red points) of the File Haidar sandstone formation and correlative units in southern Sweden. Modified after Nielsen and Schovsbo (2011). Red shaded area has experienced later erosion, so thicknesses are minima. Green area shows no evidence of deposition of the File Haidar Formation and it is interpreted to have remained emergent. C. Cambrian sea level changes modified after Haq and Schutter (2008). Sea level curves show a long term, overall transgression, and short-term retrogression-transgression cycles, based on onlap curves, based on sequence stratigraphic analysis of sections and boreholes that document base level changes. The blue line is an imaginary datum, which (if the datum is stable) experienced 14 flooding and retrogression cycles.*

Figure 1-9. *Horizontally-bedded Middle to Late Cambrian alum shale and Early Ordovician limestone at Diabasbrottet, Halleberg. The stratigraphy is described in Bergström et al. (2004).*

1.2.4 Later Palaeozoic deep burial

At the time of the Caledonian orogeny, large volumes of sediment accumulated on the craton surface in southern Sweden but the depth of burial remains controversial (Larson et al. 1999, Hendriks and Redfield 2005, 2006, Larson et al. 2006). Vitrinite reflectance indicates < 2 km of cover (Samuelsson and Middleton 1998, Lecomte et al. 2017), concordant with (U-Th)/He thermochronometry (Söderlund et al. 2005a) and oxygen isotope data for limestones (Tullborg et al. 1995). These values are approximately half those suggested by Apatite Fission Track analysis (AFTA) (Zeck et al. 1988, Larson et al. 1999, Japsen et al. 2016). The Late Silurian to Middle Devonian interval represents the period of maximum burial of the basement in southern Fennoscandia (Puura et al. 1996). After Early Palaeozoic sedimentation, the unconformity surface and its cover was disrupted by faulting, but the timing of faulting is uncertain (Ahlin 1987) but likely dates from the early Permian (Månsson 1996, Timmerman et al. 2009). The Phanerozoic erosion and burial history of the basement around Trollhättan is summarised in Figure 1-10.

During the Late Carboniferous – Early Permian interval, dolerite sills were intruded into thick sedimentary cover (Timmerman et al. 2009). Modelling of the emplacement of sills of similar type and age in central Scotland indicates that a linear relationship exists between sill thickness and the depth of intrusion (Goulty 2005). Using this relationship, the thickness of the Permian sills at Kinnekulle (60 m) and Halleberg (40 m) suggests that 1.2–1.3 km of sedimentary cover remained at the time of intrusion at ~290 Ma. The full Cambro-Ordovician stratigraphic sequence is < 200 m thick (Nielsen and Schovsbo 2011), implying that at the time of sill emplacement ~1 km of Devonian to Carboniferous sedimentary rocks likely remained over the early Palaeozoic rocks. Early Permian magmatism was associated with fault movement in Västergötland (Ahlin 1982) and Bohuslän (Samuelsson 1967). Permian fault movements also dislocated U2 and its overlying Early Palaeozoic cover in Närke and Östergötland (Alm and Sundblad 2002). Effects of Middle Triassic cooling and exhumation, beginning between 245 and 240 Ma, are apparent in apatite fission-track data across much of southern Sweden (Japsen et al. 2016). In Västergötland, Middle Triassic palaeotemperatures may have reached 75–90 °C below a cover of Palaeozoic to Lower Triassic rocks that was later thinned by erosion associated with Middle Triassic uplift and block faulting (Norling and Bergström 1987, Gabrielsen et al. 2015).

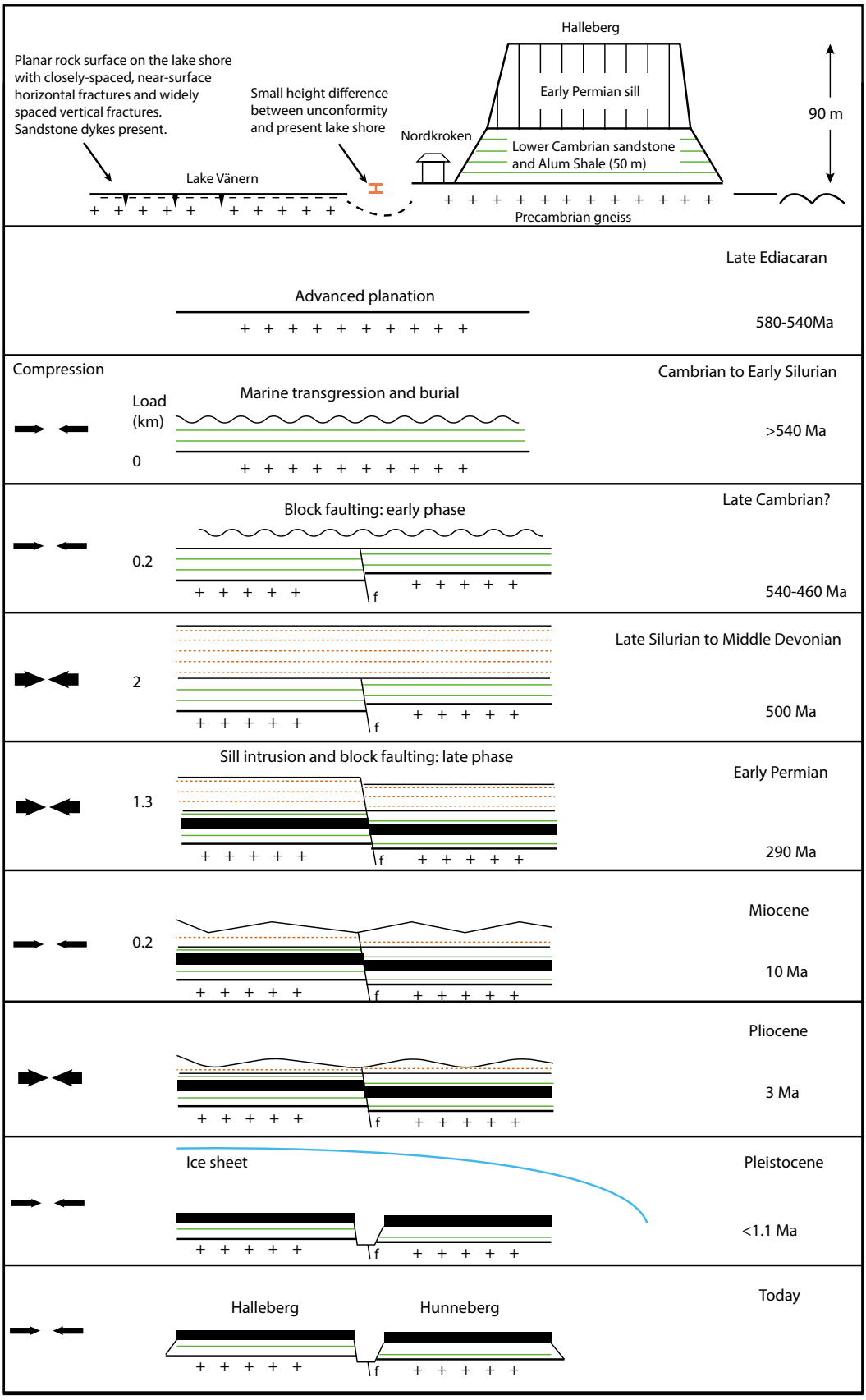

Figure 1-10. *Cartoons of the exposure and burial history of the basement at Nordkroken, Trollhättan. The top panel is a schematic representation of the key elements of the geology and basement relief around Halleberg. Compression and loading are schematic and based on changing estimated thicknesses of sedimentary cover thickness through the Phanerozoic outlined in Section 1.2 and ice sheet loading in the Pleistocene in Section 1.3.*

1.2.5 Exhumation and erosion of the sub-Cambrian unconformity

In southernmost Sweden, Palaeozoic cover was not only thinned by erosion but, at least locally, it was removed (Japsen et al. 2016). This exhumation is recorded by three major episodes of cooling in the Late Triassic-middle Jurassic, middle Cretaceous and Neogene (Figure 1-11). Exhumation of basement is recorded by sub-Triassic, – Jurassic and – Cretaceous clay-rich, kaolinitic weathering profiles (Lidmar-Bergström 1993, Ahlberg et al. 2003, Fredin et al. 2017). Volcanic necks of Early Jurassic to Early Cretaceous age in Skåne (Bergelin 2009) were emplaced beneath thin Mesozoic cover. Weathering and erosion led to destruction of the exhumed sub-Cambrian planar basement unconformity. New basement planation surfaces formed and were buried by sediment to form the sub-Triassic unconformity (U3a) and the sub-Late Cretaceous unconformity (U3b). U3a and U3b show a distinctive undulating, hilly relief developed as deep weathering exploited fracture zones during etching (Lidmar-Bergström et al. 2012). Hilly relief was later buried below Late Cretaceous and younger sediments. Early Miocene uplift, block faulting and consequent erosion (Japsen et al. 2016) led to development or reactivation of the South Swedish Dome. The dome crest was stripped of remaining sedimentary cover and eroded to form the South Småland Peneplain (SSP) (Lidmar-Bergström 1988, Lidmar-Bergström et al. 2017). This *epigene* planation surface has been exposed since formation and never buried (Twidale 2009). The SSP carries immature, grus-type weathering remnants (Lidmar-Bergström et al. 1997, Olvmo et al. 2005). Early Pliocene uplift raised the South Småland Peneplain to its present elevation of 100–150 m in southernmost Sweden, and subsequent erosion, including Pleistocene glacial erosion, led to re-exposure of sub-Cretaceous hilly relief near the present coastline (Japsen et al. 2016).

Significant differences exist between the erosion and burial histories of south-west and southernmost Sweden. AFTA data indicate that palaeo-temperatures in Västergötland remained at ~60 °C in the Early Miocene (23–15 Ma). As numerous Early Palaeozoic outliers still exist at present, these palaeo-temperatures require widespread persistence of these cover rocks in the Neogene (Japsen et al. 2016). Also, whereas weathering residues of Mesozoic and Cenozoic age are widespread in southernmost Sweden (Lidmar-Bergström 1995, Lidmar-Bergström et al. 1997), neither kaolinitic nor grus-type weathering residues have been reported from the Trollhättan area of Västergötland. Hence evidence is lacking that the basement in the Trollhättan area was exposed to weathering through the Mesozoic and into the Cenozoic. The implication is that the basement remained buried beneath Early Palaeozoic sedimentary cover throughout this period.

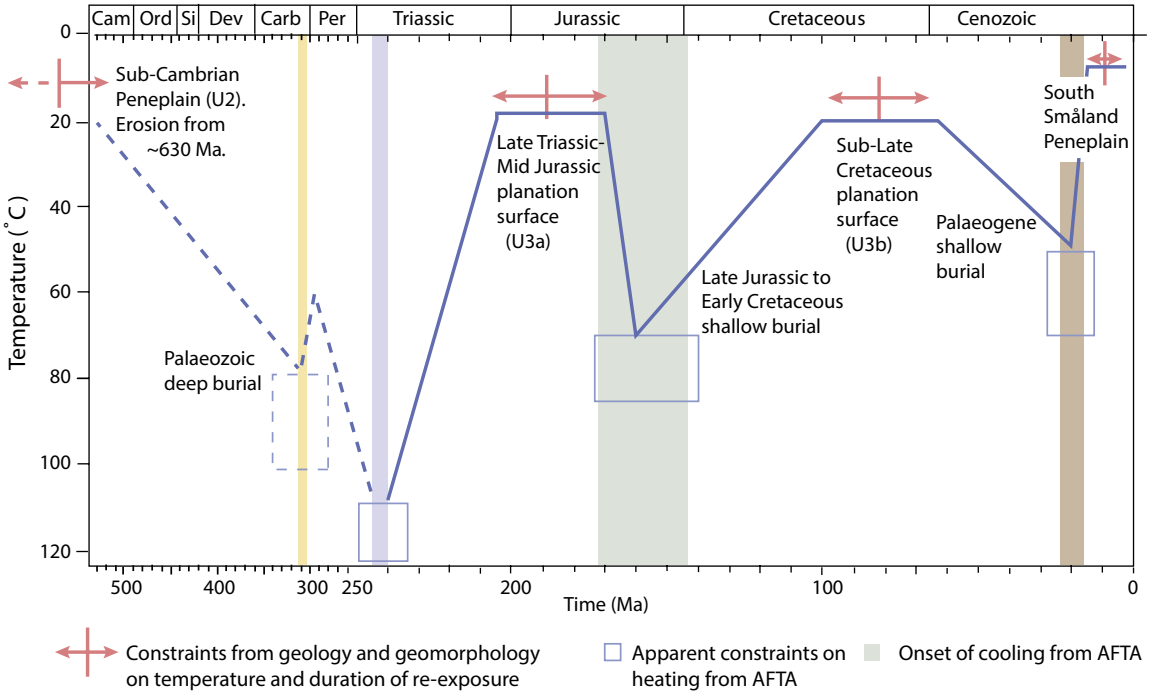

Figure 1-11. *Phanerozoic burial and temperature history in relation to the basement unconformities of southernmost Sweden. AFTA data provides estimates of initial rock temperatures prior to cooling in response to regional exhumation. The width of the vertical bars indicates the uncertainty of the onset of timing of the individual cooling episodes. Modified from Japsen et al. (2016). Unconformities after Lidmar-Bergström (1988).*

Whilst minor uplift in southern Norway has been identified in the offshore sedimentary record (Sømme et al. 2019), across much of southern Scandinavia, relief remained low through the Palaeogene, with extensive and deep weathering (Rasmussen 2018). Major uplift of the Norwegian passive margin occurred from the Oligocene to the mid Miocene, with eastward tilting of the shield (Lidmar-Bergström et al. 2007, Ebert et al. 2011). Uplift in SW Norway triggered widespread and deep erosion, represented by the substantial volumes of sediment that were deposited to the S and SW (Bijlsma 1981).From the early Miocene, large deltas prograded into the eastern part of the North Sea Basin (Kuhlmann et al. 2004, Rasmussen 2018). Miocene sands in Denmark have yielded heavy mineral and zircon ages which indicate that these sediment wedges were sourced in part from Västergötland (Olivarius et al. 2014). The heavy minerals may have been derived directly from erosion of basement or recycled from overlying sandstones. The Miocene sands represent a major phase of uplift and erosion in SW Sweden (Rasmussen 2018) and mark a major phase of thinning and partial removal of the remaining sedimentary cover. The presence of Cambrian quartzite pebbles in the sands (Rasmussen et al. 2010), however, indicates the persistence of Early Palaeozoic cover rocks in Västergötland into the Neogene. To the NW of the South Swedish Dome, late Neogene drainage was via the Vänern basin (Olivarius et al. 2014, Lidmar-Bergström et al. 2017). This drainage and the wider Baltic River system (Bijlsma 1981) ceased to function after ~1.1 Ma following erosion by the Menapian ice sheet (Overeem et al. 2001). The large numbers of Cambrian and Ordovician sedimentary and Permian dolerite erratics in Middle and Late Pleistocene tills in Jutland (Weidner et al. 2015) and northern Germany (Geyer et al. 2004), sourced from Västergötland, indicate that Early Palaeozoic cover rocks and dolerite cap rocks remained extensive in Västergötland into the Pleistocene.

1.3 Quaternary glaciation

The mountains of western Norway and Sweden provided one of the principal ice accumulation centres in Eurasia during the Pleistocene. The Fennoscandian Ice Sheet (FIS) may have expanded onto the shield lowlands of Sweden and Finland on several occasions since 2.75 Ma (Flesche Kleiven et al. 2002) but the number and total duration of glacial phases to which the basement surface has been exposed in the Trollhättan area is largely unknown due to uncertainty over the extent of Early to Middle Pleistocene glaciations in southern Scandinavia (Sejrup et al. 2000). Intensification of glacial erosion is likely during and after the Middle Pleistocene Transition (1.2–0.7 Ma) to 100 ka glacial cycles and the switch to thicker and more extensive ice sheets (Clark et al. 2006, Willeit and Ganopolski 2019). The FIS extended onto the shelf off SW Norway and excavated or deepened the Norwegian Trench during the Menapian Stage (Marine Isotope Stage (MIS) 36 or 34) at ~−1.2–1.1 Ma (Sejrup et al. 2005, Reinardy et al. 2017, Ehlers et al. 2018). After this phase, the distinctive Baltic Gravel Assemblage, which largely consists of clasts derived from the Lower Palaeozoic rocks of southern Scandinavia (Gibbard and Lewin 2016), disappears from the Pleistocene sequences in Denmark and northern Germany (Bijlsma 1981). The change indicates final disruption of the northern part of the Neogene drainage, including the Bothnian river system. The onset of excavation of the overdeepened basins of the Skagerrak (Houmark-Nielsen 2004) and Bothnian and Baltic Seas (Hall et al. 2019) probably also dates from this time.

The maximum extent of the FIS in Denmark, Germany and Poland was in MIS 12 (Elsterian) (Mangerud et al. 1996), with similar thickness and extent reached in MIS 6 (Saalian) (Lambeck et al. 2006, Batchelor et al. 2019). The Elsterian glaciation represents a major phase of glacial erosion, with removal of almost all earlier sediment from around the present Bothnian and Baltic Seas (Šliaupa and Hoth 2011), erosion of the Åland rapakivi granites, as shown by large numbers of these clasts in tills in Poland (Czubla et al. 2017), cutting of tunnel valley networks in the southern Baltic (Flodén et al. 1997) and remodelling of the drainage systems of northern Germany (Ehlers et al. 2011).

The Trollhättan region was situated at or beyond the limits of mountain ice sheets but within the outer, wet-based, erosive zone of the FIS at its maximum extent (Kleman et al. 1997) (Figure 1-12). Trollhättan stands at a similar distance from main ice centres as Forsmark (Kleman et al. 2008) but the magnitude of post-glacial isostatic rebound was lower at Trollhättan (~200 m) than Forsmark (~500 m) (Fredén 1994), indicating that ice thicknesses were lower. Modelled ice thicknesses at the Last Glacial Maximum were ~2 km at Trollhättan, compared to ~3 km at Forsmark (Forsstrom et al. 2003). Modelled glacial sliding distances are high for the last FIS in SW Sweden, implying high glacial abrasion rates (Näslund et al. 2003).

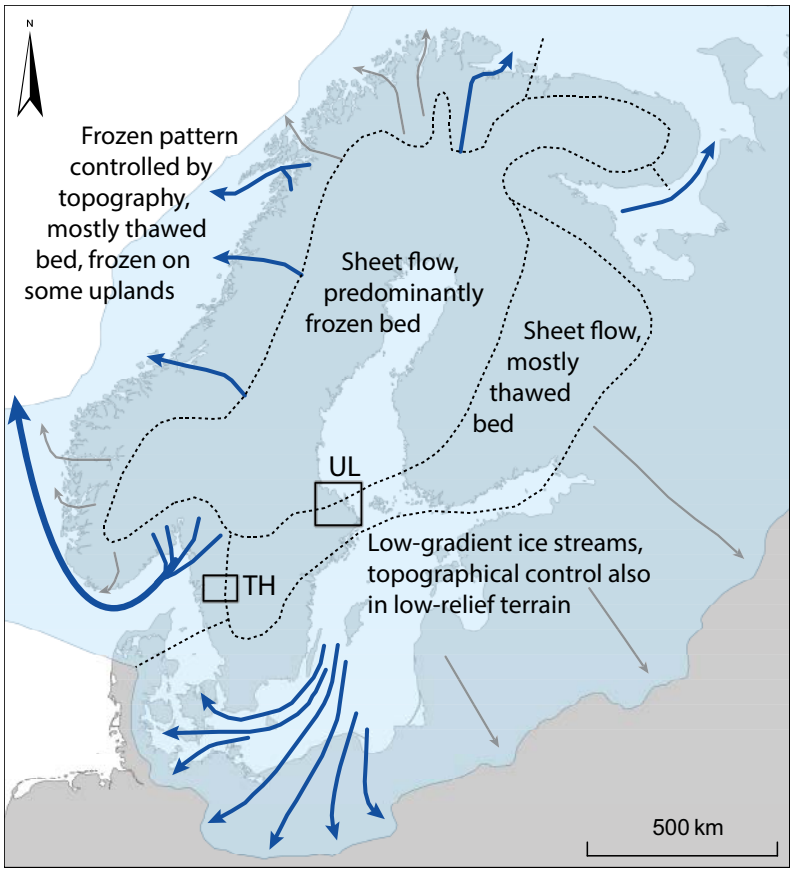

Figure 1-12. *Basal thermal regime of the Fennoscandian Ice Sheet, modified from Kleman and Glasser (2007). Trollhättan lies in the zone of low-gradient ice streams. TH Trollhättan. UL Uppland.*

Ice flow was from NE or NNE during the last deglaciation (Hillefors 1979) and Last Glacial Maximum (Houmark-Nielsen and Kjær 2003). The Trollhättan area became ice-free at ~13.6 ka (Stroeven et al. 2016). The highest postglacial marine shoreline on Hunneberg has an elevation of 133 m a.s.l. (Digerfeldt 1979). Final emergence of lower ground around the southern shore of Lake Vanern at ~45 m a.s.l took place around 9.5 ka (Björck and Digerfeldt 1991).

1.4 Terminology relating to the sub-Cambrian unconformity

The term *sub-Cambrian peneplain* has been used widely to identify the low relief basement surface that emerges from beneath Cambrian strata in Sweden and Norway (Högbom 1910, Lidmar-Bergström 1999, Gabrielsen et al. 2015). The term, however, usually refers to the basement *unconformity* and to its age, form and origin, elements that are known to differ across Fennoscandia. It is important to identify these differences in order to use consistent terminology, to understand the origins of the basement surface and to identify the relationships between the unconformity surface and the present basement surface.

1.4.1 Age

The regional basement unconformity developed on the Fennoscandian shield through the Late Neoproterozoic and into the Early Palaeozoic and so it is a *diachronous* denudation surface. Marine transgression extended across Baltica from the south-east, beginning in the Late Ediacaran in Poland (>551 ± 4 Ma) (Moczydłowska 2008) and continuing into the Early Cambrian in Sweden (Nielsen and Schovsbo 2011), a period of >11 Ma. On the sea bed near Forsmark (Söderberg and Hagenfeldt 1995) and in the impact structure at Siljan (Lehnert et al. 2013), basement is overlain by Late Cambrian

Alum Shales and by Early Ordovician limestones. Here the sub-Cambrian unconformity was likely stripped of unconsolidated sands during the Hawke Bay Event (Nielsen and Schovsbo 2015). Across Baltica, final burial of the basement spans a period of at least 50 Myr. Hence "sub-Cambrian" is an age descriptor for the unconformity that is strictly applicable only to parts of Sweden and Norway and which refers only to part of a longer period of erosion.

1.4.2 Morphology

The geomorphological term *peneplain* currently lacks a closely defined morphometry (Ebert 2009). A basement planation surface can be described as a peneplain where it is "almost a plain" (Fairbridge and Finkl 1980) or where a low relief surface is gently rolling or undulating and of regional extent (Twidale 1982). Recently, however, the use of the term has been extended in Fennoscandia to include sub-Mesozoic and epigene Cenozoic planation surfaces with a relative relief of > 100 m (Green et al. 2013).

An emphasis has been placed on the flatness of the sub-Cambrian unconformity in Västergötland since its first descriptions:

'The line of contact between the granite and the shale is striking, as it is practically horizontal. It is hard to understand how the Precambrian basement can have obtained such a horizontal surface along such a long distance' (translation from original in German). Keilhau (1838, p 418).

The unconformity also has been regarded as so flat in the Trollhättan region as to be effectively planar (Rudberg 1970). As such, the unconformity can be classified as an *ultiplain,* a flat, extensive and featureless plain (Twidale 1983). The recognition of this flatness is important for distinctions between the Early Cambrian basement unconformity in Västergötland found adjacent to Early Palaeozoic outliers and the greater relief typical of younger, cross-cutting exhumed and epigene planation surfaces found in southern Sweden (Lidmar-Bergström 1993) and on present basement surfaces distant from Early Palaeozoic outliers (Figure 1-13).

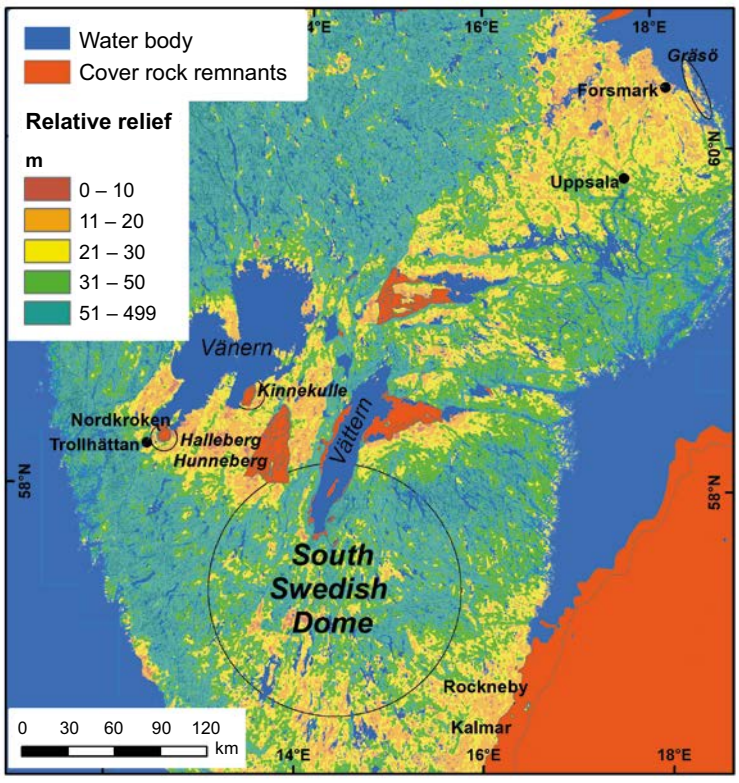

Figure 1-13. *Relative relief in southern and east-central Sweden based on Lantmäteriet elevation data. Relative relief is < 20 m per km in the areas around Trollhättan, Kalmar and N of Uppsala that have been interpreted as little-modified fragments of the sub-Cambrian peneplain. Main Early Palaeozoic outliers shown as cover rocks.*

1.4.3 Origin

A further difficulty with the term *peneplain* is that it can refer to both the landform and to its origins (Ebert 2009). Where a genetic definition is used, following Davis (1902), then the sub-Cambrian peneplain must be a surface of low relief that formed by prolonged subaerial denudation operating close to base level (Ebert 2009). Evidence of a subaerial evolution of the sub-Cambrian unconformity surface on Baltica is provided by the presence locally of palaeosols and saprolites on the buried basement surface (Elvhage and Lidmar-Bergström 1987, Liivamägi et al. 2015). Yet large areas of the unconformity lack records of weathering covers (Gabrielsen et al. 2015), suggesting that either Neoproterozoic regolith did not form in these areas or that any regolith was removed prior to or during Ediacaran to Early Ordovician marine transgression. Moreover, the Early Cambrian sediments that rest directly on the sub-Cambrian unconformity in Sweden are of marine, rather than terrestrial origin (Nielsen and Schovsbo 2011). Hence the final development of the unconformity was as a marine rock shelf, albeit one that developed from grading of a pre-existing subaerial planation surface. The unconformity is thus a re-exposed, *polygenetic* planation surface. The erosional level of the unconformity is the end-product of deep erosion through the Neoproterozoic under fluvial, marine and, in western and northern Norway, Cryogenian glacial environments (Martinsson 1974). The present erosional level of basement around the Bothnian Sea (Flodén 1977, Hall et al. 2019) and in southern Norway (Gabrielsen et al. 2015) remains close to Mesoproterozoic unconformities, where low and hilly basement relief emerges from below Mesoproterozoic sandstones (Högbom 1910). Persistence of low basement relief on large parts of the craton is indicated (Brunsden 1993), a response to prolonged burial, limited uplift and slow denudation of the craton surface (Hall et al. 2019).

1.4.4 Terminology used in this study

In Uppland and around the Bothnian basin, the basement became stable and was reduced close to its present erosion level earlier than in Västergötland. In these locations, a widespread basement unconformity emerges from beneath Mesoproterozoic sandstones. This *sub-Jotnian unconformity* is the oldest preserved unconformity of regional extent found on the Fennoscandian shield and it is referred to in short form as U1 (Hall et al. 2019). In this study of Västergötland, and also in Uppland, the basement surface beneath Early Cambrian sandstone is referred to as the *sub-Cambrian unconformity.* Its components are referred to as U2. U2 forms part of the wider *Late Neoproterozoic-Early Palaeozoic unconformity* in Fennoscandia and on the East European Platform. The weathered unconformities before Late Triassic to Early Jurassic (U3a) and Late Cretaceous (U3b) sedimentary covers in southernmost Sweden (Ahlberg et al. 2003) may be grouped as diachronous parts of the *sub-Mesozoic unconformity* (U3). The *present basement surface* carries the imprint of Quaternary glacial erosion and locally buried by Late Pleistocene sediment and is referred to as UQ.

An unconformity may remain *buried* where it is preserved beneath cover rocks or may be *exposed* where cover rocks have been removed but subsequent erosion has been slight. The *present basement surface* in proximity to sedimentary outliers developed after exhumation from cover rocks and, as it has been eroded, stands below the original unconformity. Where elevation differences between high points on the buried unconformity and on the exposed basement in its vicinity are low then the form of the unconformity is *inherited* by the present basement surface. Under these circumstances, bedrock highs provide pinning points for *summit envelope surfaces* that can be used to model the form of an unconformity and its tilting and dislocation by Phanerozoic faulting (Lidmar-Bergström 1988, Jarsve et al. 2014). Phanerozoic *fault blocks* and *fault scarps* have been re-exposed after removal of Early Palaeozoic and younger cover (Ahlin 1987). In parts of Fennoscandia, the *Late Neoproterozoic-Early Palaeozoic unconformity* was exposed to weathering and erosion during the Mesozoic, Palaeogene and Neogene, leading to its modification and destruction (Lidmar-Bergström et al. 2012). In parts of Uppland and Västergötland, re-exposure of U2 was likely a result of erosion by the FIS (Section 4.7.1). In these areas, modification of U2 has been mainly due to processes of glacial erosion.

Features associated with the sub-*Cambrian unconformity* in Västergötland include *sandstone dykes*, where vertical fractures in the gneiss have fills of quartz sandstone. The sandstone dykes provide evidence of formerly more extensive Early Cambrian sandstone cover and its proximity to the present basement surface (Mattsson 1959). Around Trollhättan, a striking component of the basement surface is the presence of *planar flats*. In Swedish, these are referred to as *slättbergen.* Planar flats are low,

tabular hills or rock flats up to 0.9 km long developed in granite gneiss. The planar flats have been regarded as inherited with little or no subsequent modification from the sub-Cambrian unconformity (Rudberg 1970, Johansson et al. 2001b). At Kinnekulle, the unconformity surface is exposed locally with patches of basal marine conglomerate and sandstone (Högbom and Ahlström 1924) and shows features typical of a *shore platform*.

Where relief is < 10 m in 1 km long sections on the buried U2, the unconformity surface is described in this study as an *ultiplain* (Twidale 1983). The same term is used for summit envelope surfaces on the exposed basement where summits remain accordant within an elevation range of < 10 m in 1 km^2 windows. Where relief is > 10 m in the same windows, the term *peneplain* is used here to describe the surface morphology. Phanerozoic tilting of U2 requires corrections for down-dip elevations to allow for gradients of 2–4 m/km. Ultiplains and peneplains may include isolated hills or clusters of hills (Ebert 2009).

1.4.5 Key questions for investigation

Key terminology and questions for investigation are illustrated in a schematic section for the Trollhättan area (Figure 1-14).

- What is the form and inclination of the buried sub-Cambrian unconformity at different scales?
- How deeply weathered, if at all, was this gneiss surface prior to burial and its re-exposure?
- To what extent does the form and elevation of the presently exposed basement surface (UQ) conform to that of the buried unconformity (U2)?
- What is the pattern of Phanerozoic block faulting in the basement across U2? What are the vertical throws across individual faults?
- What were the patterns and rates of scarp retreat around the mesas of Halleberg and Hunneberg?
- What are the depths of glacial erosion of basement below the former unconformity since re-exposure?
- What were the depths and rates of glacial erosion on basement highs during the last glaciation?

In examining these questions, we test the hypotheses that

- parts of UQ remain at similar elevations to and so are largely inherited from U2,
- U2 was displaced by post-Ordovician faulting, and that these fault scarps and blocks are present in the landscape today, and
- the dislocated sub-Cambrian unconformity can be used as a reference surface for estimating Pleistocene glacial erosion of the basement.

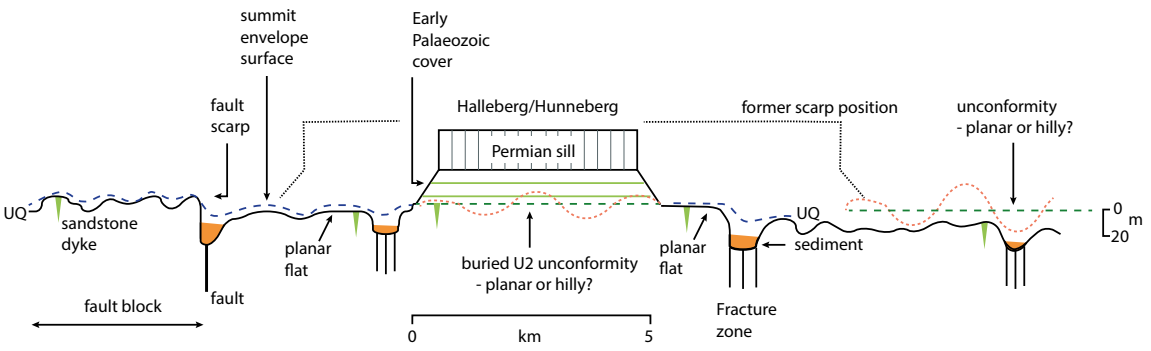

Figure 1-14. *Terminology used to describe key elements of the sub-Cambrian unconformity around Trollhättan.*

2 Methods

Previous work has indicated that the relief on the sub-Cambrian unconformity is low, and that a nearly planar surface is found exposed locally (Johansson 1999, Johansson et al. 1999, 2001b). The comparison of U2 and UQ is important because where U2 and UQ are closely-spaced in elevation, the present basement surface must be largely inherited from the sub-Cambrian unconformity. Moreover, if the buried unconformity is planar and its inclination is known then it can be projected across basement in areas close to Early Palaeozoic outliers. Where basement summits at distances of several kilometres from outliers remain accordant in elevation and pin summit envelope surfaces and topographic profiles that conform to the buried unconformity, summit lowering by erosion since re-exposure likely also has been limited. Alternatively, a hilly buried unconformity would be evident on exposed basement surrounding sedimentary outliers as a hilly surface, with summits at different heights,

In this study, the elevation and form of the buried sub-Cambrian unconformity and of the present basement surface are reconstructed. Following earlier work (Johansson 1999, Johansson et al. 1999, Johansson et al. 2001b) but now using high resolution LiDAR data, the form of the sub-Cambrian unconformity is modelled in summit envelope surfaces and topographic profiles. The modelled unconformity is then used as a reference surface for identifying (i) Phanerozoic dislocation by faulting and (ii) the pattern of erosion since the exhumation of the unconformity. Where re-exposure was completed in the Pleistocene, glacial erosion of basement is represented by the sum of the rock depth lost from summits and the elevation difference between the summit envelope surface and the present rock surface.

2.1 Digital data attribution and processing

Extensive use is made throughout this study of digital geological data provided by the Swedish Geological Survey (SGU) and of digital elevation data from Lantmäteriet (The National Swedish Land Survey). Data sets include the elevation and position of bedrock highs and depths of Quaternary sediment. Landforms have been superimposed in ArcGIS on SGU datasets for rock type, fractures, Quaternary geology and depth to bedrock. Soil depth data, representing the total depth of Quaternary deposits above bedrock, is modelled by SGU from borehole, well and outcrop data and its accuracy varies according to point data coverage (Dahlke et al. 2009). Where necessary, the DEM's (2 m and 50 m) were resampled to a 10 m resolution, using ArcMap 10.6 to improve visual interpretation. Maps and diagrams from previous studies were first georectified using the overview map provided by SGU as a base map. Features such as faults and lithologies were then superimposed as a separate layer and modified in ArcMap 10.6 and Adobe Illustrator CS 6.

2.2 Regional bedrock relief of Västergötland

Regional maps were generated to show surface relief, bedrock relief and major fractures and compared to maps of geology and structure. The elevations of the buried unconformity and the exposed basement in its immediate vicinity are plotted where both elevations are known around Early Palaeozoic outliers.

2.3 Relief on the buried unconformity

2.3.1 Evidence from geological mapping

The sub-Cambrian unconformity is largely concealed today by talus around the flanks of Halleberg and Hunneberg. Only small, widely-spaced exposures of U2, retaining patches of basal conglomerate, occur today on the shore of Lake Vänern at Kinnekulle (Calner et al. 2013). However, the overlying Early Cambrian sandstone, the early Middle to Late Cambrian Alum Shale and the Early Ordovician limestone were formerly quarried at many locations around these hills (Maletz et al. 1996), providing exposures that were described in 19th and 20th century reports (Högbom and Ahlström 1924, Mattsson 1962, Rudberg 1970). The basement-cover contact, based in part on these records, is shown on SGU maps and constrains the relief on the buried unconformity.

The elevation of the edge of the buried unconformity can be estimated where it is concealed beneath talus and Quaternary sediments. The Early Palaeozoic sedimentary cover is horizontally bedded and the main units, the Early Cambrian sandstone, the early Middle Cambrian Alum Shale and mainly Early Ordovician limestone beds, together with constituent sub-units, maintain thicknesses over several kilometres (Sidenbladh 1870). This layer-cake stratigraphy allows the elevation of the unconformity to be estimated from geological maps and from contacts between overlying sedimentary units of known thickness. The elevation of the unconformity is constrained to within a few metres of elevation where the upper surface of the basal Early Cambrian Mickwitzia Sandstone is exposed. Locations where the full Early Palaeozoic sequence, 60–62 m thick (Maletz et al. 1996), is present retain early Middle Cambrian Alum Shale and Early Ordovician limestone beds, exposed locally in numerous abandoned mines on the hill flanks (Figure 2-1). The elevation of the basement unconformity can be estimated by subtracting thicknesses of the early Palaeozoic sedimentary cover rocks from the elevations of contacts between the sandstone, shale and limestone and of the base of the sill.

On Halleberg, the base of the sill is in contact with Cambrian rocks, whereas on Hunneberg the contact is with Early Ordovician limestones (Martinsson 1974). For example, the thickness of sedimentary rocks between the base of the dolerite cliff named Skäktefallet and the basement near Nordkroken is only 21–26 m. Both Alum Shale and limestone are missing (Sidenbladh 1870) and hence no old mine workings occur on this segment of the hill flank. The upper units were displaced vertically during intrusion of the Early Permian dolerite sill which thickens here (Sidenbladh 1870). The elevations of the base of the dolerite sill at either end of the Lilleskog valley also show a height difference of ~30 m whereas the elevation of the unconformity along strike remains at 53–59 m a.s.l. At these locations, the elevation of the buried unconformity can only be estimated where the elevation of the top of the Mickwitzia Sandstone is known.

Older literature indicates that sandstone dykes occur extensively in vertical fractures, often associated with planar flats (Mattsson 1962, Martinsson 1974). We add new sites discovered during field survey.

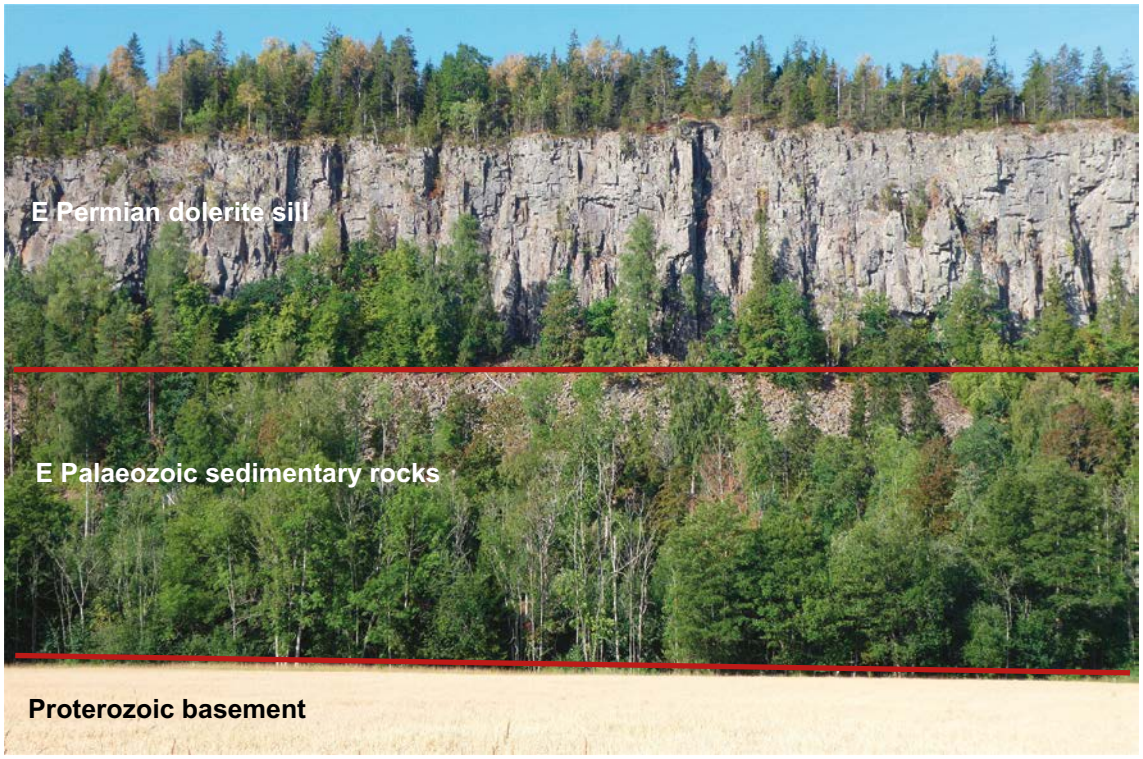

Figure 2-1. *View W from Hulan, Gaddesanna. The elevation of the sub-Cambrian basement unconformity can be estimated here using the elevation of the base of the sill in old Alum Shale mines and the thickness of Early Palaeozoic sedimentary sequence.*

2.3.2 Comparison of elevations on the buried unconformity with adjacent exposed basement

A straightforward approach towards estimation of the elevation and maximum relief of the unconformity around Halleberg and Hunneberg is to compare the elevations along the edge of the Cambrian cover as shown on SGU solid geology maps and visible in DEMs with those of the gneiss bedrock in its vicinity. In this study, the relief on the buried unconformity is examined in detail in four locations around Halleberg and Hunneberg (Figure 2-2) and along the lake shore at Kinnekulle.

2.3.3 Relief on the unconformity

The relief of the sub-Cambrian unconformity in Västergötland has been regarded previously as very low (Rudberg 1970, Johansson et al. 2001b). The maximum height of hills and depth of valleys on the buried unconformity is constrained by the sinuosity and elevation of the mapped edge of the Early Cambrian sandstone. A linear contact indicates low relief whereas a sinusoidal contact indicates the presence of hills and valleys. Further constraints on relief on an unconformity may be provided by sediment fills in basins, valleys and clefts that were cut into basement surfaces prior to burial, as on the sub-Torridonian unconformity in NW Scotland (Williams 1969). Constant or slowly increasing or decreasing elevations provide further evidence of a horizontal or inclined, near planar unconformity.

The edge of the unconformity is apparent in DEMs locally around Hunneberg. Where summit elevations on the adjacent basement remain within a few metres of the elevation of the edge of the buried unconformity and show similar increases or decreases in elevation then the summits represent the lowered surface of the unconformity. The location, form and height of former hills on the unconformity is indicated by the elevations of the highest points across the exposed basement relative to the projected unconformity. Similarly, if broad valleys existed on the buried unconformity then such exhumed valleys should form low elevation corridors on the exposed basement surface below the elevation of the projected preserved unconformity. Such corridors should provide protection from erosion and so may be expected to retain patches of Cambrian sediment.

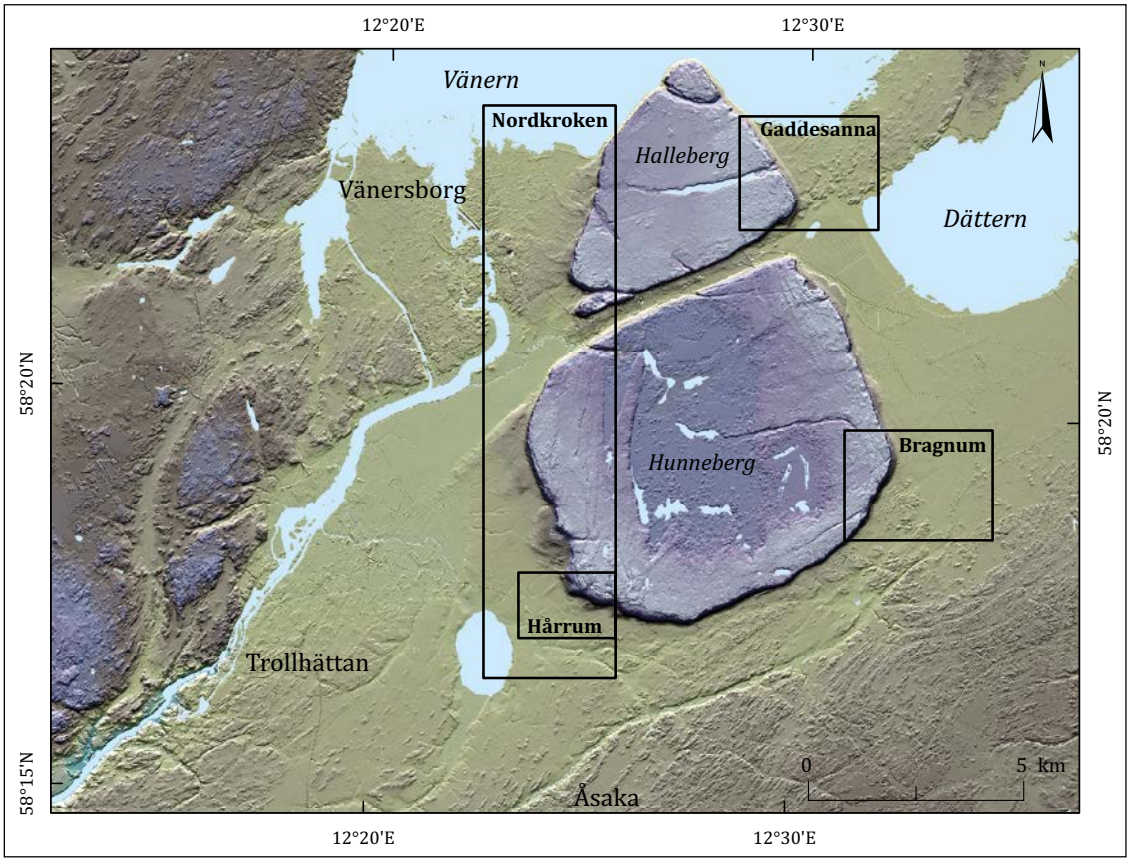

Figure 2-2. *Detailed study areas along the edge of the buried unconformity around Halleberg and Hunneberg. A. Western flank. B. Gaddesanna C. Bragnum. D. Hårrum. DEM based on Lantmäteriet data.*

The most direct and striking evidence for the form of the sub-Cambrian unconformity comes from exposures of basement and overlying Early Cambrian sandstone along the lake shoreline at Kinnekulle, 75 km NE of Trollhättan. Current exposures, along with important early observations of the unconformity made during low lake water levels (Högbom and Ahlström 1924), provide information along ~10 km of lake shoreline. The overlying basal sandstones and conglomerates provide important evidence for understanding the processes that operated on the unconformity at the onset of marine transgression in the Early Cambrian.

2.4 Morphology of the exposed basement

Landforms in this report are considered across different scales: *landscape* (10–100 km), *regional* (1–10 km), *local* (0.1–1 km), *macro* (10–100 m), *meso* (1–10 m) and *micro* (< 1 m) scales, as in the companion Forsmark report (Hall et al. 2019).

The basement around Trollhättan forms a large (> 1 000 km^2), contiguous area of low (< 20 m) relative relief (Figure 1-3), incised by the deep valley of the Göta River (Rudberg 1954, Lidmar-Bergström 1988). Existing models of the sub-Cambrian peneplain were based mainly at the landscape scale and were based on contour maps and early digital elevation data (Elvhage and Lidmar-Bergström 1987, Tirén and Beckholmen 1992, Johansson 1999, Johansson et al. 1999). Here we re-examine the morphology of the exposed basement at regional to macro-scales in relation to the sub-Cambrian unconformity using topographic profiles and DEMs based on more detailed LiDAR data at 2 m and 20 m resolution for the Trollhättan region.

We examine the morphology of the basement surface across the Trollhättan region and four local areas where bedrock is widely exposed at increasing distances from the edges of Halleberg and Hunneberg (Figure 2-3). The detailed study areas are:

Area 1. Vargön on the Vänern shore on the western flank of Halleberg.

Area 2. Väne-Åsaka on the southern flank of Hunneberg.

Area 3. Trollhättan.

Area 4. Sjuntorp.

The morphology of the exposed basement is examined below for the four study areas at the regional and local scales. The morphology is reconstructed from summit envelope surfaces and topographic profiles and linked to rock type and fracturing using evidence from available exposures in road sections and quarries. The morphology of the presently-exposed basement surface is compared to the elevation and relief of the buried unconformity at increasing distances from Cambrian outliers.

Planar flats have been interpreted previously as little modified erosional forms inherited from the unconformity (Johansson et al. 2001b). Here we map planar flats, recognising well-preserved, fragmented and degraded forms based on field evidence and recognition in DEMs. Planar flats are most common in Areas 1 and 3. We use 2 m resolution LiDAR data to examine the tilt of planar flats in profiles. Flat rock surfaces include structural landforms where horizontal structures, including bedding planes and lava flows, control surface slopes. Good examples are provided by raised shore platforms developed on horizontal or gently-inclined lava flow tops in Scotland (Smith et al. 2019). Quarry sections and road cuts show that extensive horizontal fractures (HF) or sub-horizontal fractures (SHF) are not widely developed in the gneiss terrain of Västergötland. However, some granite gneisses, notably at Nordkroken on the southern shore of Lake Vanern, show development of horizontal fractures. In the Trollhättan region, the frequency and distribution of such fractures was checked in large quarries and in man-made exposures. Fracture patterns were also mapped around localities with planar flats. The results are used to test hypotheses that the flatness of the present basement surface at the regional and local scales is structurally determined and that individual planar flats are structural landforms.

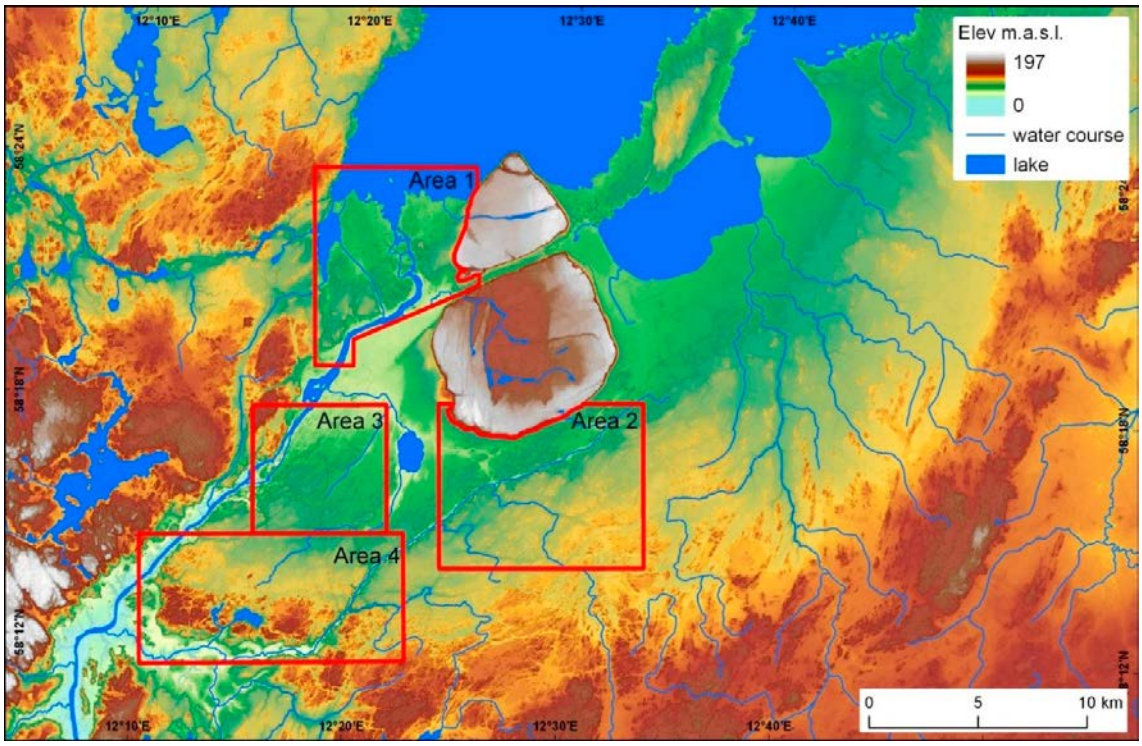

Figure 2-3. *DEM of the Trollhättan area, showing four areas selected for detailed study of the exposed basement surface. Area 1 Vargön. Area 2 Väne-Åsaka. Area 3. Trollhättan. Area 4. Sjuntorp. Elevation data from Lantmäteriet.*

2.4.1 Topographic profiles

Bedrock is exposed widely on high points in the Trollhättan region; hence topographic profiles provide good visualisations of bedrock morphology. We generate topographic profiles across planar flats to identify the inclinations of these bedrock surfaces. We also run profiles joining individual planar flats on both sides of the Lilleskog Fault.

2.4.2 Summit envelope surfaces

We model the form of the unconformity in areas of exposed basement using rock summit elevations to pin summit envelope surfaces (Figure 1-14). The summits of rock risers mainly occur where the spacing of vertical fractures is wide, rendering summits resistant to erosion. The depth of lowering on the unconformity by glacial erosion is expected to be low in comparison to adjacent zones with closely-spaced fractures. As a check on depths of lowering, we compare summit elevations on the buried unconformity, on the exposed basement in proximity to the edge of the buried unconformity and over the wider area of the exposed unconformity.

Summit envelope surfaces were generated on the basis of a modelled DEM of the bedrock surface. The bedrock surface DEM was generated by subtraction of the 2 m resampled 20 m soil depth (source: SGU data) from the 2 m resolution LIDAR elevation model (source: Lantmäteriet data). Summit envelope surfaces were then generated by firstly calculating maximum surfaces of elevation on search windows of different radii, and secondly calculating a mean surface from the maximum surface with the same radius. The resulting maximum-mean surface represents a summit envelope surface. All calculations were conducted in the GIS-software ArcGIS Pro. The effect of the summit envelope surface (the maximum-mean surface) is to fill in low points in the terrain (rock trenches and basins). The procedure gives DEMs showing smoothed surfaces at different scales that represent models of the former unconformity (the former bedrock surface). (See Table 2-1 for a step-by-step description). Confidence in the models is highest where the elevation of the buried unconformity is closest to the elevation of bedrock highs in surrounding exposed basement.

Table 2-1. Steps for estimation of glacial erosion depths in GIS in the Trollhättan region.

Input Data (source)	Calculation(s)	Result
2 m LIDAR DEM (Swedish National Land Survey). 20 m soil depth (Swedish Geological Survey).	Resampling of the 20 m soil depth to 2 m. Subtraction of the soil depth from the 2 m LIDAR DEM.	2 m DEM of the present bedrock surface.
2 m DEM of the present bedrock surface.	Focal statistics: Generating a maximum surface using circular search windows of different radii. The GIS picks the highest pixel value within the circle of the given radius.	A 2 m maximum surface with circles and steps between these well visible.
2 m maximum surface.	Focal statistics: Generating a mean surface using a circular search window with the identical radius that the input maximum surface was based on.	A 2 m maximum-mean (smoothed) surface (a **summit envelope surface**).
2 m summit envelope surface. 2 m DEM of the present bedrock surface.	Subtraction of the bedrock surface from the summit envelope surface.	A 2 m raster showing the elevation differences between the summit envelope surface and the bedrock surface for every pixel in the raster – the **modelled erosion depth**.

The procedure was conducted in different geographical areas of different scales, with different radii for generating the maximum-mean surface. The term **focal statistic** is used in Arc-GIS to refer to the calculation for each input cell location of a statistic of the values within a specified surrounding neighbourhood.

2.5 Faulting and fracturing

Large, post-Ordovician fault blocks have been identified previously in the Trollhättan area from analysis of contour maps, trend surfaces and topographic profiles (Figure 2-4). Differential block movement (throw) across faults has been identified previously from differences in the elevation of the unconformity on rock blocks on either side of a fault (Ahlin 1987, Jarsve et al. 2014). Tilting of a rock block is evident from the inclination of the originally near-horizontal unconformity and from the presence of a bounding fault scarp (Johansson et al. 1999). Previously, the low resolution of elevation data allowed only the identification of rock blocks across faults with >25 m of displacement (Ahlin 1987, Johansson 1999). The availability of high resolution LiDAR data offers the possibility of identifying faults with smaller (5–20 m) vertical throws (Jarsve et al. 2014). A limit on the identification of small displacements across faults is provided, however, by uncertainties for the elevation and form of the unconformity prior to glacial erosion (Ahlin 1987). Comparisons are made with the block-faulted sub-Cambrian unconformity surface at Närke (Hall et al. 2019) and Motala where spatial patterns of glacial modification of fault scarps and block tops can be linked to changes though time via the progressive exhumation of fault blocks from cover rocks by glacial erosion during the Pleistocene.

We reassess the importance of structure in controlling the detailed form of the sub-Cambrian unconformity across scales in the Trollhättan area. At the regional and local scales, lineaments interpreted as fractures were mapped from LiDAR data. At the local scale, due to the low relief of the study area, rock fracture patterns were observed mainly in large quarries and in other man-made sections. Lineament orientations and length were mapped from DEMs and were used to produce weighted mean rose diagrams of fracture orientations. Sub-horizontal and inclined fractures were mapped around planar flats in the field around Trollhättan.

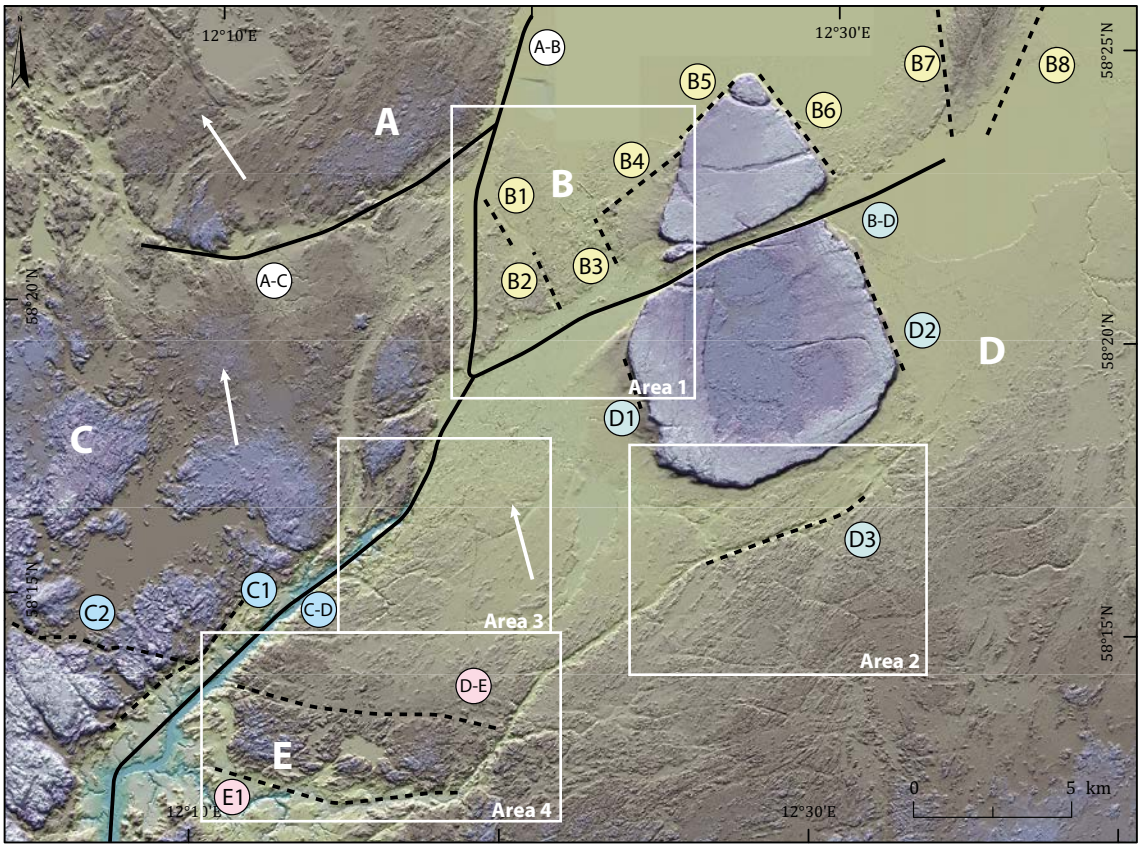

Figure 2-4. *Potential Phanerozoic faulting in the Trollhättan area. Letters A–D refer to fault blocks recognised previously by Johansson et al. (1999). Solid lines: inter-block faults identified in previous studies (Ahlin 1987, Johansson et al. 1999). Dashed lines: intra-block, fracture-guided lineaments that may include faults active in the Phanerozoic. Each lineament is given a block code letter and number. White arrows indicate the dip of fault block tops. DEM based on Lantmäteriet data.*

2.6 Glacial modification of the exhumed unconformity

2.6.1 Glacial landforms

Glacial landforms developed by erosion of bedrock are evident at different scales in the study area (Table 2-2). Micro-scale (< 1 m), meso-scale (1–10 m) and macro-scale (10–100 m) forms of glacial erosion are widely distributed but are considered below only in relation to the glacial modification of planar flats. The distribution, frequency and dimensions of local (0.1–1 km), regional (1–10 scale) and landscape (> 10 km) features provide information on the progressive modification of the unconformity surface. Fracturing is a major control on glacial landforms (Krabbendam and Bradwell 2013) and its role is considered here through examination of lineament patterns in DEMs and through inspection of sections in working quarries and road cuts. As distance increases from the Halleberg and Hunneberg outliers, it is likely that the time since re-exposure of basement has also increased. Hence, comparisons of proximal and distal locations allow space-time substitutions (Thornes and Brunsden 1977, Huang et al. 2019) that allow the identification of the progressive modification of the basement unconformity.

Table 2-2. Inventory of the main landforms of glacial erosion at different scales. Scale boundaries are the same as those used in the Forsmark area (Hall et al. 2019).

Landform Group	Scale	Positive relief	Negative relief
Microforms	< 1 m A-axis length		Polish, striae, grooves, conchoidal fractures, P-forms, lee-side cliff, stoss-side cliff, flank cliff, box socket, prismatic socket.
Mesoforms	1–10 m	Smoothing, stoss edge rounding, flank rounding.	P-form, lee-side cliff, stoss-side cliff, flank cliff, box socket, prismatic socket.
Macroforms	10–100 m	Whaleback, roche moutonnée.	Cleft, lee-side cliff, stoss-side cliff, flank cliff, disrupted bedrock.
Local forms	0.1–1 km	Box hill, roche moutonnée, streamlined hill or ridge.	Lee cliff, fracture valley, box or star basin, disrupted bedrock.
Regional forms	1–10 km	Flyggberg, non-streamlined (box and rectilinear) hills, weakly streamlined to streamlined hill or ridge.	Fracture valley, box or star basin, flank depression, lee depression.

2.6.2 Elongation ratios

Elongation parallel to ice flow is a measure of glacial streamlining (Principato et al. 2016). The elongation ratios of the positive landforms of glacial erosion were derived following the method of van Boeckel (2018). The first step is to use a hill shade and a slope map of the surface elevation DEM created in ArcMap 10.5 to digitize the outlines of the bedrock highs from bounding slopes. The elongation ratios of the mapped landforms were calculated using the minimum bounding geometry tool in ArcMap 10.5. This tool creates a new shape file that is comprised of rectangles that represent the minimum geometry that fits the polygon of the landform. The long axis of the rectangle corresponds to the widest diameter of the polygon. The short axis corresponds to the widest diameter perpendicular to the long axis. The new shape file contained the orientation, the length (long axis) and the width (short axis) of the minimum rectangle that fits the polygon. This information was used to calculate the elongation ratio of the landforms by dividing the length and width of the rectangle relative to paleo-ice flow. Elongation ratios were calculated for four sub-areas in the Sjuntorp detailed study area. The landforms of each sub-area were plotted in frequency diagrams according to their aspect ratio and plotted in rose diagrams according to the orientation of the long axis, relative to the course of the paleo-ice flow, using Stereonet.

2.6.3 Topographic roughness

Glaciated shields are typically characterised by exposed bedrock landscapes of high topographic roughness, with numerous knolls or ridges and a multitude of lake-filled basins, termed *cnoc and lochain topography* (Krabbendam and Bradwell 2013). In this study, we estimate topographic roughness as a measure of the progressive modification by glacial erosion of the initially smooth, near planar U2 surface. To provide a preliminary visualization of basement surface roughness, mean, minimum and maximum elevation surfaces with 10×10 cell search windows were created based on the 2 m LIDAR DEM from the Swedish National Land Survey. The RTP (Relative Topographic Position) was calculated using the raster equation (mean-min)/(max-min) (Table 2-3). To improve the visual output, a mean surface model based on a 50×50 cell search window was generated from the 10×10 cell based RTP map. (See Table 2-3 for more detailed workflow). For comparison, terrain roughness was calculated also by the Standard Deviation (SD) method using a standard deviation of elevation in neighbouring cells within a 100 m radius (Figure 2-5). Terrain roughness is scale dependent (Falcini et al. 2018) and the focus here is on visualizing the roughness of basement terrain at the regional and local scales for the detailed study areas.

Table 2-3. Steps for generating a terrain roughness map using the RTP (Relative topographic position roughness index). Based on Cooley (2013) and Jenness (2004).

Input Data (source)	Calculation(s)	Result
2 m LIDAR DEM (Swedish National Land Survey)	Focal statistics: Generating a mean elevation surface using a 10 × 10 cell search window. The GIS picks the mean pixel value within the search window.	mean DEM (mean)
2 m LIDAR DEM (Swedish National Land Survey)	Focal statistics: Generating a minimum elevation surface using a 10 × 10 cell search window. The GIS picks the minimum pixel value within the search window.	minimum DEM (min)
2 m LIDAR DEM (Swedish National Land Survey)	Focal statistics: Generating a maximum elevation surface using a 10 × 10 cell search window. The GIS picks the maximum pixel value within the search window.	maximum DEM (max)
Mean DEM Min DEM Max DEM	Raster calculator: (mean-min)/(max-min)	RTP map with 2 m resolution based on 10 × 10 cell search window
RTP map based on 10 × 10 cell search window	Focal statistics: Generating a mean surface using 50 × 50 cell (i.e. 100 × 100 m) search windows	RTP map with 2 m resolution based on the 50 × 50 cell mean (improved visual output)

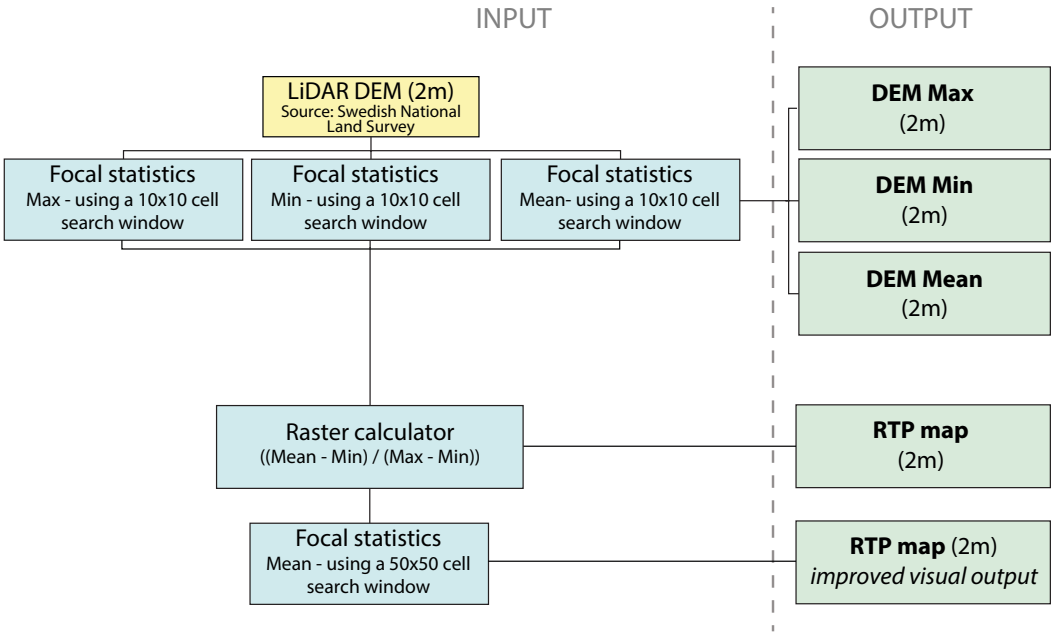

Figure 2-5. *Methods applied for the calculation of surface roughness using the Standard Deviation (SD) method.*

2.6.4 Estimating depths of glacial erosion

Depths of glacial erosion in basement are estimated by subtracting the present bedrock surface from the summit envelope surface (See 2.2.1 and Table 2-1 for a step-by-step description of the generation of the input surfaces). To these values should be added the depth of rock lost from summits. Maximum values for summit erosion are provided around the flanks of Halleberg and Hunneberg by the height differences between the buried unconformity and adjacent exposed basement summits. The main uncertainties in this procedure derive from the elevation and form of the buried unconformity surface and its planar projection from below the flanks of Halleberg and Hunneberg. Depths of erosion in basement do not represent total Pleistocene glacial erosion in the Trollhättan region. The removal of former Phanerozoic sedimentary rocks and Early Permian dolerite from above the sub-Cambrian basement unconformity must also be considered.

Rock trenches and basins represent locations where glacial erosion has been relatively deep compared to summits (Krabbendam and Bradwell 2014). In considering the glacial modification of U2, it is important to quantify the contribution of trench and basin erosion to the total erosion budget. Areas with rock trenches and basins in the study area can be identified by elevations > 5 m or > 10 m below summit envelope surfaces. The percentage of rock loss for each study area is calculated by dividing the number of pixels within a certain erosion depth with the total amount of pixels for each study area. The number of pixels excluded from the total amount of pixels were set to < 5 m and < 10 m. The volume of rock loss is calculated by the sum of the total pixel values within an area where the total erosion depth is higher than a certain value. First, the sum of the pixels with an erosion depth > 5 m was calculated by excluding the pixels with an erosion depth lower than 5 m by using the Classification Statistics in ArcGIS. The sum of the pixels was then multiplied by the cell size for each pixel (2 × 2m) to obtain volume units in m^3 of rock loss for each study area. The same process was done for pixel values with larger than 10 m erosion depths.

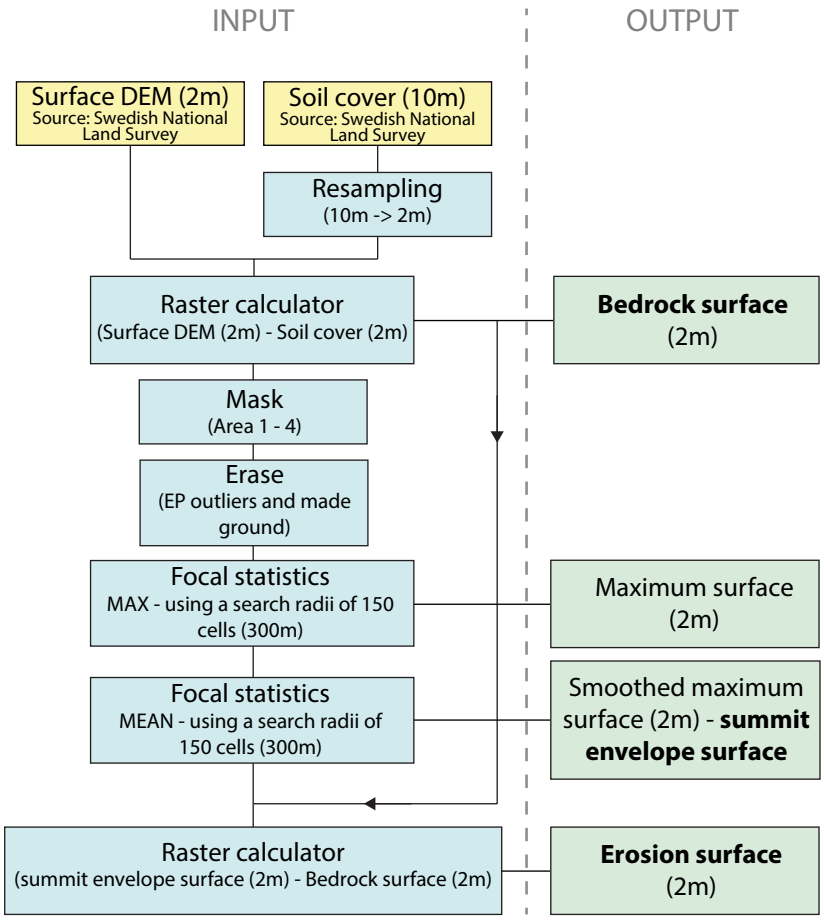

Figure 2-6. *Methods applied for calculation of the erosion depth.*

2.7 Cosmogenic nuclide inventories in bedrock and depths of erosion in the last glaciation

Cosmogenic nuclide analysis has been frequently used to study the timing of glaciations (Balco et al. 2002, Stroeven et al. 2016), duration of burial under ice (Fabel et al. 2002, Stroeven et al. 2002b, Li et al. 2008), and glacial erosion (Stroeven et al. 2002a, Goodfellow et al. 2014, Jansen et al. 2019). Here we use measurement of ^{10}Be (half-life: 1.39 Ma; (Chmeleff et al. 2010, Korschinek et al. 2010)) and ^{26}Al (half-life: 705 ka; (Nishiizumi 2004)) concentrations in bedrock surfaces to determine potential glacial erosion depths in the Trollhättan area, southern Sweden, during the late Quaternary.

The methodology builds on the fact that specific cosmogenic nuclides, such as ^{10}Be and ^{26}Al, are produced in minerals (typically quartz) when exposed to cosmic rays. The production of cosmogenic nuclides in rocks is rapidly attenuated with depth below the surface so that most production occurs in the uppermost decimetres of the rock and the production is close to zero at depths larger than three metres. The rate of cosmogenic nuclide production is known from calibration studies with cosmogenic nuclide measurements of surfaces with a known duration of exposure to cosmic rays (Nishiizumi et al. 1989, Balco et al. 2008, Goehring et al. 2012, Heyman 2014, Stroeven et al. 2015). A measured cosmogenic nuclide concentration can therefore be used to calculate either the duration of exposure to cosmic rays or, if the duration of cosmic ray exposure can be independently determined, the rate (or depth) of erosion.

In formerly glaciated regions where the glacial erosion was deep enough to remove the full inventory of previously produced cosmogenic nuclides, the concentration of cosmogenic nuclides will reflect only the duration of exposure to cosmic rays since the last deglaciation. If, on the other hand, there are cosmogenic nuclides inherited from ice-free periods prior to the last ice cover period, the cosmogenic nuclide inventory may be used to constrain the depth of glacial erosion.

2.7.1 Sampling and sample preparations

Our sampling strategy was designed to test erosion by the Fennoscandian Ice Sheet over the flattest landscape elements in the investigation area, all of which have traditionally been regarded as examples of intact sub-Cambrian Peneplain. In addition, we sampled two convex surfaces at the south-eastern base of Hunneberg at Bragnum, in an area where extensive flat surfaces are non-existent. Given the results of sampling two such flat surfaces in 2000 (Hjortmossen and Sandhem; Stroeven et al. 2016), we expected to measure concentrations higher than those generated by exposure since deglaciation of the FIS, and emergence through water due to isostatic uplift. If so, the presence of inheritance would allow us to calculate depths and rates of glacial erosion over recent glaciations, based on reconstructed durations of ice cover. Were the FIS to have removed rock sufficiently thick to leave a surface with essentially no cosmogenic nuclide inventory, no further insight on glacial erosion rate can be gleaned using this technique.

Thirteen bedrock samples have been measured from four different geographic locations; Nordkroken (n=3) along the southern shore of Vänern, Hjortmossen (n=4) and Sandhem (n=4) in Trollhättan, and Bragnum (n=2) at the south-eastern base of Hunneberg. Two samples at Nordkroken were located on the rock flat on the shore of Lake Vänern and one sample was located south of a string of dunes at the flat that is used as a car park. Two samples from Hjortmossen come from its top surface (sampled in 2000, now below a sports arena) and two from its flank. Three samples from Sandhem were taken from within a fenced-in area used as a waste site and one sample was collected from the adjacent Slättbergen in year 2000. The two samples from Bragnum are on bedrock surfaces that protrude through fine-grained sediments that fill the depression aligning the south-eastern base of Hunneberg.

Samples were collected during the summers of 2000, 2016 and 2017 with a rock saw, hammer, and chisel. We recorded coordinates using handheld GPS and subsequently determined the sample elevation based on a 2 m resolution LiDAR elevation model based on Lantmäteriet data. We measured geometric shielding (Dunne et al. 1999) for some sample locations where the topographic horizon was more than 10° above a horizontal plane. Measurements of topographic shielding are used to correct local nuclide production rates.

To calculate erosion based on inheritance, it is imperative that we know the duration of exposure following deglaciation. The timing of deglaciation is well-constrained through the FIS retreat reconstruction by Stroeven et al. (2016), with the timing of ice retreat from the Trollhättan moraine around 13.6 cal ka BP. We assign individual deglaciation ages for our sample sites based on the Stroeven et al. (2016) reconstruction, yielding ages of 13.45–13.70 ka before sampling. At the time of deglaciation, the Trollhättan region was covered by water and the sea level was then lowered due to glacial isostatic adjustments and rebound. To accurately calculate the production of cosmogenic nuclides, we therefore need to take into account the water depth following the deglaciation and the timing of emergence from the sea. We use a single shoreline displacement curve from Hunneberg for all samples (Påsse and Daniels 2015) and constrained by radiocarbon data (Björck and Digerfeldt 1991).

Sample preparation and measurement of ^{10}Be and ^{26}Al was completed at PRIME Lab, Purdue University, using standard methods (Kohl and Nishiizumi 1992). This includes separation of quartz, addition of ^{9}Be and ^{27}Al carrier, extraction of ^{10}Be and ^{26}Al, and AMS measurements of ^{10}Be/^{9}Be and ^{26}Al/ ^{27}Al ratios. Total Al concentrations were determined by ICP measurements. Isotope measurements were standardized against the 07KNSTD standard for ^{10}Be (Nishiizumi et al. 2007), and the KNSTD standard for ^{26}Al (Nishiizumi 2004).

2.7.2 Exposure age calculations

This section is a modified version of Section 5.2.2 of Hall et al. (2019), describing the exposure age calculation method.

We calculate simple apparent exposure ages from the measured ^{10}Be and ^{26}Al concentrations using the expage calculator (http://expage.github.io/calculator v. 201902, see also additional material in Hall et al. (2019), Appendix 5). This calculator is based on the original CRONUS calculator of Balco et al. (2008) but adopts the nuclide-specific LSD production rate computations (Lifton et al. 2014). Production rate from spallation varies over time and is calibrated against a global set of ^{10}Be and ^{26}Al production rate calibration sites. Production rate from muons is constant over time (Marrero et al. 2016), includes a minor modification to reduce a potential near-surface artefact (Balco 2017), and is calibrated against the Beacon Heights ^{10}Be and ^{26}Al sandstone bedrock core data(Borchers et al. 2016, Marrero et al. 2016, Phillips et al. 2016, Balco 2017).

We followed the approach of Stroeven et al. (2015) in also taking account for shielding during glacial isostatic uplift through the water column in the expage calculator (expage_sealevel.m). We calculate the mismatch in time (yr) between a simple exposure age and an expected exposure age given a reconstructed deglaciation age and the shoreline displacement curve. The deglaciation age is based on the Stroeven et al. (2016) deglaciation reconstruction and ranges from 13 424 to 13 703 years before sampling.

The attenuation length of spallogenic production of ^{10}Be and ^{26}Al is calculated from atmospheric pressure and a time-dependent geomagnetic rigidity cut-off, similar to the CRONUScalc calculator (Marrero et al. 2016). For the Trollhättan region, this results in an average attenuation length of 152 g cm^{-2}. We use a rock density of 2.65 g cm^{-3} and a water density of 1.0 g cm^{-3} in our calculations. We assume that there has been no post-emergence shielding by vegetation, snow, or sediments. We believe the possibility of shielding by sediments is generally low (after all, on wide almost level surfaces sediment transport trends to very low values, and surfaces immediately below lake level in Lake Vänern are conspicuously free of sediment), but notable risk samples are the Nordkroken samples and the Sandhem samples near the storage site.

2.7.3 Glacial erosion simulations

This section is a modified version of Section 5.2.3 of Hall et al. (2019), describing the glacial erosion simulation method.

To simulate site-specific glacial erosion based on ^{10}Be and ^{26}Al concentrations, we use a modified version of the expage glacial erosion calculator by also including shielding by sea water after deglaciation (glacialE_sealevel.m, see additional material in Hall et al. (2019), Appendix 5). In this calculator, a glaciation history is defined by a cut-off value for the benthic δ^{18}O record from the LR04 stack (Lisiecki and Raymo 2005). We assume that the growth and decay of the FIS has followed this proxy

for global ice volume (cf. Stroeven et al. 2002b). Because the duration of cosmic ray exposure since the last glaciation is of major importance for the erosion rate estimate, local last deglaciation is set independently by the Stroeven et al. (2016) reconstruction. During periods of ice coverage, the ^{10}Be and ^{26}Al production rates are assumed to be zero. During ice-free periods the production rates are computed from sample shielding depth, which is a function of the integrated glacial erosion, the integrated non-glacial subaerial erosion, submergence, and the densities of rock and water.

Glacial erosion simulations are run in two modes of operation: (1) constant erosion rate and (2) constant erosion depth. In the first case, the glacial erosion depth of each ice cover period scales with the duration of ice coverage. In the second case, the glacial erosion depth of each ice cover period is constant, independent of the duration of ice coverage, and the total glacial erosion instead scales with the number of ice coverage periods. Whereas the former may mimic the effect of wet-bed glaciation, the latter may mimic glaciations dominated by dry-bed conditions but experiencing erosion during wet-bed deglaciation (Kleman et al. 1992, Harbor et al. 2006, Cowton et al. 2012, Sugden et al. 2019). We acknowledge that this is a simplification of natural conditions under ice sheets. For example, conditions conducive for either mode of operation may have co-occurred or have switched-on or switched-off within any single glaciation.

Subaerial erosion is assumed to operate at a constant rate for all ice-free periods. Again, this is a necessary simplification of a complex reality, but one which appears reasonable for an area which has most likely remained low-relief over the course of Pleistocene glaciation. Inundation by sea and glacial lake water occurs following each ice cover period because of glacial isostatic depression. While submerged, the samples experience neither glacial nor subaerial erosion. To calculate emergence through the water column, we use the shoreline displacement curve for the last deglaciation and a filtering approach-derived displacement curve following previous ice cover periods. For the latter, the ice cover history of the preceding 30 ka determines the sea level displacement curve. This filtering approach (subfunction uplift_preLGM, see additional material in Hall et al. (2019), Appendix 5) is calibrated against the shoreline displacement curve for Forsmark for the last deglaciation and modelled sea level displacement in Forsmark following the MIS 4 glaciation (SKB 2010).

Erosion rates have been calculated in two ways. First, in a simple calculation for single nuclides (^{10}Be or ^{26}Al), glacial erosion is computed for a specific ice cover (δ^{18}O cut-off value) and subaerial erosion rate couple, based on an interpolation of 50 simulated nuclide concentrations derived from a suite of glacial erosion rates or suite of glacial erosion depths (Fu et al. 2019). We use this method to investigate the sensitivity of glacial erosion to perturbations of specific model parameters.

Second, following a more sophisticated approach, predefined minimum and maximum values for glacial erosion, subaerial erosion, and δ^{18}O cut-off values are all imposed to allow for a search of the parameter space yielding the target nuclide concentration within measurement uncertainties plus propagated production rate uncertainties. This is done iteratively to approach the minimum and maximum parameter values that yield the target nuclide concentrations. The iterative search for the parameter space yielding the measured cosmogenic nuclide concentrations is done with repeat computations of cosmogenic nuclide production for a range of scenarios, with the minimum and maximum values for each of the three parameters searched with decreasing step size down to a maximum of 0.01 mm/ka or 0.01 cm/ice cover period for glacial erosion, 0.01 mm/ka for subaerial erosion, and 0.01 ‰ for the δ^{18}O cut-off value. Because the relation between the input parameters values and the resulting cosmogenic nuclide concentration is potentially non-linear and discontinuous, we use a guided Monte Carlo approach to search for the full range of parameter limits and potential erosion depths over time. This is done first focused around the iteratively determined minimum and maximum parameter values searching actively for lower minimum values and higher maximum values for each of the three parameters using five Monte Carlo runs with 150 scenarios each for each of the six parameter limits. Finally, Monte Carlo runs with 150 random scenarios using parameters drawn from ranges defined by the determined minimum and maximum parameter limits each decreased and increased, respectively, by 10 %, are run iteratively to generate at least 1 000 cosmogenic nuclide concentration solutions or for a maximum of 100 runs. For full details of the erosion simulations, we refer to the supplementary function glacialE_sealevel.m, see additional material in Hall et al. (2019), Appendix 5. With this method, we can find the range of glacial erosion rates that satisfies the measurements for assumed subaerial erosion rates and reasonable ice cover histories (see below). This method also enables the calculation of erosion histories for ^{26}Al/^{10}Be pairs. Specifically, only certain scenarios will yield a match with both measured nuclide concentrations, and we use this method to simulate the erosion history of the Trollhättan surfaces.

2.7.4 Input parameter constraints

This section is a modified version of Section 5.2.4 of Hall et al. (2019), describing the parameter constraints for the glacial erosion simulation.

To constrain the potential ice cover history of the Trollhättan region, we use a minimum $\delta^{18}O$ cut-off value of 4.4 ‰ and a maximum value of 4.7 ‰. For the last glacial cycle, this yields glaciation during MIS 2 and potentially most but not all of the period from MIS 4 to MIS 2. These two cut-off values allow for a range of possible glaciation histories. Through the last glacial cycle (from ~115 ka) and the Quaternary (from ~2.6 Ma), the total durations of ice cover become 18–49 ka and 104–340 ka, respectively. This corresponds well with previous interpretations of average Quaternary ice sheet extent and indicates that the Trollhättan region has remained ice free for most of the Quaternary (Porter 1989, Kleman et al. 1997, 2008).

Subaerial erosion is assumed to operate at a constant rate for all ice-free periods. For the subaerial erosion rate, we set the minimum and maximum values to 0 and 5 mm/ka, respectively. The upper limit of 5 mm/ka is somewhat higher than estimated Holocene erosion rates (André 1996, 2002) to account for potentially higher average subaerial erosion rates if weathering accelerates under longer ice-free periods.

We run the simulations starting from various points back in time with the cosmogenic nuclide concentration starting at zero. For a case where the sample starts at great depth with a minimal cosmogenic nuclide production rate, this zero-nuclide assumption is perfectly valid. For a case where the sample starts a shallow depth with a notable cosmogenic nuclide production rate, the zero-nuclide assumption implies that the bedrock must have been shielded from cosmic rays prior to the point in time when the simulation starts. In such a situation, we can mentally equate the start of our simulation to follow a sudden and instantaneous erosion of the sedimentary cover rocks that completely shielded the underlying basement rock surface from cosmic rays. Because it is difficult to determine the timing of cover rock removal with certainty, we ran the simulations starting from 130 ka, 0.5 Ma, 1.0 Ma, 2.588 Ma, and 10 Ma. These starting points cover a wide range of scenarios, including likely end-members where cover rock removal occurred as recently as the penultimate glaciation (130 ka) or as long as 10 Ma ago, through non-glacial processes.

Because the constant glacial erosion scenarios are crude simplifications of a much more complex reality, we considered two end-member scenarios starting at 10 Ma which assume no glacial erosion (1) between 10 Ma and 130 ka and (2) after 55 ka. We do not consider these end-members to be particularly likely, but they are chosen simply to explore the boundaries of our model space. In the first scenario, all glaciations prior to the last glacial cycle are non-erosive and the only glacial erosion is that which occurs in the last glacial cycle. This scenario requires intense glacial erosion during the last glacial cycle up to the late Weichselian to account for measured concentrations. In the second scenario, there is no glacial erosion in the ice cover period(s) after MIS 4. Because the samples will be exposed at or close to the surface for the full subaerial period after MIS 4, glacial erosion in MIS 4 and earlier ice cover periods will be higher than in the constant glacial erosion scenarios. As with the other simulations, we ran these extreme scenarios with both constant glacial erosion rate and constant glacial erosion depth. Table 2-4 specifies simulation specific parameters for all 14 simulation scenarios.

Table 2-4. Glacial erosion simulations. All simulations have the same predetermined parameter boundaries for the $\delta^{18}O$ cut-off value (4.4–4.7 ‰) and the subaerial erosion rate (0–5 mm/ka).

Simulation	Starting point	Glacial erosion
1	130 ka	Constant glacial erosion rate
2	130 ka	Constant glacial erosion depth
3	0.5 Ma	Constant glacial erosion rate
4	0.5 Ma	Constant glacial erosion depth
5	1.0 Ma	Constant glacial erosion rate
6	1.0 Ma	Constant glacial erosion depth
7	2.588 Ma	Constant glacial erosion rate
8	2.588 Ma	Constant glacial erosion depth
9	10 Ma	Constant glacial erosion rate
10	10 Ma	Constant glacial erosion depth
11	10 Ma	10 Ma–130 ka: no glacial erosion; 130–0 ka: constant glacial erosion rate
12	10 Ma	10 Ma–130 ka: no glacial erosion; 130–0 ka: constant glacial erosion depth
13	10 Ma	10 Ma–55 ka: constant glacial erosion rate; 55–0 ka: no glacial erosion
14	10 Ma	10 Ma–55 ka: constant glacial erosion depth; 55–0 ka: no glacial erosion

2.7.5 Sensitivity tests of the glacial erosion simulations

This section is a modified version of Section 5.2.5 of Hall et al. (2019), describing the sensitivity tests for the glacial erosion simulation.

To test the sensitivity of the glacial erosion simulations to specific scenario parameters, we ran a set of ^{10}Be simulations for four particular samples (TROLL-16-07, 16-09, 17-01, and 17-03) in which we varied one parameter at a time. The four samples were chosen to cover a range of cosmogenic nuclide inheritance and to include the samples that have potentially been covered by sediments. As reference scenario, we use a $\delta^{18}O$ cut-off value of 4.55 ‰, a subaerial erosion rate of 2.5 mm/ka, and we start the simulation from 1 Ma. We varied the $\delta^{18}O$ cut-off value, the subaerial erosion rate, the simulation starting point, and the sediment cover, and we ran simulations in the constant erosion rate and the constant erosion depth modes. These tests help us to evaluate the reliability of derived glacial erosion rates.

3 Results

3.1 Regional bedrock relief of Västergötland

The topography of south-west Sweden is dominated by three relief elements at the landscape scale (Figure 3-1):

1. Large table mountains or mesas (Swedish: *platåberg*) where remnants of Early Permian dolerite sills have protected underlying Early Palaeozoic sedimentary rocks from erosion.
2. Surrounding, rather smooth gneissic basement surfaces where relative relief is <20 m per km at distances of up to 70 km from Early Palaeozoic outliers (Figure 1-13).
3. Rougher basement areas to the west and south (Fredén 1982) where relative relief is widely >40 m per km and where fracture-guided valleys and basins are prominent.

The boundary between the smooth and rough terrains occurs in a 5–10 km wide zone over a distance of ~125 km (Figure 3-1). This boundary does not correspond to known lithological or structural contrasts (Figure 1-4). Sharp terrain boundaries may exist, however, beneath former ice sheets at the edges of zones of glacial erosion. In such cases, each zone displays distinct assemblages of glacial and non-glacial landforms (Sugden 1978). Terrain boundaries that lie parallel to former ice flow lines may reflect sustained differences in glaciological conditions beneath former ice sheets (Glasser and Bennett 2004), as between zones of slow and fast ice flow (Kleman 1994) or between zones of non-erosive, cold-based ice and erosive, warm-based ice (Kleman et al. 2008). Terrain boundaries that lie across former ice flow lines may represent former ice stream onset zones, where ice streaming was triggered by changes in bed gradient (Kleman and Applegate 2014).

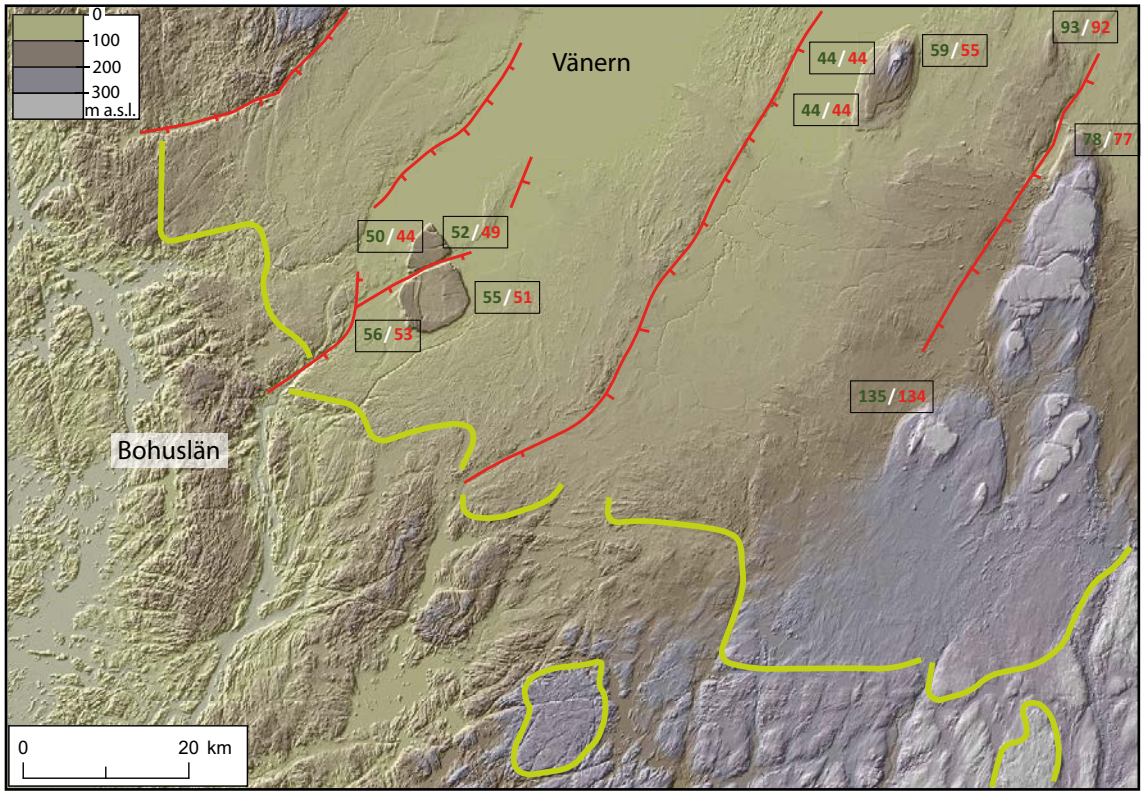

Figure 3-1. *Relief of SW Sweden. Terrain boundary between the little modified parts of the sub-Cambrian unconformity to the NE and the sub-Mesozoic etchsurface to the SW is shown by the green line. Major faults shown in red. Elevation (in metres a.s.l.) of the buried sub-Cambrian unconformity around outliers is shown in green and of summits in the adjacent exposed basement in red. DEM based on Lantmäteriet data.*

The terrain boundary in Västergötland runs across former ice flow lines (Kleman et al. 1997). The terrain boundary is unlikely to represent an ice stream zone for several reasons. Firstly, Västergötland was peripheral to the ice stream that flowed from the Oslo Graben into the Skagerrak in the Late Weichselian (Houmark-Nielsen and Kjær 2003). Secondly, the terrain boundary in Västergötland extends south-eastwards across a large part of southern Sweden (Figure 3-1). The width and orientation of the terrain boundary is inconsistent with an origin as an onset zone for ice streaming towards the Skagerrak. Thirdly, no onset zone for an ice stream across southern Sweden is apparent in recent glaciological models of the last FIS (Patton et al. 2016). Fourthly, in the Sjuntorp area, which straddles the terrain boundary to the south of Trollhättan, similar assemblages of glacial bedforms, but with different relative relief, exist on both sides of the terrain boundary, including asymmetric hills, trenches and rock basins (Section 3.5.4). The configuration of the terrain boundary and the continuity of the glacial erosion forms across it is not consistent with a primary origin as a ice stream onset zone beneath former ice sheets. In the absence of clear geological and glaciological controls, other explanations should be sought for the roughness contrasts.

The smooth basement surface found around the Early Palaeozoic outliers in Västergötland has been interpreted as an expression of the re-exposed, planar sub-Cambrian unconformity (Lidmar-Bergström 1993). Evidence is lacking that U2 was exposed to prolonged weathering and erosion during the Mesozoic, Palaeogene and Neogene in Västergötland. In contrast, the rougher landscape of Bohuslän, with its trenches, basins and hills, has been described as a joint-valley landscape (Johansson 1999) or undulating hilly relief (Lidmar-Bergström 1999). Similar rough basement surfaces are found below Mesozoic sedimentary rocks offshore in the Skagerrak (Green et al. 2013). The terrain resembles etched relief found further south (Johansson et al. 2001b) that retains deep weathering on the U3a (Ahlberg et al. 2003) and U3b unconformities (Lidmar-Bergström 1995). Bohuslän also retains the roots of grus-type saprolites of likely Neogene age (Johansson et al. 2001a). The terrain boundary across Västergötland lies at the break of slope between U2 and U3. According to Johansson et al. (2001b), the U2 has been uplifted, and eroded along its raised, south-western edge, The topographic contrasts between Västergötland and Bohuslän across the terrain boundary in SW Sweden are interpreted as mainly products of the pre-Pleistocene denudation history of the basement (Lidmar-Bergström et al. 2017), with locally increased glacial erosion along the break of slope between U2 and U3.

Three components of basement topographic roughness can be identified in Bohuslän. The first derives from fracture-guided weathering and erosion that developed during the Mesozoic and later, denudation that led to modification and destruction of the exposed sub-Cambrian unconformity (Green et al. 2013). The second derives from removal of deep weathering mantles of Mesozoic and Neogene age, particularly from fracture zones, by glacial erosion during the Pleistocene (Johansson et al. 2001a). The third component is the product of glacial erosion of unweathered basement, also operating mainly along fracture zones in Bohuslän, below former basal surfaces of weathering (Olvmo et al. 1999). Where, as in other parts of SW Sweden, including the Trollhättan area, the basement at the sub-Cambrian unconformity was not widely exposed to deep weathering prior to the Pleistocene, topographic roughness derives largely from this final component with exploitation of fracture zones by Pleistocene glacial erosion.

3.2 Relief on the buried unconformity

The detailed morphology on the sub-Cambrian unconformity is evident where basement emerges from beneath the Early Palaeozoic outliers. The relative elevations of the basement on the buried sub-Cambrian unconformity and on adjacent exposed summits vary by only a few metres around the Early Palaeozoic outliers in Västergötland (Figure 3-1). The relief on the buried unconformity at Halleberg-Hunneberg and at Kinnekulle is examined below.

3.2.1 Halleberg-Hunneberg

The sub-Cambrian unconformity around Halleberg and Hunneberg is concealed today beneath till, slope deposits and made ground (Figure 3-2). Basement highs are neither exposed on lower hill flanks nor protrude through the beds of Early Cambrian sandstone exposed at the base of Hunneberg on its SW flank. The edge of the Early Cambrian sandstone is shown as a smooth line on SGU maps, also suggesting that no large (> 10 m) hills or deep (> 10 m) valleys occur on the unconformity around the base of each hill. Bedrock exposure is locally extensive, but no outliers of basal Early Cambrian sand-

stone have been mapped in basement lows around Halleberg and Hunneberg, indicating a lack of clefts, trenches and valleys on the former unconformity surface. The unconformity along the eastern flanks of the hills is depicted in cross-section parallel to the dip of the early Palaeozoic cover as near planar and gently inclined to the N, with relief of < 5 m over a distance of > 10 km (Sidenbladh 1870) (Figure 3-3).

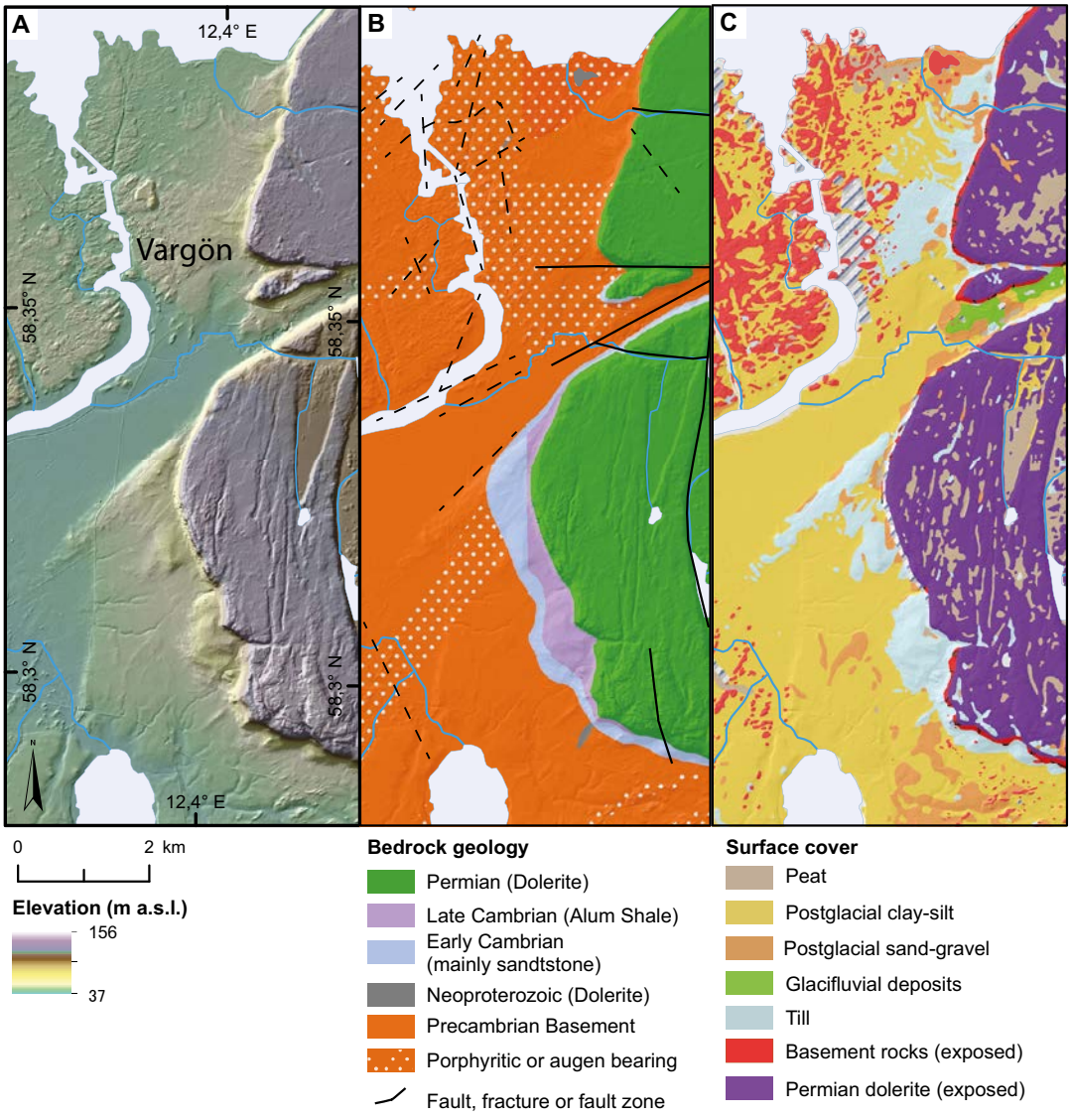

Figure 3-2. *The western flank of Halleberg and Hunneberg. A. 2 m DEM based on Lantmäteriet data. B. Map of solid geology based on SGU data. C. SGU Map of Quaternary geology based on SGU data.*

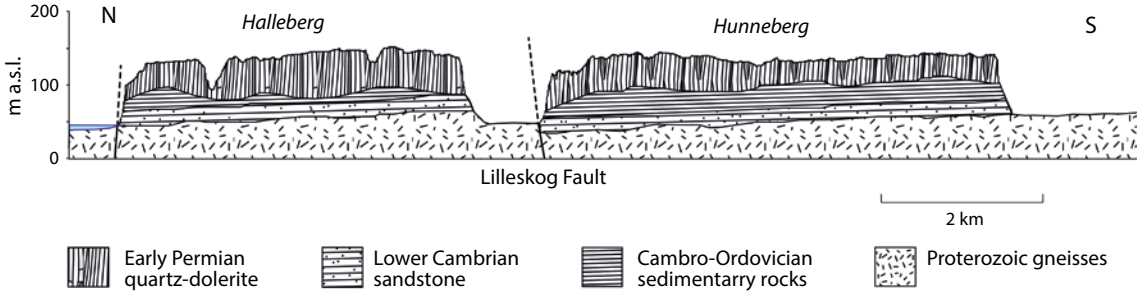

Figure 3-3. *Cross section along the eastern flank the Halleberg and Hunneberg Palaeozoic outliers (based on Sidenbladh (1870) and modified from Johansson et al. (1999). Permian vertical throw across the fault is slightly greater than the 24 m thickness of the Lower Cambrian Mickwitzia sandstone. The Cambro-Silurian sedimentary layers on both sides of the fault dip at ~0.3 % northwards (Sidenbladh 1870).*

The relief of the basement in close proximity to the buried unconformity is apparent from summit heights on rock knobs at four locations (Figure 2-2) around Halleberg and Hunneberg: Gaddesanna, Bragnum, Hårrum and Nordkroken. Further information is available from summit envelope surfaces for those parts of Areas 1 and 2 that lie along the edges of these hills (see Sections 3.3.1 and 3.3.2).

Gaddesanna

At Gaddesanna on the NE flank of Halleberg, the exposed basement is seen at a distance of 0.2 to >3 km from the edge of the buried contact with the Early Cambrian Mickwitzia Sandstone (Figure 3-4). In proximity to the base of Halleberg, elevations of the summits of gneiss rock knobs vary by <3 m. Further from the hill flank, the highest summits in the exposed basement rise 3–8 m above adjacent summits over distances of 0.5 km but nowhere exceed the estimated heights along the edge of the buried unconformity. The edge of the Early Cambrian sandstone as marked on SGU maps is overlain by thicknesses of 3 to >10 m of Late Pleistocene deposits. Hence, the elevation of the base of the Cambrian sandstone has an uncertainty of several metres but, when projected from beneath Halleberg, U2 appears to stand a maximum of 3–9 m above adjacent gneiss knobs. The estimated gradient on the buried unconformity at Hulan is 0.25 % whereas the exposed basement summit surface adjacent to the unconformity has a gradient of 0.36 % to the NNW.

The elevation of the base of the Early Permian dolerite sill is at 115 m a.s.l. at the abandoned Alum Shale mine on the path from Hulan up to the summit of Halleberg. The planar flat at Gaddesanna has an elevation of 51 m a.s.l. and other rock knobs close to the break of slope rise to 53 m a.s.l. (Figure 3-5). Assuming that the full 60–62 m thickness of the Early Palaeozoic sequence is preserved, the estimated elevation of the basement unconformity is 53–55 m. The difference in height between the buried unconformity and the present basement summit surface is estimated at ≤0–4 m.

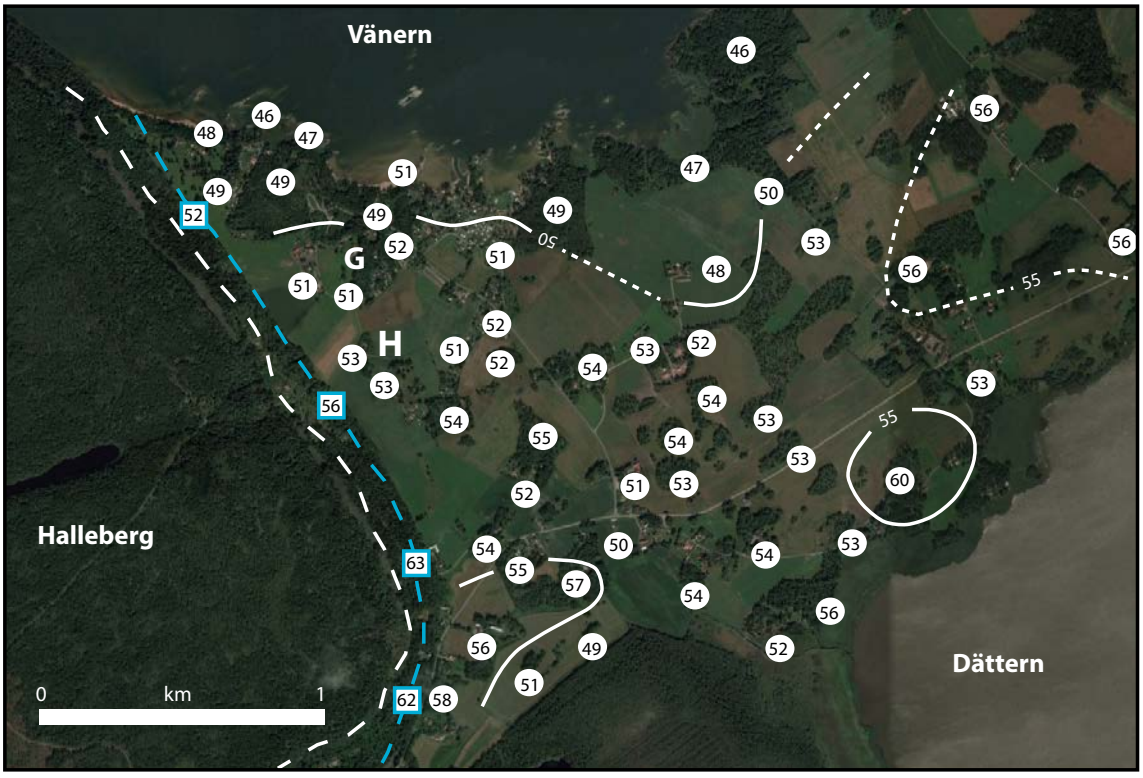

Figure 3-4. *Relief of the re-exposed basement unconformity NE of Halleberg (heights in metres and interpolated contours at 5 m intervals). Lithological boundaries from SGU mapping; elevations from Lantmäteriet data. Base of Early Cambrian sandstone outcrop shown in blue. Edge of Early Permian dolerite sill shown in white. G Gaddesanna, H Hulan.*

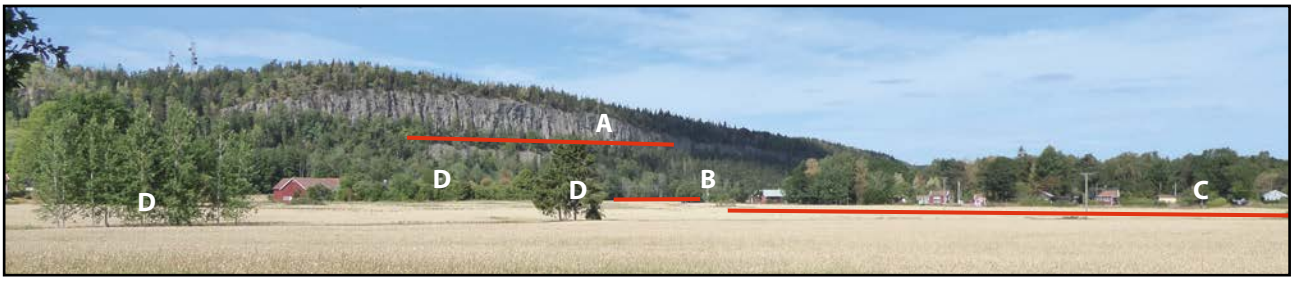

Figure 3-5. *View west from Hulan towards Halleberg. A. Base of the dolerite sill at 115 m a.s.l. B. Break of slope close to the buried contact of Early Cambrian sandstone and basement at 55 m a.s.l. C. Planar flat at 51 m. D. Wooded rock knobs at 53 m.*

Bragnum

At Bragnum on the SE flank of Hunneberg, the basement is exposed at distances of 0.2 to >2 km from the contact with the Early Cambrian Mickwitzia Sandstone (Figure 3-6). Along the edge of Halleberg, the summits of gneiss knobs lie within an altitude range of <3 m over wide areas. Further from the hill flank, the highest summits in the exposed basement rise 3–5 m above neighbouring bedrock highs over distances of 0.5–1 km. No highs on the exposed basement exceed the estimated heights on the unconformity. SGU maps indicate that the edge of the Early Cambrian sandstone is overlain by 3 to >10 m of Late Pleistocene deposits. The elevation of the base of the Cambrian sandstone has an uncertainty of several metres but stands a maximum of 4–6 m above adjacent gneiss knobs.

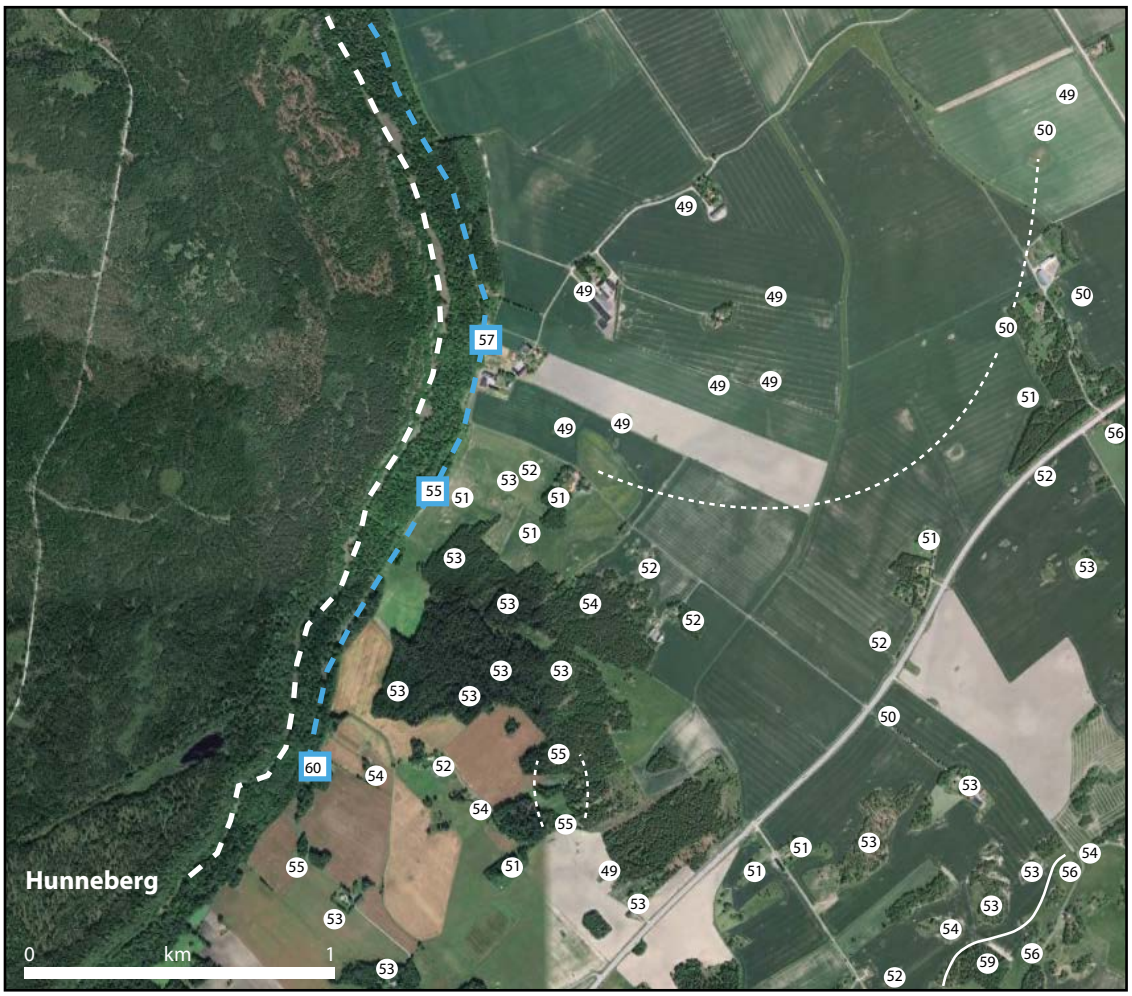

Figure 3-6. *Relief of the re-exposed basement unconformity SE of Hunneberg (heights in metres). Lithological boundaries from SGU solid and Quaternary geology mapping data. Base of Early Cambrian sandstone outcrop shown in blue. Edge of Early Permian dolerite sill shown in white.*

Hårrum

At Hårrum, on the SW flank of Hunneberg, the basement is seen in places within 100 m distance of the contact with the Early Cambrian Mickwitzia Sandstone (Figure 3-7). The summits of the gneiss rock knobs show an elevation range of 4 m over a distance of 1.2 km. The edge of the Early Cambrian sandstone is covered by 2–10 m of Late Pleistocene and Holocene deposits, but exposures of the sandstone shown on SGU maps indicate that drift cover is locally zero. The edges of sub-horizontal sandstone beds are also apparent as steps in LiDAR DEMs (Figure 3-8). The basement unconformity stands a maximum of 2–6 m above the tops of nearby gneiss knobs. No highs on the exposed basement exceed the estimated heights on the unconformity. The gneiss summits and the elevation of the unconformity rise gently to the SE of Sköstorp towards a low basement ridge.

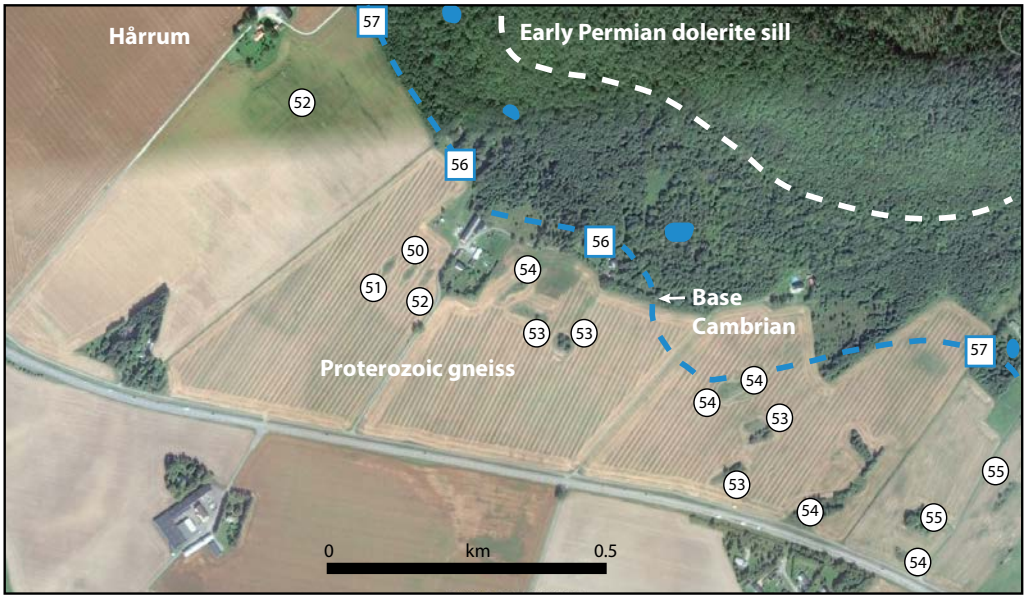

Figure 3-7. *Relief of the re-exposed basement unconformity at Hårrum, south of Hunneberg (heights in metres). Gneiss outcrops and lithological boundaries modified from SGU solid and Quaternary geology mapping data. Base and outcrops in Early Cambrian sandstone shown in blue. Edge of Early Permian dolerite sill shown in white. Elevations from Lantmäteriet data.*

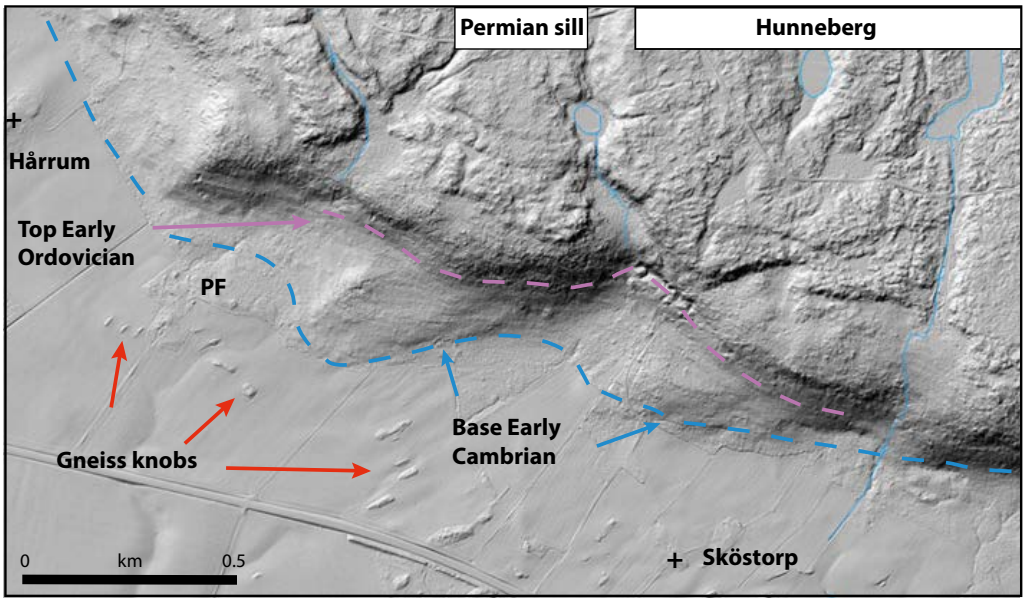

Figure 3-8. *DEM of the SW flank of Hunneberg at Hårrum. The elevation of the base of the dolerite sill is at 118 m a.s.l. at the western waterfall and 116 m a.s.l. at the eastern waterfall. Subtraction of the full 58–60 m thickness of the Early Palaeozoic successions indicates that the basement unconformity should lie at 56–60 m a.s.l., whereas its actual elevation is 54–57 m. PF Planar flat in gneiss. DEM based on Lantmäteriet data.*

Nordkroken

At Nordkroken on the NW flank of Halleberg, the basement is seen within a horizontal distance of 0.4 km of the contact with the Early Cambrian Mickwitzia Sandstone (Figure 3-9). The strikingly flat gneiss surface has an elevation range of 1 m for 0.6 km on the lake shore. The unconformity is covered by talus at Nordkroken but shown at an elevation of ~50 m a.s.l. on SGU maps. The basement unconformity on the hill flank stands a maximum of 6 m above the flat surfaces on the lake shore. A concealed, minor SW-NE oriented normal fault may account for all or part of this height difference. The planar granite surface dips N below the lake at a gradient of ~0.36 %.

Summary

The altitude range of gneiss rock knobs close to the unconformity at Halleberg and Hunneberg is widely < 10 m along km-long stretches of hill flank. Low, small hills of up to 8 m in height and 0.25–1 km in wavelength are also apparent from the present summit topography in the nearby basement. Large hills are absent from the adjacent basement and not seen along the lower flanks of the hills. No Early Cambrian outliers are mapped on the surrounding basement, apart from numerous sandstone dykes. At locations where elevations of the buried unconformity and exposed basement are closely constrained, the projected unconformity stands a maximum of 2–6 m above the elevation of the tops of nearby rock knobs. Uncertainties on these estimates are no more than a few metres.

3.2.2 Kinnekulle

The basement at Kinnekulle is mainly granitic migmatite gneiss (1.7–1.0 Ga) (SGU 1:50 000 Solid Geology map). The basement unconformity is exposed at locations along the Lake Vänern shoreline where it is overlain by patches of Early Cambrian Mickwitzia conglomerate and sandstone (Högbom and Ahlström 1924, Lindstrom and Vortisch 1978). The overlying Lower Palaeozoic sedimentary rocks are flat-lying, or nearly so, and extend into the lower Silurian Kallholn Shale (Llandovery) (Calner et al. 2013). The total thickness of the sedimentary succession at Kinnekulle is approximately 215 m below an originally more extensive dolerite sill that acted as a cap rock and protected the underlying sedimentary sequence from erosion (Nielsen and Schovsbo 2011) (Figure 3-10).

Figure 3-9. *View E along the shore of Lake Vanern towards Halleberg, with elevations of bedrock surfaces. The flat granite gneiss surface dips gently towards the N below the lake surface but remains visible as the lake bed in air photos for 0.8 km (Figure 3-23). The base of the Early Permian sill is covered by talus but stands 21–26 m above the nearest basement outcrop, 380 m to the W. The height difference indicates the maximum thickness of Cambrian and Ordovician strata on this flank of Halleberg. The sub-Cambrian unconformity on Halleberg stands ~6 m above the flat gneiss surface in the foreground. A minor fault runs between the planar flat and the hill base.*

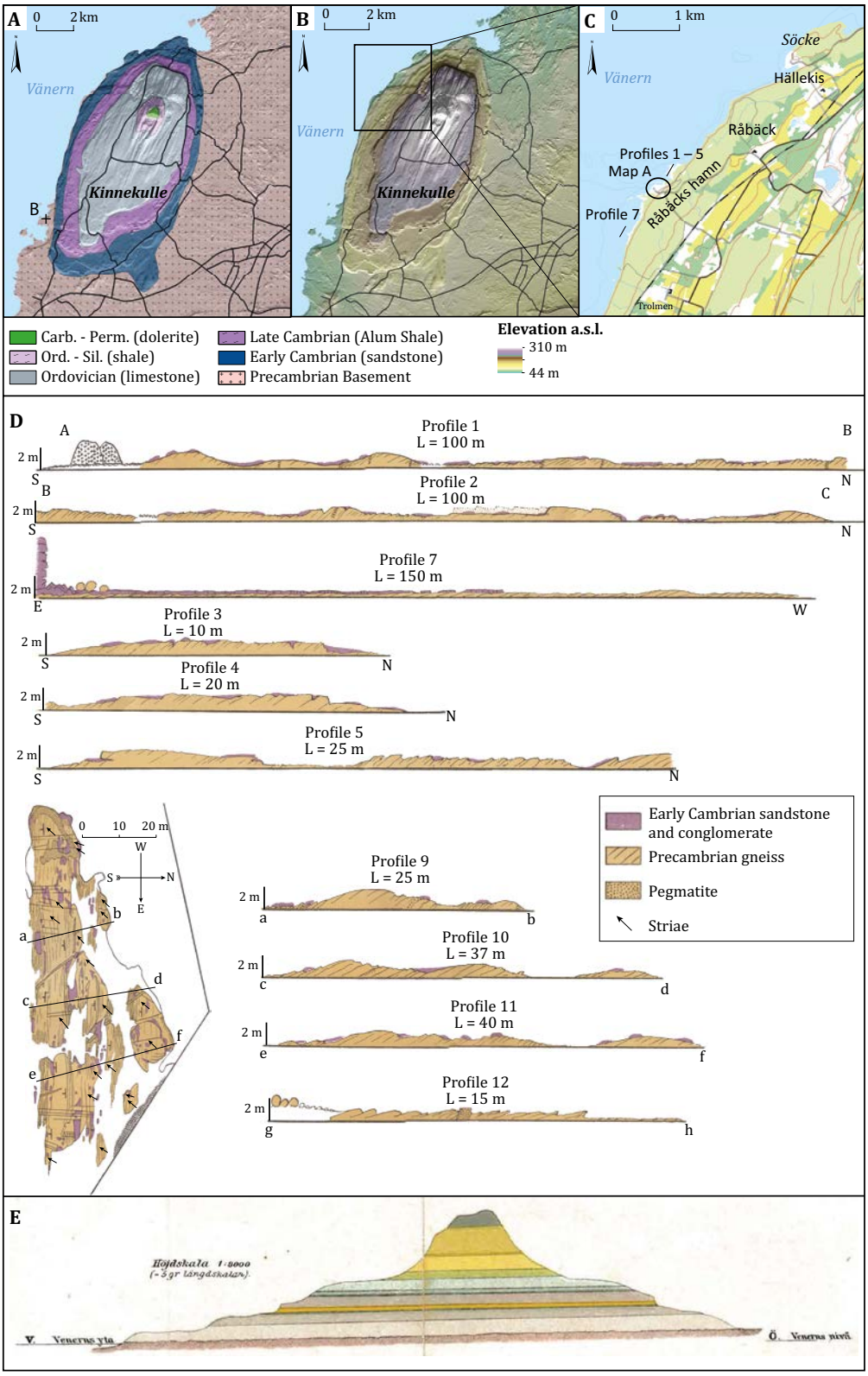

Figure 3-10. *The sub-Cambrian basement unconformity at Kinnekulle. A. Geology based on SGU data. The edges of flat-lying beds of resistant Cambro-Silurian sedimentary rocks are seen as breaks of slope. B. Topography based on Lantmäteriet data. Kinnekulle has a drumlinoid form. The hill surface is fluted and shows drumlins and megagrooves. C. Locations of map and profiles. D. Profiles mapped during low lake levels on Vänern around 1920. Redrawn from Högbom and Ahlström (1924). The amplitude of the relief on the unconformity is < 2 m over distances of > 100 m. E. Geological cross section from Råbäcks Hamn eastwards across the summit of Högkullen showing the near planar basement unconformity overlain by horizontal units of Cambrian and Silurian sedimentary rocks and the Kinnekulle quartz dolerite (Holm 1901). The sequence has been tilted at 0.4 % towards the west. Geological data from SGU; elevation data from Lantmäteriet.*

The unconformity is inclined westwards at 0.4 % but maintains a constant elevation close to lake level and along strike for >6.5 km along the Lake Vänern shoreline (Holm 1901), indicating a near planar form. The strike of beds in the overlying, horizontally bedded Mickwitzia Sandstone is parallel to the unconformity, indicating deposition on a near flat basement surface (Holm 1901). The smooth outline of the edge of the basal Early Cambrian Mickwitzia Sandstone around the base of the hill and summit elevations for basement hills E of the hill indicate that no large (>20 m) hills or valleys occur in the basement (Figure 1-13).

Rudberg (1970, p 161) describes the unconformity relief as follows:

"At the base of Mt Kinnekulle and close to the shore line…(the unconformity) is now normally hidden below the water of the regulated lake. The erosion surface is very flat in some places but in others it is undulating with small hillocks 1–2 m high, partly covered by minute slabs of Cambrian conglomerate or sandstone, partly polished and striated by the inland ice. They look like smooth roches moutonnées, but it is obvious that the form is mainly original and of pre-Cambrian age. The hills are orientated according to the strike of the gneiss."

The most detailed account of the geology and morphology of the unconformity comes from Högbom and Ahlström (1924) who observed the shoreline of Lake Vänern during drawdown of the lake (Figure 3-10). The unconformity is mainly cut across fissile granite gneisses with fractures inclined at low dips to the N (Figure 3-11). Low, rounded ridges aligned roughly W-E are developed where vertical fractures in the gneiss are spaced >1 m apart. The ridges stand <2 m above adjacent fracture-aligned furrows. The gneiss surface exposed today lacks saprolite (Figure 3-11) but Högbom and Ahlström (1924) report decomposition of the top cm to dm of the rock surface in places. Kaolin was not observed except as small patches in otherwise intact gneiss. Biotite is discoloured and orthoclase has been partly replaced by calcite. The latter replacement suggests that the limited alteration of primary minerals post-dates cutting of the unconformity in basement. Alteration may relate to diagenesis after burial (Harper et al. 1995).

The gneiss surface is covered by horizontally-dipping, thinly-bedded conglomerate and sandstone (Figure 3-11). Based on observations at Råbäck, Högbom and Ahlström (1924, p 82) estimated that sandstone dykes in vertical fractures in the gneiss had depths of only a few metres. On the presently-exposed unconformity, pebble conglomerates infill vertical fissures and shallow depressions on the gneiss surface (Figure 3-11), indicating passive gravel infill of open fissures on the Early Cambrian shoreline. The basal conglomerate pebbles are of angular vein quartz derived from local pegmatites (Martinsson 1974) and many are sub-rounded to sub-angular. Few gneiss clasts are seen in the conglomerate but occasional clasts of penecontemporaneous sandstones, shales and phosphorites are recorded (Martinsson 1974). Far-travelled pebbles of other rock types are very rare (Högbom and Ahlström 1924, Calner et al. 2013). Quartz pebbles are reported to display ventifacts at Råbäcks Hamn but in fewer numbers than at Lugnås (Hadding 1929) and Billingen (Högbom and Ahlström 1924). Ventifacts have been attributed to aeolian erosion by silt and sand in a sterile, rocky landscape before Cambrian transgression reached the area (Calner et al. 2013) or on rock shorelines during the transgression (Martinsson 1974). The medium- to coarse-grained basal sandstones show well-developed ripple marks. At Trolmens Hamn, the ripples in the basal sandstone have a wavelength of ~10 cm with a ripple index of l, indicating the operation of swash in shallow water (Tanner 1967). The thin basal conglomerate is interlayered with pure sandstones and mud lenses, indicating formation as a transgressive lag deposit under conditions of slow sedimentation (Jensen 1997). Storm wave activity is indicated higher in the Mickwitzia sequence by individual, thick, upward-fining sand units (Jensen 1997).

Recent observations on the Kinnekulle shore largely confirm previous reports. Large hills and deep valleys are not apparent at the regional and local scales (Figure 3-10). The unconformity shows <2 m relief at the macro- scale, with shallow steps and clefts (Figure 3-11). Planar flats are exposed at Trolmens Hamn and Blomberg (Figure 3-11). The exposed gneiss surface shows only a shallow, slightly weathered layer. It is uncertain if the weathered layer relates, wholly or partly, to weathering prior to, during or after the Early Cambrian marine transgression. The unconformity is overlain by thin, horizontal beds of pebble conglomerate and sandstone, consistent with deposition under conditions of very low wave energy, shallow water and a very gently-shelving rock shoreline (Nielsen and Schovsbo 2011).

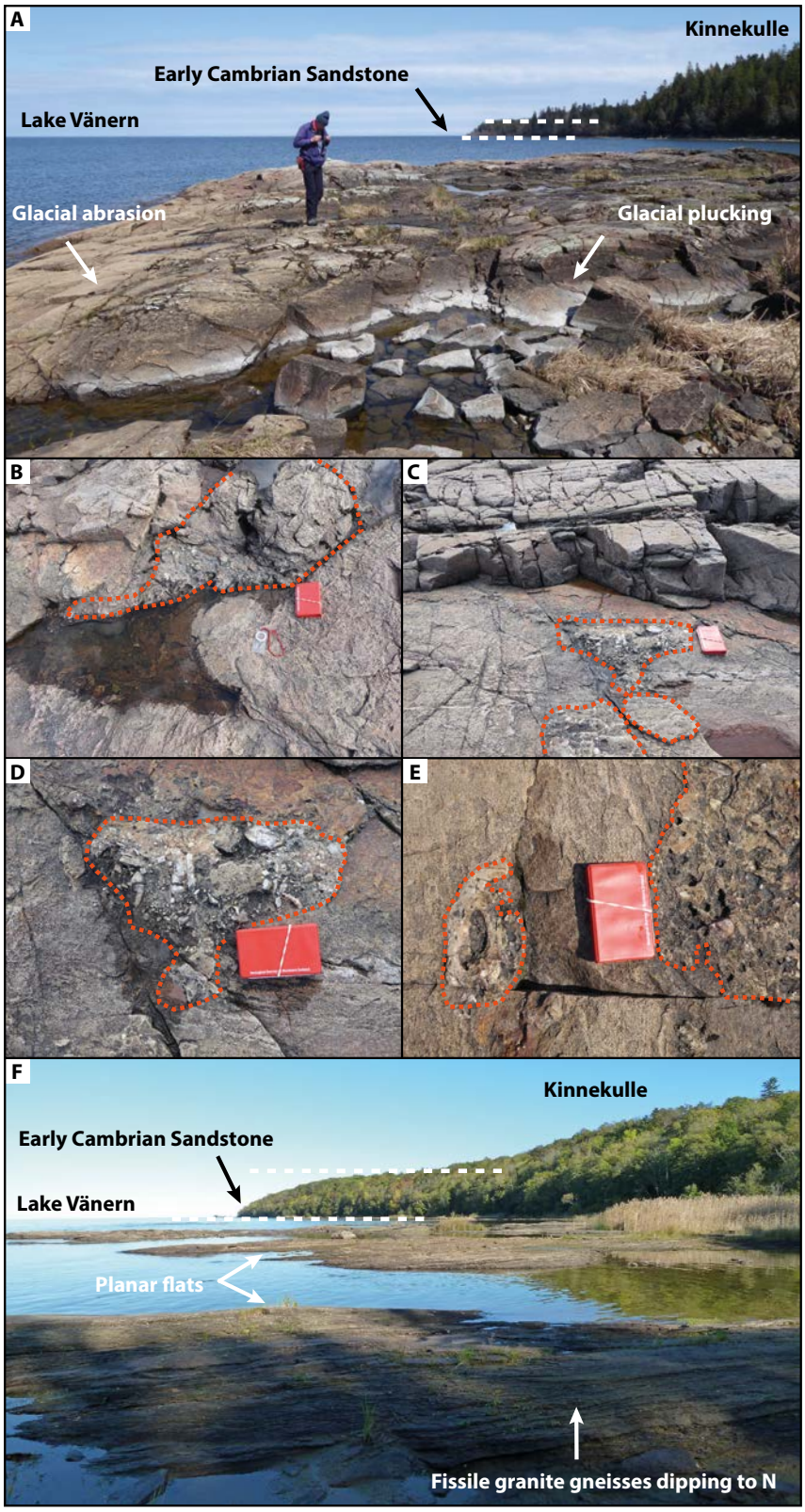

Figure 3-11. *Re-exposed Early Cambrian shore platform on the Vänern shoreline at Kinnekulle. A–E Råbäcks Hamn (Figure 3-10C). A. General form, with low, rounded rock surfaces split by fracture-aligned clefts. Former ice movement towards the camera. B. Vertical view of a cleft in granite gneiss with its infill of basal quartz conglomerate. The notebook is 18 cm long. C. Patch of basal conglomerate on a gneiss surface adjacent to a rock step. The original position of the step edge is marked by the iron-staining on the gneiss surface. D. Detail of C, showing angular pebbles and granules of vein quartz in the basal conglomerate overlain by horizontally-laminated sandstone. E. Patches of medium- to coarse-grained sandstone, with vein quartz clasts, overlying the smooth, unweathered surface of the granite gneiss. F. Planar flats on the unconformity at Blomberg (B in Figure 3-10A). Former ice movement towards the camera.*

3.3 Morphology of the exposed basement

Topographic profiles across the region show general trends across the basement surface (Figure 3-12). Bedrock summits generally are in narrow elevation bands that drop in elevation gently towards the NNW across the surfaces of fault blocks. The lowest elevation ranges for basement summits are on Fault Blocks B and D where inclined surfaces of > 10 km length and with summit elevation ranges of < 10 m along strike pass beneath Early Palaeozoic sedimentary cover rocks at Halleberg and Hunneberg.

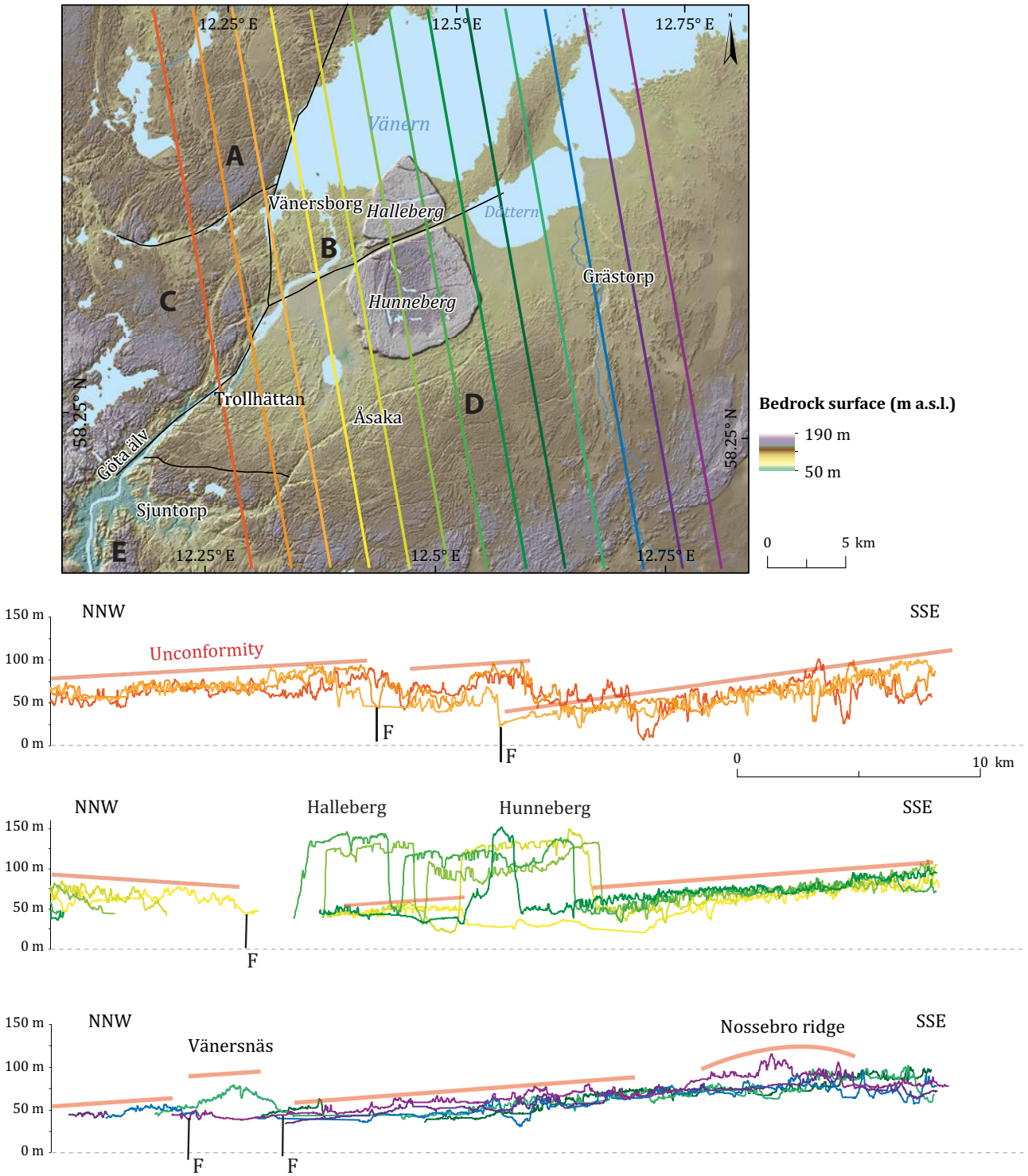

Figure 3-12. *Bedrock profiles for the Trollhättan region. Profiles oriented 350–170° to accommodate the reported inclinations of fault blocks A–E (Figure 2-4). Profiles based on Lantmäteriet elevation data.*

A summit envelope surface for the Trollhattan region (Figure 3-13) shows the major features of the basement morphology. The edges of the Fault Blocks A–E are apparent as 10–50 m high steps. The surface of each block has a low elevation range, with a gentle northward inclination. Large, isolated hills are not present. The major relief feature in the basement is a bedrock ridge lying to the NE of Grästorp developed partly in ultrabasic and basic gneisses (Figure 1-5). The ridge is 1–4 km wide and rises 20–40 m above terrain on its western flank. The ridge extends NNE and is bounded on its eastern flank by a fault with ~30 m of post-Cambrian displacement (Ahlin 1987).

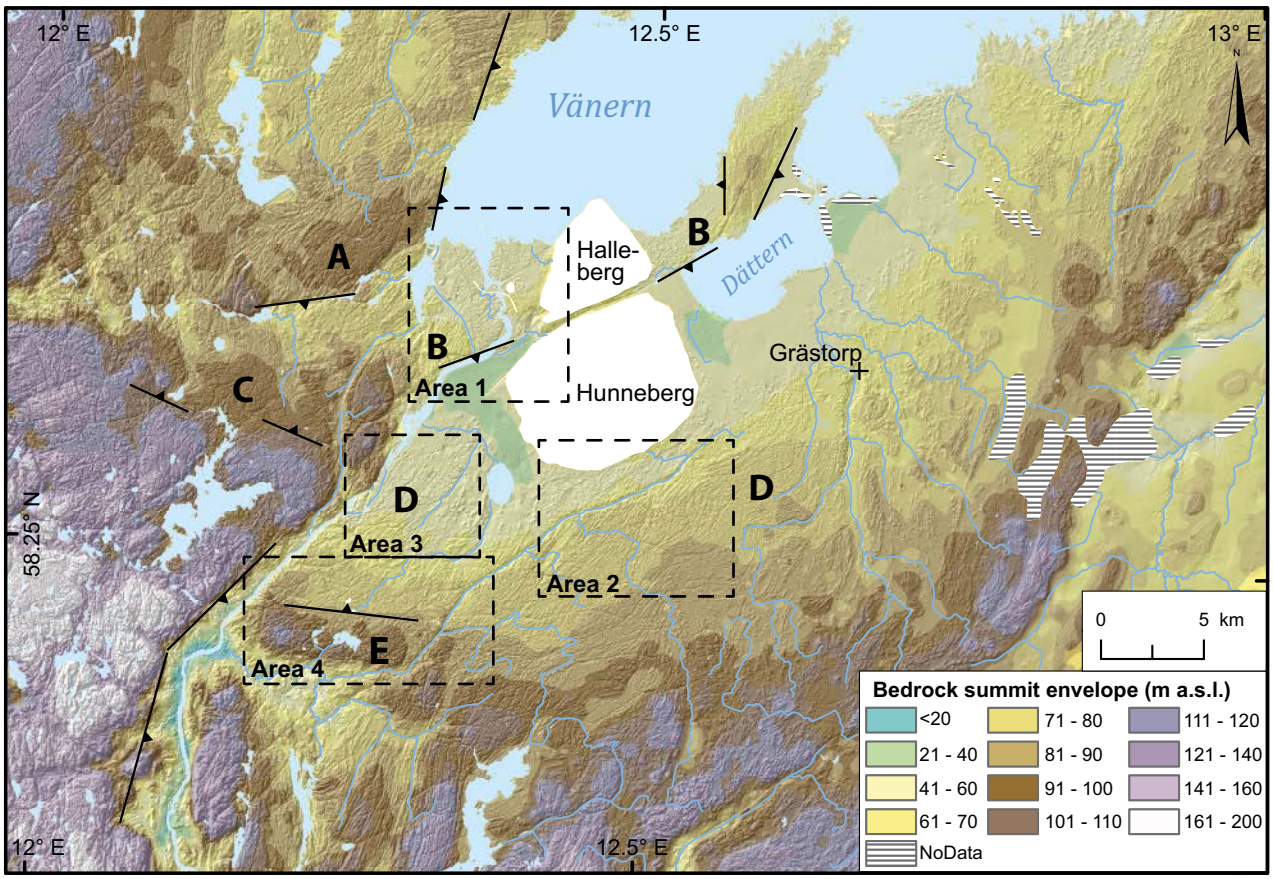

Figure 3-13. *Bedrock summit envelope surface at 0.3 km spacing for the Trollhättan region.*

3.3.1 Morphology of the Vargön area

The Vargön area (Area 1) stands on the western part of Fault Block B, extending along the southern shoreline of Lake Vänern towards the Göta Älv and with the settlements of Vargön and Vänersborg (Figure 3-14). The geology is dominated by coarse-grained to porphyritic granite gneisses (Figure 3-14A). The main lineaments west of Halleberg run NE-SW (Figure 3-14B).

The surface relief is very subdued, with large parts of the Vargön area having elevation ranges of < 3 m per km^2 (Figure 3-14B). Soil depths are generally low, and bedrock is exposed widely (Figure 3-14C). A bedrock depression is developed in basement around the western base of Halleberg. Pleistocene deposits reach a thickness of 40 m in boreholes in a closed rock basin SE of Vargön (Figure 3-14C). Basement is concealed to the south of the Lilleskog Fault, in part due to down-faulting of the adjacent fault Block D to the S. The Göta river channel follows the Lilleskog Fault in a 2 km wide trench where Pleistocene deposits are up to 20 m thick (Figure 3-14B).

In areas where basement is exposed or concealed beneath thin sediment cover, the relief of the rock surface is low (Figure 3-14D). Large hills are absent (Figure 3-14D) and no large basement hills emerge from below talus and cover rocks along the western flank of Hunneberg. Basement summit elevations between Vänersborg and Nordkroken remain at 47 ± 2 m a.s.l. for 5 km (Figure 3-15). On S-N transects, the elevation range of summits is 3 m and the rock surface is inclined to the N at 0.3 % (Figure 3-16). Along a strike section on the lake shoreline, bedrock is widely exposed and varies by a maximum of 5 m in elevation over 5 km (Figure 3-16). The broad valley (V) (Figure 3-15) indicated by basement summit contours at the intake of the Göta Älv is < 3 m deep. Widely-spaced high points (H) in the summit topography stand up to 6 m above their surroundings and have wavelengths of 0.5–2.0 km. The summits of the exposed basement highs equal or only slightly exceed the 55–58 m a.s.l. elevation of the preserved unconformity along the SW flank of Halleberg. Small differences in height occur between parts of the three bedrock blocks found W of the Karls grav, between the canal and the river and E of the river that probably relate to differential movement across minor faults (Section 3.4.1). Bedrock surface roughness is very low across basement highs but increases along edges and along and within rock trenches and basins (Figure 3-14E).

North of the Göta River, a basement summit envelope surface at 250 m spacing shows an inclined surface dipping to the N at an average inclination of 0.45 % (Figure 3-14F), a similar trend and inclination to that seen in profiles (Figure 3-16). The summit envelope surface is near planar but shows two low (5 m high) hills and ridges, with wavelengths of 0.5–1 km (Figure 3-14E). Basement summit elevations to the SW of the Göta Älv drop towards the NNW at a gradient of 0.2–0.3 %. Subtraction of the present basement surface from the summit envelope surface indicates erosion depths of < 5 m over wide areas but reaching < 30 m in trenches (Figure 3-14G).

In summary, in the Vargön area, on the western flank of Halleberg, the summit envelope surface has a near planar form. It stands up to 6 m below the buried unconformity, but field relations may be complicated by minor faulting and the actual height difference may be less. The relief on the summit envelope surface is 4–5 m and it is inclined to the N at 0.45 %. The small height difference between the buried unconformity and the exposed basement and the similar inclinations indicate that the summit envelope surface is a close approximation to the re-exposed unconformity. U2 in this area was a gently tilted near planar surface.

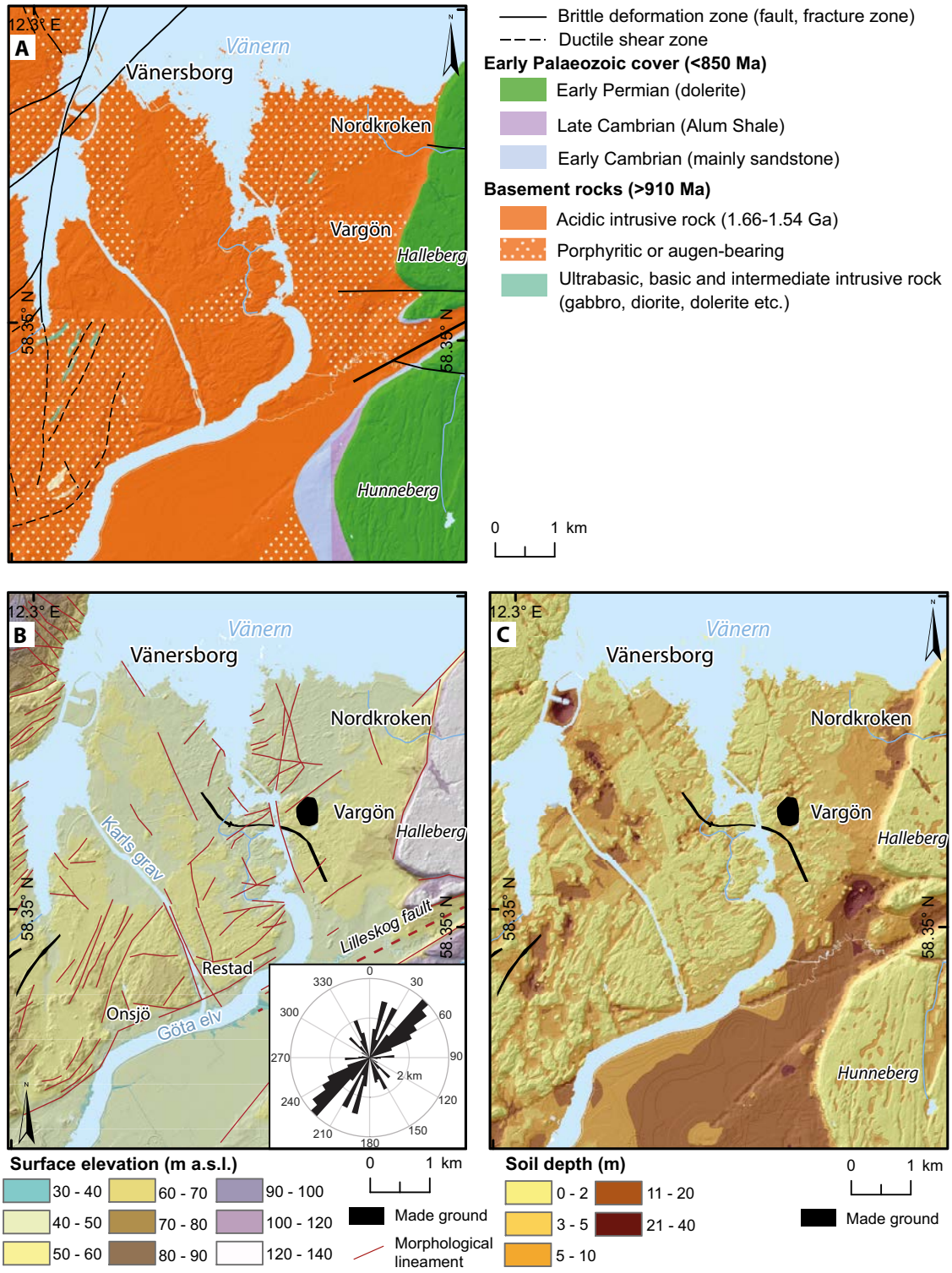

Figure 3-14. *Vargön area. A. Geology. SGU solid geology data for the Vänersborg area is inconsistent and shown here as undifferentiated acidic intrusive rock (1.66–1.54 Ga). B. Surface elevation (m a.s.l.) shown in a digital elevation model. Made ground includes mineral heaps at Vargön and a road embankment. DEM based on Lantmäteriet data. Red lines are topographic lineaments. The rose diagram shows the total length of lineaments in 5° orientation classes. C. SGU data on soil depth. A gneiss outlier marked on SGU maps at 60 m a.s.l. at CN 6473841 and CE 348596 is not seen at outcrop. Mapping is likely in error here as a small sand pit of a volleyball court occurs at this location that could be mistaken in air photos for a gneiss outlier. C. SGU modelled soil depths. D. Bedrock surface elevation (m a.s.l.) based on SGU data. E. Surface roughness based on standard deviation (SD) of basement bedrock elevations. F. Basement bedrock summit envelope surface. G. Erosion depth derived by subtracting D from F.*

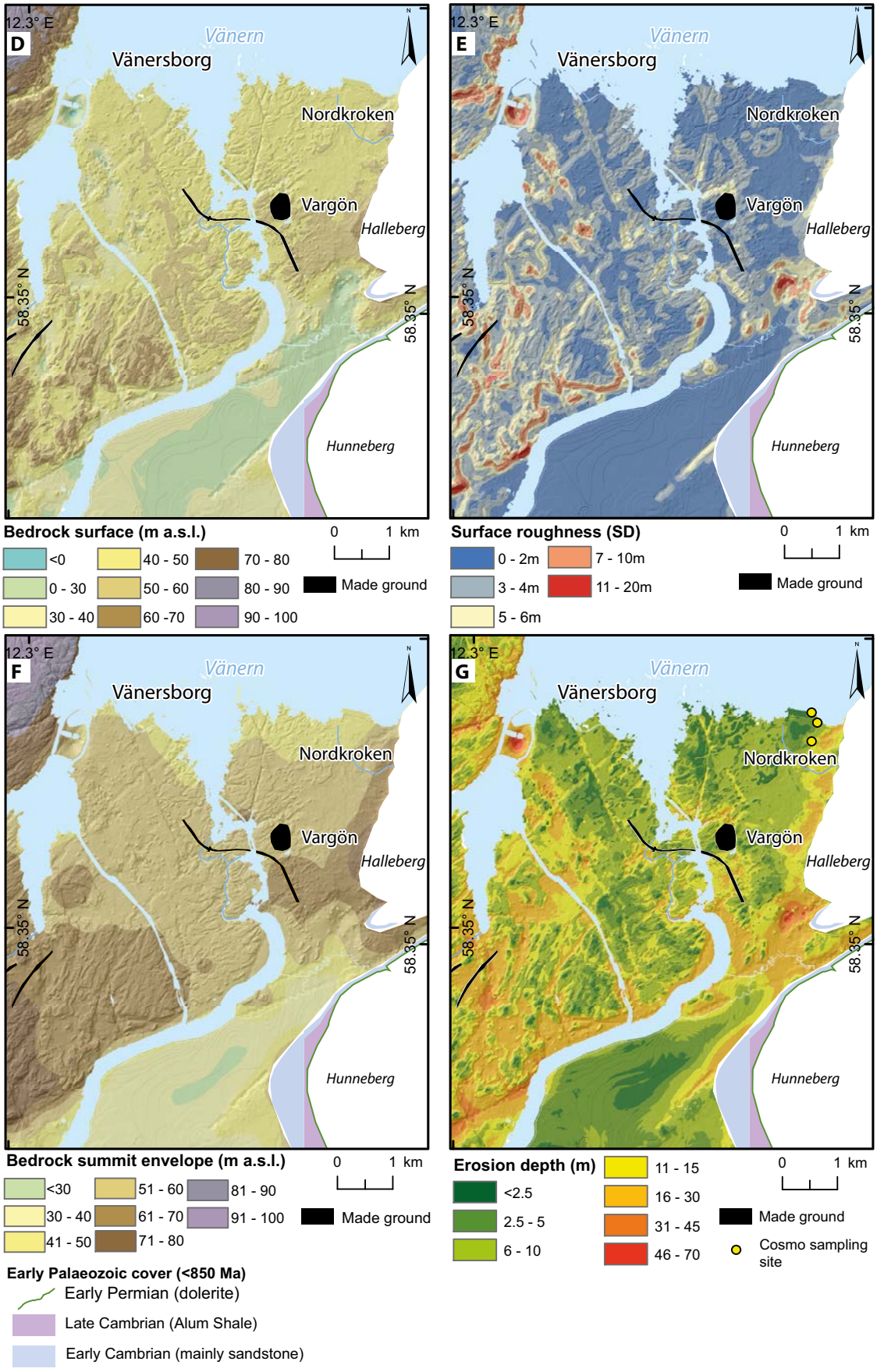

Figure 3-14. Continued.

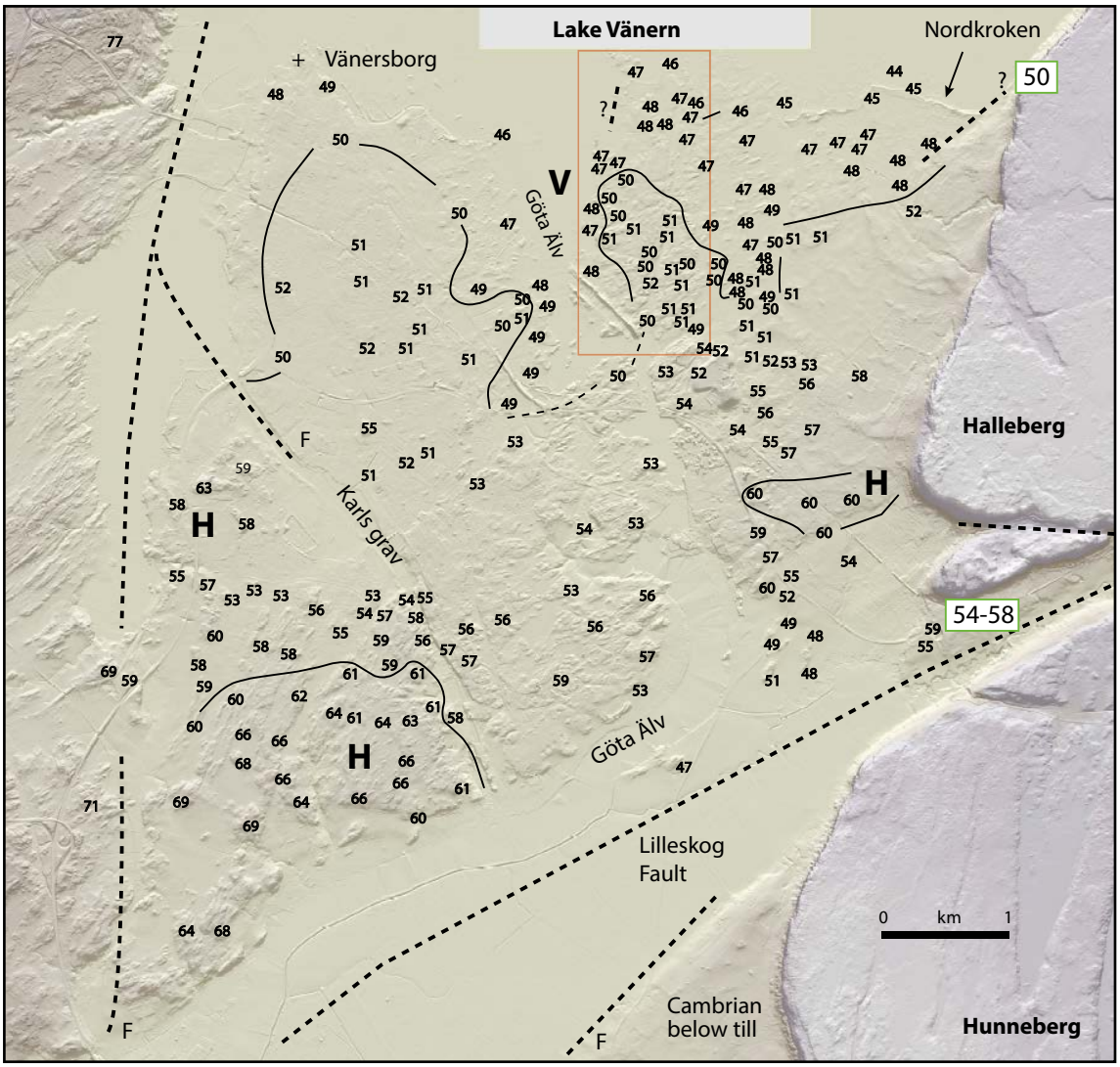

Figure 3-15. *Spot heights (m) based on Lantmäteriet data for exposed basement bedrock summits around Vargön, with interpolated contours. H hill. V valley. Heights along the edge of Halleberg refer to the elevation of the unconformity as shown on SGU maps.*

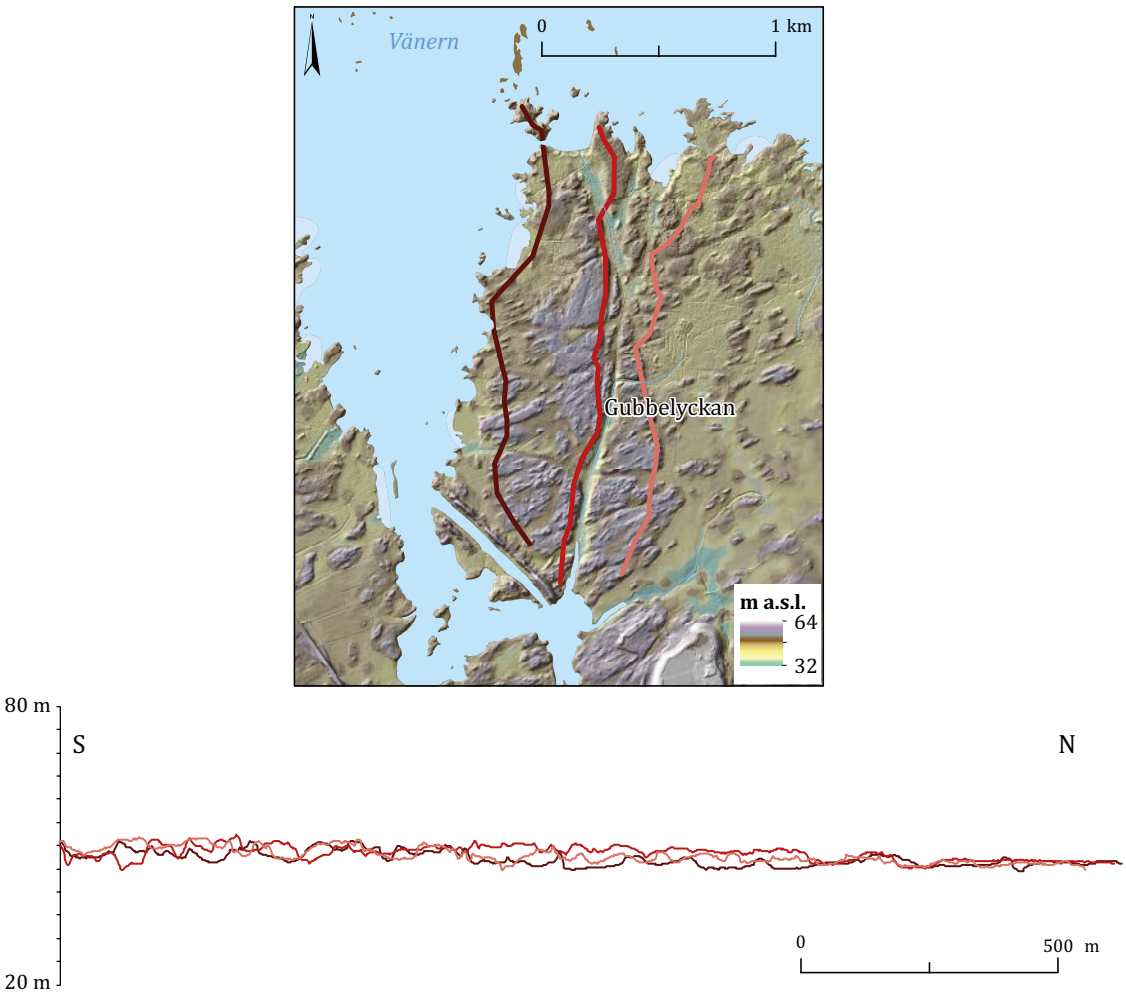

Figure 3-16. *Profile S-N on bedrock summits from Vargön to the shore of Lake Vänern. Area of sections shown as a red box in Figure 3-15. DEM and profiles based on Lantmäteriet elevation data.*

3.3.2 Morphology of the Åsaka area

The Åsaka area (Area 2) stands on Fault Block D and extends southwards from Hunneberg (Figure 3-17). The basement geology is dominated by granite gneisses, locally augen-bearing or pegmatitic. A few, small (< 1 km long) mafic and ultramafic gneisses also occur (Figure 3-17A). The main faults and fracture sets are expressed in topographic lineaments as NE-SW oriented trenches (Figure 3-17B). Gneissic foliation and banding follow a similar strike direction with a low amplitude sinuosity. The quarry at Kuleskog, just S of this area (Figure 3-33), provides sections parallel and normal to the main structural trends (Figure 3-36). Gently sinuous ridges that are a striking feature of DEMs (Figure 3-17D) are seen to follow gneiss foliation in strike-parallel zones of low fracture spacing.

The surface relief is subdued, descending northwards towards Hunneberg and more steeply north-westward towards Hullsjön (Figure 3-17B). No hills rise > 10 m above the general summit level (Figure 3-17B). Along the southern flank of Hunneberg, basement summits stand 2–5 m below the unconformity (Figure 3-7). Granite gneiss bedrock is exposed over wide areas or covered by thin glacial deposits (Figure 3-17B). Thick Pleistocene deposits are confined mainly to the western edge of the area with depths of < 10–20 m (Figure 3-17C).

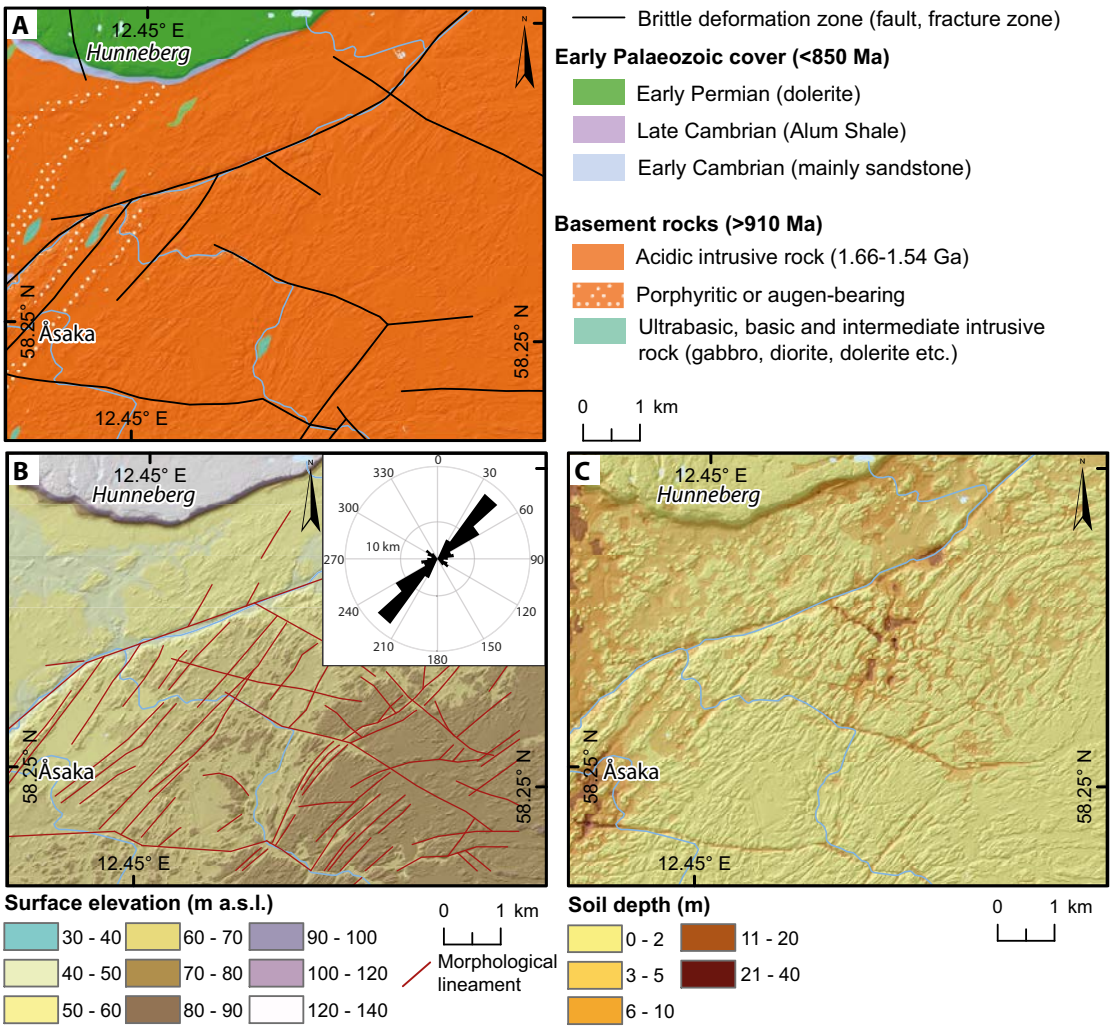

Figure 3-17. *Åsaka area. A. Geology based on SGU data. B. Surface elevation (m a.s.l.) shown in a digital elevation model. DEM based on Lantmäteriet data. Red lines are topographic lineaments. The rose diagram shows the total length of lineaments in 5° orientation classes. C. SGU modelled soil depths. D. Bedrock surface elevation (m a.s.l.) based on SGU data. E. Surface roughness based on standard deviation (SD) of basement bedrock elevations. F. Basement bedrock summit envelope surface. G. Erosion depth derived by subtracting D from F.*

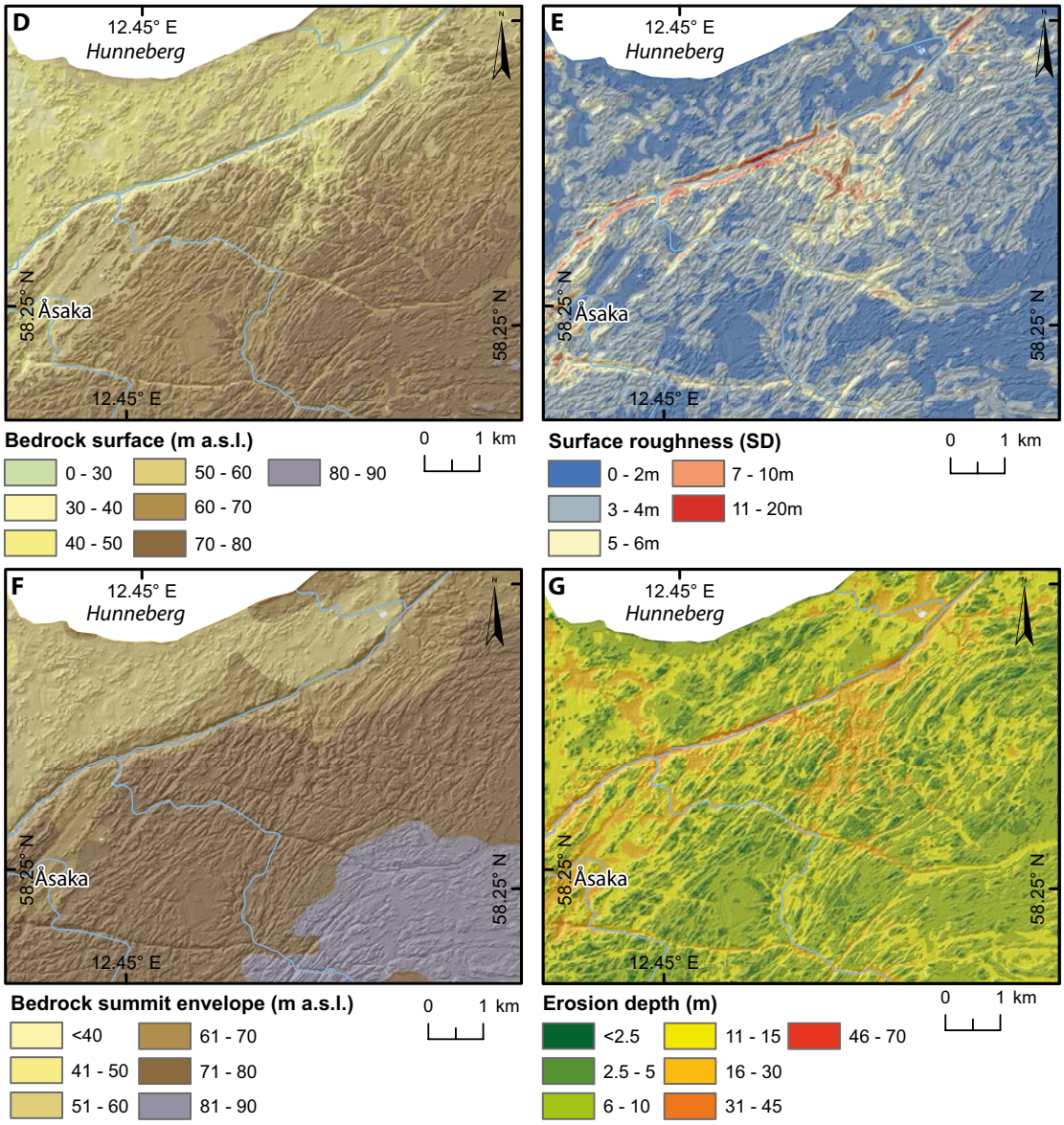

Figure 3-17. *Continued.*

The basement bedrock surface (Figure 3-17D) shows the strong influence of sinuous, NE-SW aligned bedrock structures. Basement surface roughness remains low across basement highs (Figure 3-17E) but is generally slightly greater than in the Vargön area. The bedrock summit envelope surface at 1 km spacing is near planar and inclined towards the NNW (Figure 3-17F). Subtraction of the present basement surface from the summit envelope surface indicates erosion depths of < 5 m across basement highs but widespread erosion of strike-aligned trenches to depths of < 15 m (Figure 3-17G).

In summary, in the Åsaka area, the summit envelope surface has a near planar form. It stands 2–5 m below the buried unconformity south of Hunneberg. The relief on the summit envelope surface is < 10 m and it is inclined to the NNW at 0.25 %. The small height difference between the buried unconformity and the exposed basement south of Hunneberg and the similar inclinations between the summit envelope surface and the buried unconformity on the SW flank of Hunneberg indicate that the summit envelope surface provides a close approximation to the re-exposed unconformity. U2 in this area was also a gently tilted, near planar surface.

3.3.3 Morphology of the Trollhättan area

The Trollhättan area (Area 3) is centred on the town and stands on Fault Block D, 5–7 km W of the base of Hunneberg (Figure 2-4). Red, coarse-grained to porphyritic granite gneisses predominate, with more mafic lithologies only appearing W of the Göta Älv (Figure 3-18A). Gneissic foliation dips towards the NW and NNW (Samuelsson and Lundqvist 1988). Many fractures are aligned NNE-SSW along strike (Figure 3-18B). The Göta Älv follows a major shear zone (Tirén and Beckholmen 1992) along the Vänern-Göta Fault, with a pronounced fault scarp west of the river on the edge of Block C (Figure 3-31).

The surface relief is subdued and the ground slopes towards the NNE (Figure 3-18B). Soil depths are low, and bedrock is exposed widely (Figure 3-18C). At Hullsjön, to the E, the Quaternary fill thickens to a maximum depth of 30 m in a 2–3 km wide linear depression, oriented to the NNW.

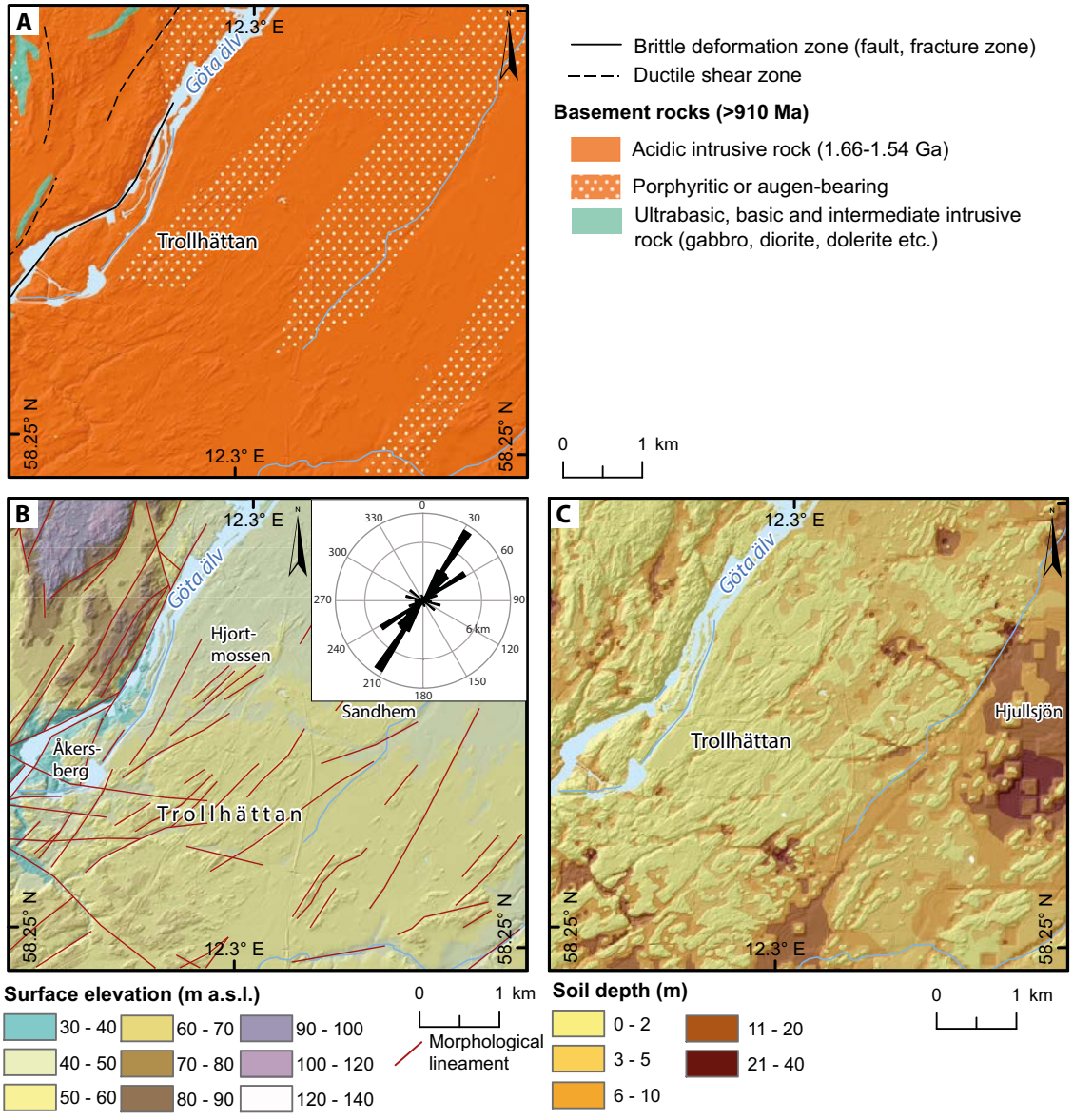

Figure 3-18. *The Trollhättan area. A. Geology based on SGU data. B. Surface elevation (m a.s.l.) shown in a digital elevation model. DEM based on Lantmäteriet data. Red lines are topographic lineaments. The rose diagram shows the total length of lineaments in 5° orientation classes. C. SGU modelled soil depths. D. Bedrock surface elevation (m a.s.l.) based on SGU data. E. Surface roughness based on standard deviation (SD) of basement bedrock elevations. F. Basement bedrock summit envelope surface. G. Erosion depth derived by subtracting D from F.*

The uplifted fault Block C to the NW of Trollhättan reaches elevations of > 100 m a.s.l. The bedrock surface E of the Göta Älv, however, is subdued and descends northwards from 67 to 45 m a.s.l. (Figure 3-18D). Elevation differences between neighbouring rock summits are small (< 4 m) and no large hills rise above general summit levels. Strike-aligned edges and trenches show the strong influence of NE-SW oriented bedrock fractures. Southwest of Trollhättan, the relief increases slightly, with scattered low, flat-topped hills, rising 5–20 m above the surrounding sediment-filled lows (Fredén 1982, Johansson et al. 2001b).

Bedrock surface roughness is high along the Göta Älv and on fault Block C. Roughness is very low around Trollhättan, increasing towards the SW and SE (Figure 3-18E). The summit envelope surface at 0.25 km spacing is near planar on Block D and slopes at 0.3 % to the NNE (Figure 3-18E). Estimated erosion depths are < 5 m over wide areas around Trollhättan but reach < 45 m in trenches and basins on Block C and < 30 m in depressions SW, S and SE of the town (Figure 3-18G).

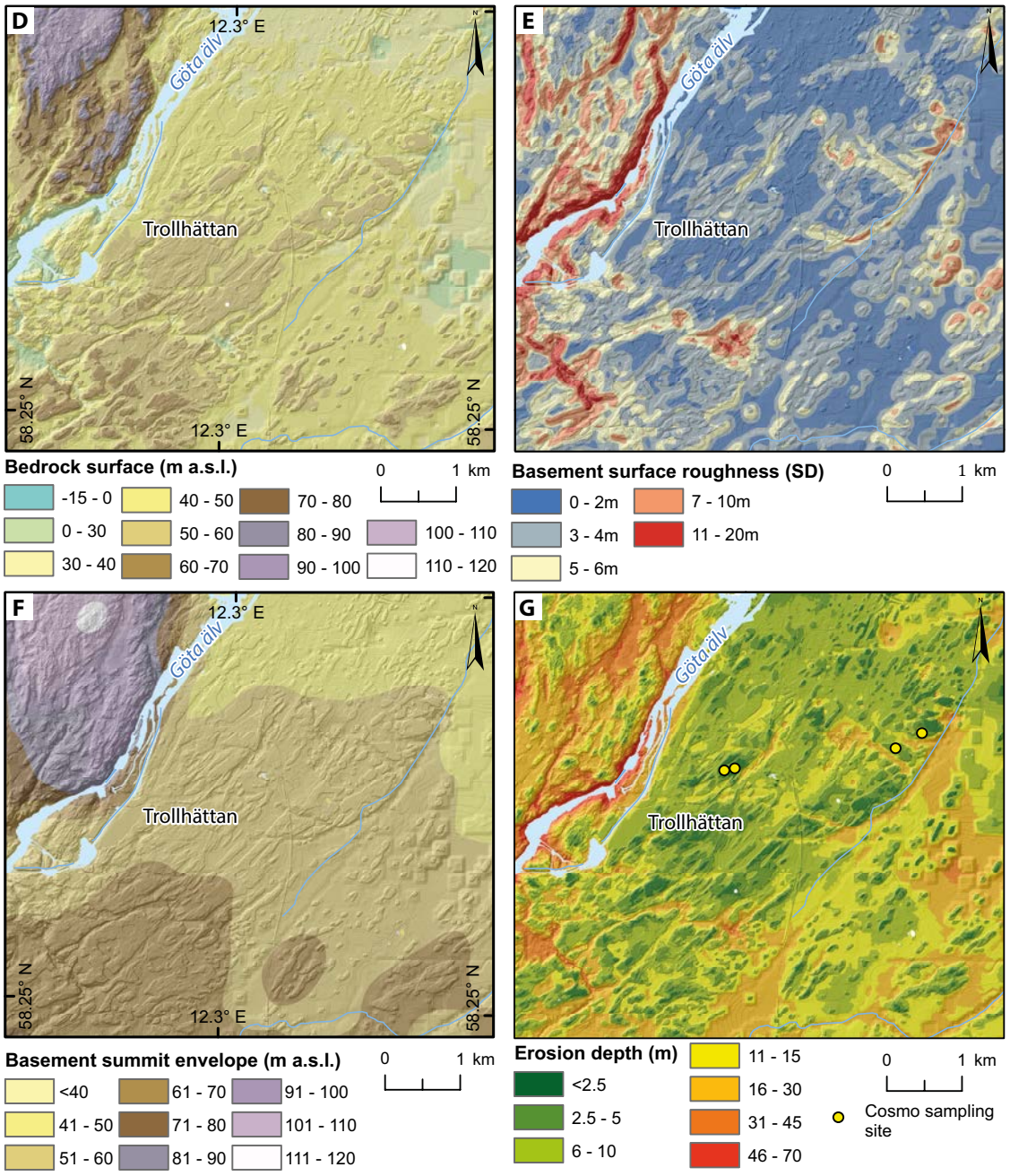

Figure 3-18. *Continued.*

In summary, in the Trollhättan area, the summit envelope surface has a near planar form. The relief on the summit envelope surface is generally < 4 m. The form of the summit envelope surface is similar to that in the Vargön area which lies immediately to the N across the Lilleskog Fault. The inclination of the surface (0.3 %) is close to that of the equivalent surface in the Åsaka area (0.25 %) that also stands on Fault Block D. These similarities in form and inclination indicate that the summit envelope surface around Trollhattan closely approximates to U2.

3.3.4 Morphology of the Sjuntorp area

The Sjuntorp area (Area 4) stands 10–15 km SW of Hunneberg on Fault Block D. Grey and red granite gneisses predominate, with frequent quartz and pegmatite veins. Gneisses of intermediate to basic composition also occur locally (Figure 3-19A). The main fracture sets are NE-SW oriented shear zones (Figure 3-19B) and a WNW-ESE joint system (Larsson 1963).

The surface relief descends northwards from an elevation of 100 m to below 50 m a.s.l. (Figure 3-19B). The Slumpån Älv occupies a SW-NE oriented trench. A shallower trench runs W-E, following a fracture between Sandbacken and Visslaån. Bedrock is exposed over wide areas but glacial deposits thicken towards the NE, exceeding depths of 20 m in the Hullsjön and Saint Bredäng depressions (Figure 3-19C).

The bedrock surface (Figure 3-19D) shows clear contrast across the Sjölanda Fault, with the numerous and deep, structurally-aligned depressions and valley floors up to 20 m below summits found S of the Fault. Basement surface roughness also increases sharply across the Fault (Figure 3-19E). To the N, the bedrock terrain is smooth, with rectilinear rock hills showing summit elevations within a 10 m height range, oriented SW-NE and rising < 5 m above sediment-filled depressions (Figure 3-20). To the S, across a marked topographic step, up to 15 m high, the terrain is rougher (Figure 3-21). Hilltops are restricted in extent, show a 20 m elevation range, and have rounded tops and plucked lee faces. Rock basins and trenches cover 40 % of the area, with rectilinear, fracture-guided shapes. The southern part of the Sjuntorp area has the deepest depressions, highest summit elevation range and greatest roughness (Figure 3-19E) found in the detailed study areas. The bedrock summit envelope surface at 0.25 km spacing shows a step across the Sjölanda Fault, with inclination on blocks towards the N (Figure 3-19F). Estimated erosion depths are < 10 m over wide areas N of the Sjölanda Fault (Figure 3-19G). On the block S of the Fault, erosion depths in trenches are < 30 m but reach < 70 m in the broad trenches along the Slumpån valley.

In summary, in the Sjuntorp area, the summit envelope surface has a near planar form only to the N of the Sjölanda Fault. The relief on the summit envelope surface here is generally < 8 m, with inclination of 0.3–0.5 % to the N. This northern area represents a continuation of the topography found to the N at Trollhattan. South of the Fault, summit altitudinal range increases to 20 m and surface roughness and relief increase sharply. Here the summit envelope surface morphology is interpreted to represent more advanced glacial modification of U2.

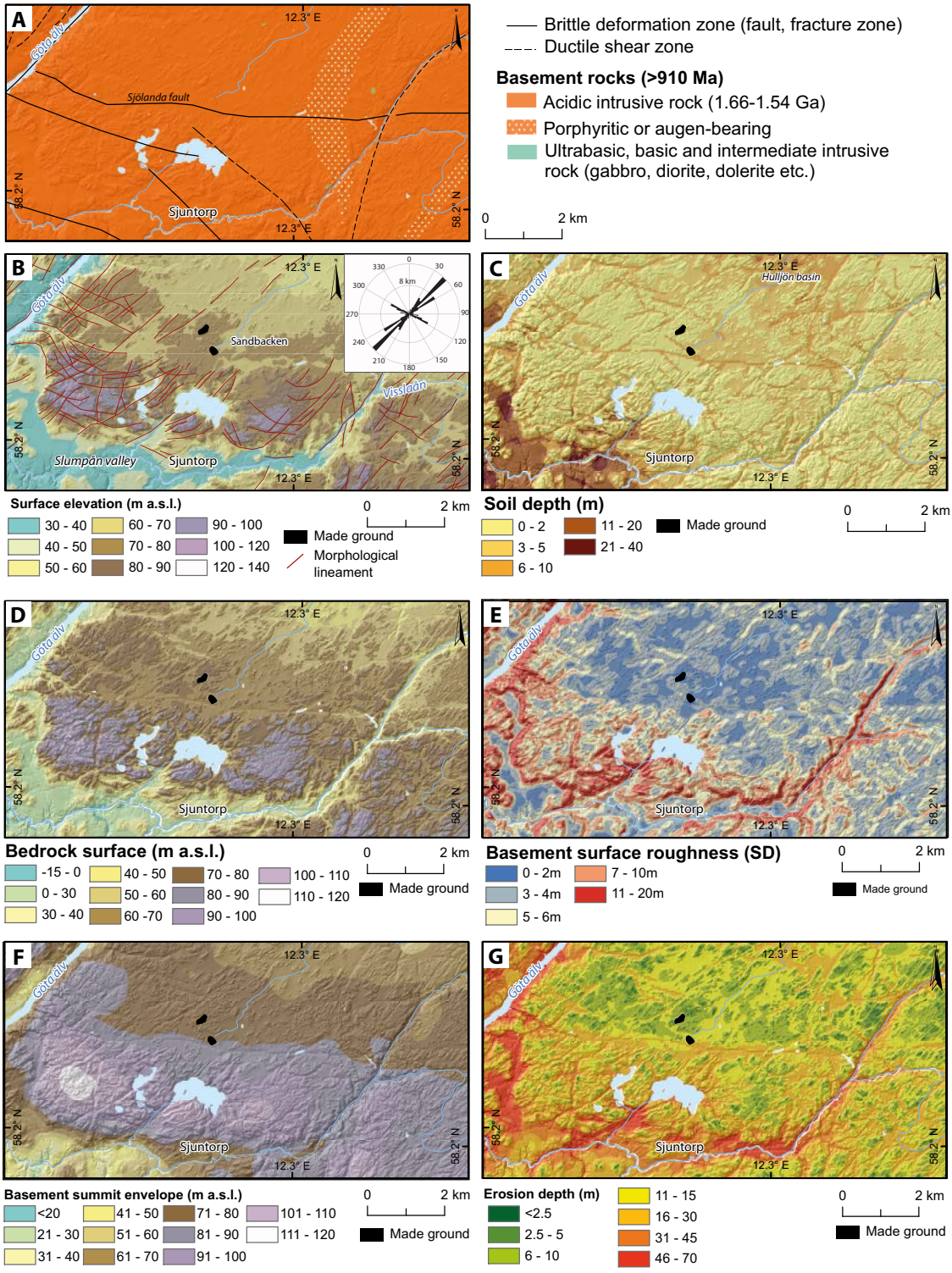

Figure 3-19. *Sjuntorp area. A. Geology based on SGU data. B. Surface elevation (m a.s.l.) shown in a digital elevation model. DEM based on Lantmäteriet data. Red lines are topographic lineaments. The rose diagram shows the total length of lineaments in 5° orientation classes. C. SGU modelled soil depths. D. Bedrock surface elevation (m a.s.l.) based on SGU data. E. Surface roughness based on standard deviation (SD) of basement bedrock elevations. F. Basement bedrock summit envelope surface. G. Erosion depth derived by subtracting D from F.*

Figure 3-20. *Lindveden, 3.3 km N of Sjuntorp, part of the subdued terrain N of the Sjölanda Fault. A. DEM showing the landfill mound (tip) and the surrounding low bedrock terrain. Note the strong control on topography from the SW-NE oriented fracture set. B. View N towards Trollhättan from the landfill mound across a clear-cut area within forest with low bedrock risers (arrowed).*

Figure 3-21. *Fornborg, 2 km NW of Sjuntorp. A. DEM showing the roughened terrain S of the Sjölanda Fault. Hilltops remain accordant at 104–108 m a.s.l. but are separated by 100 m wide rock trenches and basins with till-covered floors at 80 m a.s.l. B. Prominent rock knob viewed from the NNE rising 15 m above its base (photo location and orientation shown in box in A). Granite gneiss with bounding N-S oriented fractures.*

3.3.5 Planar flats

Slättbergen or *planar flats* are smooth, bare bedrock surfaces with relief of < 1–2 m over distances of 0.1–0.9 km flanked by steep rock slopes. Planar flats are found mainly in the low relief terrain between the western flanks of Halleberg and Hunneberg and the valley of the Göta Älv at Trollhättan (Figure 3-22). Small planar flats occur east of the hills at Gaddesanna (Rudberg et al. 1976) and, more extensively, on the southern shore of Dättern (Figure 3-22). Close to the Vänern shoreline, the planar flats stand < 4 m above their immediate surroundings and form extensive rock surfaces (Figure 3-23). Around Trollhättan, planar flats form rectilinear, flat-topped hills and ridges, edged by rock cliffs and slopes, separated by fracture-guided, sediment-filled valleys up to 8 m deep. Nearby rock summits are accordant or a few metres lower in elevation, but no planar flats have been recognised on lower ground. Planar flats have been reported previously at Nordkroken (Munthe 1915) and at three locations within the town of Trollhättan (Mattsson 1959, 1962). Six new planar flat localities have been identified from DEMs and confirmed by field inspection (Figure 3-22). The planar flats are most numerous in Areas 1 (Vargön on Fault Block B) and 3 (Trollhättan on Fault Block D) and are described in detail for those areas below. Planar flats also occur on where the basement unconformity emerges from beneath basal Mickwitzia Sandstone on the lakeshore at Kinnekulle (Figure 3-11F).

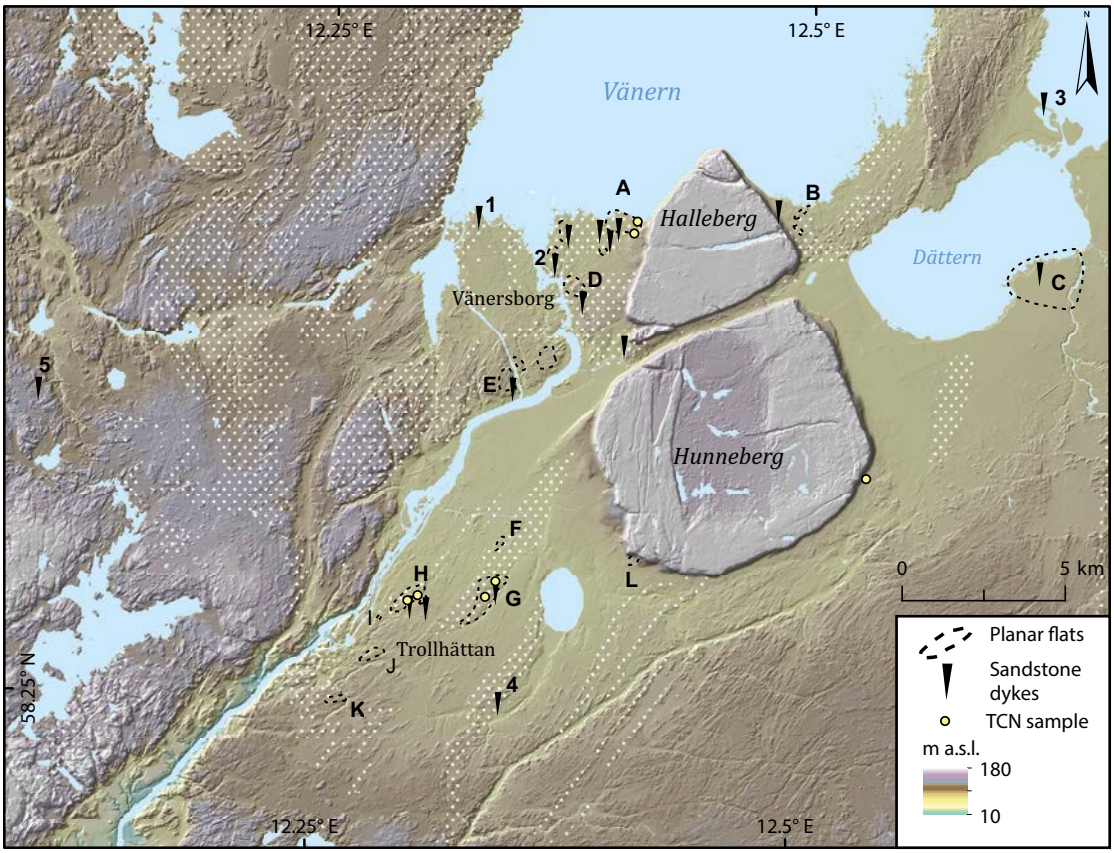

Figure 3-22. *Planar flats and sandstone dyke localities in the Trollhättan region. Planar flats: A. Nordkroken. B. Gaddesanna. C. Nybölet. D. Vargön. E. Onsjö. F. Kåtene. G. Sandhem. H. Hjortmossen. I. Starkodders. J. Eriksro. K. Ryrbäcken. L. Hårrum. Sandstone dykes: 1.Vänersborg. 2. Gubbelyckan. 3. Marieholme. 4. Altorp Cross. 5. Väne-Ryr. Dots indicate porphyritic granite gneiss types (from SGU data). Terrestrial cosmogenic nuclide (TCN) sample sites indicated. DEM based on Lantmäteriet data.*

Planar flats around Trollhättan are found only in coarse-grained to porphyritic or augen-bearing granite gneiss. The distribution of this rock type as shown on SGU maps is, however, much wider than that of planar flats (Figure 3-22). Planar flats are seen in DEMs and in the field to be developed across the steeply-inclined gneissic foliation and the main vertical and inclined fracture sets. Spacing of vertical or steeply-inclined fractures on planar flats exceeds 10 m locally but spacing of > 4 m is more common. Fractures of < 1 m spacing on planar flats are found only in narrow rock bands which are enclosed by large rock blocks with > 5 m spacing that have provided protection from glacial erosion. The vertical fractures occur as long (> 10 m), single cracks, seen locally *en echelon* at Hjortmossen.

Area 1 includes, at Nordkroken, a type site of the SCP, first described over a century ago (Munthe 1915), as well as extensive planar flats and a high frequency of sandstone dykes (Figure 3-22). Planar flats drop in elevation northwards from 54 m a.s.l. at Vargön to 44 m a.s.l. at the Lake Vänern shoreline (Figure 3-23). Planar flats and summits N of Vargön conform in profiles to a near-planar basement surface inclined at 0.3 % to the N (Figure 3-16). Adjacent summits with curved upper surfaces and plucked lee faces stand at similar elevations (Figure 3-15). At Nordkroken, a remarkably flat surface is exposed in granite gneiss, over 500 m wide and dipping to the NW (Figure 3-23). Similar flat surfaces, although generally more fragmented, and standing slightly higher than their surroundings, can be traced westwards for 2.8 km and southwards towards Vargön (Rudberg et al. 1976) and Onsjö (Figure 3-22). The flat surface at the Lake Vänern shoreline is separated from the base of Halleberg at Nordkroken by a 300 m wide depression (Figure 3-14). The height difference between the planar flat and the base of the Early Cambrian sandstone at the foot of Halleberg is estimated at ~6 m (Figure 3-9). Relationships are complicated however by the possibility of minor displacement along a fault that passes between the lake shore platform and the hill (Section 3.4.1).

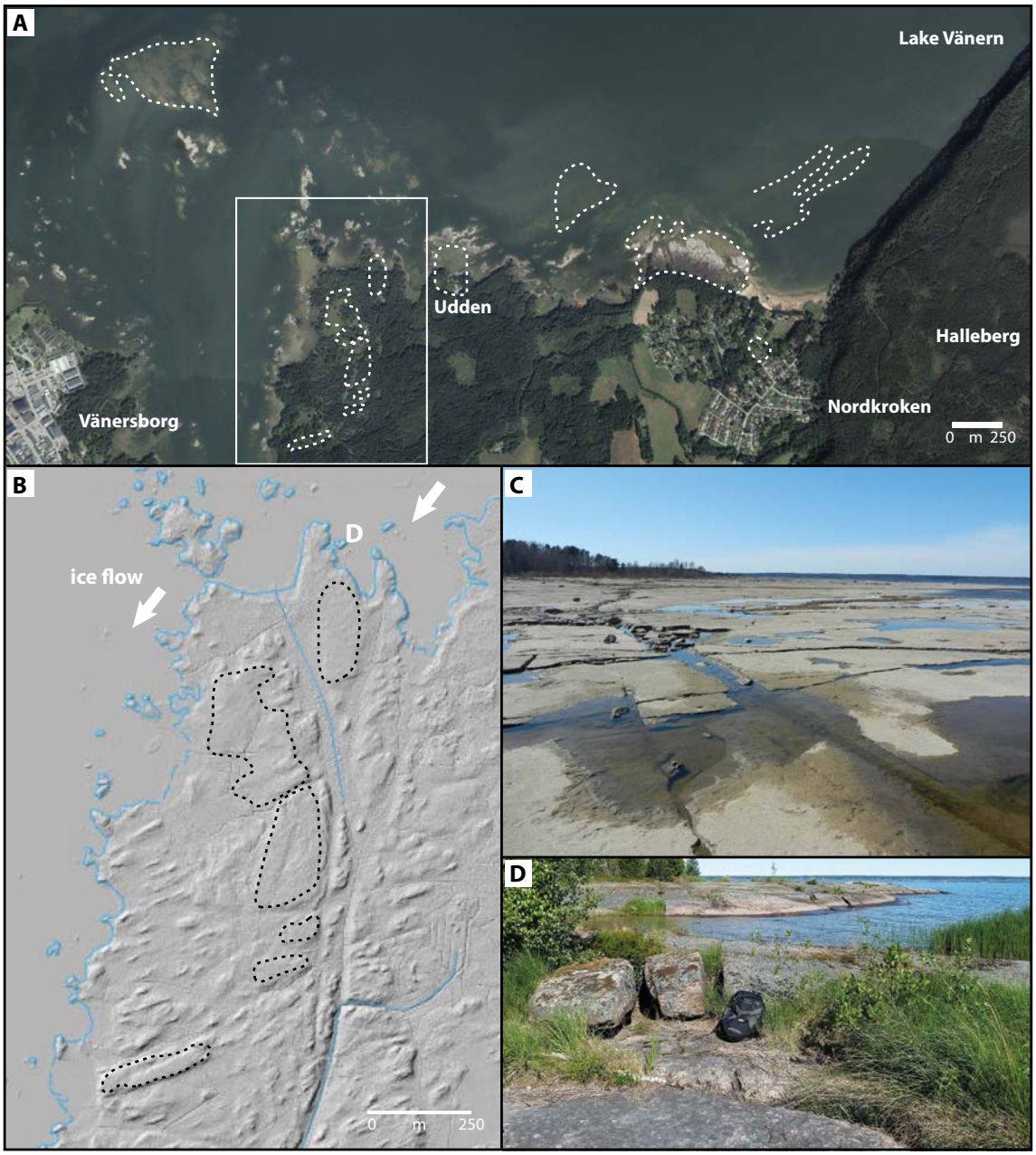

Figure 3-23. *The gneiss surface along the shoreline of Lake Vänern, W of Nordkroken. A. Vertical air photo showing the near-planar basement surface dipping to the N beneath the lake but maintaining a constant elevation from W to E towards concealed Early Palaeozoic cover rocks at Halleberg. Main planar flats shown as dashed white lines. B. DEM of the western part of the area based on Lantmäteriet data. Relief is < 4 m between planar flat tops (delineated by dotted lines) and adjacent depressions. S-N profiles across this area are shown in Figure 3-16. C. The shoreline at Nordkroken, looking W. Porphyritic granite gneiss with orthogonal vertical fractures with spacing of 2 to > 10 m. Horizontal fractures with ~10 cm spacing occur to at least shallow depth. D. Shoreline W of Udden. Ice movement from R to L. Rounding of stoss faces and loosening of blocks along closely-spaced vertical fractures seen on lee faces. Stoss-side rounding is apparent on many bedrock risers in B.*

On Fault Block D, planar flats rise southwards from 45 m a.s.l. at Kåtene, through the town of Trollhättan to a final degraded fragment at 67 m a.s.l. at Ryrbäcken (Figure 3-22), with an average gradient of 0.3 % (Figure 3-24). The planar flats are box-shaped and elongate in a SW-NE direction, with lengths of 0.5–1.7 km and widths of 0.3–0.9 km. In the town of Trollhättan, planar flats, up to 0.5–0.75 km long, form low, tabular hills at Eriksro, Hjortmossen and Sandhem with summits at 60–48 m a.s.l. (Figure 3-25). Surrounding bedrock highs stand 1–5 m lower in elevation but lack planar flats and instead show typical roche moutonnée forms. At Kåtene (Figure 3-26) and Starkodders, the planar flats are residual features, found as small (~100 m long), low (1–4 m above surrounding rock outcrops), isolated, tabular hills. The surfaces of individual planar flats dip at 0.3–0.4 % to the N (Figure 3-24). Intervening zones of more closely-spaced fractures have been exploited by glacial erosion to form fracture-guided valleys up to 8 m deep.

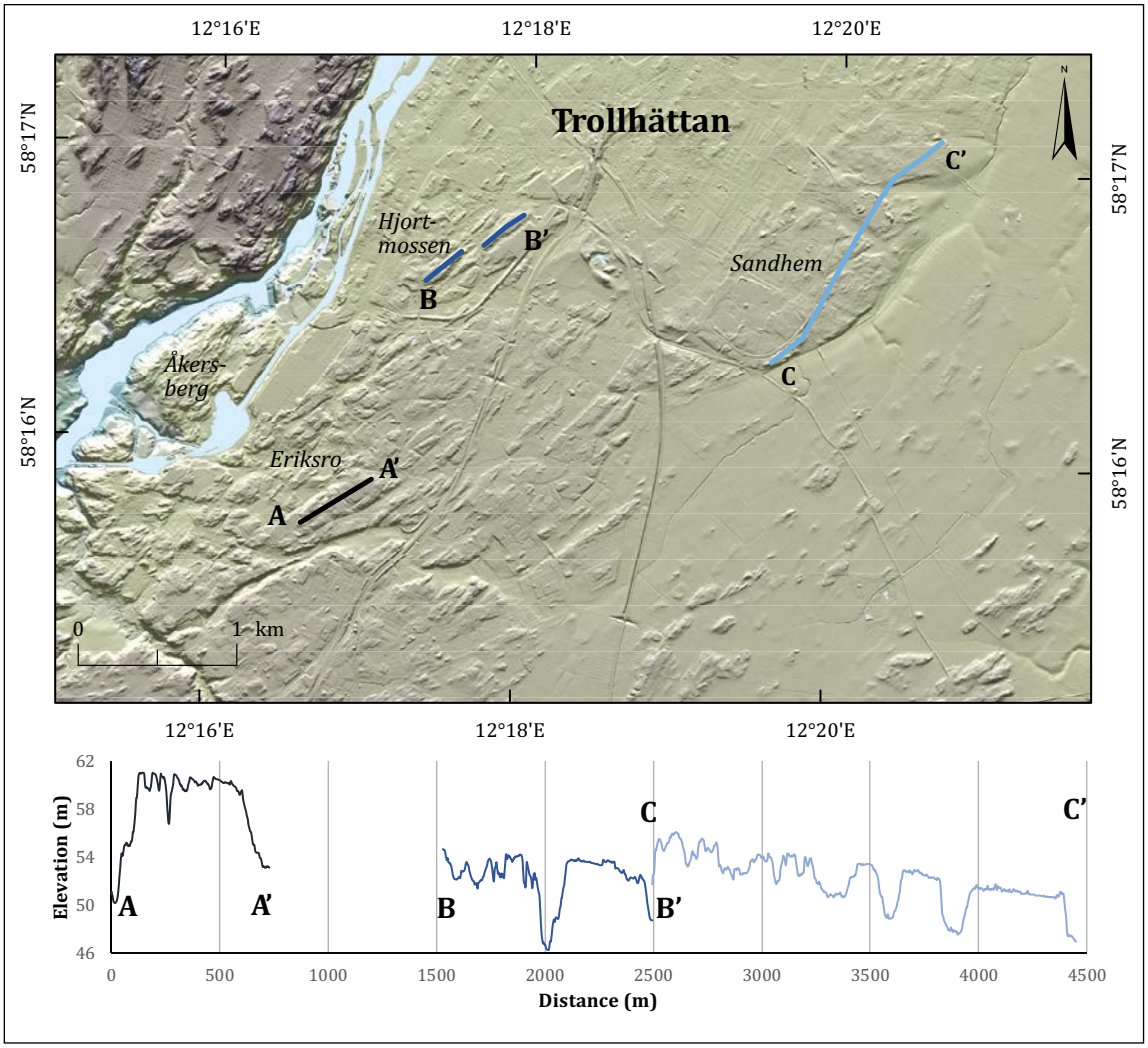

Figure 3-24. *Slope profiles for planar flats at Trollhättan plotted SW-NE parallel to gneiss foliation. DEM based on Lantmäteriet elevation data.*

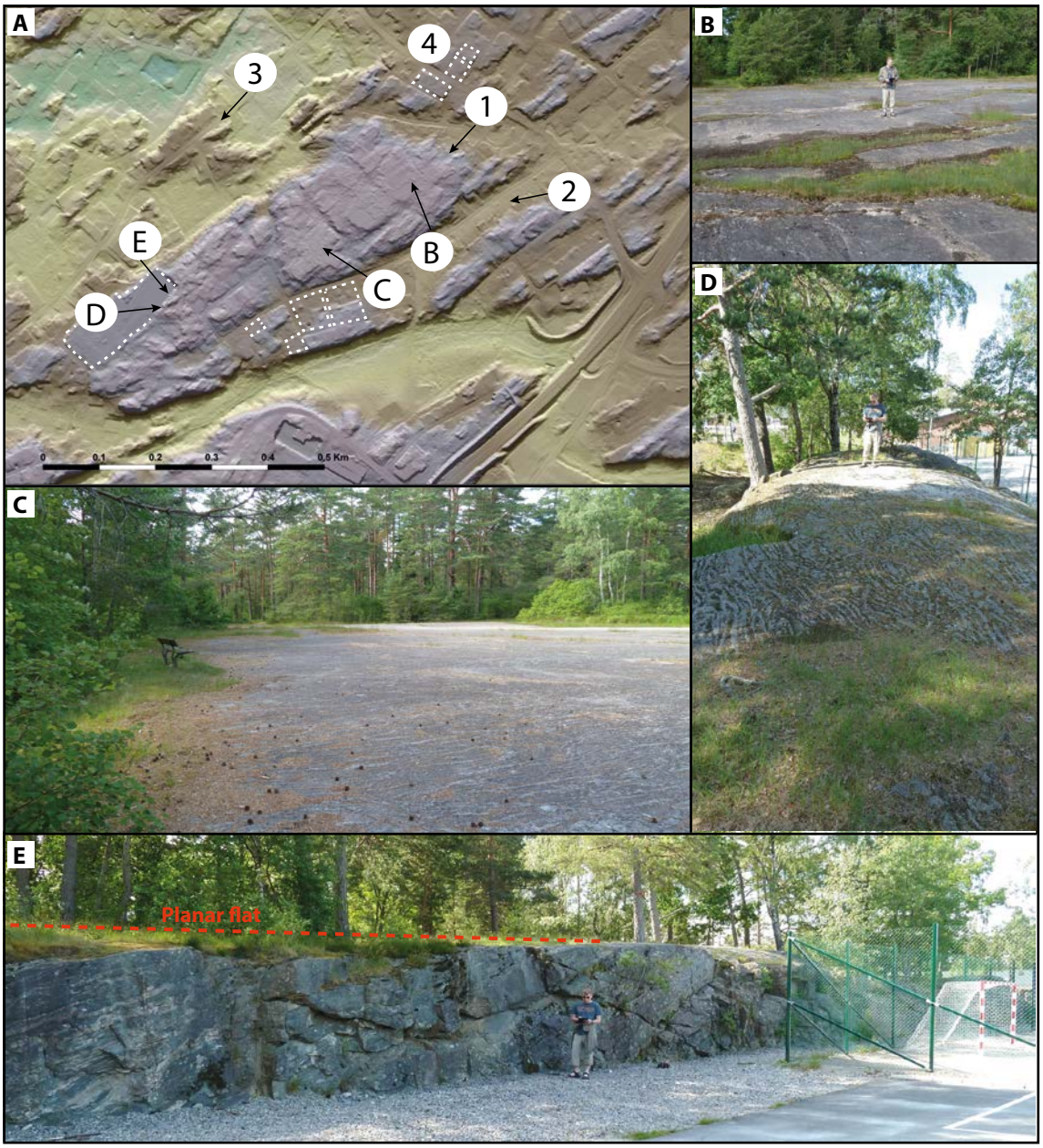

Figure 3-25. *Planar flats at Eriksroparken, Trollhättan. A. DEM of topography at Eriksroparken. B–E refer to photo locations. 1. Rounded stoss face of hill. 2. Valleys excavated along fractures. 3. Slope conforming to inclined fractures oriented SW-NW and with the grain of the basement topography seen in A. 4. Footprints of man-made structure in the vicinity of Eriksroparken. B. Glacially-polished surface, with shallow grooves and low ridges after glacial abrasion. C. Large planar flat dipping 0.25° to the NE. D. Small planar flat remnant on narrow ridge with lateral plucking of edges. E. Quarry section in the side of the ridge in F showing development of this planar flat across inclined and near-vertical fractures.*

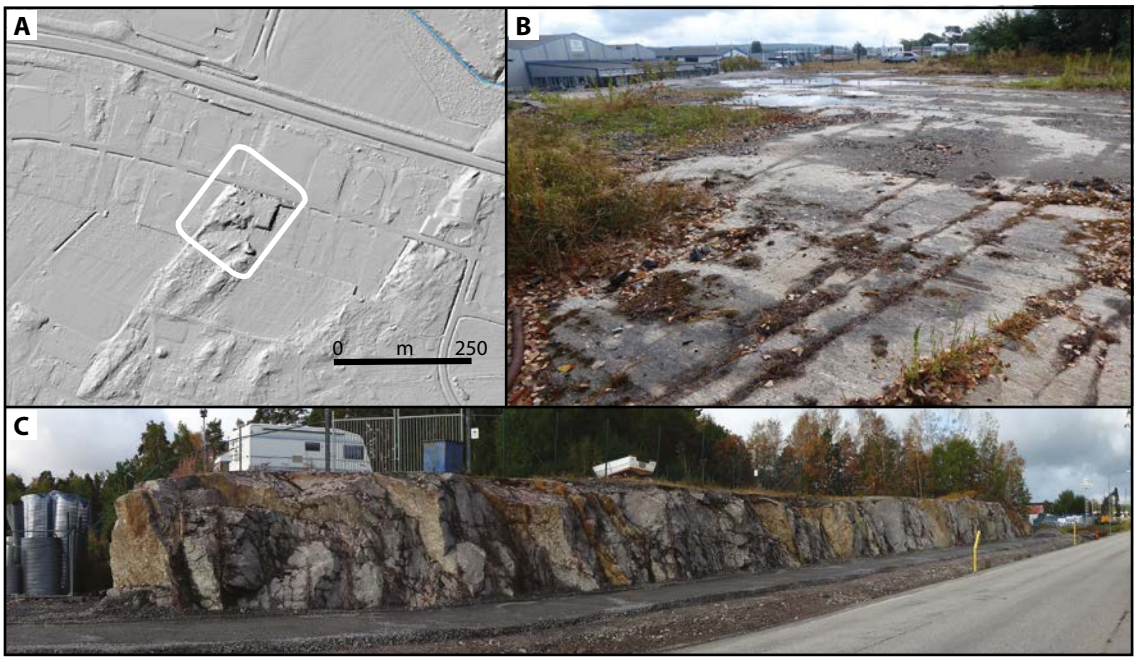

Figure 3-26. *Kåtene. A. DEM based on Lantmäteriet data showing planar flat location. B. Planar flat surface. C. Planar flat in section. Note the prominent fracture set dipping to the NW with gneiss foliation. Sheet fractures are absent; the surface slope is developed across steeply inclined fractures. Former ice flow was southwards, perpendicular to the section. No sandstone dykes were observed.*

3.3.6 Weathering on the buried and exposed unconformity

In Sweden, weathering of basement rocks below U2 is generally thin or absent (Hall et al. 2019). In Västergötland, weathering profiles below the sub-Cambrian unconformity, if present at all, were generally only metres to decimetres thick (Calner et al. 2013). At Lugnås, the weathered layer is 1.5 m to several metres deep (Holm 1901, Mattsson 1962) but has been partially re-cemented (Lidmar-Bergström et al. 1997). Cementation, probably developed during diagenesis of the overlying sandstone, has prepared the uppermost basement surface for mining of gneiss blocks for millstones (Lindstrom and Vortisch 1978). At Kinnekulle, previous observations indicate that the weathered layer on U2 is cm to dm thick beneath the Early Cambrian unconformity (Högbom and Ahlström 1924). At both locations, it is uncertain to what extent this thin, weathered layer represents subaerial weathering before Early Cambrian transgression, burial diagenesis, brine circulation (Harper et al. 1995) and/or low-grade metamorphism. No saprolite has been reported or observed during this survey on the buried Cambrian unconformity or from the exposed basement in Trollhättan region exposed in quarries (Section 3.4) and other man-made sections. Where Cambrian sandstone dykes occur in vertical fractures, the fracture surfaces are fresh but may retain mineral coatings (Mattsson 1959). These fractures were formed or opened in granite gneisses on basement surfaces that carried little or no weathering at the time of dyke formation in the Early Cambrian. As variable mineralogy and fracturing give uneven depths of weathering in gneissic bedrock (Hall 1986, Olvmo et al. 1999, Krabbendam and Bradwell 2014, Hall et al. 2015), the general lack of a thick weathering or soil layer on U2 at the time of burial is consistent with the continuous, smooth, planar form of the buried unconformity and its exposed edge along the shore of Lake Vänern.

In Västergötland, evidence for significant weathering of U2 after re-exposure is also lacking. Surficial, likely post-glacial, weathering of mafic dykes is found locally on the exposed basement surface (Mattsson 1962). Brown iron oxide coatings are developed to ~2 m depth in vertical and steeply-inclined fracture faces at Sandhem (Figure 3-27A), Kåtene and elsewhere (Mattsson 1962) and to depths of > 10 m in the Vänersborg Quarry (Figure 3-34) and to shallower depths at Kuleskog (Figure 3-36).

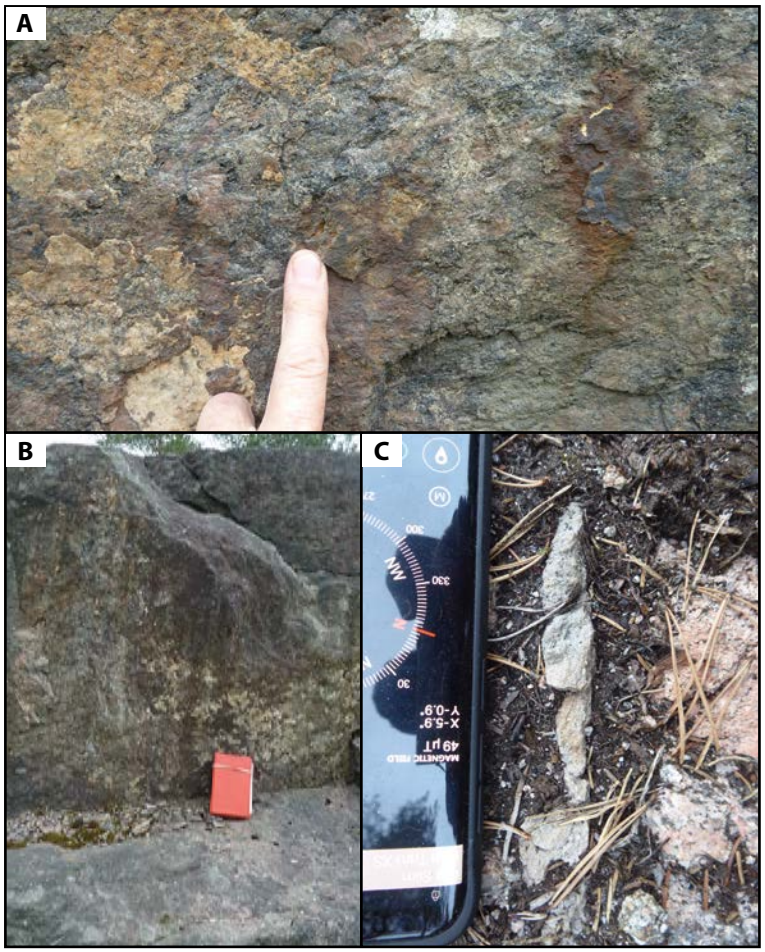

Figure 3-27. *Limited weathering of fracture surfaces below planar flats. A. Sandhem planar flat. Vertical fracture surface at < 1 m depth with Fe oxide and calcite coatings. B. Sandhem planar flat. Vertical fracture surface at < 1 m depth with calcite coatings. C. Onsjö planar flat. Unweathered coarse-grained sandstone dyke in vertical fracture in porphyritic granite gneiss.*

Similar iron oxide staining is seen immediately below the sub-Cambrian unconformity at Kinnekulle (Figure 3-11). It is unclear how the iron oxide coatings relate to pre- and sub-Cambrian, Pleistocene and recent weathering episodes. The widespread preservation of calcite (Figure 3-27B) and other weathering-susceptible mineral coatings in the near surface (Mattsson 1962) indicates very limited weathering of the basement since re-exposure. The Cambrian sandstone dykes, where preserved on the present basement surface, also remain unweathered (Figure 3-27C). The absence of saprolite and presence of unweathered sandstone dykes and calcite fracture coatings are features consistent with recent re-exposure of basement at the sub-Cambrian unconformity.

3.3.7 Comparison of the buried unconformity and surrounding exposed basement surfaces

Around the flanks of Halleberg and Hunneberg, the edge of the preserved unconformity where it remains buried by Early Cambrian sandstone has an elevation range of 4–9 m that compares to a range of 4–5 m for summits on the exposed basement nearby (Table 3-1). At Kinnekulle, the re-exposed sub-Cambrian unconformity has a relative relief of < 3 m (Figure 3-10). Available evidence indicates that the buried unconformity surface at these localities is nearly planar and smooth at the macro- and local scales (Figure 3-3 and 3-10), with only metre-scale roughness at the meso-scale (Figure 3-10). At Halleberg and Hunneberg, the sedimentary cover overlying the unconformity, the unconformity itself and summit envelope surfaces for the surrounding basement beds are inclined to the N to NNW at gradients of 0.21–0.42 %. The maximum height difference between the preserved unconformity

and adjacent basement summits is generally 2–6 m, reaching 9 m on the SE flank of Halleberg (Figure 3-4). Small height differences are also apparent around the edges of other Early Palaeozoic outliers in Västergötland (Figure 3-1). The close similarities between the form, elevation and inclination of the buried unconformity and the surrounding basement summit elevations indicate that the exposed basement in proximity to these hills closely approximates to the glacially modified surface of the sub-Cambrian unconformity.

Profiles on Block D along the southern flank of Hunneberg allow direct comparison of the morphology of the preserved unconformity with the present basement surface over a wider area (Figure 3-28). Along this 20 km long belt, no hill rises > 10 m above its neighbouring summits. Profiles 1–3 join basement summits that lie within an elevation range of < 15 m at distances of 2–11 km from the unconformity edge along the profiles. The mid-section of Profile 2 follows basement along the edge of the unconformity (c.f. Figure 3-7). The equivalent section of Profile 3 is seen to be lower in elevation and rougher in relief. Block D is gently inclined to the north at ~0.3 % (Johansson et al. 1999). After allowing for this inclination, the difference in elevation between summits on the edge of the preserved unconformity and on the exposed basement is < 5 m. The smooth, near-planar form of the buried unconformity is maintained at a slightly lower elevation when projected across exposed basement summits (Figure 3-28).

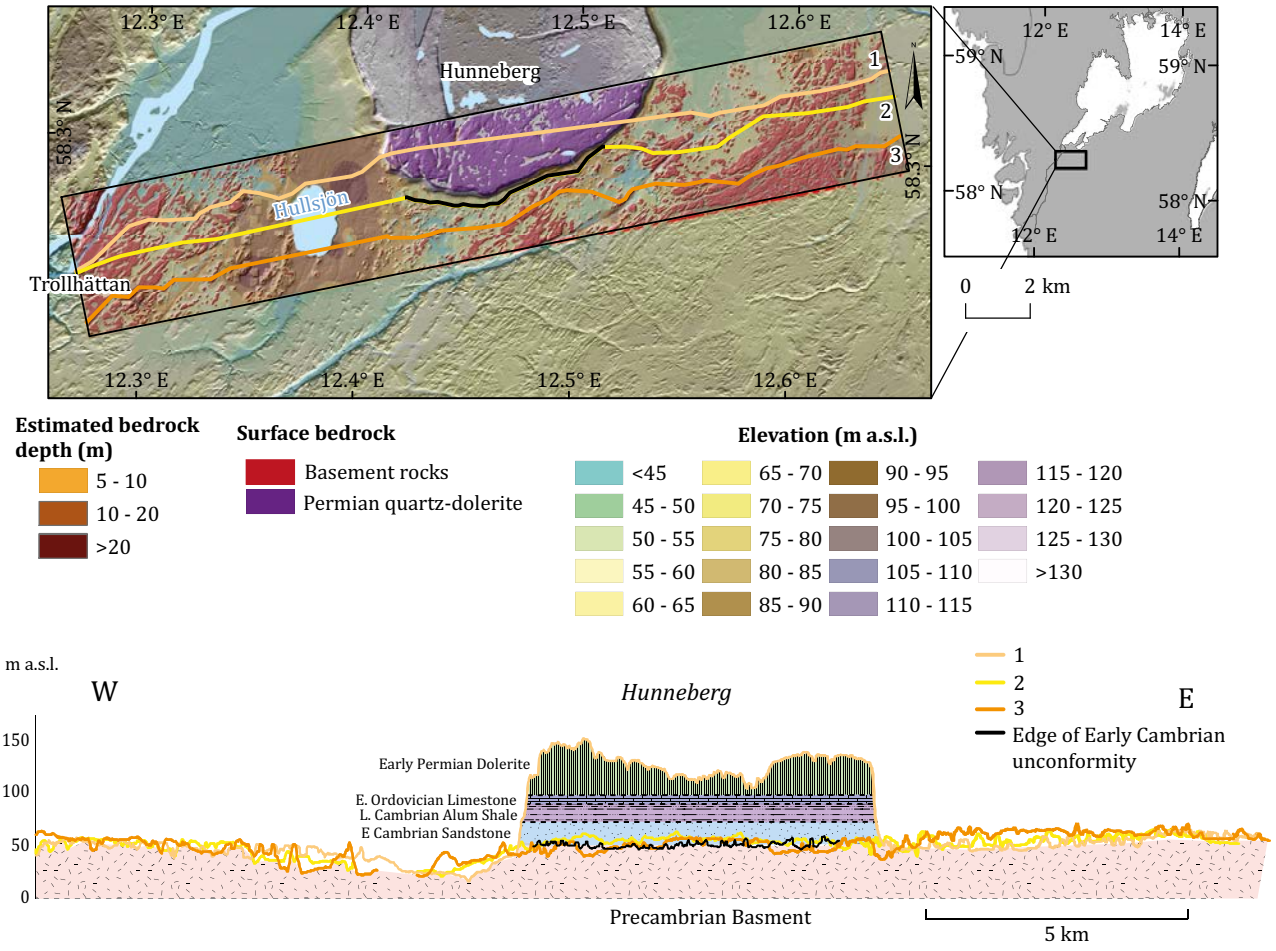

Figure 3-28. *Topographic profiles along the southern flank of Hunneberg. The panel shows estimated depths to bedrock based on SGU soil depth data along the swath. Profiles 1, 2 and 3 follow exposed rock summits where crossing basement. The middle part of Profile 2 follows basement summits < 200 m from the edge of the sub-Cambrian unconformity (see also Figure 3-7). DEM and profiles based on Lantmäteriet elevation data.*

The summit elevation surfaces for the Trollhättan region (Figure 3-13) and for Areas 1 to 4 (Figure 3-14 and Figures 3-17 to Figure 3-19) have similar low relief, elevation and inclination to the unconformity and to the adjacent exposed basement around Halleberg and Hunneberg. Planar flats form local highs and so are integral to the summit envelope surfaces. This coincidence requires that, at least close to the edge of Halleberg and Hunneberg, the planar flats, like other summits, remain, at most, only a few metres below the original unconformity. Summit envelope surfaces maintain elevations within 2–15 m of the buried unconformity at distances 0–11 km from outliers. No hills rise > 6 m above surrounding summits in Areas 1 and 3 or > 10 m above the projected preserved unconformity (Figure 3-28). These results provide strong support for the previous use of summit elevations in trend surfaces and profiles to map the sub-Cambrian peneplain in Västergötland (Johansson 1999, Johansson et al. 1999, 2001b). The summit envelope surfaces represent the slightly lowered basement unconformity and so provide reference surfaces for assessments of its dislocation by faulting and its modification by glacial erosion.

Table 3-1. Comparison of elevations, height differences and gradients for the preserved sub-Cambrian unconformity and the exposed basement. Inclinations are estimated along lines of transects based on available basement exposure.

Criterion	Maximum summit elevation range (m/km) on buried unconformity	Inclination (%) on the buried unconformity	Maximum elevation difference (m) between buried and exposed basement	Inclination (%) of exposed basement	Maximum summit elevation range (m/km) on exposed basement	Transect orientation	Reference or source
Dip of sedimentary sequence		0.30				N	(Sidenbladh 1870)
Edge of unconformity							
Halleberg W flank	6	0.32				N	SGU maps
Hunneberg W flank	4	0.23				N	
Halleberg E flank	7	0.69				NNW	
Hunneberg E flank	5	0.24				NNW	
Gaddesanna	5–8	0.25	3–9	0.36	4	NNW	Figure 3-4
Bragnum	6–9	0.25	4–6	0.25	5	NNW	Figure 3-6
Hårrum	4	–	2–4		4	–	Figure 3-7
Planar flats							
Nordkroken			5	0.36	4	N	
Vargön				0.35	8	N	
Sandhem				0.32	4	N	
Hjortmossen				0.30		NE	
Eriksro				0.23		NE	
Fault Blocks							
A				0.40		N 34 W	(Johansson et al. 1999)
B				0.21		N 8 W	
C				0.26		N 10 W	
D				0.38		N 15 W	
Summit Envelope Surfaces							
Area 1: Restäd to Vänersborg				0.21		NNW	Figure 3-14
Area 2: Åsaka				0.42		NNW	Figure 3-17
Area 3: Trollhättan				0.40		NNE	Figure 3-18
Area 4: Velanda				0.40		NNE	Figure 3-19

3.4 Faults and fractures on the exposed basement

In this section, evidence is presented for the influence of faulting and fracturing on the morphology of the presently exposed basement surface. Faulting of the unconformity is examined in bedrock profiles over distances of 1–10 km. Fracture patterns in the basement at the local scale are well exposed in large quarries with faces of 0.1–0.6 km lateral extent. Fracture patterns at shallow depth are also exposed in road cuts across the surfaces and flanks of planar flats over distances of 0.1–0.9 km. Planar flat surfaces expose numerous sandstone dykes in vertical fractures. Fracture zones may preserve remnants of saprolite in glaciated shield terrain (Krabbendam and Bradwell 2014) and so represent the most likely locations to find evidence of sub-Cambrian and younger weathering in the Trollhättan area.

3.4.1 Faulting and dislocation of the sub-Cambrian unconformity

The sub-Cambrian unconformity in the Trollhättan region has been interpreted as broken by post-Ordovician faulting into tilted blocks of different sizes (Ahlin 1987, Lidmar-Bergström 1991, Johansson 1999) (Figure 2-4). Along the Lilleskog Fault which separates Halleberg and Hunneberg, Early Palaeozoic beds are displaced by ~30 m (Martinsson 1974, Ahlin 1987). The block surfaces have estimated slope gradients in trend surfaces that vary between 0.21 and 0.40 % (Johansson et al. 1999) (Table 3-1). In this section, we present evidence for fault movements at rock block edges and for displacement along fractures within individual blocks.

Where the reconstructed summit envelope surface has a maximum relief of < 5 m between Trollhättan, Vänersborg and Nordkroken, it is possible to identify fault scarps with > 5 m relief. In Area 4 and in terrain W of the Göta Älv, relief on the summit envelope surface is locally > 10 m and here it is only possible to identify potential fault scarps with > 10 m displacement.

Inter-block faults

Four main fault blocks (A–D) have been identified previously (Ahlin 1987) in the Trollhättan region (Figure 2-4). We recognise another fault block (E) in the Sjuntorp area. Profile codes refer to blocks on each side of the faults that define the block margins.

Fault throws across blocks indicated by the profiles can be summarised as follows (Figure 3-29):

- Profile A–B across the Dalbobergen segment of the Vänern-Göta Fault indicates a throw of ~60 m (E side down) between Blocks A and B where it runs along the W shore of Lake Vänern (Figure 3-29).
- Profile A–C indicates a throw of ~23 m (S side down), assuming that summits S of the fault remain close to their original elevation on the unconformity. Ahlin (1987) estimated 30 m of displacement across this fault. Maximum bedrock elevation at the E end of the lineament is 95 m a.s.l. on the gently-inclined summit surface of Block A but 72 m a.s.l. on isolated rock ridges on Block C. Further W at Väne-Ryr the bedrock elevation rises above 100 m a.s.l. N of the fault, but to 83 m a.s.l. immediately to the S before rising to 110 m a.s.l. The small elevation differences here may be solely a result of greater glacial erosion of the fractured basement. The elevation differences along the fault are consistent with dip of Block C towards the N and strike towards the NE.
- Profile B–D crosses the Lilleskog Fault that separates Halleberg and Hunneberg. Halleberg has been moved upward relative to Hunneberg with displacement of the Early Permian sill by > 24 m (Sidenbladh 1870) or by ~30 m (Martinsson 1974, Ahlin 1987). Linear projection of a 0.3 % gradient from the Kåtene planar flat, 3.2 km to the S, indicates a basement elevation of ~34 m a.s.l. against the Lilleskog Fault, 26–32 m below summits on the southern edge of Block B to the N of the river (Figure 3-30). A similar projection E of Halleberg from gneiss knobs around Dättern indicates that the concealed unconformity stands at an elevation of ~35 m a.s.l., 30 m below the highest points to the N. Profile B–D indicates a throw of 30–35 m (Figure 3-29), seen in elevation differences across the fault scarp at Onsjö (Figure 3-30). The consistent heights of throw along the Lilleskog Fault indicate little or no internal dislocation of Block B. The similar throw along the Lilleskog Fault beneath cover at Halleberg and Hunneberg and on the same fault blocks exposed to the west indicates very limited erosion of the raised edge of Block B at Onsjö since its re-exposure from beneath Early Palaeozoic cover rocks.

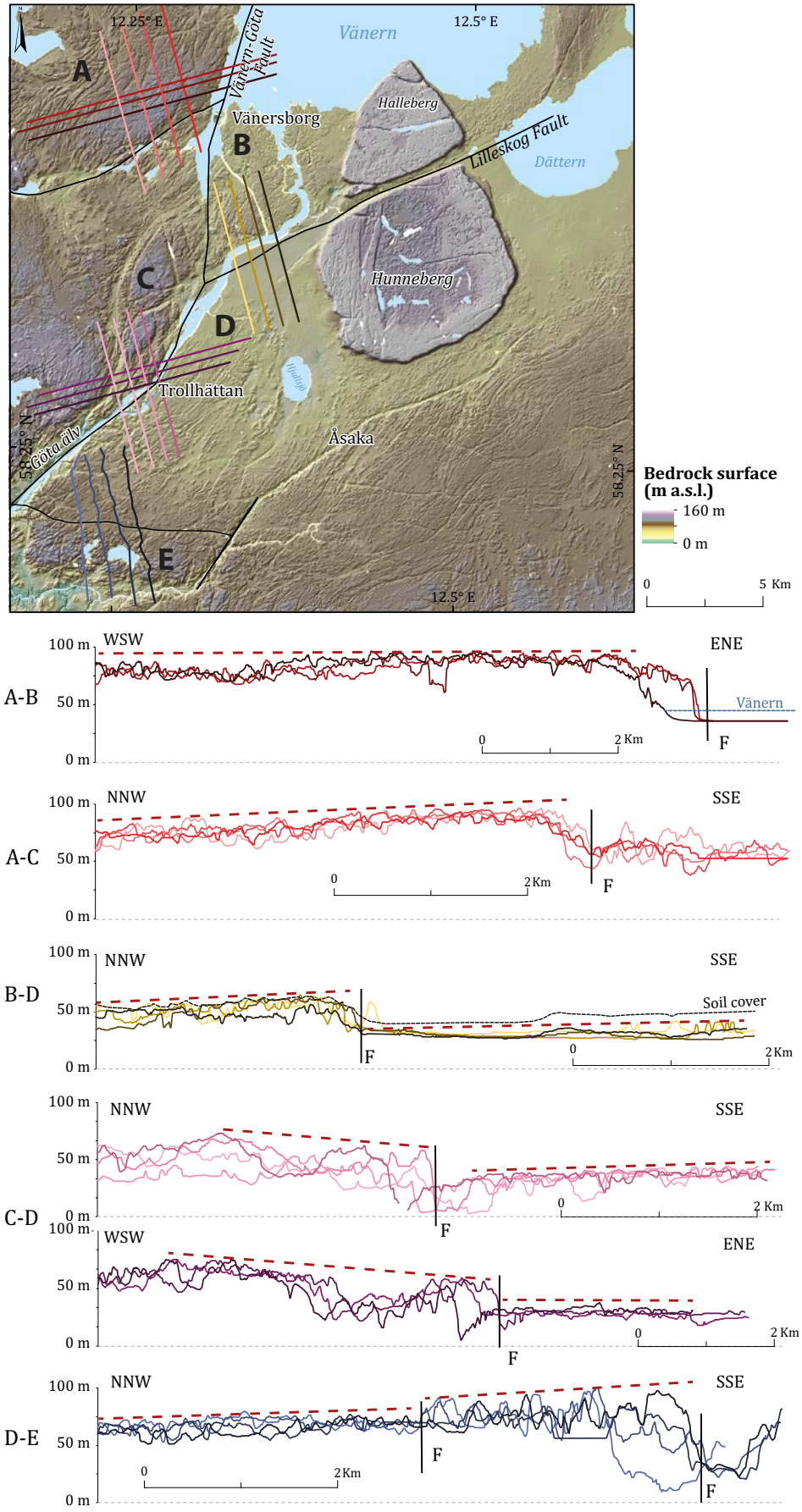

Figure 3-29. *Topographic profiles across faults separating rock blocks in the Trollhättan region. Dashed line marks the trend of the exposed unconformity on the basement. Note the rock loss from fault scarp edges in profiles. DEM and profiles based on Lantmäteriet elevation data.*

- Profiles C–D indicate a throw of 32–43 m on both the NNW-SSE and WSW-ENE profiles along the Vänern-Göta Fault near Trollhättan (Figure 3-29). This throw is consistent with elevation differences between the highest points across the fault (Figure 3-31). Further south, bedrock topography on Block C rises to 150 m a.s.l. Bedrock highs that rise above the river reach 71 and 81 m a.s.l. to the NW and SE of the river, respectively. Step-wise down-faulting along minor faults within the Göta Älv shear zone is likely (Ahlin 1987).
- Profiles D–E indicate throw of ~10 m (N side down) across the Sjölanda Fault N of Sjuntorp, also seen in DEMs (Figure 3-19).

Taken together, the profiles indicate minor vertical displacements of a few tens of metres that are broadly consistent with previous estimates of fault throws (Ahlin 1987).

Figure 3-30. *Scarp on the NW bank of the Göta Älv at Onsjö. The basement rises to 66–64 m a.s.l on planar flats on the crest of the forested slope. Fields in the foreground are underlain by 5–10 m of Quaternary deposits.*

Figure 3-31. *Scarp of the Vänern-Göta Fault at Trollhättan. The basement W of the Göta Älv rises to 92 m a.s.l. at the base of the mast. On the opposite bank, planar flats at Hjortmossen stand at 54 m. A vertical throw of ~38 m is indicated.*

Intra-block lineaments

Profiles across intra-block lineaments allow possible minor faulting to be identified and displacement to be estimated (Figure 3-32).

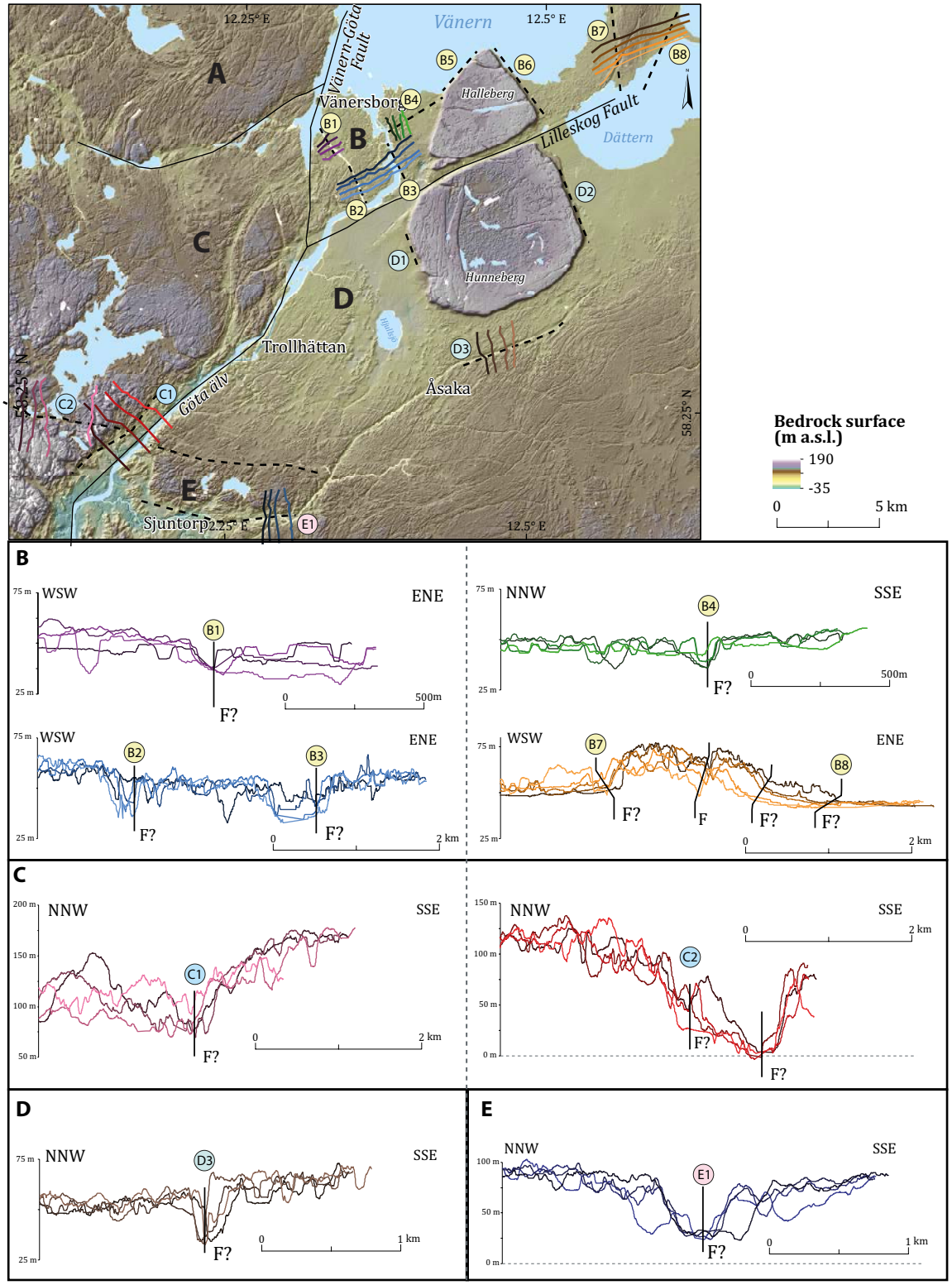

Figure 3-32. *Bedrock profiles across possible intra-block faults. Codes refer to block letters and intra-block lineament numbers. DEM and profiles based on Lantmäteriet elevation data.*

Block B

Intra-block lineaments B1–B3 are oriented NNW-SSE and follow faults marked on SGU maps. Lineament B1 runs close to the line of the Karls grav (canal) and shows a ~7 m height difference between higher ground to the SW of the lineament and that to the NE. Its continuation, Lineament B2, follows the southern section of the canal. Here the equivalent height difference between facing planar flats is ~9 m. Minor vertical displacement across the fault is likely. Lineament B3 however has no apparent fault displacement.

Lineament B4 is oriented WSW-ENE and follows a fault marked on SGU maps that separates augen-bearing from non-augen-bearing types of granite gneiss. A 10–15 m high ridge rises S of the lake shoreline at Nordkroken. A single bedrock outlier is marked on the ridge on SGU Quaternary maps but this has not been traced in the field and it is likely in error (Section 3.1.2). The depth of Quaternary deposits below the ridge is estimated on these maps as 10–20 m. No displacement on lineament B4 is apparent from bedrock summit heights across the lineament N of Vargön (Figure 3-32).

Lineaments B5 and B6 are represented by straight segments on the E and W flanks of Hunneberg, respectively. No displacement of basement is apparent across the southern ends of either lineament.

Lineaments B6 and B7 are oriented N-S and NNE on Vänersnäs. A fault shown on SGU bedrock maps runs SW-NE close to the axis of the Vänersnäs ridge but lacks topographic expression. Lineament B6 follows the NW flank of the ridge with a drop in elevation across the lineament of ~12 m. Lineament B7 defines the SE flank of the ridge, with a height difference of ~14 m between bedrock summits across it. Vänersnäs appears to be a low basement horst.

Block C

The intra-block lineaments towards the southern edge of Block C fall within a zone of high glacial roughening where differential block movements are difficult to assess. There is a possible vertical displacement of up to 25 m across lineament C1 and up to 40 m across C2.

Block D

Lineament D3 forms a straight segment of the Slumpån valley to the S of Hunneberg. An apparent vertical displacement of ~10 m is seen in profiles across the lineament.

Block E

Lineament E1 shows no apparent height differences between rock summits in profiles.

Taken together, profiles across the intra-block lineaments indicate likely minor faulting within Blocks B, C and D. Elevations across several lineaments, however, are similar and indicate the lineaments either follow faults with small displacements or other types of fracture without displacement.

3.4.2 Fracture patterns at the local and macro-scales

Topographic lineaments within Areas 1–4 (Figure 3-14 and Figures 3-17 to 3-19) show the dominant influence of the regional NE-SW to NNE-SSW oriented fracture set that runs subparallel to gneiss foliation.

Three large quarries are operational in the Trollhättan area (Figure 3-33). Each quarry is set into low relief bedrock terrain in which adjacent bedrock summits have elevation ranges of 5–10 m at the local and regional scales that are typical of wider summit envelope surfaces that represent the lowered sub-Cambrian unconformity. Hence the quarries expose fractures in basement at shallow depth below the former unconformity.

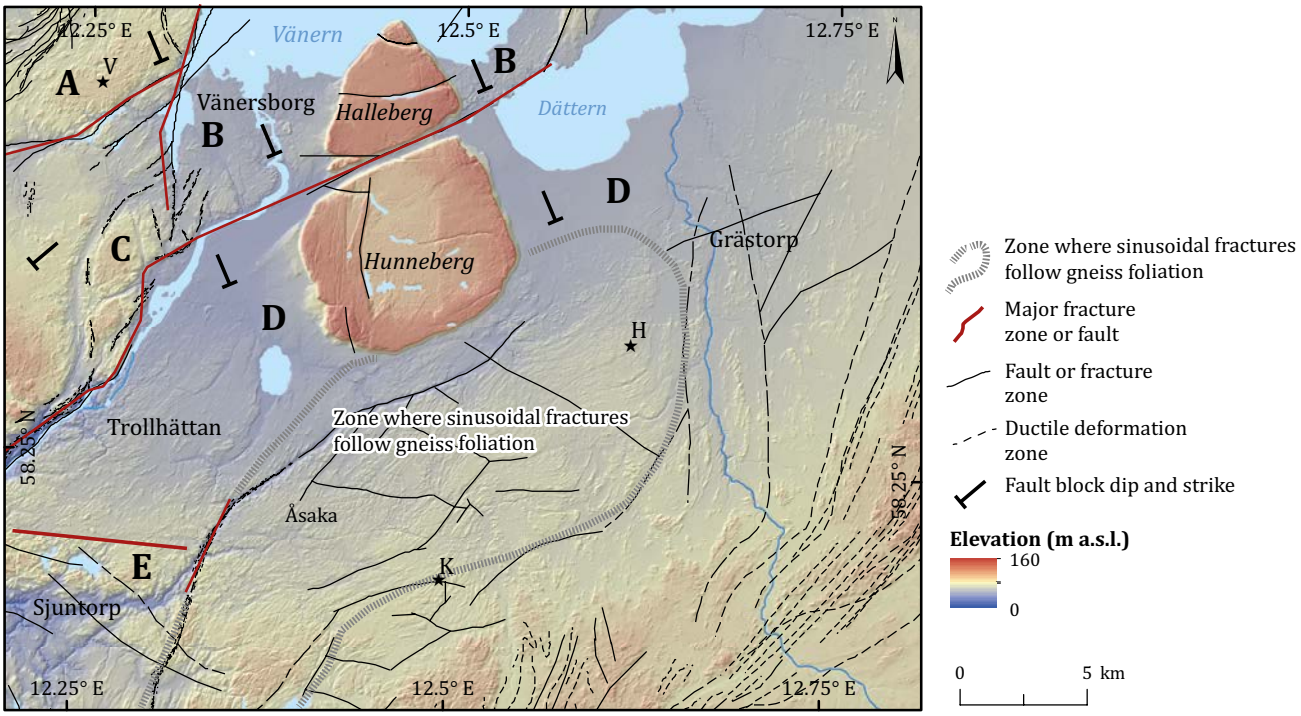

Figure 3-33. *Major fractures and fracture patterns in the Trollhättan region based on SGU data. V Vänersborg Cross Quarry. H. Håberg Quarry. K. Kuleskog Quarry. A–E refer to fault blocks. Elevation data from Lantmäteriet.*

Steeply-inclined fractures are generally spaced at 0.5–3 m with more closely-fractured Proterozoic mafic dykes and fracture zones at Vänersborg Cross (Figure 3-34), Håberg (Figure 3-35) and Kuleskog (Figure 3-36). Gently-inclined fractures have somewhat wider spacings of 1–4 m. Sub-horizontal or sheet fractures are not widely developed. Around these quarries, the exhumed sub-Cambrian unconformity is developed indiscriminately across variably fractured rocks of mainly felsic but locally mafic composition.

Figure 3-34. *Vänersborg Cross Quarry. Mesoproterozoic granitic gneiss with mafic bands. Steeply-dipping vertical fracture zones and mafic dykes follow the foliation strike to the NNE.*

Figure 3-35. *Håberg Quarry. Grey, coarse-grained granite gneiss. Steeply-inclined fractures oriented mainly N-S and WNW-ENE.*

Figure 3-36. *Kuleskog Quarry, Vane-Åsaka. Granite gneiss with foliation dipping to NNW. Zones of more widely-spaced fractures form low WSW-ENE trending ridges between shallow, strike-parallel valleys.*

3.4.3 Fracturing and planar flats

Planar flats are very gently inclined rock slope facets developed in coarse-grained to porphyritic granite gneiss. In order to establish whether the flat upper surfaces on planar flats are mainly erosional forms inherited from the sub-Cambrian unconformity, it is necessary to examine the extent to which these distinctive, local scale, bedrock landforms are structurally-controlled.

In planform, individual planar flats often have edges oriented parallel to NNE-SSW fractures. At Eriksroparken (Figure 3-25) and Hjortmossen (Figure 3-38), the north-western flanks of planar flats conform in inclination to these fracture surfaces.

North of Vargön, the dominant topographic lineaments run WSW-ENE and N-S (Figure 3-23), in contrast to areas around Vänersborg and Onsjö to the west where lineaments are mainly oriented NNE-SSW following the strike of gneiss foliation (Figure 3-14B). The very gently inclined, flat rock surfaces on the lake shore at Nordkroken, W of Halleberg, display extensive, 4–8 cm thick, near-surface, horizontal to very gently inclined fractures (Figure 3-23). At Udden, 1.5 km W, near-surface fractures have dm spacing and are horizontal to sub-horizontal (< 10°) in inclination and planar to gently curved in form. Thinly-spaced, surface parallel, curved sheets are also evident on rounded, stoss-side slopes of low roches moutonnées at the lake shore (Figure 3-23). Gently-inclined, thinly-spaced, near-surface rock sheets are also seen on planar flats at Dättern, E of Halleberg (Figure 3-22). Shallow sheet fractures provide local structural control on planar flats and on glacial and wave erosion forms developed locally on rock surfaces on these parts of the Lake Vänern shoreline (Figure 3-9).

The near-surface, closely spaced sheet fractures appear to cross-cut sandstone dykes at Dättern and Nordkroken. No sandstone fills are reported in near-surface, horizontal sheet fractures from these locations. The presence of Cambrian sandstone dykes and pre-Cambrian fracture coatings (Mattsson 1962) indicate, however, that a *structural fabric* (Vidal Romaní 2008) of horizontal, sub-horizontal and vertical fractures had largely developed in the granite gneisses below the surface of U2 before the Early Cambrian marine transgression. The closely-spaced sheet fractures are younger but conform to this structural fabric.

Elsewhere, control of planar flat surfaces by horizontal fractures is limited or absent. Exposures to the south along the Karls grav canal lack prominent, long, and continuous sub-horizontal fractures. Curved sheet fractures are seen close to the locks at Restad (Figure 3-37). Horizontal and sub-horizontal fractures are not widely developed on the edges of planar flats or in other exposures around the town of Trollhättan. An absence or scarcity of long HFs and SHFs is evident in man-made sections at planar flat localities (Figure 3-22) at Kåtene (Figure 3-26), Starkodders, Ryrbäcken (Figure 3-49) and Eriksro (Figure 3-25). At Hjortmossen, planar flats are seen in multiple man-made shallow sections to be cut across the main fracture set that follows the NE-SW strike of gneissic foliation and is inclined at 45–70° NW (Figure 3-38). At Sandhem, SHFs are more common but are short and dip gently to the south in contrast to the northward dip of the planar flat surface (Figure 3-39); in other words, the SHFs are not parallel to the planar flat surfaces. Around Trollhättan town, many man-made exposures occur at lower elevations than the planar flats. HFs and SHFs are not widely developed, indicating that the basement on which the town is built lacks extensive sheet jointing and that sheeting is not generally developed at depth. No planar flats are seen at these lower elevations where bedrock risers typically have roche moutonnée forms (Section 4.7.4).

Figure 3-37. *Sections aligned N-S along the Karls grav viewed from Rosenlund between Onsjö and Restad (Figure 3-14). A. Former quarry showing prominent fractures inclined to the NW and with NE-SW strike. B. Canal cut with curved sheet joints. C. Canal cut with fractures inclined to the NW. Planar flats occur on the highest ground on either side of the canal.*

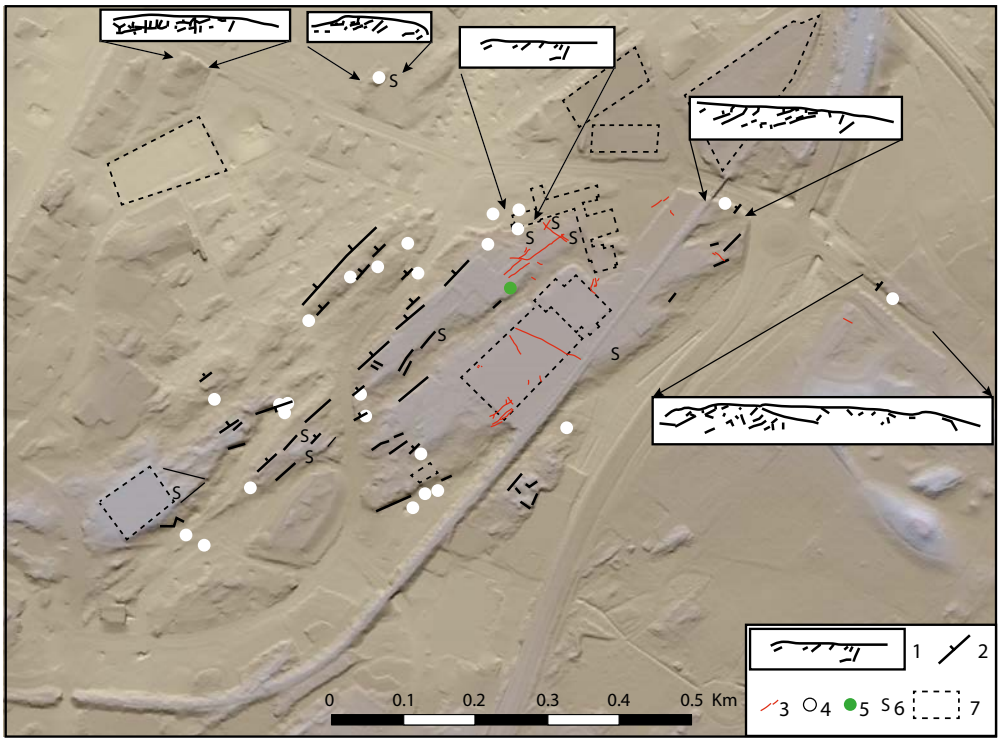

Figure 3-38. *Major lineaments and fracturing around planar flats at Hjortmossen, Trollhättan. 1. Fractures mapped along Gärdhemsvägen, where man-made cliffs provide sections across the dominant NW-SE fracture set. 2. Strike and dip of mapped fractures. 3. Sandstone dykes after Nordblom (1961, cited in Rudberg et al. 1976). 4. Cliff lacking significant horizontal fractures. 5. Prominent sub-horizontal fracture. 6. Thin, curved sheet joints present on block edges. 7. Building outline. Elevation data from Lantmäteriet.*

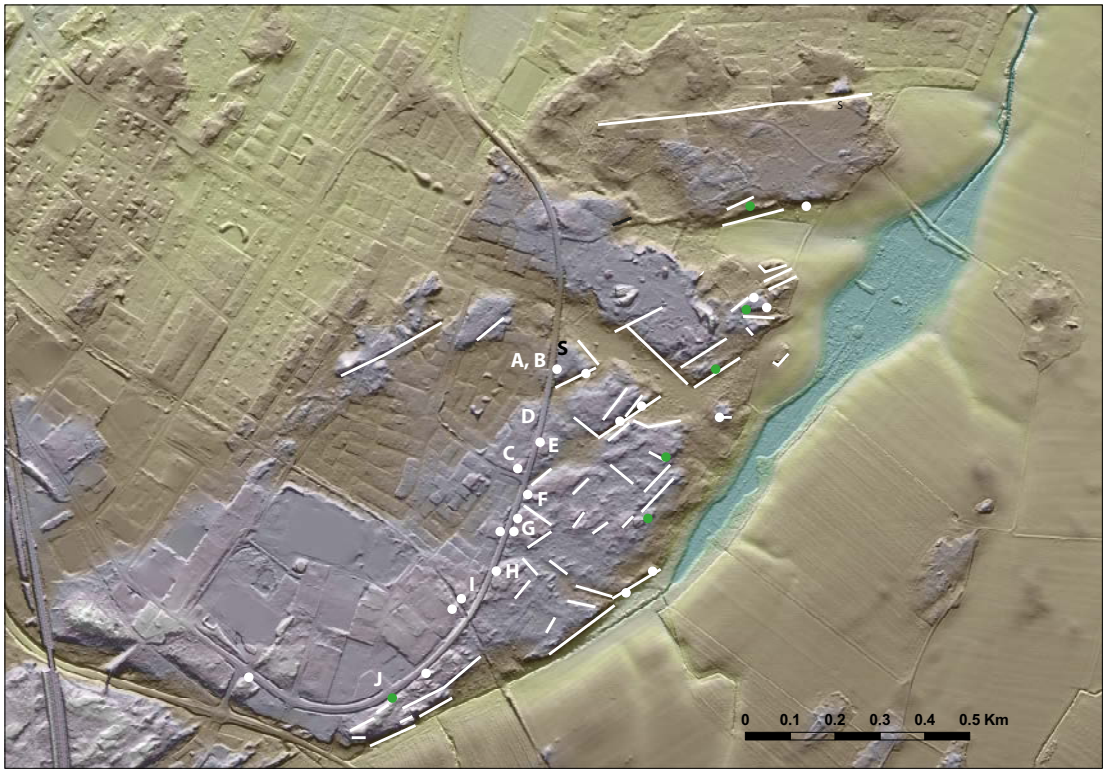

Figure 3-39. *Major lineaments and interpreted fractures around Sandhem. Green dots indicate presence of a sub-horizontal fracture; white dots are sites where no significant sub-horizontal fractures are seen. These planar flats have local parallelism with sub-horizontal fractures but sheet structures are absent from the low cliffs along the road section. Letters refer to photo locations in the next figure. Elevation data from Lantmäteriet.*

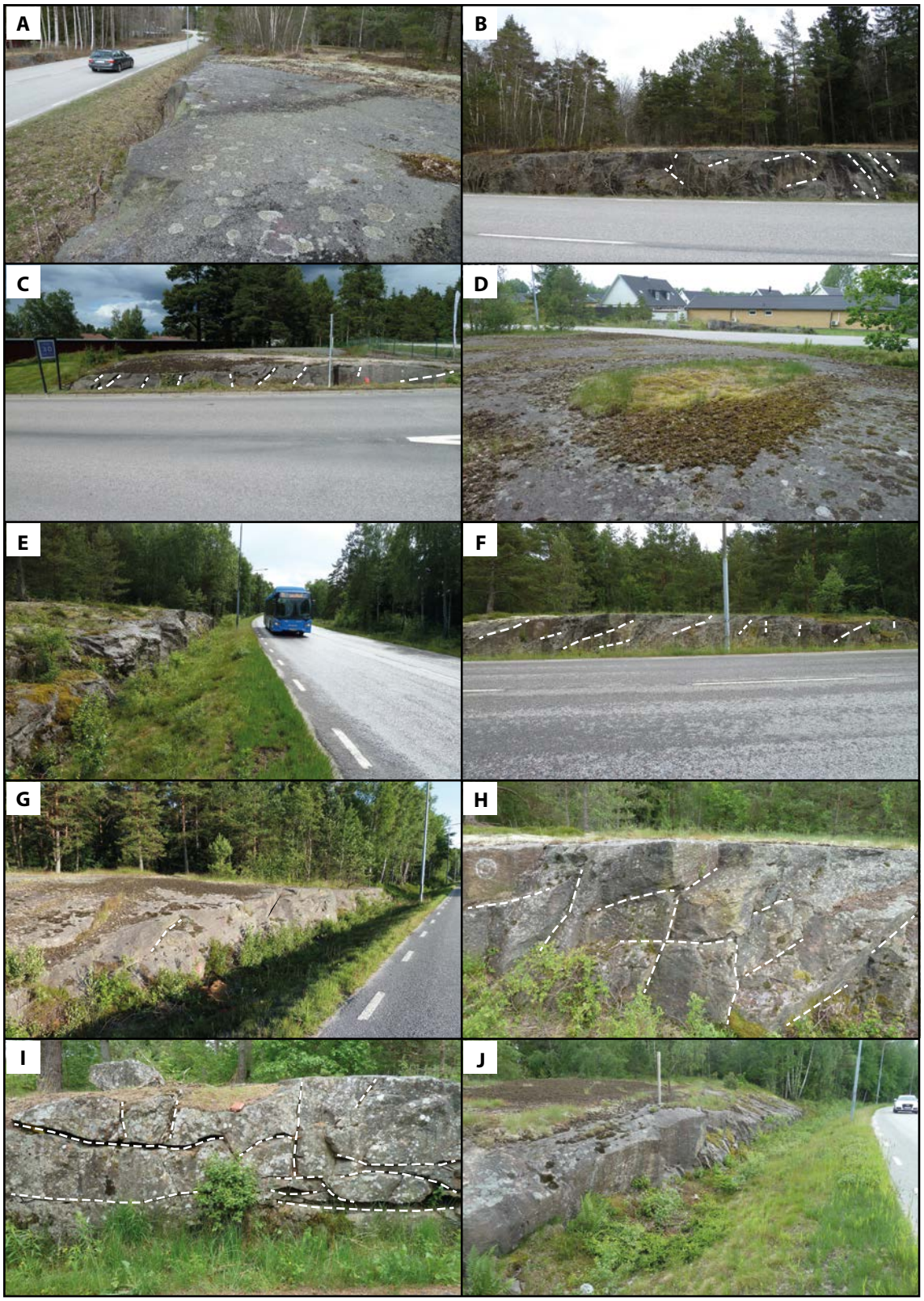

Figure 3-40. *Planar flats and fractures along the road section at Sandhem. Photo locations shown on previous figures. A. Surface of planar flat. B. Section through surface at A with fractures marked by dashed lines. C. Planar flat fragment with glacial abraded edges. Ice flow towards camera. Note the inclined fractures. D. Surface of planar flat fragment. E. Edge of planar flat fragment. F. Section of E, with inclined fractures. G. Abraded, curved edge of a planar flat fragment. H. Section in planar flat fragment showing variably oriented fractures. I. Section in underpass with horizontal, gently inclined and vertical fractures. J. Section in edge of planar flat fragment with curved fractures.*

Minor, thin and curved sheet fractures are developed locally in the near-surface on the abraded flanks and stoss sides of planar flats and roches moutonnées where vertical fractures are widely spaced. This fracture set lacks mineral coatings and crosscuts all other fractures and so appear to be relatively recent features. These fractures, however, do not show radial inclinations typical of sheet joints on low granite domes (Jahns 1943) but appear to preferentially located at the rounded edges of granite gneiss blocks. One potential model for their formation is in response to increasing curvature on these edges (Martel 2016) after progressive glacial excavation of bounding fracture zones.

3.4.4 Sandstone dykes

Many planar flats expose sandstone dykes that fill vertical fractures in the gneisses (Mattsson 1962, Rudberg et al. 1976). The sandstone dykes generally can only be easily recognised where the rock surface is unweathered, and the fractures are free of soil. The fracture fills comprise mainly rounded, medium to coarse quartz grains (Mattsson 1959). The Early Cambrian brachiopods *Mickwitzia monilifera* and *Torellella laevigata* have been recorded in sandstone dykes on the south-western shore of Lake Vänern (Gavelin 1909, Martinsson 1974), indicating fill at shallow depth coeval with deposition of the overlying Cambrian sands. Sandstone fills extend only along short (20 m long) exposed sections of a few vertical fractures at Nordkroken (Mattsson 1962) but at Hjortmossen dykes up to 120 m in length have been mapped (Nordblom 1961, cited in Rudberg et al. 1976) (Figure 3-38). The dykes are often only a few mm wide but reach a width of 20 mm (Figure 3-41).

Sandstone dykes seen penetrating planar flat surfaces at Nordkroken stand at a maximum elevation of ~6 m below the nearby preserved sub-Cambrian unconformity (Figure 3-9). At Gaddesanna, a roche moutonnée with a summit at 46 m a.s.l. (Figure 3-4) shows a sandstone dyke (Rudberg et al. 1976) at an elevation ~6 m below the buried unconformity. Sandstone dykes on planar flats at Hjortmossen have tops at up to 54 m a.s.l. but no dykes have been reported or observed from outcrops in Trollhättan town centre at elevations below 48 m a.s.l. The short and narrow sandstone dykes today found at elevations close to the buried unconformity represent vertical fractures originally infilled at shallow depth below U2. Sandstone dykes may penetrate to greater depths around Trollhättan, but none has been observed or reported.

The fractures were originally filled by unlithified Early Cambrian sands overlying the unconformity (Hadding 1929). Both existing, mineral coated fractures and new uncoated fractures were opened, most likely in earthquakes during and shortly after the marine transgression (Scholz et al. 2009, Friese et al. 2011). Most fractures that host sandstone dykes are aligned WSW-ENE parallel to gneiss foliation (Mattsson 1959, Nordblom 1961, cited in Rudberg et al. 1976), At Vargön (Mattsson 1962) and Hjortmossen (Nordblom 1961, cited in Rudberg et al. 1976) (Figure 3-38), sandstone dykes also have W-E orientations The different orientations within the Trollhättan area suggest that the opening of existing and new fractures was related to multiple events under different stress fields. The sand fills were lithified during deep burial in the Palaeozoic (Bruun-Petersen 1975). Calcite coatings are associated with the sandstone dykes (Mattsson 1962) but are more widely developed in vertical fractures with no recorded sandstone dykes (Mossmark et al. 2015). In eastern Sweden, these younger coatings likely formed beneath thick Palaeozoic cover rocks but at much greater depths in the basement than the sandstone dykes (Drake et al. 2009b). Calcite, fluorite and galena veins also crosscut sandstone dykes (Alm and Sundblad 2002, Drake et al. 2009a). The presence of unweathered sandstone dykes (Figure 3-41) and calcite coatings (Figure 3-27) indicates limited weathering of the basement surface since its re-exposure from beneath Early Palaeozoic cover.

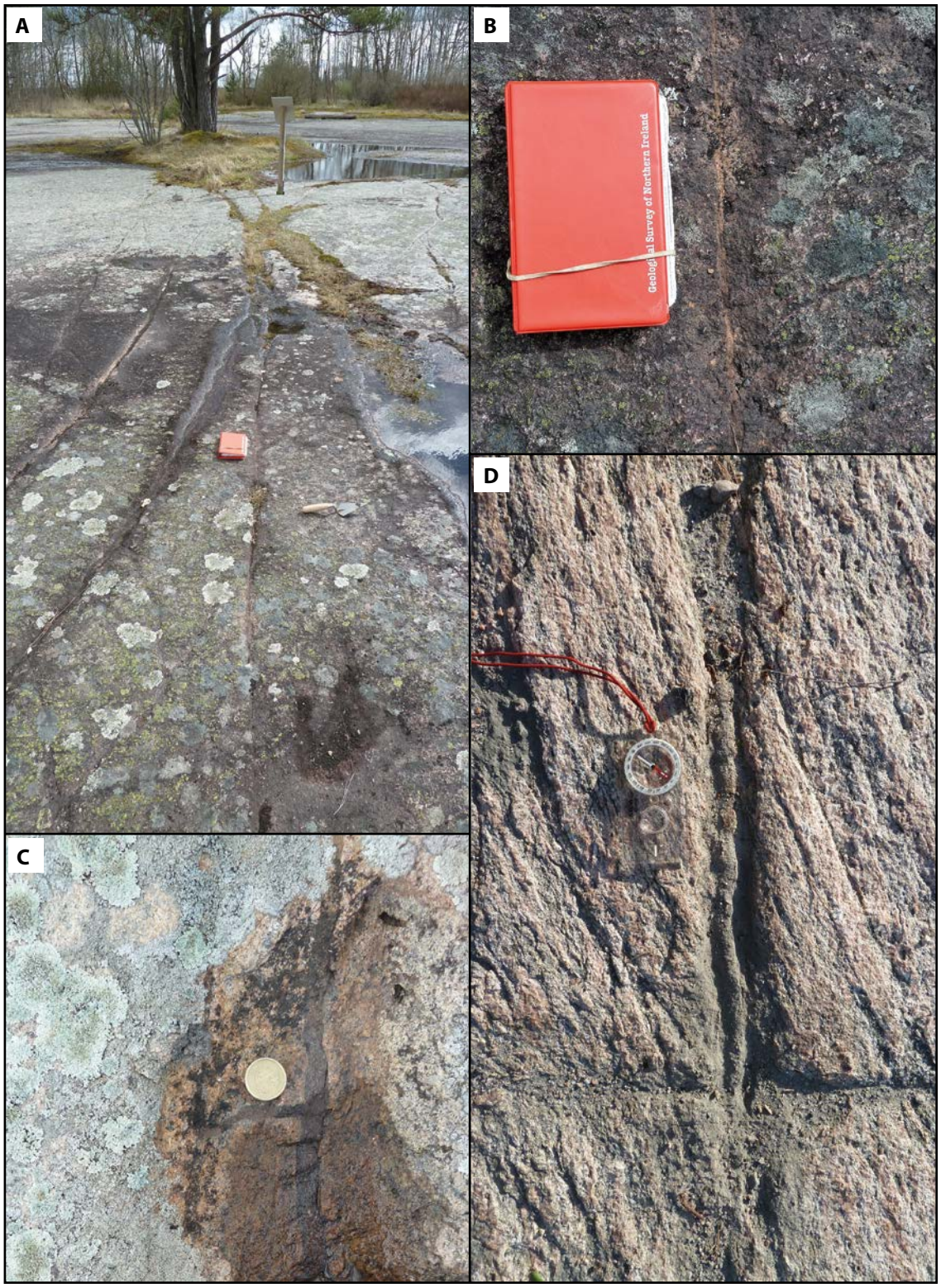

Figure 3-41. *Sandstone dykes. A and B. Sandhem. Notebook is 19 cm long. C. Dättern. D. Hjortmossen. Site locations on Figure 3-22.*

3.5 Glacial erosion of the sub-Cambrian unconformity

Modelling of the basement surface of the sub-Cambrian unconformity provides an unusual opportunity for identifying the pattern and depth of glacial erosion subsequent to the re-exposure of a largely unweathered, near-planar basement surface. In most formerly glaciated areas, the landsurfaces on which the inception of glacial erosion took place at the beginning of the Pleistocene were of complex form, with saprolite covers of varying depths (Hall and Migoń 2010). The evidence presented above indicates that (i) the buried sub-Cambrian unconformity in Västergötland is nearly flat over wide areas, (ii) weathering depths on the buried unconformity were low or zero and (iii) summits on the exposed unconformity remain at elevations a few metres below those on the buried unconformity. These characteristics allow summit envelope surfaces to be used as reference surfaces to identify patterns and depths of erosion by the FIS across exposed basement.

3.5.1 Components of glacial erosion

Ice sheets in the Trollhättan region have eroded five different rock substrates (Figure 3-42). In vertical sequence, these substrates are:

A. Any Palaeozoic cover rocks that formerly rested on the upper surface of the dolerite sill.

B. Early Permian dolerite, hard, with widely-spaced, orthogonal joint sets (Figure 2-1).

C. Early Palaeozoic sandstone and limestone, relatively soft, with closely-spaced, horizontal bedding planes and vertical joints (Figure 1-9).

D. Top basement immediately below the sub-Cambrian unconformity (Figure 3-11), with a fractured and, in places, a weathered surface of shallow depth.

E. Pre-Cambrian basement gneiss, hard and unweathered, with variably spaced vertical, inclined and sub-horizontal fractures (Figures 3-50 to 3-52).

Component A, the rock removed from above the present summits of the table mountains, is of unknown depth. Components B and C are today confined to Halleberg and Hunneberg. The volume of dolerite and Early Palaeozoic sandstone and limestone erratics present in Middle to Late Pleistocene deposits in Jutland and sourced from Västergötland (Weidner et al. 2015) indicates that these rocks were much more extensive earlier in the Pleistocene. Component D included variably fractured granite gneisses on the unconformity surface. Additionally, at Lugnås (Lidmar-Bergström et al. 1997), Närke (Lundegårdh et al. 1973) and at other locations on the sub-Cambrian unconformity (Gabrielsen et al. 2015), a ≤5 m-thick horizon of saprolite and saprock is present locally on the buried unconformity. At Kinnekulle, however, and also at many other locations (Gabrielsen et al. 2015), the buried unconformity surface is unweathered. Around Halleberg and Hunneberg, no evidence has been reported or observed for the presence of saprolite on U2. Also, sandstone dykes and calcite coatings remain unweathered at shallow depths below U2 (Figure 3-27). The elevation difference between the buried sub-Cambrian unconformity and adjacent summits on the exposed basement indicates a maximum thickness for Component D of 2–6 m above present summits (Section 3.3.6). Erosion of underlying basement, Component E, is represented by the rock removed between the summit envelope surface, representing the lowered unconformity, and the present rock surface (Figure 1-14).

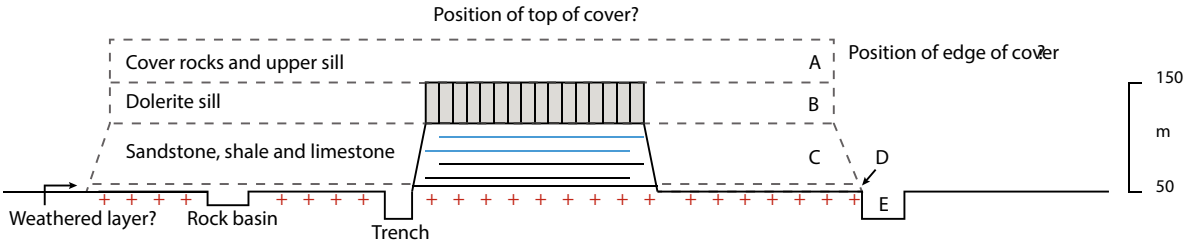

Figure 3-42. *Rock components of glacial erosion around the table mountains of Västergötland.*

3.5.2 Landscapes and landforms of glacial erosion

The largest glacial landforms of the Trollhättan region occur at the landscape and regional scales and include the Vänern basin, the Halleberg and Hunneberg table mountains and major basins and valleys (Figure 3-43). Each of these landforms has been modified or reshaped in various ways by glacial erosion by the FIS during the Pleistocene.

Lake Vänern basin

Lake Vänern is the largest in Sweden, covering 5 655 km^2. Unlike Lake Vättern, the Vänern basin lacks a graben structure (Andréasson and Rodhe 1990) but instead occupies a shallow N-facing basement depression that extends beyond the northern limit of the study area (Figure 1-2). The western shore of the southern lake basin abuts the fault scarp along the Vänern-Göta Fault (Figure 3-29). Lake Vänern has an average depth of 27 m, reaching a maximum of 106 m in the eastern sub-basin of Värmlandsjön (Kvarnäs 2001). In its southern part, towards Vänersborg, the lake is < 20 m deep, with a basement floor gently inclined towards the north. Cambrian sandstone dykes are found around its southern margins (Mattsson 1962, Greiling et al. 1988). The shallow floor of the Vänern basin in this area remains close to the sub-Cambrian unconformity. . Early Palaeozoic cover was likely removed through erosion by the FIS (Amantov 1995). The southern Vänern basin is a mainly inherited topographic feature formed after removal by glacial erosion of sedimentary cover from the inclined, block faulted surface of U2.

Progressive glacial erosion of table mountains

The dolerite table mountains of Västergötland provide a range of forms that represent progressive glacial erosion (Figure 3-43). Where Permian sills remain extensive and thick, as at Mount Billingen (~50 m thickness) and at Halleberg and Hunneberg (40 m thickness), the hills have distinctive mesa forms. Bounding cliffs are developed in the dolerite cap rock, near rectilinear slopes are found across the Early Palaeozoic sedimentary sequence and the foot slope is developed in talus cover and meets the flat surface of the basement unconformity and its overlying Late Pleistocene deposits (Figure 3-5). These slope forms are typical of mesas developed in unglaciated areas where weak sedimentary strata are protected from erosion beneath cap rocks and develop through slope retreat (Duszyński et al. 2019). Across the more extensive Billingen area, the dolerite cap is fragmented, and individual sill remnants are reduced in area (Figure 3-43). Where dolerite cap extent is reduced in area to < 1–2 km^2, the remnants of the sill retain thicknesses of 30–40 m but the edges of the dolerite cliffs have been rounded by glacial erosion. At Kinnekulle, only a small (0.25 km^2), thin (~25 m) dolerite cap remains and extensive areas of the underlying Ordovician limestone have been exposed to glacial erosion with development of glacial lineations (Figure 3-10). At Lugnås, the dolerite cap rock is missing entirely (Calner et al. 2013). Space-time substitutions indicate that progressive glacial erosion has led to fragmentation of formerly more extensive plateaux, as at Billingen. Lowering of the upper surface of sills has been limited because dolerite caps on neighbouring mesas are of similar thickness. On the tops of Halleberg and Hunneberg, orthogonally jointed dolerite appears to have been eroded mainly through the removal of gently-inclined rock sheets (Figure 3-22). Dolerite has been removed from the bounding cliffs during scarp retreat, leading to exposure and erosion of underlying Early Palaeozoic sedimentary rocks. Complete removal of dolerite cap rock, as at Lugnås, leaves the underlying fissile and soft Early Palaeozoic strata vulnerable to removal by glacial erosion.

Indicator glacial erratics of Cambrian sandstone, Ordovician limestone and Permian dolerite occur within or rest on Late Weichselian tills in positions down-ice from the Västergötland mesas. Dolerite sourced from Halleberg and Hunneberg makes up 5–10 % of the till clasts in the northern parts of the Göta valley (Hillefors 1979). Dolerite and Ordovician limestone boulders are common in tills on Kinnekulle (Gillberg 1970). These indicator rocks can be traced as field stones for > 10 km S of Kinnekulle. A fan of Early Palaeozoic erratics, > 3 000 km^2 in area extends for 45 km southwards from the Billingen table mountains (Gillberg 1965). The indicator erratics represent the removal of substantial volumes of rock from the Early Palaeozoic mesas, consistent with significant glacial erosion of these mesas during the last glacial cycle.

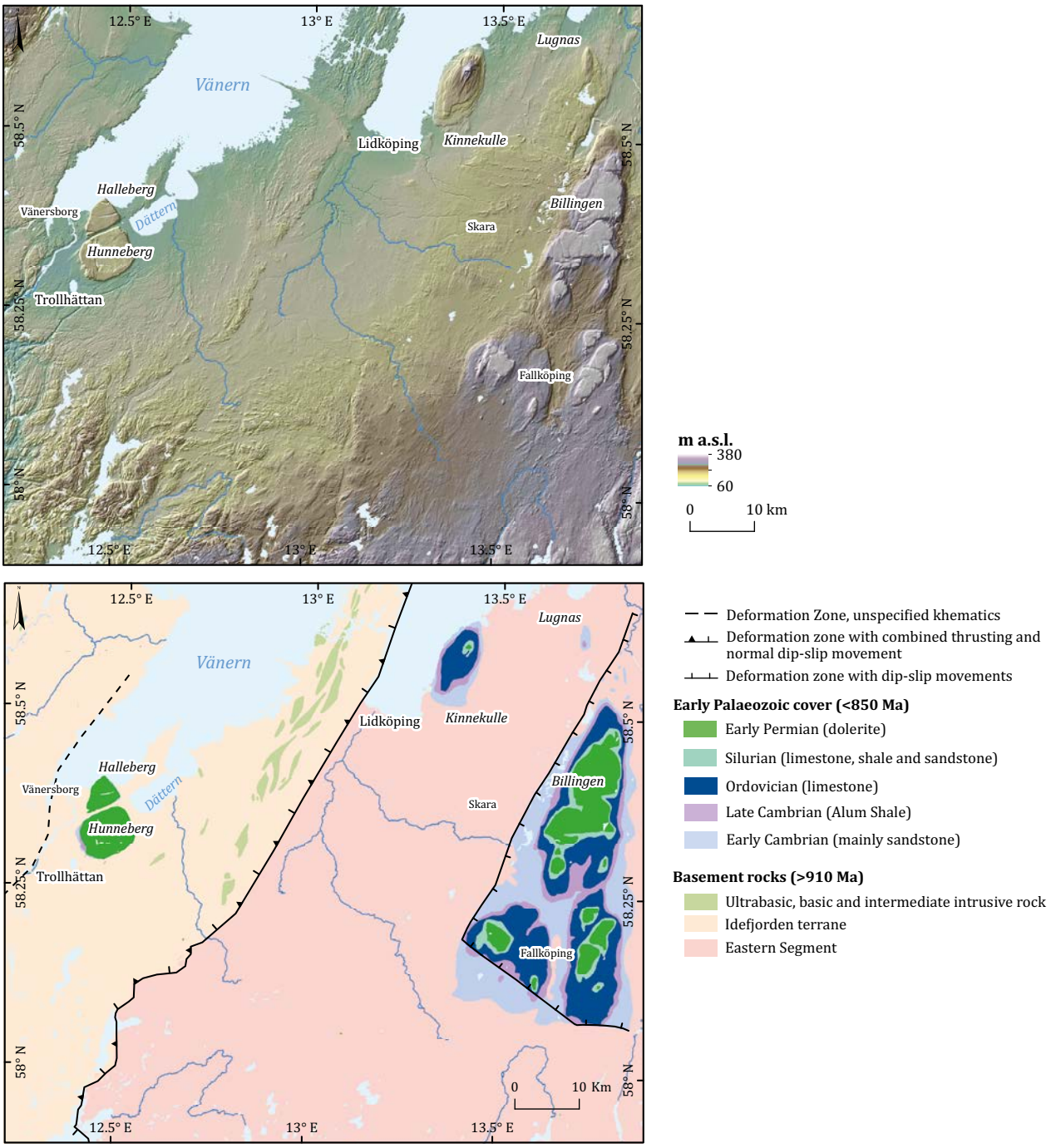

Figure 3-43. *Table mountains capped by Early Permian dolerites in Västergötland. The present forms of the hills and the distribution of cap rocks and cover indicate progressive glacial erosion of outliers. DEM based on Lantmäteriet elevation data. Geology map based on SGU data.*

Major rock basins and valleys

DEMs for sediment thickness (Figure 3-44) and bedrock elevation (Figure 3-45) show the main negative relief features of glacial landscapes in Västergötland. Sediment thickness exceeds 20 m only in the SE part of the study area, in the Hullsjön depression and at Sjuntorp and adjacent parts of the Göta Älv (Figure 3-44). Bedrock elevation maps indicate that sediments partly infill trenches that are mainly < 5 km long and < 20 m deep (Figure 3-44). Rock basins become apparent around Sjuntorp and reach depths of > 50 m in the SE part of the study area. Large trenches, depressions and rock basins however are mainly confined to the higher ground W of the Göta Älv, the Göta valley itself, and to a meltwater spillway to the W. Channelling of ice and meltwater flow (Bergsten 1994) have led to deep excavation along the Göta Älv shear zone.

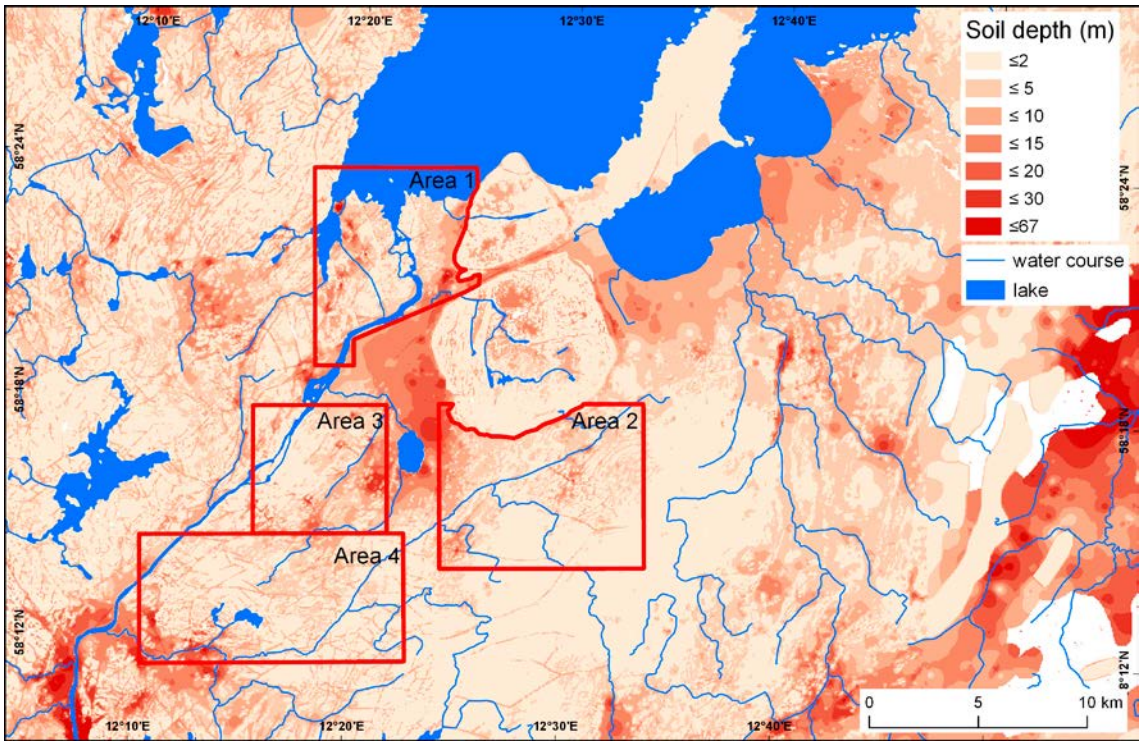

Figure 3-44. *Soil depth (depth to bedrock) map centred on Halleberg and Hunneberg. Based on SGU data.*

Depressions around the base of the Halleberg and Hunneberg reach depths of 30 m but do not form continuous, lunate features around the base of these hills (Figure 3-44). The over-deepened Hullsjön basin stands up to 3 km W from the hill flank of Hunneberg (Figure 3-45). The location of this depression likely relates to fracture spacing in the basement but over-deepening is also suggestive of topographically channelled ice flow around Hunneberg. The high density of Cambrian sandstone dykes and frequency of planar flats at Trollhättan (Figure 3-22) indicates the late persistence in that area of one or more Cambrian outliers. The Lugnås outlier, stripped of its cap rock and awaiting removal in future glaciations, provides an analogous situation today. Hence, it may be speculated that the Hullsjön depression developed between a more proximal flank of Hunneberg and a former hill mass developed in Early Palaeozoic sedimentary cover in the Trollhättan area. Subsequent glacial erosion led to retreat of the scarp around Hunneberg and to complete removal of the purported Trollhättan outlier. Alternatively, and more simply, the Hullsjön depression may represent glacial excavation along a fracture zone.

Missing features of glacial erosion

Several major landforms of glacial erosion at the landscape scale that are typical of the shield surface elsewhere in Sweden are absent from the Trollhättan region. Hilly topography with flyggbergs (Rudberg 1992), large asymmetric hills produced by glacial erosion of inselbergs (Ebert and Hättestrand 2010), does not occur on basement in the Trollhättan area. This absence is consistent with the lack of large (>10 m in height) hills on the buried sub-Cambrian unconformity (Section 3.2). Glacial streamlining of gneissic bedrock is also largely absent at the landscape scale (Figure 3-15). Disrupted bedrock surfaces and boulder spreads, features that are diagnostic of the glacial ripping process set seen in parts of eastern Sweden (Hall et al. 2019), also have not been reported or observed around Trollhättan.

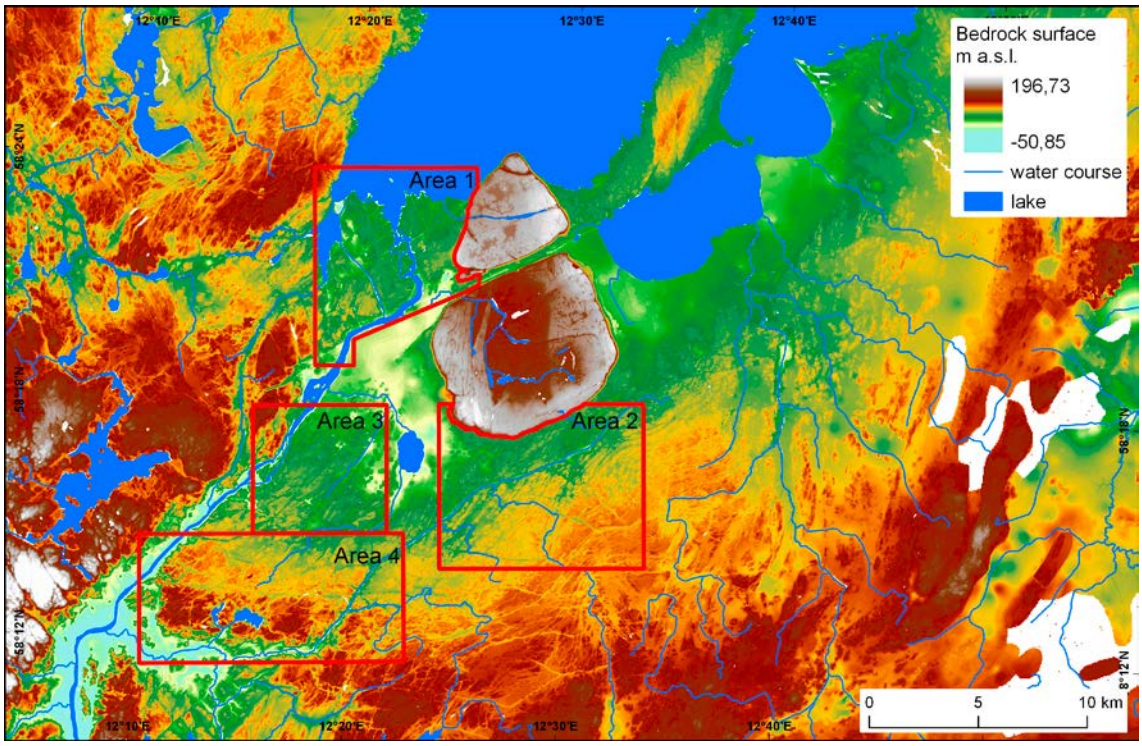

Figure 3-45. *Bedrock surface (2 m DEM minus soil depth). Method outlined in Table 2-1. DEM based on SGU soil depth and Lantmäteriet elevation data.*

3.5.3 Terrain roughness and streamlining

The local scale roughness of the buried sub-Cambrian unconformity at Halleberg, Hunneberg and Kinnekulle is low, consistent with similar low roughness as reported from exposures on the buried unconformity elsewhere in Scandinavia (Gabrielsen et al. 2015). Re-exposure of basement in proximity to Early Palaeozoic outliers is very likely the product of Pleistocene erosion by the FIS (Section 4.7.1). As sandstone-filled rock trenches and basins are not reported on the buried Early Cambrian unconformity or from the adjacent exposed basement, rock trenches and basins represent erosion by the FIS. Assuming that low roughness extended uniformly across the buried unconformity, the present-day topographic roughness, in large part represented by the trenches and basins found across the exposed basement around outliers, represents the product of glacial erosion operating selectively on hard, variably fractured basement.

At the landscape and regional scales, topographic roughness mapped using Relative Topographic Position (RTP) is generally low (Figure 3-46). Low roughness at these scales is due to widespread inheritance of bedrock topography from the flat and smooth sub-Cambrian unconformity. Terrain roughness increases with distance from the Lake Vänern basin but areas with high RTP values are of restricted extent.

At the regional to local scales, topographic roughness based on standard deviation (SD) varies between and within the detailed study areas (Figure 3-47). In Area 1, around Vargön, surface roughness is low. Topographic profiles show that bedrock highs vary in elevation by <5 m and are separated by hollows <10 m deep (Figures 3-15 and 3-16). Only a few linear, fracture-guided trenches, 1 km long and 50 m wide, run N-S in the Vargön area (Figure 3-14). In Area 3, at Trollhättan, surface roughness is also low, particularly in the slightly elevated area, with its planar flats, on which parts of the town are built. Surface roughness increases to the W towards the Göta valley and E towards the Hullsjön depression. In Area 2, at Åsaka, surface roughness is a direct expression of the excavation of closely-spaced SW-NE fractures, giving bevelled ridge and furrow topography, with only a few shallow basins (Figure 3-17B). In Area 4, at Sjuntorp (Figure 3-19), surface roughness increases sharply at the local scale, notably on hill and basin edges found S of the Sjölanda Fault (Figure 3-29). Rock basins increase in size and depth, occupying 40–50 % of the ground area. Rock trenches reach widths of 300 m. Hill masses are more widely spaced but also more prominent, rising 10–15 m above surroundings (Figure 3-21).

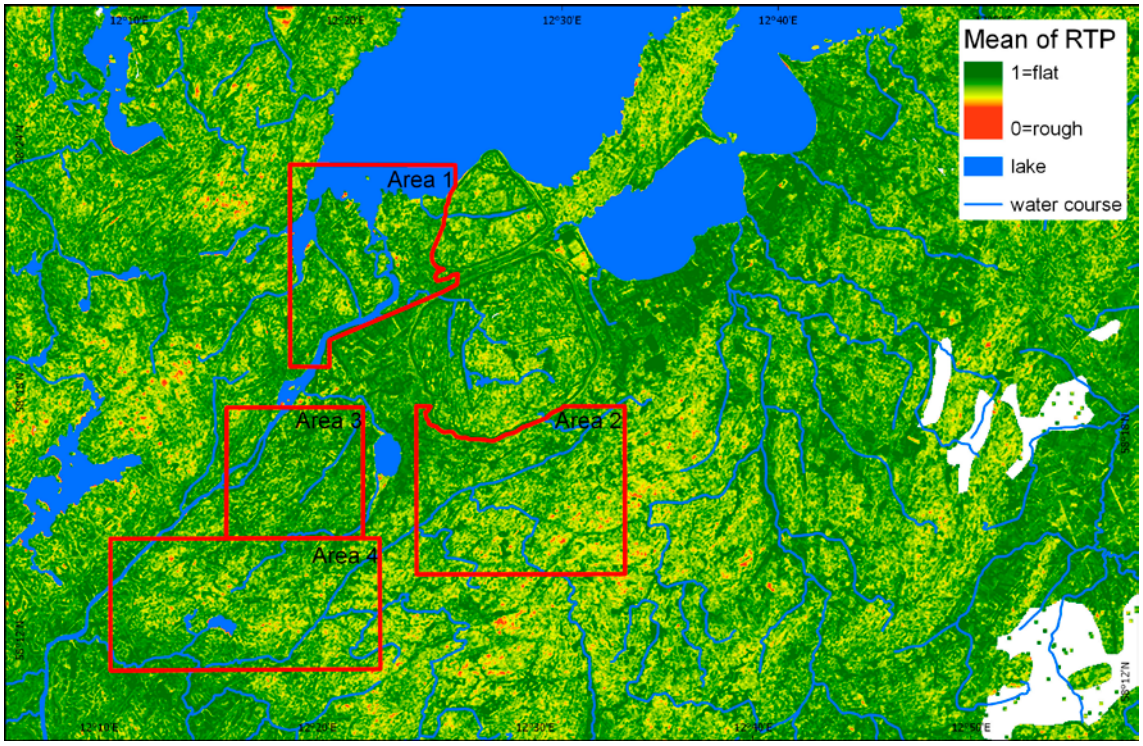

Figure 3-46. *Topographic roughness (RTP) of the bedrock surface in the Trollhättan region. Mean of RTP based on 10 × 10 cell calculation. Mean based on 50 × 50 cells (i.e. 100 × 100 m windows) to improve the visual output of the RTP (Table 2-3). DEM based on Lantmäteriet elevation data.*

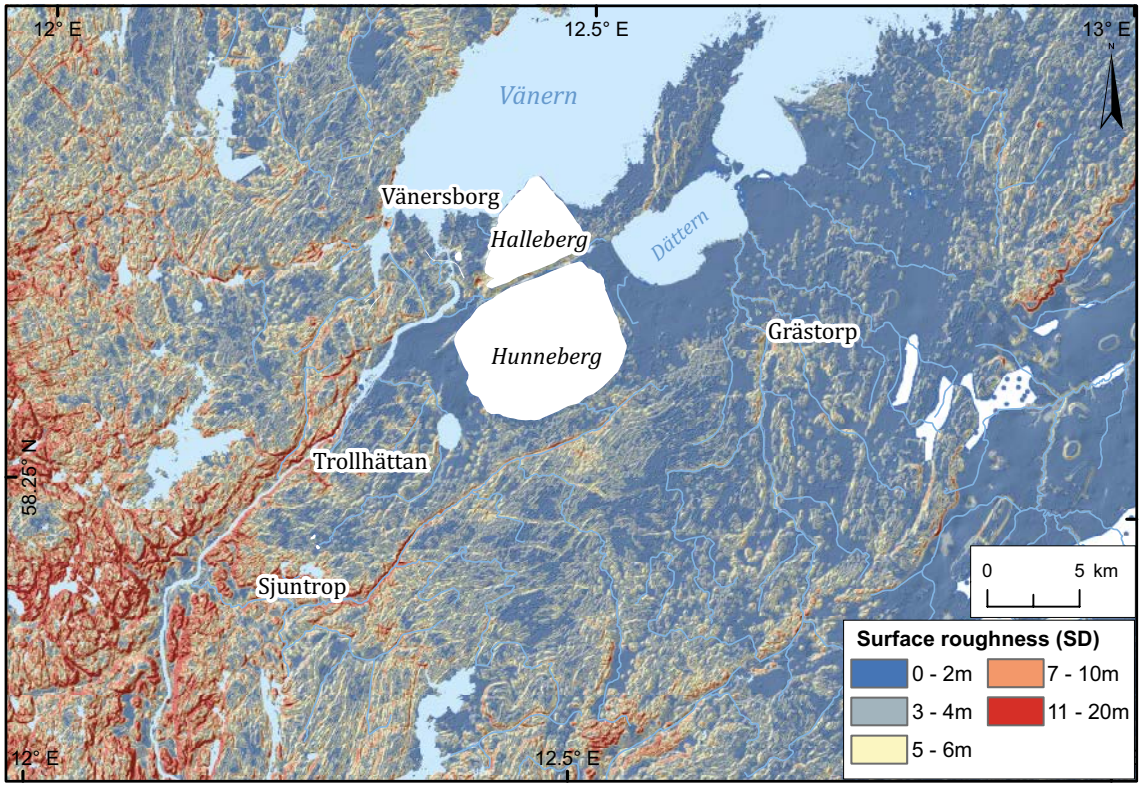

Figure 3-47. *Surface roughness (SD) in metres of the bedrock surface in the Trollhättan region. SD is the standard deviation of elevation in neighbouring cells within a 100 m radius (Figure 2-5). DEM based on Lantmäteriet elevation data.*

Regional ice flow was from between NNE and NE (Hillefors 1979, Houmark-Nielsen and Kjær 2003), a direction that was slightly oblique to NE-SW trending fracture patterns. Parallelism between ice flow directions and fracture orientations is often a feature of glacially streamlined bedrock (Roberts and Long 2005, Hall et al. 2013, Krabbendam et al. 2016). In the study area, however, glacial streamlining is neither widely nor strongly developed at the landscape to local scales. In the Sjuntorp area, the intensity of glacial erosion shows a sharp transition across the Sjölanda Fault between Fault Blocks D and E. To the N, relative relief is low (Figure 3-20) and trenches are <20 m deep. To the S, relative relief is higher, with isolation of hills and hill groups (Figure 3-21) through trench excavation and deepening of rock basins that extends to depths of >40 m. Whilst small bedrock knolls are often elongate in this southern area, the orientation of the knolls is oblique to the former ice flow direction (Figure 3-48).

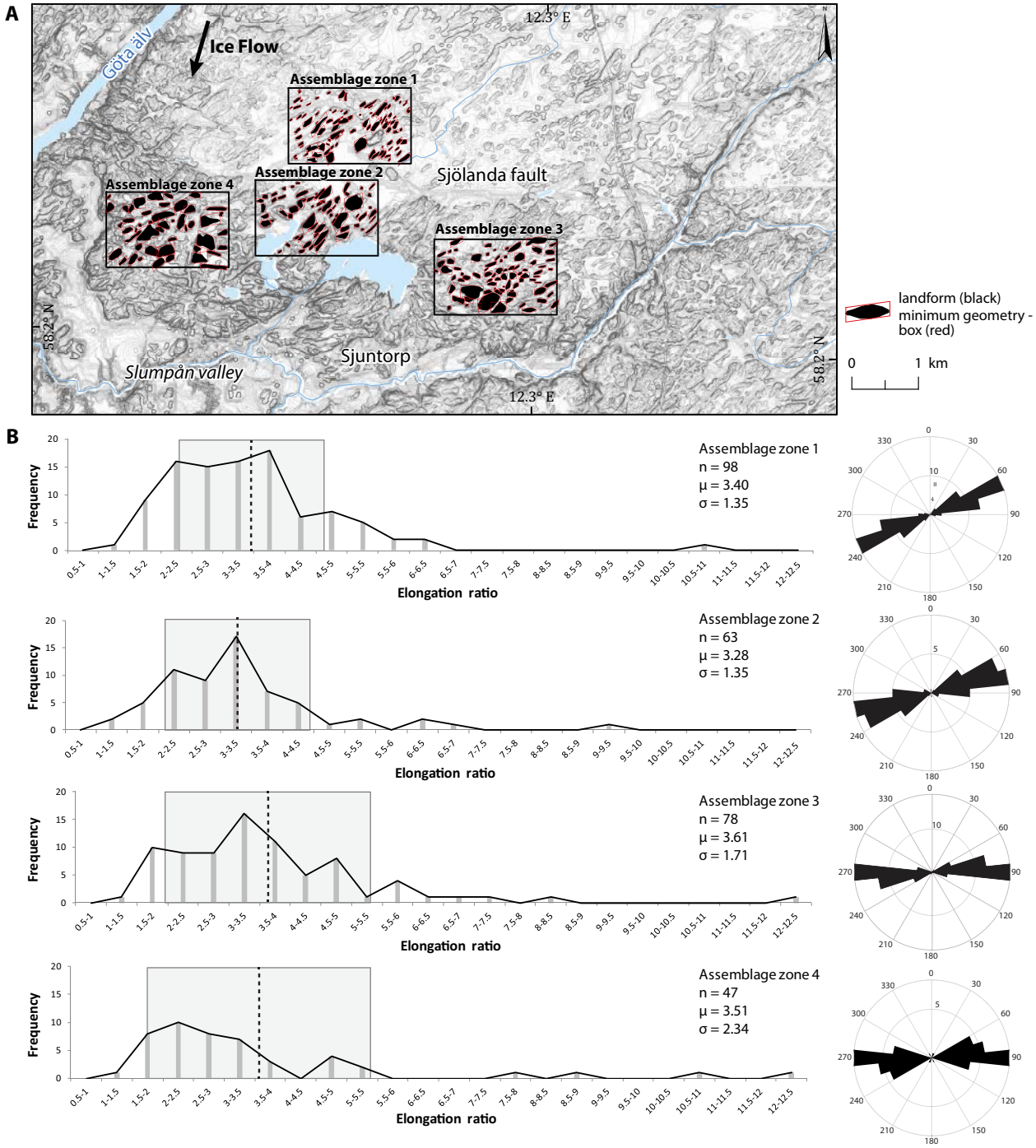

Figure 3-48. *Elongation ratios for bedrock highs in the Sjuntorp area. A. Outlines of bedrock highs in 4 sub-areas. B. Elongation ratios of the mapped landforms plotted in frequency diagrams according to their aspect ratio and plotted in rose diagrams according to the orientation of the long axis. Hillshade is based on Lantmäteriet data.*

Rather, hill orientation follows structural weaknesses, particularly along crush and shear zones oriented towards the N and NE and also fracture zones oriented WNW-ESE (Larsson 1963). Hence, erosion below the unconformity in the southern area is not accompanied by glacial streamlining of bedrock.

It is instructive to compare the bedrock terrain in Västergötland with cnoc and lochan topography in its type area of Assynt, NW Scotland, a well-studied landscape of areal scouring developed on Archaean and Paleoproterozoic Lewisian gneisses (Krabbendam and Bradwell 2013). The present terrain in Assynt formed after glacial erosion of an epigene denudation surface of Neogene age (Godard 1961). The coastal lowland of Assynt has a rugged landscape with hundreds of rock hills or *cnocs* and lake-filled rock-basins or *lochains*. Hill summit elevations vary by 20–30 m in relatively smooth terrain and by 50–80 m in rougher areas. The main landforms of glacial erosion in topographic lows are trenches and star basins, with whalebacks and roches moutonnées on topographic highs (Krabbendam and Bradwell 2013). Very little till occurs. Within the Trollhättan area, the Sjuntorp terrain is relatively highly modified by glacial erosion but still has a somewhat lower relative relief than Assynt, even in the roughest terrain on Fault Block E. The Sjuntorp area has greater till thicknesses in depressions (Figure 3-19). Sjuntorp has a similar array of fracture-bounded hills showing stoss-and-lee forms (Figure 3-21), but with a weaker development of the rounded and smooth outlines typical of stoss slopes in cnoc and lochain terrain. The accordant summits, including flat-topped slättbergen, however, are quite distinctive and unlike the round-topped hillocks at different elevations that are typical of cnoc-and-lochain landscapes (Krabbendam and Bradwell 2014). Elongation of hills in the direction of former ice flow is only weakly developed at Sjuntorp and lee and flank cliffs also generally remain sharp. Hill masses have varied and angular planforms (Figure 3-48). The rectilinear and star basins seen at Sjuntorp (Figure 3-48) resemble structurally-controlled rock basins found west of the study area (Gillberg 1955), in Bohuslän (Olvmo and Johansson 2002) and in cnoc-and-lochain terrain in Scotland (Krabbendam and Bradwell 2014). These morphological differences between Assynt and the area S of Trollhättan imply a greater role for glacial abrasion on the cnoc and lochain terrain on the Lewisian gneiss and a dominance of block removal at Sjuntorp.

3.5.4 Glacial modification of basement highs at the local scale

Landforms of glacial erosion at the local scale include box hills. The term *box hills* refers to rock highs, bounded by fractures that are seen as rectangular or trapezoidal shapes in DEMs (Hall et al. 2019). Good examples are seen in Assemblage Zone 1 at Sjuntorp (Figure 3-48). The box hills are 0.5–2 km in A-axis length and low, rarely rising > 5–10 m above surrounding terrain. Low cliffs are common on southern and eastern flanks, consistent with lee and flank plucking. Intervening depressions include box and star basins, 50–400 m in A-axis length, formed where fracture zones intersect, and trenches, up to 1 km long, following single fracture zones. On the box hills are superimposed whalebacks and roches moutonnées of 10–200 m A-axis length.

Slättbergen are a form of box hill where the hill tops include planar flats and occur at near accordant elevations with neighbouring summits. Progressive glacial modification of planar flats is evident from comparisons of well-preserved, degraded and reshaped forms (Figure 3-49). Well-preserved planar flats retain extensive areas with glacially-polished and planed off phenocrysts, chipped surfaces of quartz and pegmatite veins but few conchoidal fractures. Other glacial microforms include shallow grooves and dm-scale whalebacks (Figure 3-49A and B). Glacial abrasion forms dominate on the upper surfaces of planar flats. Thin till cover is retained in patches on planar flats and may have been more extensive formerly, as planar flats at Sandhem and Kåtene have man-made ridges of soil at their edges that have been removed from adjacent rock surfaces. The northwest faces of planar flats are preferentially aligned along fractures that follow the strike of gneiss foliation, with slopes that conform to the dip of foliation (Figure 3-38). Dells and trenches between slättbergen represent progressively excavated fracture zones that now have shallow infills of Quaternary deposits (Figure 3-49C).

Degraded forms retain smaller planar flats but show greater hill top relief due to differential abrasion and to the loss of blocks from fracture bounded sockets on hill summits, flanks and lee slopes (Figure 3-49D and E). Stoss and flank rounding is widely developed around slättbergen (Johansson et al. 2001b). Edge rounding is partly structurally controlled, as shown by near-surface, closely-spaced, curved sheet fractures (Figure 3-23). Roches moutonnées with well-developed stoss and lee asymmetry occur at elevations only a few metres lower than planar flats (Figure 3-49F), indicating that these classic bedforms of glacial erosion can develop after only very limited lowering of rock surfaces on the former sub-Cambrian unconformity. The topography at elevations below planar flats

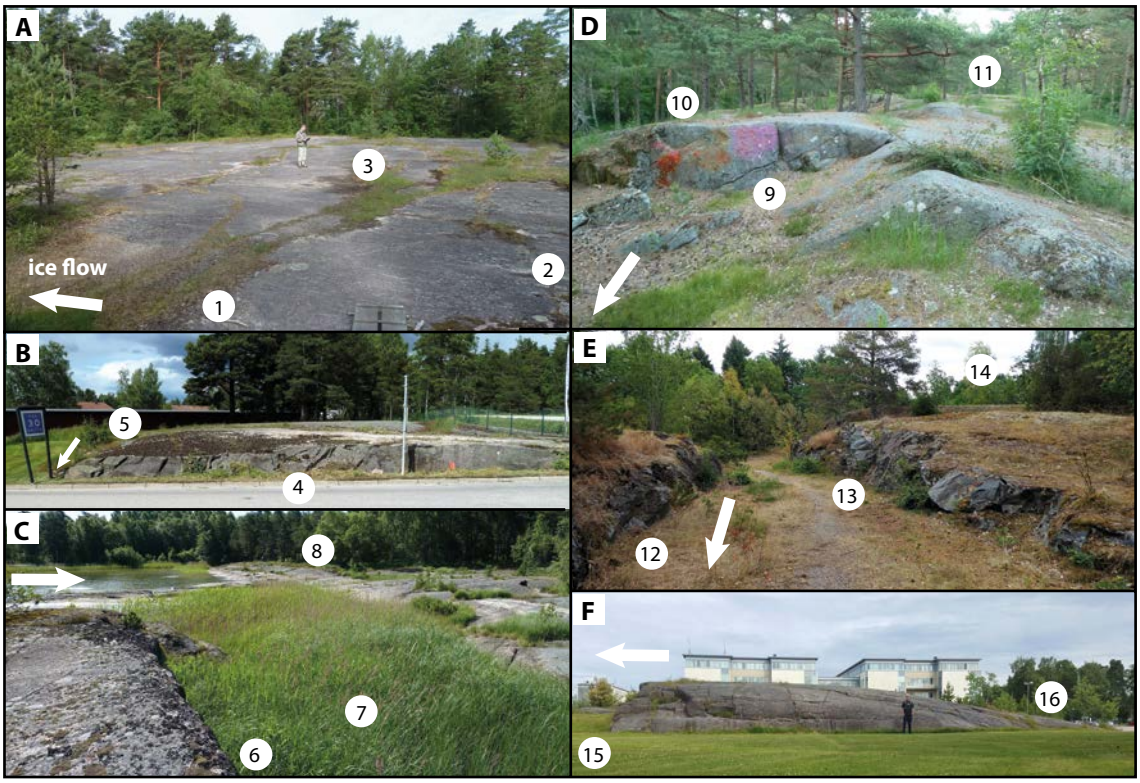

Figure 3-49. *Progressive glacial modification of planar flats (locations on Figure 3-22). A. Eriksro. B. Sandhem. C. Udden. D. Hjortmossen. E. Ryrbäcken. F. Gärdhemsvägen High School. 1. Vertical fractures with < 1 m spacing set within wider granite gneiss surface where fracture spacings generally exceed 4 m. 2. Shallow (< 10 cm deep) grooves from glacial abrasion. 3. Surface of planar flat. 4. Shallow road cut showing inclined fractures dipping to NW along the strike of the gneiss foliation. 5. Whaleback ~ 1 m high. 6. Low lee-side cliff at the edge of a massive block of gneiss. 7. Cleft excavated in more fractured gneiss. 8. Abraded stoss slope. 9. Plucked lee face 10. Plucked lee face ~ 1 m high. 11. Degraded planar flat, after block removal, edge rounding and slight surface lowering. 12. Inclined fractures dipping to NW. 13. Man-made cut showing variably fractured granite gneiss. 14. Degraded planar flat. 15. Plucked lee face of roche moutonnée at an elevation 2–3 m below that of planar flats at Hjortmossen, 270 m to the SE. 16. Curved stoss face of roche moutonnée.*

does not conform to the stepped, flat or gently-inclined surfaces typical of structurally-controlled glacial erosion forms developed in other horizontally fractured, hard, massive, rock substrates. Examples include the horizontally bedded Torridonian sandstone in parts of NW Scotland (Krabbendam and Glasser 2011) and gently dipping rock layers on the Laurentian shield and its Mesoproterozoic cover in north-east Minnesota (Zumberge 1955).

The planar flats can be interpreted as remnant facets of the unconformity preserved in massive zones in granite gneiss. Top surfaces have been lowered slightly by abrasion, but edges have been significantly rounded and have lost blocks to lateral and lee-side plucking (Figure 3-49). Planar flats have become isolated through the removal of blocks by plucking and other glacial erosion processes from intervening zones of more closely fractured gneisses.

3.5.5 Selective exploitation of rock fractures and associated glacial landforms

The links between basement fracturing and landforms of glacial erosion at the local scale are most apparent in and around the three large quarries in the Trollhättan region. DEMs for the surroundings of the quarries near Vänersborg (Figure 3-50) and Håberg (Figure 3-51) show fracture-bounded trapezoidal and rectangular box hills in planform. Similar features are visible at Kuleskog (Figure 3-52), but here ribbed topography is also developed due to the closer spacing of NE-SW fractures. Bedrock profiles oriented N-S and roughly parallel to former ice flow show low elevation ranges for summits. Hill asymmetry is only weakly developed at the local (0.1–1 km) scale. Fracture-guided trenches reach depths of mainly 5–15 m, reaching 20 m in a major fracture zone at Kuleskog.

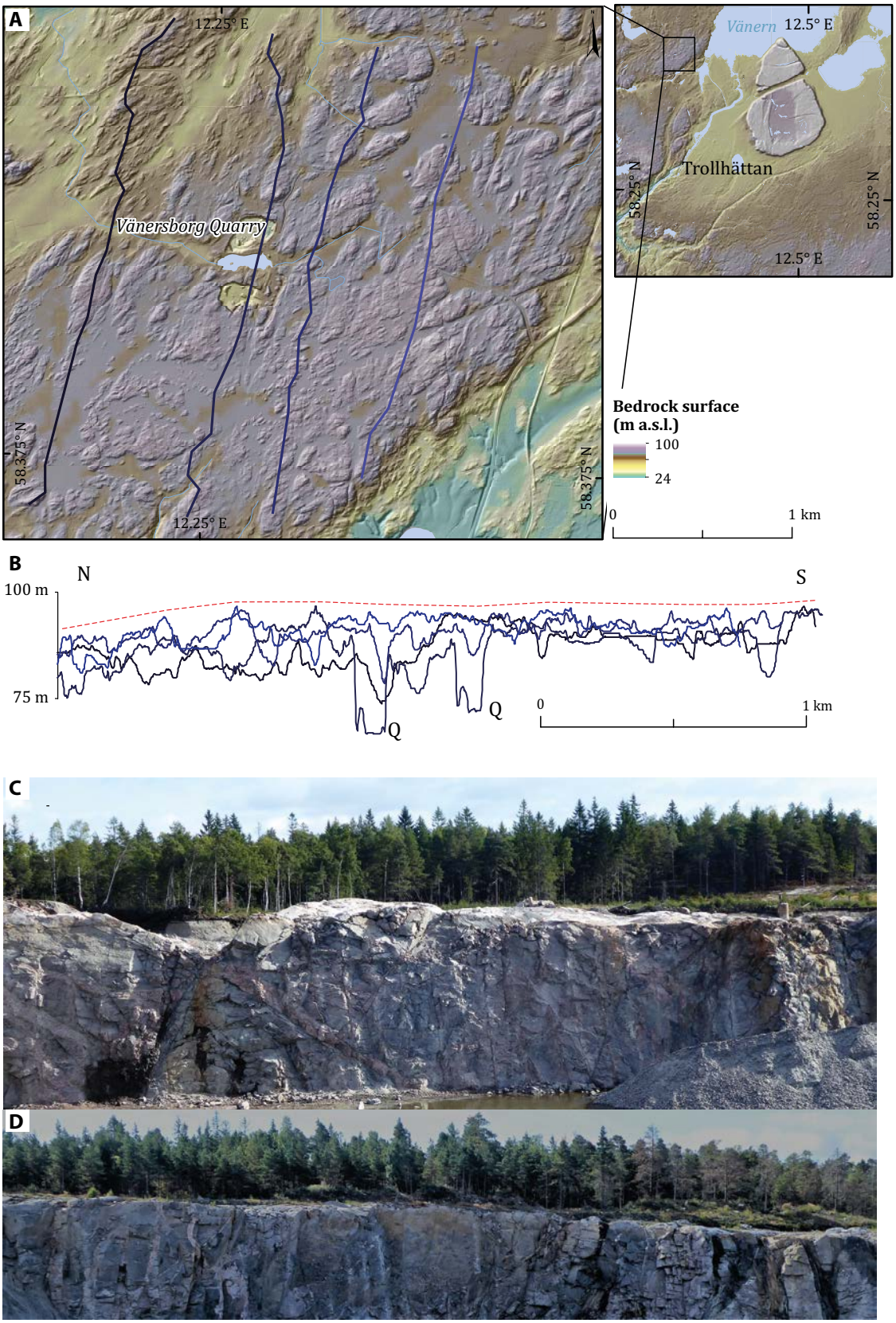

Figure 3-50. *Vänersborg Quarry on Block A, with a summit envelope surface gently tilted towards the N. A. DEM of surroundings. B. Bedrock profiles parallel to ice flow. Dashed line is summit envelope surface. Q quarry excavation. C. North face of north quarry, looking towards the direction of ice flow. D. East face of south quarry, looking across ice flow. See also* Figure 3-34. *DEM and profiles based on Lantmäteriet elevation data.*

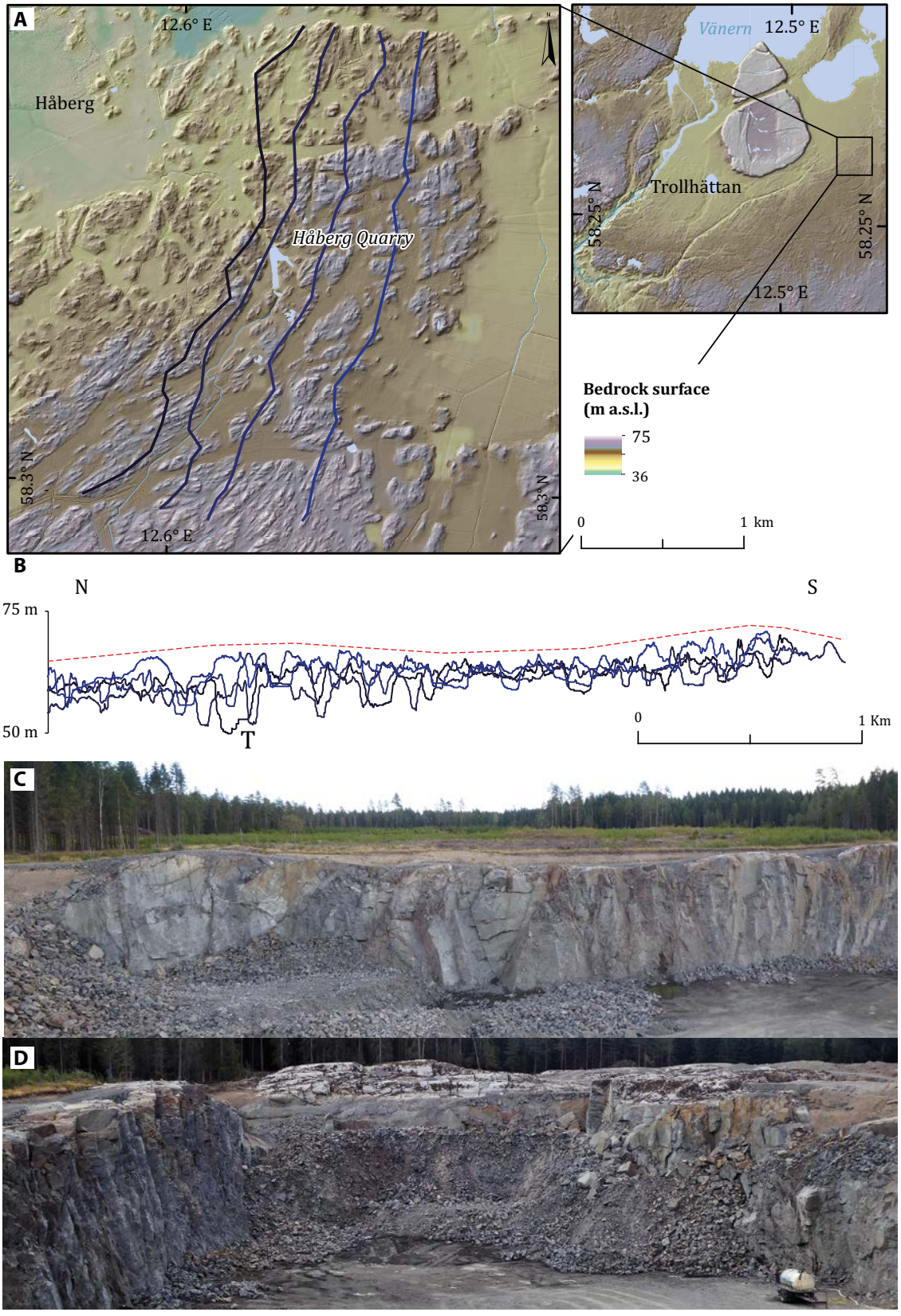

Figure 3-51. *Håberg area, SE of Hunneberg (see also* Figure 3-35*). A. DEM of surroundings. Main fracture sets running ENE-WSW, N-S and NNE-SSW define trapezoidal rock blocks (box hills) 200–400 m in length. B. Bedrock profiles parallel to ice flow. Dashed line is summit envelope surface. T Deep rock trench. C. Håberg Quarry, WNW face, looking towards the direction of ice flow across low roches moutonnées. D. Håberg Quarry, SSE face. Ice moving L to R. Glacial erosion across the top of the rock blocks has roughened surfaces through the exploitation of minor fractures, with development of stoss and lee forms at the macroscale. DEM and profiles based on Lantmäteriet elevation data.*

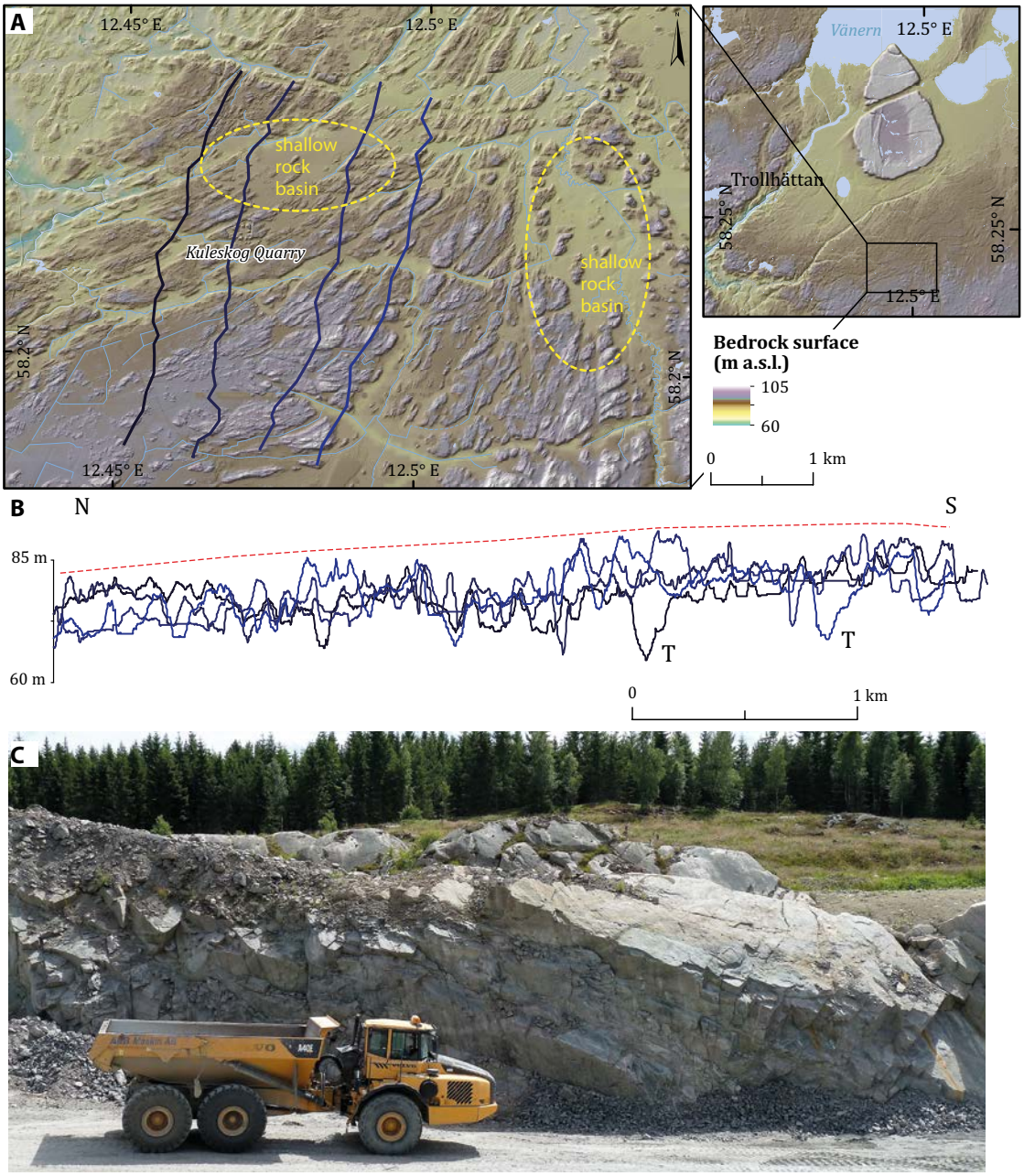

Figure 3-52. *Glacial erosion forms around Kuleskog Quarry, SE of Åsaka. A. DEM of surroundings. B. Bedrock profiles parallel to ice flow. Red dashed line is summit envelope surface. T deep trenches. C. West face of quarry, looking across ice flow. Main fracture sets run WNW-ESE, NE-SW and N-S. The dominant NE-SW set runs parallel to gneiss foliation and defines ridges up to 750 m in length but mainly < 100 m. Intervening trenches are up to 100 m across and 15 m deep but the largest depression are rectilinear basins up to 1 km across but generally only up to 10 m deep. The summit envelope surface here has an elevation of ~90 m. Bedrock is exposed widely, with depths of Quaternary deposits of < 5 m depressions. The ridges when seen in section are asymmetric, with steeper slopes following the strike of the gneisses to the NW. See also* Figure 3-36**.** *DEM and profiles based on Lantmäteriet elevation data.*

Quarry sections parallel and normal to ice flow at Vänersborg (Figure 3-50) and Håberg (Figure 3-51) show links between fracturing and bedrock forms. Closely-spaced vertical fracture zones are associated with shallow clefts. Intervening zones with wider fractures show development of 25–130 m long roches moutonnées and whalebacks. Lee-side and flank cliffs, <3 m high, follow fractures on the southern and eastern flanks of the hills. Erosion below the sub-Cambrian unconformity in these localities has led to the excavation of clefts, trenches and basins in fracture zones, the isolation of massive rock compartments and the weak development of asymmetry across these bedrock highs.

3.5.6 Depths of glacial erosion in basement

Depths of glacial erosion of basement across the Trollhättan region (Figure 3-53) are derived by subtracting the present basement surface from the summit envelope surface, regarded as a close approximation of the former position and form of the U2 reference surface (Section 2.4.2). Extensive areas show removal of <5–10 m depths of basement. Glacial erosion is greatest in trenches and basins that reach depths of 40 m W of the Göta Älv and 80 m in parts of the Göta trench and in basins S of Sjuntorp. The average depth of erosion below a summit envelope surface across the Trollhättan study area is 14.4 m.

These depths are broadly consistent with those estimated for Areas 1–4. Around Vargön (Area 1), estimated depths of erosion below the summit envelope surface are <5 m over wide areas, with an average depth of 10.7 m across Area 1, consistent with the widespread survival of planar flats (Figure 3-14G). Around Trollhättan (Area 3), glacial erosion of basement also has been <5 m in parts of the town, where planar flats are common, and <15 m in the terrain to the E (Figure 3-18G). Average depth of erosion in Area 3 is 12.7 m. Around Åsaka (Area 2), erosion depths are greater but generally remain <20 m in depressions (Figure 3-17G). Around Sjuntorp (Area 4), average erosion depths are 19.4 m and reach 40 m in large basins (Figure 3-19G). The southern part of the Sjuntorp area has the largest erosion depths (Figure 3-53).

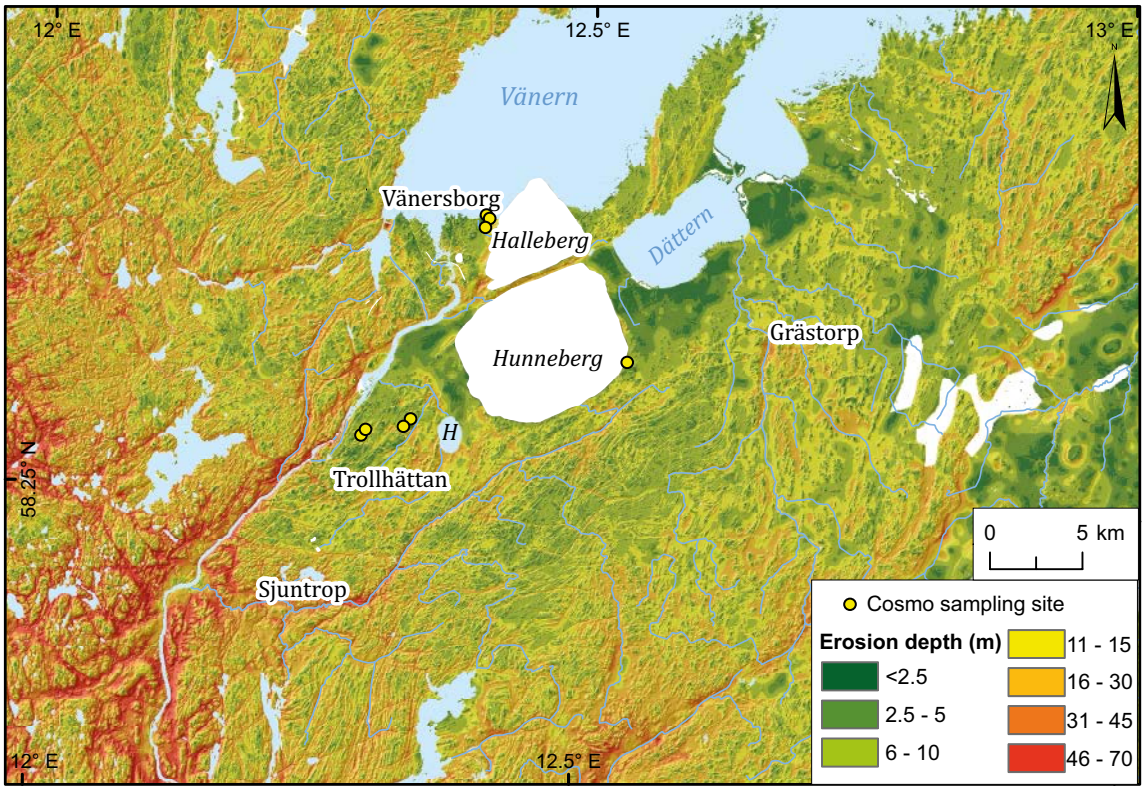

Figure 3-53. *Estimated depths of glacial erosion in basement below the unconformity. Method outlined in Figure 2-5. Note that the model underestimates erosion depths in areas where pinning points are widely spaced. This is evident for the area N of Hullsjön (H), where Quaternary sediment thickness locally exceed 20 m. This issue is not significant for Areas 1–4 (Figure 3-46) where bedrock is exposed widely. DEM based on Lantmäteriet elevation data.*

Relatively deep erosion is indicated where erosion depths below summit envelope surfaces are > 5 m, > 10 m and > 20 m. Points where erosion depths beneath the summit envelope surfaces are > 10 m cover areas of 42–53 % of Areas 1–3 (Table 3-2). Where excavation has occurred to > 10 m and > 20 m deep, trenches and basins occupy 42–53 % and 4–16 %, respectively, in Areas 1–3. In Area 4, 75 % of its area is > 10 m below, and 35 % is > 20 m below summit envelope surfaces, consistent with deeper erosion and the much more limited extent of summit areas (Figure 3-19D) compared with Areas 1–3 (Figures 3-14D, 3-17D and 3-18D). The estimated volumes of rock removed from Area 4 at > 5 m, > 10 m and > 20 m depths are also much larger than for other areas (Table 3-2). These estimates of trench and basin excavation indicate that Area 4, Sjuntorp, has been not only more deeply eroded (Figure 3-19G) but also that a large part of the volume of rock removed is derived from the extension and deepening of rock basins and trenches (Table 3-2). The bulk of the basement rock removed by glacial erosion across the Trollhättan region has come from the excavation of trenches and basins.

Table 3-2. Contribution to erosion below summit envelope surfaces of the excavation of rock trenches and basins estimated using points that stand > 5 m and > 10 m below those surfaces (Section 2.6.4).

Area number	Area rock loss (in %) from rock basins and trenches					
	> 5 m	< 5 m	> 10 m	< 10 m	> 20 m	< 20 m
1	85.7 %	14.3 %	44.4 %	55.6 %	11.8 %	88.2 %
2	75.6 %	13.9 %	42.0 %	58.0 %	4.0 %	96.0 %
3	85.8 %	14.2 %	52.5 %	47.5 %	15.8 %	84.2 %
4	95.0 %	5.0 %	74.7 %	25.3 %	34.5 %	65.5 %

Area number	Area (km^2)	Volume rock loss (in km^3) from rock basins and trenches			Average rock loss (in m per km^2) from rock basins and trenches		
		> 5 m	> 10 m	> 20 m	> 5 m	> 10 m	> 20 m
1	44.07	0.44	0.34	0.13	13.12	17.2	25.59
2	65.86	0.62	0.40	0.07	10.88	14.48	24.72
3	37.43	0.46	0.37	0.18	14.30	18.68	30.02
4	72.02	1.39	1.27	0.85	20.23	23.6	34.34

Further constraints on the estimated depths of basement erosion are provided by the heights of exhumed Phanerozoic fault scarps along block edges. Block edges have been eroded (Figure 3-29) but tops remain at similar elevations on the buried and exposed unconformity surfaces (Figure 3-15) and retain inclined, planar surfaces seen in topographic profiles (Figure 3-16). Lowering of block tops by glacial erosion is locally < 5 m (Figure 3-53). Exhumed fault scarps at block edges have not been eliminated by glacial erosion. The estimated displacement across the Lilleskog Fault derived from geological evidence (~30 m) from the buried unconformity is similar to that based on morphological evidence (26–35 m) for the continuations of the fault scarp found in exposed basement W and E of Halleberg (Section 3.4). Lowering of the raised surface on Fault Block B and the lowered surface on Fault Block D across the Lilleskog Fault has been negligible on resistant rock cores. Along the Lilleskog Fault, the exhumed fault scarp is well preserved. Other inter-block fault scarps have heights of 10–30 m, whereas intra-block fault scarps have heights of 9–20 m. Significantly greater lowering of blocks across other faults is unlikely and the heights of the preserved fault scarps represent maximum values for depths of glacial erosion.

To all erosion depths estimated from summit envelope surfaces should be added the loss of rock from basement highs. This thickness represents the height difference between the projected unconformity and the lower summit envelope surface. This loss is estimated to be 2–6 m based on the height differences between the preserved unconformity around Halleberg and Hunneberg and the hills and knolls in the immediate surroundings that provide pinning points for the summit envelope surfaces. At greater distances from outliers, glacial erosion can be assumed to have acted over a longer duration and to greater depth. Near constant summit elevations along the shore of Lake Vänern W of Hunneberg (Figure 3-15) and low summit elevation ranges across the southern flank of Hunneberg (Figure 3-28) indicate that summit erosion depths do not increase significantly with increasing distance from outliers.

3.6 Cosmogenic nuclide inventories in bedrock surfaces

3.6.1 Exposure ages

The samples were collected for the purpose of understanding the long-term erosional history of exceptionally flat bedrock outcrops in the Trollhättan area. The sample set comprises three samples of which were collected in year 2000 (MJ-13 to MJ-15), and the results of which were listed but not discussed in Stroeven et al. (2016), and ten samples which were collected in years 2016 (TROLL-16-04 to TROLL-16-10) and 2017 (TROLL-17-01 to TROLL-17-03). The samples derive from four different but closely-spaced geographical areas. Two of the areas flank the twin table mountains of Halleberg and Hunneberg (Figure 3-54).

Table 3-3 presents key exposure age data for the full set of samples and Figure 3-55 displays simple exposure ages against sample elevation. The simple ^{10}Be (^{26}Al) exposure ages range from 6.8 ± 1.4 ka (7.0 ± 1.4 ka) to 44.7 ± 2.8 ka (46.3 ± 3.5 ka), with nine samples that are younger than 14 ka (15 ka) and the remaining four samples that are older than 24 ka (18 ka). Compared to the expected simple exposure age assuming only exposure following deglaciation and taking account of the post-glacial submergence, there are two ^{10}Be exposure agesand two ^{26}Al exposure ages that are too young, three ^{10}Be exposure ages and four ^{26}Al exposure ages s that overlap within uncertainties with the expected exposure age, and eight ^{10}Be exposure ages and seven ^{26}Al exposure ages that have too old exposure ages due to prior exposure.

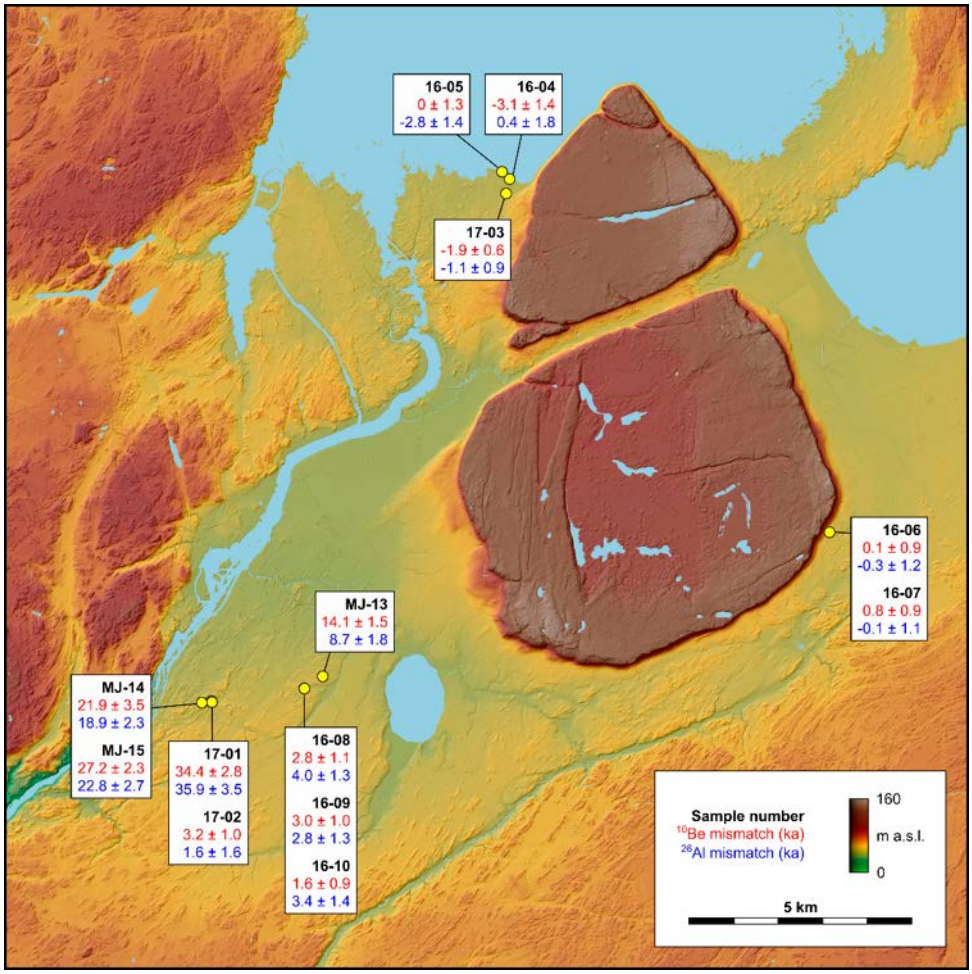

Figure 3-54. *Map of the Trollhättan region with cosmogenic nuclide sample locations. The sample ^{10}Be and ^{26}Al mismatch represents the difference between the calculated and the expected exposure age employing the deglaciation age of Stroeven et al. (2016) and taking shielding by water into account. Positive mismatch values represent cosmogenic nuclide inheritance and negative mismatch values represent samples with a cosmogenic nuclide concentration lower than expected assuming full exposure to cosmic rays after post-glacial emergence. DEM based on Lantmäteriet elevation data.*

Table 3-3. Summary of sample data and ^{10}Be and ^{26}Al exposure ages for the thirteen samples. The exposure ages are calculated assuming one single period of full exposure at the surface. The mismatch is the difference between this exposure age and the theoretical simple exposure age that the concentration expected based on the deglaciation and uplift through water would yield if the last ice sheet had removed all previously produced cosmogenic nuclides. The deglaciation, emergence, and exposure ages are all related to the individual sampling year (2016, 2017, 2000).

Sample	Latitude	Longitude	Elevation (m a.s.l.)	Deglaciation (yr)	Emergence (yr)	^{10}Be exposure age (yr)	^{10}Be exposure age mismatch (yr)	^{26}Al exposure age (yr)	^{26}Al exposure age mismatch (yr)
TROLL-16-04	58.386	12.407	45	13 452	9 615	6 771 ± 1 354	−3 054	10 273 ± 1 823	444
TROLL-16-05	58.388	12.404	45	13 452	9 615	9 817 ± 1 338	−9	7 021 ± 1 387	−2 809
TROLL-16-06	58.318	12.535	53	13 424	10 230	10 408 ± 911	64	10 078 ± 1 229	−270
TROLL-16-07	58.318	12.535	53	13 424	10 230	11 175 ± 855	831	10 238 ± 1 066	−110
TROLL-16-08	58.282	12.336	52	13 668	10 175	13 078 ± 1 132	2 804	14 242 ± 1 327	3 965
TROLL-16-09	58.282	12.336	52	13 668	10 175	13 254 ± 1 035	2 980	13 087 ± 1 277	2 810
TROLL-16-10	58.282	12.336	52	13 668	10 175	11 867 ± 945	1 594	13 719 ± 1 373	3 442
TROLL-17-01	58.279	12.301	53	13 703	10 231	44 707 ± 2 797	34 372	46 260 ± 3 507	35 922
TROLL-17-02	58.278	12.301	51	13 703	10 115	13 385 ± 1 003	3 159	11 841 ± 1 613	1 612
TROLL-17-03	58.383	12.406	47	13 453	9 823	8 123 ± 589	−1 874	8 891 ± 863	−1 110
MJ-13	58.285	12.343	51	13 635	10 101	24 371 ± 1 481	14 136	18 978 ± 1 819	8 741
MJ-14	58.278	12.297	54	13 686	10 270	32 283 ± 3 534	21 908	18 916 ± 2 269	8 538
MJ-15	58.278	12.297	54	13 686	10 270	37 612 ± 2 278	27 238	33 133 ± 2 713	22 755

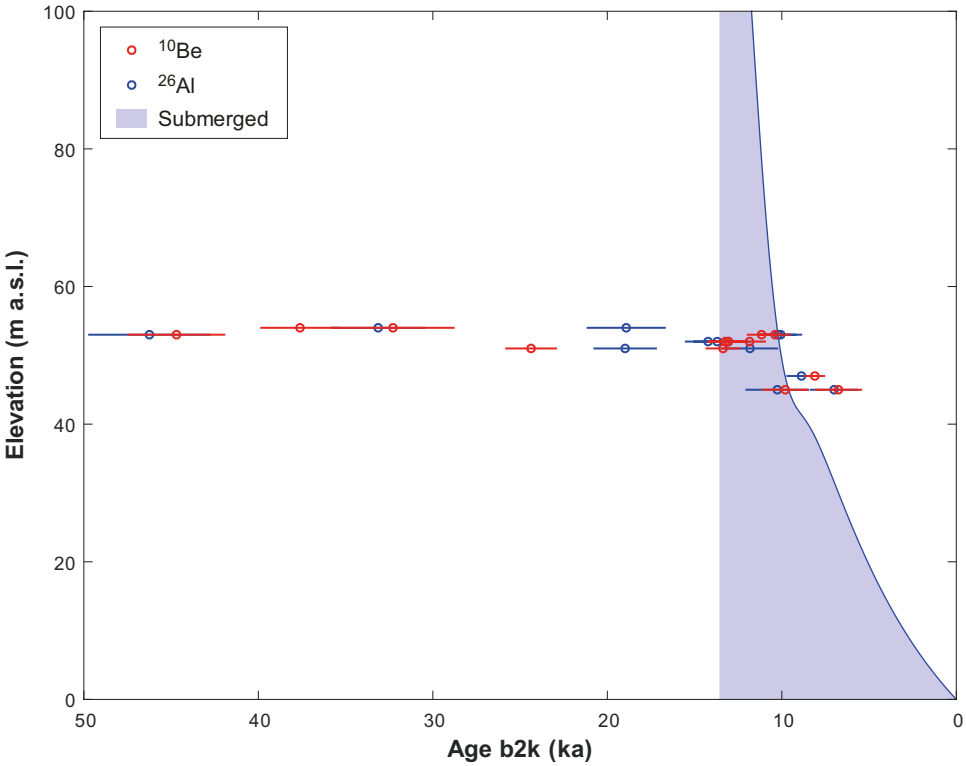

Figure 3-55. *Simple ^{10}Be and ^{26}Al exposure ages, assuming one period of full exposure to cosmic rays, and sample elevation. The blue line and area show the shoreline displacement and the post-glacial period of submergence. Surfaces that experienced glacial erosion during the last ice cover period deep enough to remove the inventory of cosmogenic nuclides overlap within uncertainty with the shoreline displacement curve. Samples with simple exposure ages that fall to the right of the shoreline displacement curve have cosmogenic nuclide concentrations lower than expected assuming full exposure to cosmic rays following emergence. Samples with simple exposure ages that fall to the left of the shoreline displacement curve have inherited cosmogenic nuclides from exposure to cosmic rays prior to the last glaciation. All ages are referenced to year 2000 (b2k) with extrapolation of the shoreline displacement curve from 1950 to year 2000.*

In order to check at-a-site variation, multiple samples have been collected from multiple sites (Figure 3-74). Apparent exposure ages from single sites generally overlap or fall close together. The best exposure age overlap occurs for samples collected from spots located close together at the Skavsta industrial site (TROLL-16-8 to -10) and at Bragnum (TROLL-16-6 and -7). The results indicate that uncertainties from at-a-site variation are small.

West of Halleberg, on the southern shore of Lake Vänern, at Nordkroken, samples TROLL-16-04 and TROLL-16-05 were collected from rock platforms at lake level (at 45 m a.s.l.). Both sites stand between a vegetated dune ridge and the lake and may formerly have been covered by dune sands. Sample TROLL-17-03 was collected from a rock surface on the landward side of the dune ridge and is unlikely to have been covered by dune sand. Sample TROLL-17-03 was from the far corner of a flat rock surface which currently is in use as a carpark (at 47 m a.s.l.). The bedrock surface of the latter sample appeared undisturbed from erosion by car traffic, but since the whole surface, at some point, also appears to have been cleared of a thin sediment cover to allow for the car park, cosmogenic results would potentially underestimate the time of postglacial exposure. The simple exposure ^{10}Be (^{26}Al) ages of these samples are 6.8 ± 1.4 ka (10.3 ± 1.8 ka), 9.8 ± 1.3 ka (7.0 ± 1.4 ka), and 8.1 ± 0.6 ka (8.9 ± 0.9 ka) for sites just above the current Lake Vänern water level. Interestingly, two of the sites underestimate our expectations for ^{10}Be with 2–3 ka, whereas one site (TROLL-16-05) is spot-on. The congruence between expected and calculated age for the latter site yields some confidence to our ability to predict exposure ages using reconstructed deglaciation ages and shoreline uplift curve. Whereas an underestimation of the time of postglacial exposure was expected for one site (TROLL-17-03), it was not for the other.

The second area, near Bragnum, is located southeast of, and is within 200 m from, the base of Hunneberg. Here we sampled two surfaces protruding above the surrounding farm fields. Samples TROLL-16-06 and TROLL-16-07 from these convex hilltops at 53 m a.s.l. yielded apparent full exposure ^{10}Be ages of 10.4 ± 0.9 ka, 11.2 ± 0.9 ka, respectively. These closely-spaced sites yielded exposure ages that are consistent with each other and overlap with the expected exposure age within uncertainties for both ^{10}Be and ^{26}Al.

The remaining two investigation areas are located within the city limits of Trollhättan. The area of Hjortmossen, nearest to the centre of town was visited in 2000 and in 2017 for sampling. Samples drawn from the edge of the summit flat in 2000 are at a site, which today is covered by an indoor hockey rink (MJ-14 and MJ-15) and could not be inspected in 2017. Of these, MJ-15 was from the summit flat proper (54 m a.s.l.), and nearby MJ-14 from a pegmatite vein set 40 cm below the summit flat in what appeared to be a plucking scarp. To align these earlier measurements with samples from 2017, we re-sampled the summit flat on another side of the hockey rink (TROLL-17-01; 53 m a.s.l.), just above a pronounced slope, and the slope 2 m below the summit flat (TROLL-17-02). The cosmogenic nuclide results from the samples collected in years 2000 and 2017 paint a consistent picture. The two surface flat samples yielded simple exposure ^{10}Be (^{26}Al) ages of 37.6 ± 2.3 ka (33.1 ± 2.7 ka) and 44.7 ± 2.8 ka (46.3 ± 3.5 ka), whereas sample MJ-14, inset slightly below the surface flat, yielded 32.3 ± 3.5 ka (18.9 ± 2.3 ka). All three sites have simple exposure ages that are much older than expected exposure ages using reconstructed deglaciation and shoreline uplift histories (22–36 ka of inheritance for all samples apart from one ^{26}Al measurement with 8.5 ka of inheritance). The fourth site, 2 m below the summit flats, has an apparent full exposure age much closer to expectation, but still has 3 ka of ^{10}Be inheritance and just about overlaps within uncertainty with the expected ^{26}Al exposure age (Table 3-3).

The final investigation area (slättbergen outcrop at Sandhem) is located east of Trollhättan. Also, this site was visited for sampling in 2000 and 2017. The sampling of a thin layer of vein quartz at 51 m a.s.l. in 2000 (MJ-13) yielded a simple ^{10}Be (^{26}Al) exposure age of 24.4 ± 1.5 ka (19.0 ± 1.8 ka). The three samples from the fenced-in area used for storage of surface material have simple ^{10}Be (and ^{26}Al) exposure ages that all overlap with each other within uncertainty, but do not overlap with the simple exposure age of sample MJ-13. Indeed, in accordance with the overlap between the simple ^{10}Be (^{26}Al) exposure ages of 13.1 ± 1.1 ka (14.2 ± 1.3 ka), 13.3 ± 1.0 ka (13.1 ± 1.3 ka), and 11.9 ± 0. 9 ka (13.7 ± 1.4 ka); 52 m a.s.l.) for samples with an identical expected exposure age, inheritance also varies moderately between the samples at 1.6–3.0 ka (2.8–4.0 ka). In contrast, inheritance for sample MJ-13 is much larger with ^{10}Be (^{26}Al) inheritance at 14.1 ka (8.7 ka).

The ^{10}Be and ^{26}Al data show similar patterns for the investigated sites. For the samples collected in 2016 and 2017, with measurements taking advantage from the use of a gas-filled magnet at PRIME Lab, the difference between the simple ^{10}Be and ^{26}Al exposure ages is less than 1 ka for all but one sample (TROLL-17-03). For the remaining four samples, the difference between the simple ^{10}Be and ^{26}Al exposure ages range from 1.6 ka to 13.3 ka.

In summary, sites on, or on the flanks of, exceptionally flat surfaces (all but Bragnum) or on summit surfaces accordant with these exceptionally flat surfaces (Bragnum) display a wide range of exposure histories from requiring post-glacial shielding (n=2; Nordkroken) and samples for which the full cosmogenic nuclide inventory can be explained by post-glacial exposure (n=3-4; Nordkroken and Bragnum plus one ^{26}Al measurement for Sandhem), to samples with varying amounts of inheritance. In the latter category are those with minor amounts of inheritance (1.6–4.0 ka, n=6; Bragnum, Hjortmossen flank, and Sandhem storage sites) to those with considerable amounts of inheritance at Hjortmossen summit flat and Slättbergen samples (n=4; 8.5–36 ka). All five samples collected just below the edge of the table mountains have cosmogenic nuclide concentrations that overlap with or is lower than expected for only post-glacial exposure to cosmic rays, while all samples from Trollhättan some kilometres away from the table mountains (except for the ^{26}Al measurement concentration of one sample) have inheritance from prior exposure.

3.6.2 Glacial erosion

The glacial erosion simulations yield output ranging from 0.3 m erosion over the last 100 ka to unlimited glacial erosion (more than 10 m). The sensitivity tests (Figure 3-56) reveal that within the specified parameter boundaries, subaerial erosion has a minor effect on the total erosion, whereas

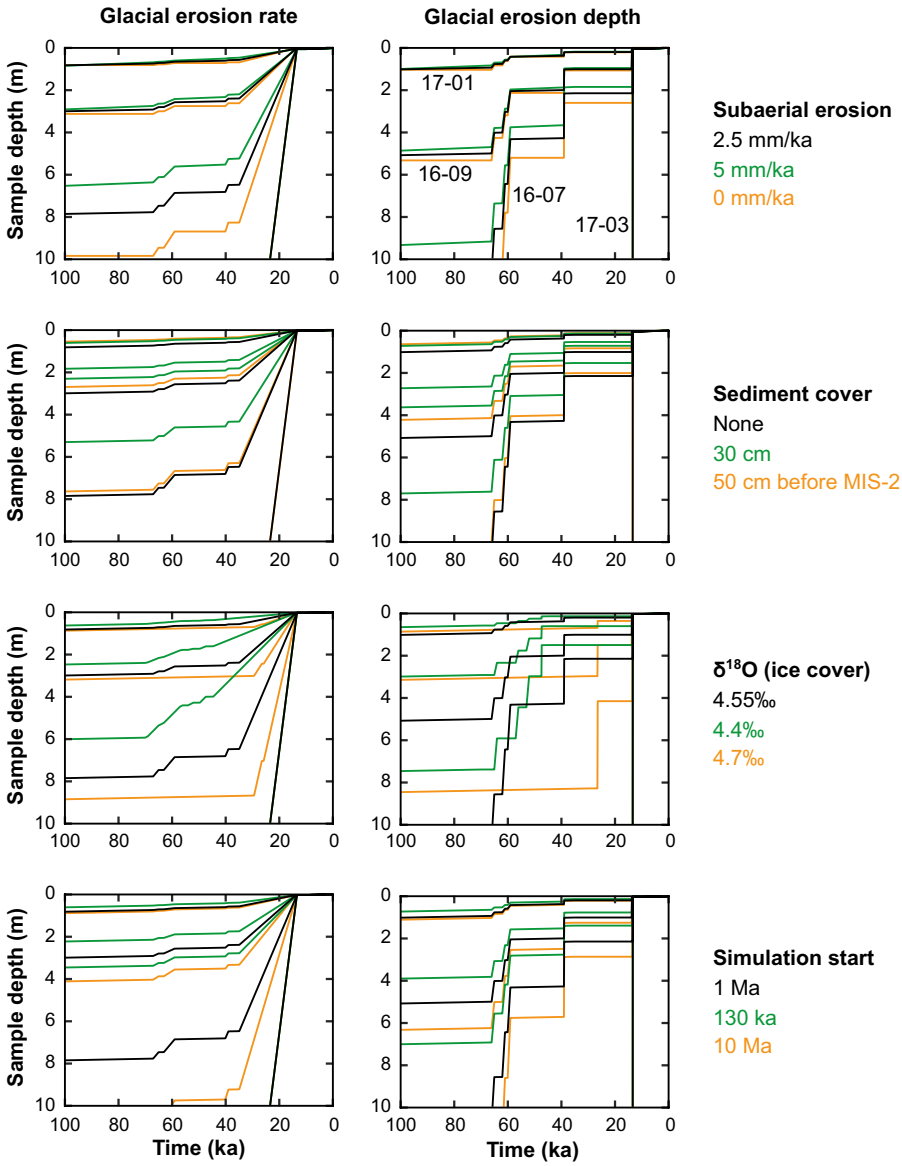

Figure 3-56. *Sensitivity tests of the erosion simulation. Each panel shows the simulated erosion (sample depth history) over the last 100 ka for four samples (TROLL-16-07, 16-09, 17-01, and 17-03) and three scenarios based on ^{10}Be. The black lines show the erosion of the reference scenario, as defined by four reference parameters, with constant glacial erosion rate (left panels) and constant glacial erosion depth (right panels). The green and yellow lines show the erosion when perturbing one of the four parameters: subaerial erosion rate, sediment cover, δ^{18}O cut-off value, and simulation start. For the predetermined parameter space, the erosion is generally more sensitive to perturbations of the ice cover history and simulation start point than to perturbation of the subaerial erosion rate. Whereas 30 cm sediment cover (density: 2.0 g cm−3) until just before sampling yields significant erosion difference, 50 cm sediment cover prior to the MIS-2 glaciation only has a limited effect on the erosion.*

perturbations of the ice cover history (δ^{18}O cut-off value) and the simulation duration have larger effect on the total erosion. In absolute values, parameter perturbations have a larger effect on the samples with minor cosmogenic nuclide inheritance compared to samples with much cosmogenic nuclide inheritance. Assuming burial under 30 cm of sediments until just before sampling affects the erosion with a similar magnitude as the ice cover history and simulation duration perturbations, and for the sample with too low ^{10}Be concentration (TROLL-17-03) it results in some ^{10}Be inheritance but still relatively large glacial erosion. Assuming burial under 50 cm of sediments prior to the MIS-2 glaciation has a minor effect with slightly reduced glacial erosion. Figure 3-58 and Figure 3-59 and Figure 3-60 display the simulated erosion histories for the full set of samples that yield a solution, for all scenarios (Table 2-4), and for ^{10}Be only (Figure 3-58), ^{26}Al only (Figure 3-59), and combined

^{10}Be and ^{26}Al simulations (Figure 3-60). To identify possible differences in erosion histories, we separate our results for samples from around Trollhättan town from those for Halleberg-Hunneberg for scenarios 3–6, covering the individual scenarios for constant erosion rate and depth starting at 0.5 Ma and 1 Ma (Figure 3-61).

For all five samples from Nordkroken and Bragnum, which overlap with or has a concentration lower than expected from the post-glacial exposure, there is no upper limit of the potential glacial erosion in all erosion scenarios and for both ^{10}Be and ^{26}Al. For the three ^{10}Be (^{26}Al) measurements with exposure ages overlapping with the expected post-glacial exposure age, the minimum total erosion over the last 100 ka range from 2.2–3.1 m (2.0–3.3 m) for scenarios 1–2 (simulation start at 130 ka) to 4.0–7.1 m (3.2–6.0) for scenarios 9–10 (simulation start at 10 Ma). With the combined ^{10}Be and ^{26}Al simulations, only the two Bragnum samples yield a solution, with minimum total erosion over the last 100 ka of 2.7–2.8 m for scenarios 1–2 and minimum total erosion of 5.5–7.1 m for scenarios 1–2.

The sample results from around Trollhättan town indicate a different erosion history (Figure 3-61). For the three samples from the fenced-in area at Sandhem, the total erosion over the last 100 ka based on ^{10}Be (^{26}Al) measurements range from 1.7-11.2 m (1.5–7.7 m) for scenarios 1–2 to 2.5–20.9 m (2.0–10.5 m) for scenarios 9–10. Sample TROLL-17-02, from the slope below the summit flat at Hjortmossen, which has a similar amount of ^{10}Be inheritance as the three samples from the fenced-in area at Sandhem, yield a similar total erosion based on ^{10}Be ranging from 1.7–6.3 m for scenarios 1–2 to 2.4–8.7 m for scenarios 9–10. With the combined ^{10}Be and ^{26}Al simulations, the three Sandhem samples yield total erosion over the last 100 ka ranging from 1.7–6.7 m for scenarios 1–2 and 2.5–9.6 m for scenarios 9–10.

For the four samples with the highest cosmogenic nuclide inheritance, from Hjortmossen and Sandhem, the total erosion over the last 100 ka based on ^{10}Be (^{26}Al) measurements range from 0.3–2.1 m (0.3–3.5 m) for scenarios 1–2 to 0.6–2.8 m (0.6–4.4 m) for scenarios 9–10. With the combined ^{10}Be and ^{26}Al simulations, one to two of the four samples yield no solution. The samples that do yield a solution yield total erosion over the last 100 ka ranging from 0.3–1.1 m for scenarios 1–2 and 0.6–1.9 m for scenarios 9–10.

The end-member scenarios 11–14 generally yield more glacial erosion compared to the constant glacial erosion scenarios 1–10. For the simulations without glacial erosion between 10 Ma and 130 ka (scenarios 11–12), the four samples with most cosmogenic nuclide inheritance yield total erosion over the last 100 ka based on ^{10}Be (^{26}Al) of 0.9–6.1 m (0.8–7.7 m). The remaining samples which do yield a solution for these scenarios, yield minimum total erosion over the last 100 ka based on ^{10}Be (^{26}Al) of 8.1–32.2 m (3.7–92.0 m). For the simulations without glacial erosion after 55 ka (scenarios 13–14), the four samples with most cosmogenic nuclide inheritance yield minimum total erosion over the last 100 ka based on ^{10}Be (^{26}Al) of 0.5–1.1 m (0.4–1.5 m) with unlimited maximum total erosion. The remaining samples which do yield a solution for these scenarios, yield minimum total erosion over the last 100 ka based on ^{10}Be (^{26}Al) of 2.9–40.3 m (2.2–5.6 m).

Figure 3-57 shows the sample ^{26}Al/^{10}Be ratios with cosmogenic nuclide concentrations normalized against long-term average surface production rates in a commonly used ^{26}Al/^{10}Be ratio plot (Lal 1991), plus examples of the ^{26}Al/^{10}Be ratio evolution through the simulation for scenario 5. In total, five samples yield no combined solution for the ^{10}Be and ^{26}Al simulations. These are the three samples with ^{10}Be and/or ^{26}Al concentration lower than expected from the post-glacial exposure and two of the samples collected in year 2000 which have too low ^{26}Al/^{10}Be ratios for the simulation to yield a solution.

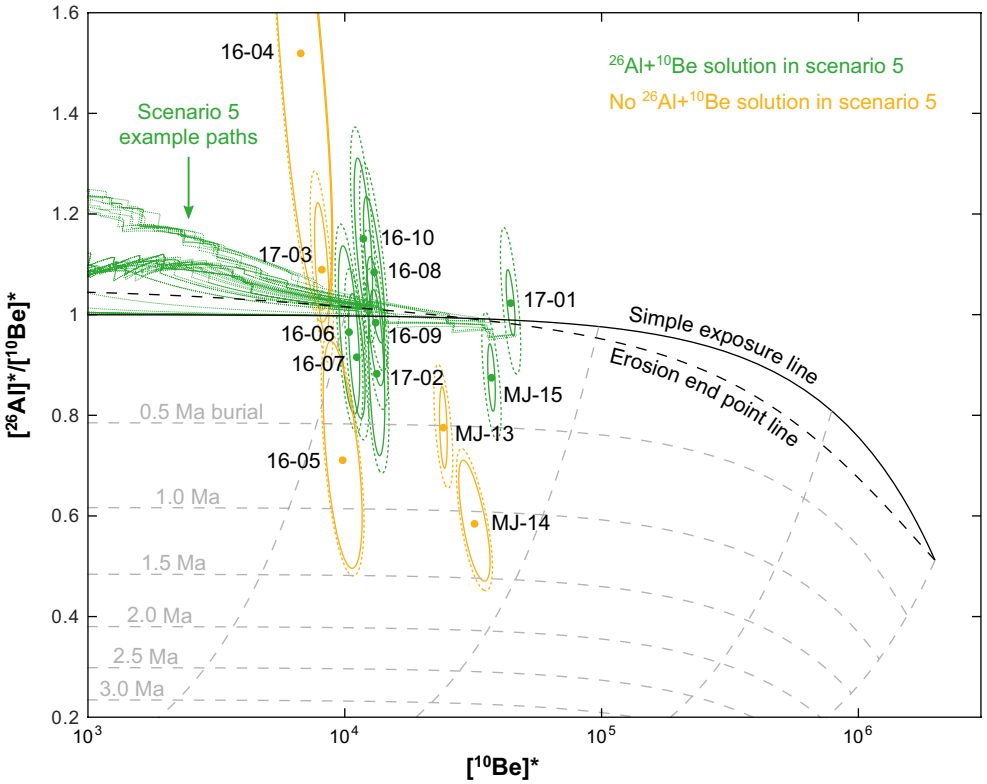

Figure 3-57. *Sample $^{26}Al/^{10}Be$ ratios with sample ^{10}Be and ^{26}Al concentrations normalized against long-term average surface ^{10}Be production rates. The simple exposure line shows the theoretical path under full exposure at the surface. The erosion end point line shows the theoretical surface ratios for various constant erosion rates. The sub-horizontal dashed curves show theoretical $^{26}Al/^{10}Be$ ratios after initial full exposure at the surface followed by burial (no cosmogenic nuclide production). The sub-vertical dashed curves show the path of $^{26}Al/^{10}Be$ ratios if buried after 10 ka, 100 ka, 1 Ma, and 10 Ma of exposure. The ellipses around the sample ratios show the uncertainty from measurement only (solid lines) and with production rate uncertainty added (dashed lines). The example paths coming in from the left edge show five examples of the $^{26}Al/^{10}Be$ ratio development for each sample that yield a solution for the combined ^{10}Be and ^{26}Al simulation with scenario 5, including the examples that yield the minimum and maximum end-point $^{26}Al/^{10}Be$ ratios. The elevated $^{26}Al/1^{0}Be$ ratios at the left edge of the plot is caused by the elevated $^{26}Al/^{10}Be$ ratios due to increased importance of muogenic production at depth.*

Similar to the glacial erosion simulations for the Forsmark area (Hall et al. 2019), the constant glacial erosion depth scenarios commonly yield somewhat deeper glacial erosion compared to the constant glacial erosion rate simulations. This is an effect of the resulting erosion history with total glacial erosion either scaling directly against duration of ice cover (erosion rate) or against number of ice cover periods (erosion depth).

To summarize, the Trollhättan sample set based on cosmogenic ^{10}Be and ^{26}Al measurements indicates glacial erosion ranging from depths of decimetre-scale over the last glacial cycle up to several metres, and potentially more than 10 m.

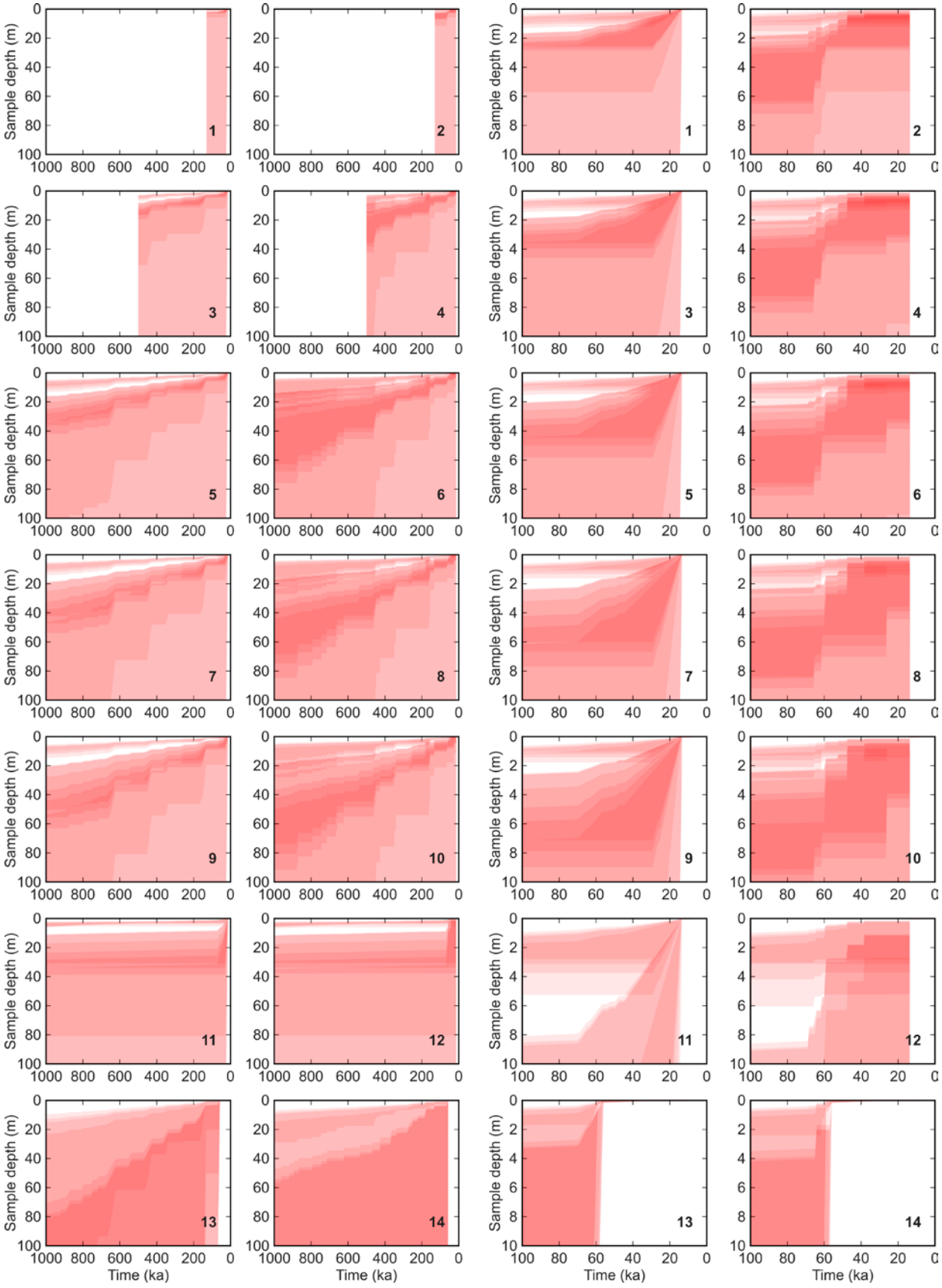

Figure 3-58. *Erosion simulation output for ^{10}Be simulations. Each simulated individual sample depth range is shown with 90 % transparency so that overlapping sample depths yield darker areas. The bold number in the lower right corner of each panel shows the simulation scenario number (Table 2–4). Odd number scenarios (columns one and three) involve constant erosion rate simulations and even number scenarios (columns two and four) involve constant erosion depth simulations. The left panels show the sample depth history over the last 1 Ma and the right panels show the sample depth history over the last 100 ka.*

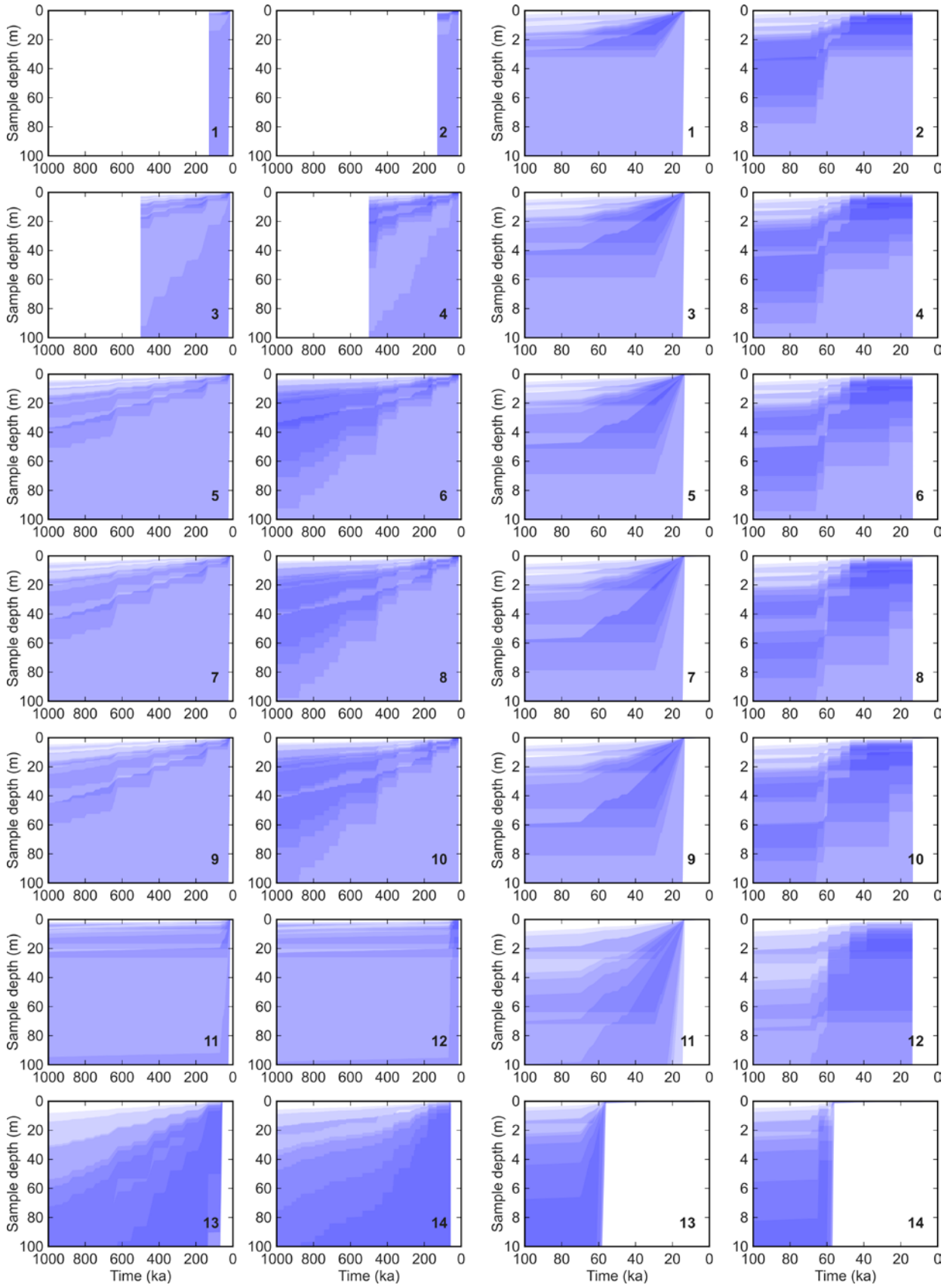

Figure 3-59. *Erosion simulation output for ^{26}Al simulations. Each simulated individual sample depth range is shown with 90 % transparency so that overlapping sample depths yield darker areas. The bold number in the lower right corner of each panel shows the simulation scenario number (Table 2–4). Odd number scenarios (columns one and three) involve constant erosion rate simulations and even number scenarios (columns two and four) involve constant erosion depth simulations. The left panels show the sample depth history over the last 1 Ma and the right panels show the sample depth history over the last 100 ka.*

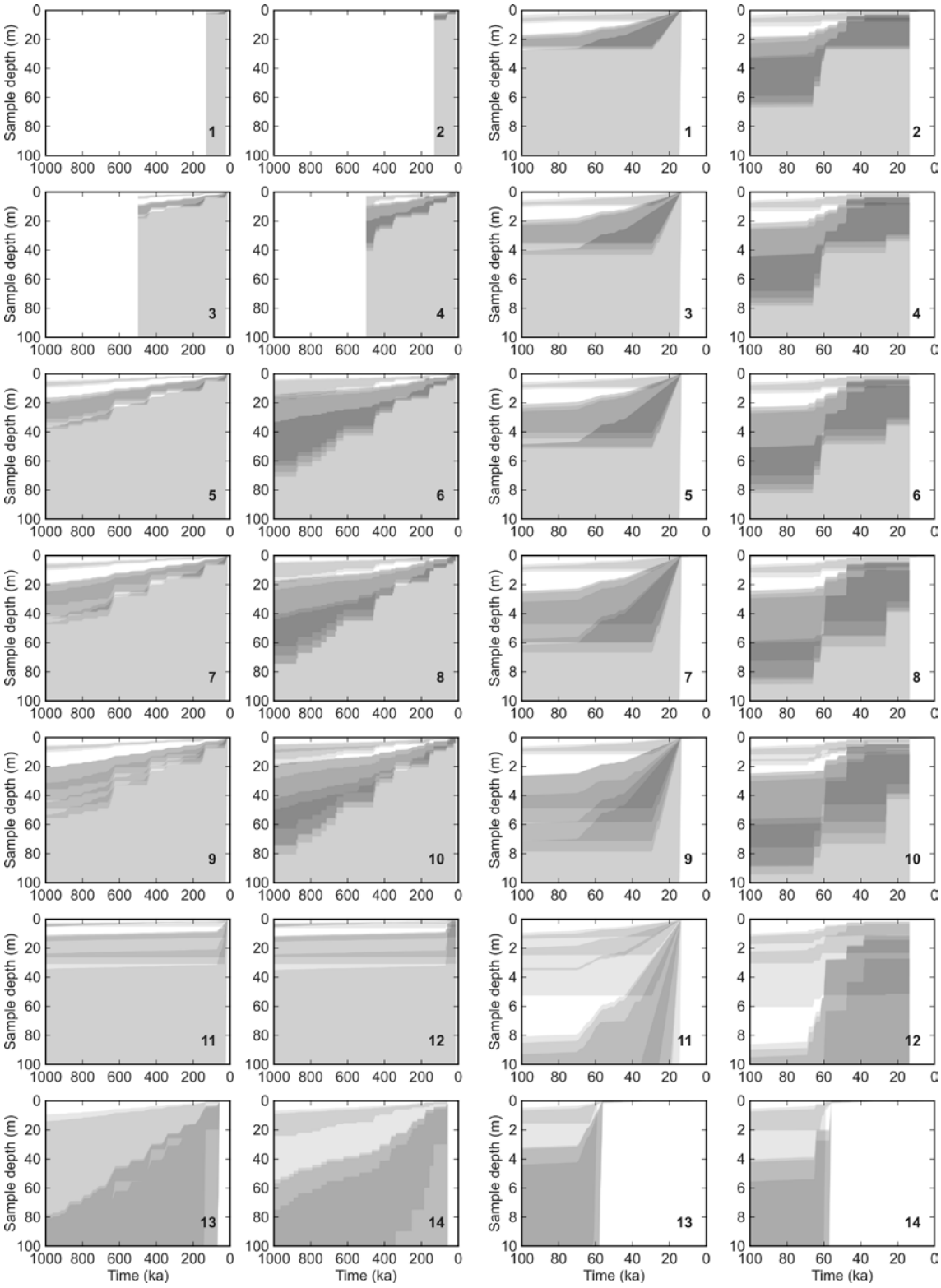

Figure 3-60. *Erosion simulation output for combined ^{10}Be and ^{26}Al simulations. Each simulated individual sample depth range is shown with 90 % transparency so that overlapping sample depths yield darker areas. The bold number in the lower right corner of each panel shows the simulation scenario number (Table 2–4). Odd number scenarios (columns one and three) involve constant erosion rate simulations and even number scenarios (columns two and four) involve constant erosion depth simulations. The left panels show the sample depth history over the last 1 Ma and the right panels show the sample depth history over the last 100 ka.*

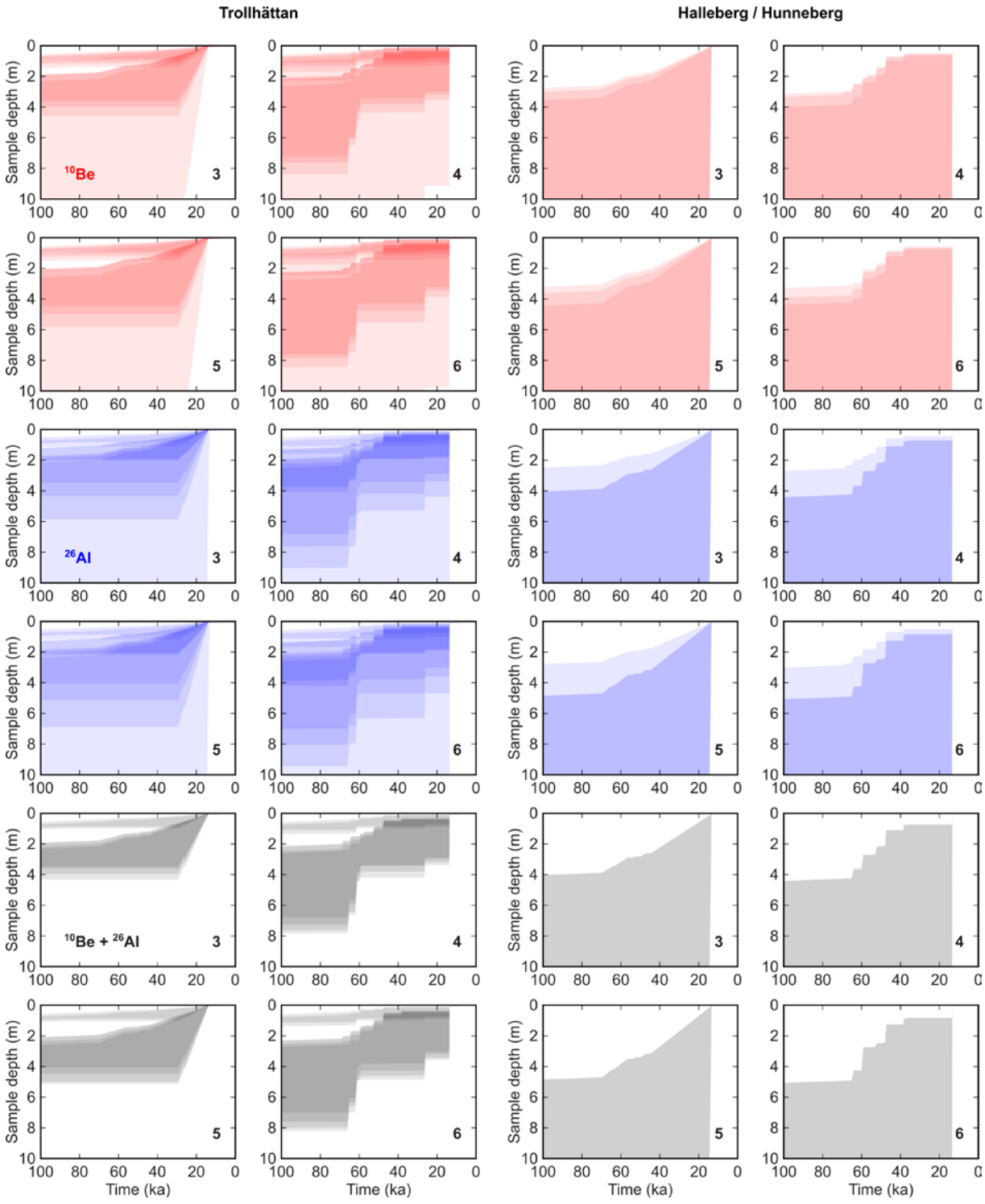

Figure 3-61. *Scenarios 3,4,5 and 6 shown separately for sites in the Trollhättan town area and around Halleberg and Hunneberg. The panels show the sample depth history over the last 100 ka.*

4 Discussion

4.1 Erosion and burial history

The sub-Cambrian unconformity is a product of three phases of denudation: (i) deep denudation of Baltica through the Neoproterozoic, (ii) planation of the stable craton surface under subaerial environments at elevations close to sea level and (iii) final grading of rock shelves during marine transgression. The unconformity in Västergötland was buried by shallow water marine sediments in the Early Palaeozoic (Nielsen and Schovsbo 2006). Further sedimentary cover was added later in the Palaeozoic during and after the Caledonian orogeny, with maximum burial of ~2 km during the Early Triassic (Figure 1-10). Denudation through the Mesozoic and into the Cenozoic led to thinning of sedimentary cover (Japsen et al. 2016) (Figure 1-11). Fault breccias found N of Goteborg with clasts of Cambrian sandstone and Ordovician limestone demonstrate retention of Early Palaeozoic cover in this area into the Permian (Samuelsson 1967, Johansson 1999). The absence of weathering remnants in the basement and the retention of calcite fracture coatings at shallow depths below the unconformity in areas proximal to Early Palaeozoic outliers in Västergötland indicates that the basement was not re-exposed to deep weathering and etching in the Mesozoic and Cenozoic, unlike in parts of southernmost Sweden (Lidmar-Bergström 1988). In the Early Miocene and also in the Early Pliocene, the South Swedish Dome was uplifted (Japsen et al. 2016) and shed large volumes of sediment southwards to basins in Denmark. Detritus sourced from SW Sweden included Early Palaeozoic quartzites (Rasmussen et al. 2010) and detrital zircons and heavy minerals from the Eastern Segment of the Sveconorwegian basement (Figure 1-4) (Olivarius et al. 2014). By 22 Ma, the source terrain in Västergötland and its surroundings included both Early Palaeozoic sedimentary cover rocks and exposed basement.

The preservation of the distinctive near-planar form of the sub-Cambrian unconformity has been recognised previously as evidence of its likely late re-exposure (Johansson et al. 2001b, Olvmo et al. 2005, Lidmar-Bergström and Olvmo 2015). Late re-exposure of sub-Mesozoic basement erosion surfaces is also likely in Skåne, with the survival of Jurassic and Cretaceous sedimentary outliers (Norling and Bergström 1987), Late Cretaceous and Palaeocene flints (Lidmar-Bergström 1982) and pockets of sub-Mesozoic weathering (Lidmar-Bergström 1995, Fredin et al. 2017). Basement re-exposure has been linked to late Neogene erosion (Johansson et al. 2001b) but little attention has been directed previously towards the likelihood that parts of the sub-Cambrian unconformity proximal to outliers were re-exposed in the Pleistocene as a result of glacial erosion of sedimentary cover rocks by the FIS. The role of glacial erosion in re-exposure of the unconformity is discussed below.

4.2 Relief on the buried sub-Cambrian unconformity

The preserved form of the sub-Cambrian unconformity in Västergötland is apparent where it remains buried beneath Early Palaeozoic sedimentary rocks and from the morphology of the basement around the edges of Early Palaeozoic outliers. At the landscape scale, the continuity of the thin, horizontally bedded basal Mickwitzia sandstone, part of the File Haidar Formation, across southern Sweden requires that the Early Cambrian sea transgressed a rock shelf with a very low gradient, estimated at 0.1 % (Nielsen and Schovsbo 2015). The layer-cake stratigraphic sequences that rest on U2 maintain similar thicknesses and facies over distances of 10–100 km (Bergström et al. 2004, Weidner et al. 2004). At the regional scale, large hills are nowhere apparent around the flanks of Halleberg and Hunneberg. At Kinnekulle, no large hills are apparent along 6.5 km of lake shore and the relief at the local scale is <3 m over 100 m-long stretches of the re-exposed unconformity (Högbom and Ahlström 1924). Low macro-scale relief is also seen in mine workings at Lugnås (Jensen 1997). In proximity to the edge of the buried unconformity, the elevation range of summits is only 4–5 m. A few low rock hills and ridges rise up to 8 m above their surroundings (Table 3-1), but these are widely spaced and have km-wide wavelengths. In terms of the competing hypotheses for a planar or hilly morphology to the unconformity (Figure 1-14), available evidence indicates that the buried sub-Cambrian unconformity around Halleberg, Hunneberg and Kinnekulle has a near planar form.

Comparisons of the heights of the buried unconformity with exposed basement tops along its edge indicate an elevation difference of 2 to 6 m, reaching 9 m locally, around Halleberg and Hunneberg. No highs on the exposed basement exceed the estimated heights on the projected preserved unconformity at distances of up to several km from the edge of Early Palaeozoic outliers (Figure 3-28). Equally, closely spaced summits maintain similar altitudes and any valleys on the former unconformity surface had depths of only a few metres (Figure 3-15). The planar form of the buried unconformity persists in accordant summits on the exposed basement nearby. Basement summits in the vicinity of the edge of the unconformity stand only a few metres below their original elevations on the unconformity.

Very low relief on the preserved unconformity and on basement exposed within a few kilometres of its edge is a characteristic feature around other Early Palaeozoic outliers on Baltica (Figure 1-13). Good examples of a near-planar form are seen at Rockneby, Kalmar (Hall et al. 2019), around the Lockne impact structure (Sturkell and Lindström 2004), at Torneträsk, northern Sweden (Ormö et al. 2017), at Slemmestad in the Oslo Graben (Calner et al. 2013) and, locally, on the Hardangervidda (Figure 4-1). Relief of < 20 m is found close to the edge of Early Palaeozoic cover rocks in eastern Sweden in the Öland–Gotland area (Flodén 1980) and beneath Early Cambrian sandstone on 125–160 km-long seismic reflection transects E of Gotland (Erlström and Sopher 2019), at locations around Kalmar (Tirén and Beckholmen 1992) and northwards to Västervik (Munier and Talbot 1993), and in Uppland (Hall et al. 2019). In Estonia, the buried sub-Ediacaran unconformity is without any major erosional depressions (Konsa and Puura 1999), carries a relief of < 20 m over wide areas (Puura et al. 1996) and maintains an average gradient of 0.15–0.35 % over a distance of > 200 km (Kirsimae et al. 1999, Eklund et al. 2007). In central Sweden, the buried unconformity close to the edge of the Caledonide nappes has topographic amplitudes of generally less than 10 m (Sturkell and Lindström 2004, Ormö et al. 2014). In northernmost Sweden, the buried unconformity is described as "exceedingly flat" for over 400 km beneath the Caledonide nappes (Ormö et al. 2017). In Finnmark, the basement surface beneath Late Neoproterozoic and younger cover shows up to 100 m relief, but this much older surface was shaped by glacial erosion in the Varangian glaciation (Rice et al. 2011) at ~630 Ma (Nystuen et al. 2008) or ~580 Ma (Jensen et al. 2018).

Preserved sub-Early Palaeozoic unconformities on Laurentia also show extensive near planar surfaces, widely described as peneplains. The buried sub-Cambrian unconformity in Scotland is planar in form for 150 km along the length of the NW Highlands (McKie 1993) beneath a layer-cake sequence of Early Palaeozoic quartz sandstones and shelf limestones (Raine and Smith 2012) (Figure 4-2). The edge of the basement unconformity where it emerges from below Ordovician carbonates in Canada is of very low relief in parts of Ontario (Mukherji and Young 1973), around Hudson Bay (Bird 1967), on SE Baffin Island (MacLean et al. 1977) and on Somerset Island (Tuke et al. 1966). The sub-Ordovician unconformity around George Bay, Ontario, however. includes small areas of low hills developed in highly resistant basement rocks such as quartzite (Johnson and Jia-Yu 1989). In Arctic Canada, along the edge of Ordovician limestone covers, exhumed basement surfaces have relief of < 15 m over many kilometres but include smaller areas with hills up to 50 m high (Bird 1967). The vast extent of such low relief basement unconformities on Baltica (Figure 1-6) and Laurentia (Peters and Gaines 2012) indicates the operation of similar sets of denudational processes acting over very long periods under the distinctive terrestrial environments of the late Neoproterozoic and early Palaeozoic.

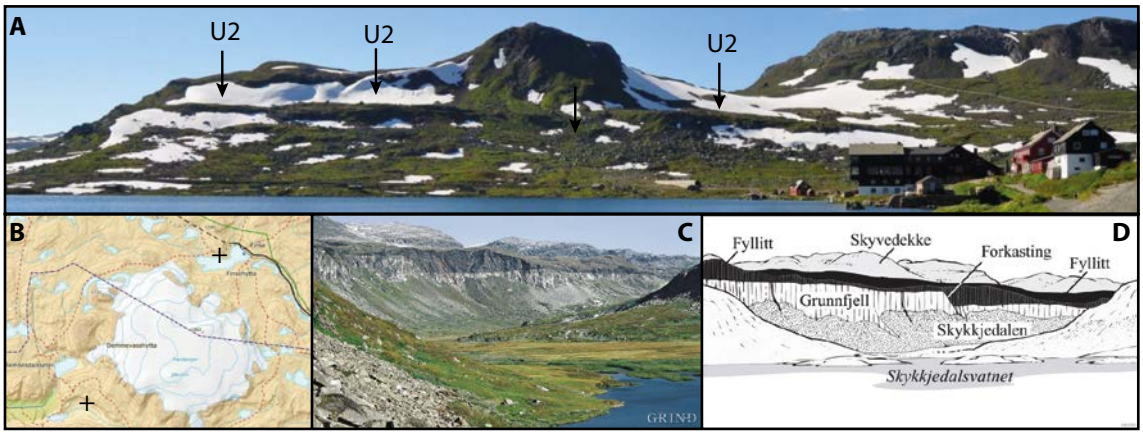

Figure 4-1. *Sub-Cambrian unconformity developed in the Finse Granite, Hardangervidda, Norway. A. Sub-Cambrian unconformity (U) at Jomfrunuten, Finse. Øvretveit (2016) records a weathered layer up to 2 m thick on the unconformity surface and sub-horizontal joints extending to a depth of 100 m below the unconformity. B. Locations of Jomfrunuten, Finse and Skytjedalen, Eidfjord. C. Photo from Svein Nord. D. Section from Johan Naterstad and Haakon Fossen on grind.no (https://www.grind.no/hardanger/eidfjord/skytjedalen) of the faulted, near planar unconformity at Skytjedalen, Eidfjord.*

Figure 4-2. *Sub-Cambrian unconformity on Laurentia. Ordnance Survey of Great Britain 3-D image of the mountain, Cranstackie, in the NW Highlands of Scotland. The tilted, near planar basement unconformity (arrowed) is cut in Lewisian gneiss and overlain by Early Cambrian quartz arenites of the Eriboll Formation. The unconformity is planar along strike over a distance of 150 km (McKie 1993).*

4.3 Morphology of the exposed basement

At the landscape scale, the bedrock relief in summit envelope surfaces around and between the Early Palaeozoic outliers in Västergötland between Lakes Vänern and Vättern has a relief of < 20 m per km (Figure 1-13). The basement surface is developed across Precambrian gneisses of felsic to mafic lithologies (Figure 1-5) and also transects the dominant regional NNE-SSW fracture set. Basement summits generally are found at < 250 m spacing but vary by < 5 m in elevation over wide areas and so pin smooth summit envelope surfaces. A notable exception to this very low relief is the 20–40 m high basement ridge that rises NE of Grästorp (Figure 3-1).

At the regional scale, around Halleberg and Hunneberg, summit envelope surfaces show similar low relief to that of the buried unconformity (Table 3-1). The highest points on the summit envelope surfaces in Areas 1–4 are low, broad hills that rise only 5–15 m above surrounding high points, with wavelengths of 0.5–1 km. The lowest relief on the summit envelope surfaces is in the Vargön area.

On a strike section along the lake shoreline, the elevation of the bedrock surface remains within an elevation range of 5 m over 5 km (Figure 3-15). Apart from around the planar flats in Trollhättan, relief increases with distance from Halleberg and Hunneberg to reach a maximum in the Sjuntorp area (Figure 3-45) (Fredén 1982, Johansson et al. 2001b). Summit envelope surfaces and profiles show gently inclinations to the NNW on both sides of the Lilleskog Fault (Figure 3-29). These inclinations conform to the dip and strike of the buried unconformity surface (Figure 3-3), local planar flats and Cambrian to Ordovician sedimentary strata beneath Halleberg and Hunneberg (Table 3-1). The consistent elevation, form and inclination of the exposed unconformity and summit envelope surfaces over wide areas of the surrounding basement indicate that the presently exposed basement surface is inherited directly from the near-planar sub-Cambrian unconformity, which was later dislocated and tilted. An original near-planar form for the unconformity is consistent with earlier models for the sub-Cambrian peneplain in Västergötland (Högbom 1910, Martinsson 1974, Johansson et al. 2001b).

The absence of large hills from the basement surrounding Early Palaeozoic outliers in Västergötland cannot be attributed to removal by glacial erosion because (i) large hills are not apparent on the buried unconformity, (ii) large hills are prominent further W in Bohuslän on exhumed and glacially modified sub-Mesozoic relief (Olvmo et al. 1999, Olvmo and Johansson 2002), yet are not present on basement terrain between Early Palaeozoic outliers in Västergötland (Figure 3-1), despite similar rock types, structures and former glaciological conditions, and (iii) glacial erosion of preglacial hills typically leads to the development of asymmetric hill forms with lee-side cliffs (Jahns 1943, Sugden et al. 1992, Ebert and Hättestrand 2010). In contrast, close to the edge of the Cambrian cover in the Baltic basin, symmetrical, low granite domes, a few tens of meters high, are seen in seismic data below Early Palaeozoic cover on Öland (Stephansson 1971, Dahlqvist et al. 2018). Similar hills are present on the exposed former unconformity surface from Kalmar county northwards (Kresten and Chyssler 1976). Whilst these hills retain features inherited from U2, notably sandstone dykes and curved sheet joints, hill forms are asymmetric, with lee-side cliffs (Lidmar-Bergström 1997). These exhumed, pre-Cambrian granite domes have been reshaped but not eliminated by erosion from the FIS. The absence of large hills around Trollhättan in Västergötland is an original feature inherited from the sub-Cambrian unconformity.

At the local scale, planar flats in the Trollhättan area occur only in massive blocks of coarse-grained and porphyritic granite gneiss. Planar flats are most extensive on Fault Block B at the Vänern shoreline in proximity to cover rocks. Individual planar flats show consistent, gentle inclinations to the N (Figure 3-24). Elevations of planar flats also drop consistently across Blocks B and D, and are consistent with vertical throw across the Lilleskog Fault (Figure 3-29). At Gaddesanna, on the NE flank of Halleberg, the planar flat elevation is < 3 m below the unconformity (Figure 3-5). Along the Vänern shore, planar flats conform locally to horizontal fractures at shallow depth but multiple, man-made cliffs around planar flats at Trollhättan indicate that horizontal fractures are not widespread. Instead, planar flats are cut across inclined fractures, including SHFs and the dominant SSW to NNE-oriented fracture set parallel to gneiss foliation (Figure 3-26). The continuity of planar flats in terms of distribution, inclination and elevation indicates that these were originally part of wider rock surfaces of low relief (Figure 3-22). Each planar flat at Trollhättan forms the highest point in its vicinity. None is observed in the lower surroundings, indicating that planar flats have not been maintained or reformed during lowering of U2 by glacial erosion. These findings are consistent with previous interpretations that planar flats are inherited, slightly modified facets from the sub-Cambrian unconformity (Johansson et al. 2001b).

The low relief basement topography exposed adjacent to Early Palaeozoic outliers in Västergötland, and its gradation into rougher basement terrain with increasing distance from outliers (Figure 3-1) resembles transitions across other extensive basement areas around Early Palaeozoic outliers in eastern and central Sweden (Figure 1-13). The basement relief below and adjacent to Early Palaeozoic sedimentary rocks on the floor of the Baltic Sea rarely exceeds 10–20 m in the Öland–Gotland area (Flodén 1980). Similar topography is seen below Cambrian and Ordovician rocks in the Bothnian Sea (Winterhalter et al. 1981) and extends as an inclined low relief surface across Ostrobothnia to the Cambrian outlier at Lauhanvuori in western Finland (Söderman 1985). Rock surface roughness increases southwards at the regional scale in Uppland away from Early Palaeozoic cover in the southern Bothnian Sea (Hall et al. 2019). The roughening of basement terrain with increasing distance from sedimentary outliers is consistent with a greater duration of glacial erosion on more remote basement surfaces as sedimentary cover was progressively removed.

4.4 Formation of the sub-Cambrian unconformity

The sub-Cambrian basement unconformity that emerges from beneath Early Palaeozoic cover rocks in Västergötland and around other outliers in Sweden has a near-planar form over wide areas which is highly distinctive and so requires explanation.

4.4.1 Neoproterozoic denudation

The unconformity on Baltica that separates the Precambrian basement from its Ediacaran to Ordovician sedimentary cover is one of the Earth's great unconformities. Other basement unconformities with equivalent time gaps of 0.15–1.50 Ga between erosion of basement and deposition of cover rocks are known from the Avalonian (Brasier 1980), Laurentian (Ambrose 1964, Dawes 2009, Peters and Gaines 2012, Parnell et al. 2014), Siberian (Sears and Price 2003) and the Arabian-Nubian (Angerer et al. 2011) shields. Each great unconformity represents an end product of syn-, late- and post-orogenic denudation of km-scale (DeLucia et al. 2017) followed, in most cases, by very long periods of erosion under cratonic regimes. Low relief on the great unconformity surfaces has been attributed to advanced subaerial planation (Parnell et al. 2014) and to marine erosion via the action of a *wave-base razor* (Peters and Gaines 2012) during landward shifts in the position of the erosive transgressive shoreface system. Surviving segments of the Earth's pre-Cambrian great unconformities have experienced long erosion and burial histories. Shield surfaces been partly stripped of Meso-proterozoic to Early Palaeozoic cover, re-exposed to renewed weathering and erosion and reburied by thin sedimentary Mesozoic to Cenozoic sedimentary sequences (Fairbridge and Finkl 1980).

On Baltica, parts of the Svecofennian basement around the Bothnian Mesoproterozoic basin were already at or close to the present erosion level by ~1.5 Ga (Hall et al. 2019). In the younger Sveco-norwegian basement province in southern Sweden and Norway, post-orogenic erosion was later, after 0.9 Ga, and low relief appears to have been established generally around intra-cratonic rift basins on Baltica by 750–700 Ma (Gabrielsen et al. 2015, Moczydłowska et al. 2018). Cryogenian tillites, carbonates and sandstones occur in N and E Greenland, Spitzbergen and N Norway (Brasier 1980) and record the 710–750 Ma Sturtian and ~635 Ma Marinoan glaciations (Arnaud et al. 2011) and, possibly, the ~580 Ma Gaskiers glaciation (Bingen et al. 2005). As on Laurentia (Keller et al. 2019), glacial erosion likely made a significant contribution through the Cryogenian to the denudation of Baltica (Paszkowski et al. 2019). The basement surface below Neoproterozoic Varangian tillite in Finnmark, however, has high topographic roughness and carries typical glacial features, including asymmetric rock knobs with abraded surfaces (Laajoki 2003).This unconformity does not resemble the near planar U2 surface preserved in Västergötland from which no overlying Proterozoic glacial sediments have been reported. The sub-Late Ediacaran to Early Cambrian unconformity in southern Sweden, Finland and on the East European Platform is > 30 Ma younger, developed under tropical climates (Bojanowski et al. 2020) and it is overlain by marine sandstones. The final shaping of the Late Neoproterozoic unconformity on Baltica took place under non-glacial environments.

4.4.2 Late Neoproterozoic ultiplains and peneplains

Marginal and intracratonic tectonics largely ceased on Baltica after ~584 Ma (Bingen et al. 1998, Nystuen et al. 2008), ~36–50 Ma before the onset of Late Ediacaran-Early Cambrian marine transgression. By ~580 Ma, Baltica was surrounded by shallow seas, with no part of its surface more than 500 km from the coast (Figure 1-7). Hilly topography remained in SW Norway (Lorentzen et al. 2019) but relief on the basement surface in Estonia was already very low by the Late Ediacaran (Puura et al. 1996).

On Laurentia, the formation of the sub-Cambrian unconformity is seen as a two-stage process, with extensive and deep weathering and supergene mineralisation followed by planation (Parnell et al. 2014). On Baltica, extensive and deep pre-Cambrian weathering is preserved only in the sub-Ediacaran basement of the Eastern European Platform. In the Baltic states, the basement was deeply weathered between ~600 and 560 Ma (Liivamägi et al. 2015). Thick, kaolinitic weathering profiles reflect intense chemical weathering during greenhouse climates and high atmospheric CO_2 (Liivamägi et al. 2015) or, alternatively, deep weathering under humid tropical climates (Driese et al. 2018). Elsewhere on Baltica, apart from an isolated locality in western Finland (Pipping and Lehtinen 1992), only minor weathering is reported from below the sub-Cambrian unconformity

in southern Norway (Gabrielsen et al. 2015), in western Sweden (Ormö et al. 2014) and southern Sweden (Elvhage and Lidmar-Bergström 1987). Supergene mineralisation beneath U2 is also localised in its extent and development beneath the edge of the Caledonide nappes (Bjørlykke et al. 1990). In Västergötland, weathering is generally absent beneath U2. Where present, as at Lugnås, weathering is shallow, less than a few metres deep (Mattsson 1962), and may relate to groundwater movement along the unconformity surface after burial. The absence of pre-Cambrian deep weathering from large parts of Baltica (Gabrielsen et al. 2015) indicates either that deep weathering profiles did not develop, or that thick weathering mantles were stripped before or during Early Cambrian marine transgression.

The basement surfaces that emerge from beneath Early Palaeozoic cover rocks on the Great Unconformities on Baltica and Laurentia are characterised by low, but subtly varied relief. At Kinnekulle, the buried unconformity shows < 10 m relief along strike for sections of 1–10 km length (Figure 3-10). In the Trollhättan area, similar relief represented in 1–10 km^2 windows by accordant summit elevations on the exposed basement (Figure 3-15). The sub-Cambrian unconformity can be described as an *ultiplain* (Twidale 1983) at the local and regional scales in these parts of Västergötland. More widely, the term *peneplain* can be applied in a morphological sense to the sub-Cambrian unconformity where it retains low, but slightly greater relief, with low (< 25 m high), widely-spaced hills and interfluves separated by plains and shallow valleys. Basement exposed along the edge of the Early Cambrian sandstone N and S of Kalmar has a peneplain form when viewed at the landscape scale, with a relative relief of 20 m over a distance of 140 km. Granite domes, singly and in groups, with heights of a few tens of metres, several with sandstone dykes, are found around Mönsterås (Alm and Sundblad 2002) and N of Kalmar (Martinsson 1974, Lidmar-Bergström 1997). Low ridges and shallow valleys are preserved beneath the Caledonian nappes in parts of the Hardangervidda (Gabrielsen et al. 2015). Isolated larger hills are rare on U2 but are represented on the buried unconformity in Estonia (Puura et al. 1996) and in the Gulf of Finland (Pokki et al. 2013). These terrains also can be described as peneplains because the inselbergs are too few and widely spaced to constitute *inselberg plains* (Ebert 2009). Comparable examples of extensive, epigene ultiplains and peneplains are present today on the Earth's cratons, including in southern Africa and western Australia (Ollier 1991). These modern analogues developed after advanced planation operating under very low rates of epeirogenic uplift (Twidale 1982) and low Cenozoic denudation rates, widely < 10 m/Ma (Beauvais and Chardon 2013) and locally < 5 m/Ma (Van der Wateren and Dunai 2001, Vasconcelos and Carmo 2018).

Present day ultiplains in semi-arid and arid environments in southern Africa and Australia include rock plains with unweathered surfaces where the development of soils and saprolites has been suppressed by the effectiveness of wash and wind action (Twidale 1982). On Baltica, in the Late Proterozoic, a period before the evolution of vascular plants, wash and wind erosion likely had similar effects across bare rock surfaces (Rudberg 1970, Martinsson 1974). Hence ultiplains and peneplains lacking thick or extensive weathering covers may have developed on basement surfaces on Baltica prior to Early Cambrian marine transgression. In comparison to Cenozoic ultiplains, the Late Neoproterozoic basement surface developed under similar conditions of slow epeirogenic uplift in the 36–50 Ma period before the onset of Late Ediacaran-Early Cambrian marine transgression. Erosion rates on Baltica during this period remain unquantified.

4.4.3 Marine grading of the sub-Cambrian unconformity

During early Cambrian to early Ordovician times, stepwise transgression caused flooding of the southernmost and westernmost parts of Baltica (Artyushkov et al. 2000, Nielsen and Schovsbo 2011, Green et al. 2013) (Figure 1-7). The period of marine transgression across Baltica was long (Konsa and Puura 1999), although still only loosely constrained by absolute dates. Flooding started in the Late Ediacaran (555–548 Ma) in Poland (Meidla 2017, Bojanowski et al. 2020) and continued through the Lower Cambrian in Sweden (534 Ma) (Slater et al. 2018) into the middle Cambrian in areas that now lie further west (Nielsen and Schovsbo 2011, Lorentzen et al. 2019). Pre-existing, Late Neoproterozoic ultiplains and peneplains standing close to sea level allowed flooding of great extent across Baltica as sea level rose from the Late Ediacaran onwards (Nielsen and Schovsbo 2011) (Figure 1-8). The extremely low topographical relief led to sediment starvation; net deposition throughout this period was generally low (Nielsen & Schovsbo 2011). Latest Proterozoic and early

Palaeozoic sediments in most places across Baltica consist of thin, condensed sequences which are nevertheless remarkably laterally extensive and often traceable over wide geographical areas (Slater and Willman 2019) (Figure 1-8). The vast extent of the Late Ediacaran – Early Ordovician deposits (Figure 1-6) support the concept that the sub-Cambrian unconformity was one of the Earth's pre-Cambrian great unconformities. Minimal lateral facies change over great distances indicate that sub-Cambrian unconformity on Baltica was a flat surface with little relief. If significant relief had existed (>100 m vertical), then more lateral facies changes would be preserved in the sedimentary record. Also, the switch from coarse clastic deposition to shale and carbonate deposition demonstrates that, after the mid-Cambrian Hawke Bay Event, there was a continent-wide shift from active erosion and deposition of clastic material to a shut-down of these processes: few hills or islands occurred in the epicontinental sea. This conceptual framework, summarised and evidenced by Nielsen and Schovsbo (2011), provides geological evidence for the overall flatness of the sub-Cambrian unconformity in Baltica.

Shoreface erosion on these rock shelves during transgression likely included the thinning and removal of pre-existing soils and saprolites. In the Baltic states, sub-Ediacaran weathering profiles decrease in depth southwards beneath a near-planar unconformity (Liivamägi 2015) probably due to shallow (a few tens of metres) erosion during transgression after tilting of the basement surface towards the Gulf of Finland. In Sweden, sub-Cambrian saprolites also may have been eroded but the planar surface of the buried Cambrian unconformity is quite unlike the irregular basal surfaces of weathering developed during the Cenozoic in crystalline rocks of heterogeneous mineralogy and fracture spacing (Mabbutt 1961, Thomas 1989). Where the weathered sub-Ediacaran unconformity has been exposed to Pleistocene glacial erosion along the Gulf of Finland, the stripped bedrock surface is rough (Eklund et al. 2007). Similarly, glacial erosion of weathered gneissic terrain facilitates development of classic cnoc-and-lochan terrain of high roughness (Krabbendam and Bradwell 2014). Other examples of irregular etchsurfaces include glacially-stripped sub-Mesozoic weathered basement surfaces in southernmost Sweden (Lidmar-Bergström 1988, Johansson et al. 2001b, Stroeven et al. 2013) and epigene Cenozoic surfaces in NW Europe (Hall 1986, Hall et al. 2015). The development of nearly flat Early Cambrian bedrock surfaces requires different mechanisms than simple stripping of saprolite.

Processes of marine erosion acting on rock shorelines are capable of forming near-planar rock surfaces or *shore platforms*. Whilst most Late Pleistocene shore platforms are narrow (<0.1 km wide) (Figure 4-3), shore platforms attained widths of 2–4 km width during the Plio-Pleistocene (Alvarez-Marrón et al. 2008) and of many tens of km on epeirogenic platform edges during the Neogene (Sandiford 2007, Thom et al. 2010, Brandano 2017). Marine platforms up to 30 km wide also developed on western European shorelines in the Neogene in an erosional response to marine transgression and with grading of pre-existing subaerial planation surfaces (Pedoja et al. 2018). Several features of buried Cambrian unconformity in Västergötland resemble those on Neogene and Pleistocene shore platforms in the Northern Hemisphere developed in crystalline rocks: (i) uniform, near planar surfaces cut across heterogeneous gneiss lithology and structure (Trenhaile 1987), (ii) a microrelief following the detailed fracture patterns on the gneiss (Figure 4-3) and (iii) a generally unweathered rock surface (Thornton and Stephenson 2006). Key differences on the sub-Cambrian rock shelf include the extent of near-planar rock surfaces over many tens of kilometres (Nielsen and Schovsbo 2011), the apparent lack of upstanding relief forms typical of modern shore platforms, such as stacks, ribs and former islets, the lack of backing cliffs and the sand units and pebble conglomerates found at the base of the Mickwitzia Sandstone (Jensen 1997) which contrast sharply with much coarser beach gravels found on many Late Cenozoic shore platforms (Figure 4-3) (Trenhaile 2004).

Evidence for the processes involved in final erosion of the preserved unconformity surface is provided by its detailed form and by the sediments that immediately overlie it. At Kinnekulle, the Early Cambrian rock shoreline was of very low relief and shallow gradient (Figure 3-10), with low rock ridges and furrows giving a micro-relief of up to 3 m (Figure 3-11). The base of the overlying Early Cambrian Mickwitzia sandstone comprises thin, horizontal beds of quartz pebbles and sand (Martinsson 1974, Lindstrom and Vortisch 1978) (Figure 3-11). Clay galls (Hagström 1987) and intercalated mud units showing desiccation cracks, indicate very shallow water depths and episodic drying (Martinsson 1974). The presence of ventifacts in thin basal conglomerates (Holm 1901, Hadding 1929, Martinsson 1974, Calner et al. 2013) suggests that rock surfaces were subject to high wind speeds and abrasion from wind-driven sand. Overlying glauconitic sands show ripple bedding, indicating the action of wave-induced currents (Calner et al. 2013). Clasts in basal conglomerates rarely exceed pebble size.

Figure 4-3. *Modern shore platform in fractured Precambrian Lewisian gneiss at Melbost Borve on the North Atlantic coast of Lewis, Outer Hebrides, Scotland. The shore platform has a maximum width of ~100 m, with high roughness at the metre scale, and a backing boulder storm beach.*

Furthermore, basal conglomerates at Kinnekulle have few gneiss fragments, even though the local gneiss has a flaggy structure and readily fragments into rock flakes and plates on the modern lake shoreline (Figure 3-11). This situation is quite unlike high energy, modern rock shorelines where storm wave impacts and currents generate and transport rock fragments of boulder size (Hall 2011). Sedimentological evidence indicates high wind energy in storms (Nielsen and Schovsbo 2011), but wave energy must have remained very low on the Cambrian rock shoreline. A possible solution to this apparent paradox is that water depths remained very shallow during the onset of marine transgressions.

Evidence of shoreline processes of weathering and erosion is seen on the preserved sub-Cambrian basement unconformity around Lockne in central Sweden. Here, Proterozoic granite gneiss at Åsan (Sturkell and Lindström 2004) and other localities (Karis and Strömberg 1998) displays irregular rounded weathering pans that are 10s of cm wide and several cm deep that hold the remnants of a filling of middle Cambrian bituminous shale, locally with a gravel layer at its base. A modern analogue for the downwearing processes involved may be provided by similar forms seen on the modern, gently-shelving lake shoreline at Nordkroken (Figure 4-4). Micro-weathering forms are widespread on lake-side rock surfaces, and include shallow pans, widened fissures along the tops of vertical fractures and phenocryst knobs (Figure 4-5). Plates and granules of granite gneiss found in fissures and ponds, together with the roughening of glacially abraded rock surfaces indicate that the rock on this shoreline is susceptible to granular disintegration and spalling. These microforms are much more prominent on the modern lake shoreline than on similar surfaces on planar flats elsewhere (Figure 3-26), showing that wetting and drying, aided by frost action, are effective weathering agents on this massive granite gneiss.

Final downwearing and flattening of the sub-Cambrian unconformity likely involved the combined operation of shoreline weathering, wind and wave action operating across very broad rock shelves. Although tidal range in the early Cambrian was low (Hamberg 1991), very low shoreline gradients would have exposed wide areas of rock to wetting and drying in each tidal cycle, whilst also attenuating wave energy. Other processes also likely contributed to weathering. The role of frost action was probably minimal as winter temperatures were high in the Late Ediacaran (Liivamägi et al. 2015) and Early Cambrian (Wotte et al. 2019) but high CO_2 concentrations in the atmosphere (Avigad et al. 2005, Liivamägi et al. 2015) and salt weathering may have contributed to enhanced rock surface disintegration. Granular disintegration acting for long periods between the high and low water marks, and operating in combination with aeolian deflation, sand movement and abrasion across unvegetated bedrock surfaces (Dott 2003), provides a plausible mechanism for lowering of

Figure 4-4. *Modern Lake Vänern as a possible analogue for the Early Cambrian marine shoreline. Note the very shallow water depth, the shallow weathering pans and pools and the platy rock fragments on the floor of the pool.*

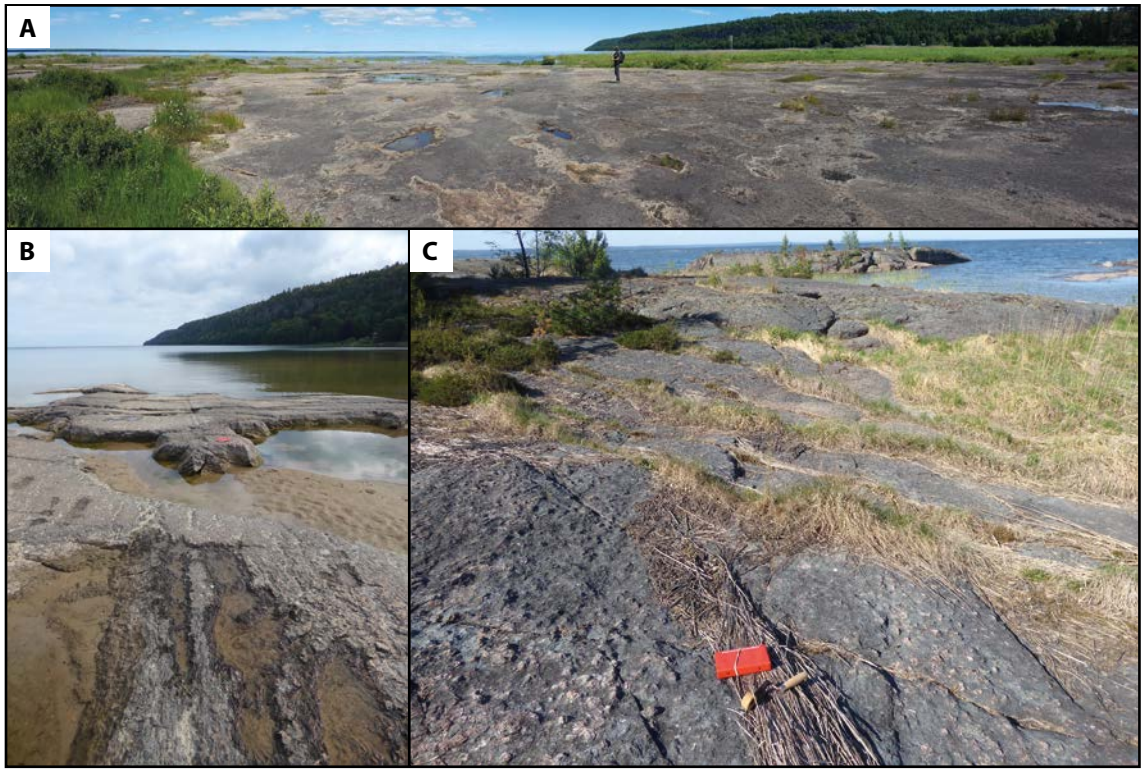

Figure 4-5. *Micro weathering and erosion of rock surfaces on the modern lake shoreline at Nordkroken. Location on Figure 3-15. A. General view of the planar flat with the NW flank of Halleberg in the background. B. Upstanding surfaces of glacially abraded porphyritic granite gneiss retaining glacial grooves. Water-filled pans have lost granules, flakes and plates of rock to weathering and wave action. C. Weathered rock surface with prominent feldspar phenocrysts.*

crystalline rock surfaces on Cambrian shorelines. Thin, granular and geochemically immature saprolites are reported from coarse grained granites on the sub-Cambrian unconformity (Söderman et al. 1983).The remarkable flatness of the planar flats now seen on parts of the exposed sub-Cambrian unconformity in the Trollhättan area may be attributed to the susceptibility of the coarse-grained granite gneisses to such granular disintegration.

On Early Cambrian shorelines, such as at Kinnekulle, reworking of sands occurred in very shallow water, under conditions of low wave energy yet with a significant component of wind action. The high maturity of Late Ediacaran sands in Estonia has been attributed to reworking of intensely weathered basement (Liivamägi et al. 2015). Concentrations of anatase in the Early Cambrian Norretorp shales that rest directly on the basement unconformity in southern Sweden also have been attributed to former intensive weathering on U2 (Erlandsson 2017). Siderite-rich pebbles in basal conglomerates in Västergötland have been linked to soil development on the underlying basement surface (Westergård 1943), although siderite also forms in marine environments (Jensen 1997). Alternatively, in southern Sweden, detrital zircon age dating results have been interpreted as indicating that the maturity of the basal Early Cambrian sandstones is the result of prolonged exposure to disintegration and reworking processes on the Cambrian marine shoreline, rather than to recycling from older sediment or to advanced subaerial weathering (Lorentzen et al. 2018, 2019). A similar scenario was proposed previously as a cause of the maturity of Early Cambrian sands resting on the sub-Cambrian unconformity on the Lewisian gneiss and Torridonian sandstone in the NW Highlands (Swett et al. 1971). Heavy mineral concentrations found in sediments that rest on the unconformity surface may be seen as variants of beach placers (Lalomov et al. 2015) under such scenarios.

The timescales over which these shoreline processes may have operated were vast. The Ediacaran to Ordovician transgression was a result of a long-term (~100 Ma) overall sea level rise of ~200 m superimposed on a series of repeated short-term high-stands and low-stands of 20–70 m amplitude (Haq and Schutter 2008). Parts of the rock shelf could have been subjected to as many as 10–20 short-term transgression-retrogression cycles over periods of up to tens of millions of years. Each of these cycles would result in a phase of coastal erosion sweeping across exposed basement surfaces. In Västergötland, a late Early Cambrian age for the basal Mickwitzia Sandstone (Jensen 1997) indicates that a period of > 10 Ma was potentially available for erosion between the start of marine transgression at the Ediacaran-Cambrian boundary and the final burial of the basement by sediment. A metaphor suggested for the equivalent development of near-planar surfaces on the sub-Ordovician unconformity in Laurentia is the *wave-base razor* (Peters and Gaines 2012). On the Early Cambrian shorelines in Västergötland, however, a *grader* seems to be a more appropriate tool because shoreline erosion in the Early Cambrian trimmed, lowered and likely further flattened an existing subaerial ultiplain. The end-product of transgressive marine grading was a near-planar rock surface that had been largely stripped of Neoproterozoic weathering mantles.

4.5 Fracturing and the sub-Cambrian unconformity

Four main generations of fracture formation and opening may be recognised in basement below the sub-Cambrian unconformity in Västergötland. The oldest generation of epidote veins formed under high pressure and temperature during the onset of brittle deformation in the Sveconorwegian orogeny (Andréasson and Rodhe 1994). Formation of the dominant SW-NE fracture set parallel to gneiss foliation also dates from this initial phase (Hegardt et al. 2007). A second generation of mineral coatings that include chlorite (Mattsson 1962, Mossmark et al. 2015), laumontite and prehnite (Mattsson 1959) occur on fracture surfaces in gneisses that cross-cut epidote veins. The Bohus Granite contains hydrothermally altered fracture zones with extensive epidote, silica or calcite impregnation (Eliasson et al. 1990). This mineral suite formed in existing and new fractures towards the close of the Sveconorwegian orogeny (Eliasson et al. 1990). A third generation of fractures formed or re-opened through the Phanerozoic. By the time of the Early Cambrian transgression, the basement at the unconformity was densely fractured. At Närke, many fractures in the basement do not continue into the overlying Early Cambrian sandstone and so are pre-Cambrian in age (Wiman 1942). The common presence of sandstone dykes at shallow depths below U2 between Vänersborg, Vargön and Nordkroken (Figure 3-22) indicates that vertical fractures opened or re-opened during or soon after the Early Cambrian transgression and were filled with sand. Hence sets of subsurface horizontal, sub-horizontal and curved fractures also observed in this area (Figures 3-37 to 3-40)

likely existed before U2. Renewed faulting, likely in the Permian when the basement was deeply buried beneath Palaeozoic rocks, led to fracture reactivation (Ahlin 1987).The youngest generation of fracture minerals likely relates to weathering. Alteration of host rocks or older fracture filling materials at low temperatures led to clay mineral formation (mainly smectite) (Eliasson et al. 1990). Clay mineral formation may relate to Mesozoic or younger deep weathering (Olvmo et al. 1999). In the Bohus Granite, the uppermost 270 m contains zones where extensive haematization occurs (Eliasson et al. 1990). Oxidation and solution of calcite coatings likely relates to downward penetration of the redox front in response to Neogene uplift (Japsen et al. 2016).

The structural fabric of the main fracture sets are displayed in the three large quarries around Trollhättan (Section 3.4.2). Whilst the regional NE-SW to NNE-SSW oriented fracture set exerts a strong control over the location of trenches and basins excavated by glacial erosion at the local scale (Figures 3-50 to 3-52), the sub-Cambrian unconformity surface is developed across these fractures in the Trollhättan area at the regional and landscape scales (Figure 1-5). Sets of horizontal fractures, including sheet joints, such as might guide surface topography are neither extensive nor widely developed in the basement gneisses (Figures 3-34 to 3-36). These cross-cutting relationships confirm that the basement unconformity at these scales in the Trollhättan area is an erosional, rather than a structural surface, cut across heterogeneous rock type and structure.

Planar flats are distinctive near-horizontal rock slope facets set within the wider surface of the exposed unconformity. At Nordkroken, planar flats conform locally to shallow and closely spaced horizontal fractures in coarse-grained to porphyritic granite gneisses (Figure 3-9). Further west along the Vänern shoreline and towards Vargön, sub-horizontal and gently curved fractures are exposed at shallow depth, locally cut by vertical sandstone dykes. These rock surfaces lie on the surface of Fault Block B that dips at 0.3 % northwards and so represent an almost horizontal strike section across the fault block surface that follows the lake shore with negligible height variation. The rock surfaces stand at elevations within 6 m of the projected buried unconformity on the flanks of Halleberg (Figure 3-9). Here, pre-Cambrian, and possibly younger, horizontal and sub-horizontal fractures provide local control on the planar form of the unconformity.

Around Trollhättan, sub-horizontal fractures are very restricted in distribution. Here planar flats are developed across vertical and inclined fractures. Examples are observed at Hjortmossen (Figure 3-38), Eriksro (Figure 3-25), Sandhem (Figure 3-40) and Kåtene (Figure 3-26). These planar flats are erosional, rather than structural forms, and lack significant control by HFs and SHFs.

Sandstone dykes, with a maximum width of a few cm, occur as fillings in vertical fractures on many planar flats (Figure 3-22). Where fracture fillings occur at the current erosion level and in proximity to and at the same elevation as the edge of the buried unconformity, as around Halleberg, the fillings currently seen were originally formed at shallow (< 10 m) depth below the unconformity. Based on available shallow exposures and without borehole logs, depths at Kinnekulle are reported as a few metres (Högbom and Ahlström 1924), and at Trollhättan as < 4 m deep (Nordblom 1961, cited in Rudberg et al. 1976). Short sandstone dykes found in narrow fracture openings may be filled down to depths of 5–10 m or more below U2 (Mattsson 1962, p 327).

In eastern Sweden, the reported depth range for sandstone dykes is substantially larger. Sandstone dykes along Kalmarsund have a maximum depth of 7 m (Martinsson 1974). Recorded depths in boreholes reach 25–75 m at Simpevarp (Drake et al. 2009a) and 50 m at Äspö (Munier and Talbot 1993). In Bohuslän, at Tosterödsvattnet, brecciated Cambrian sedimentary rocks are recorded from a fault zone (Mattsson1962, pp 257–265). Cambrian sandstone and Ordovician limestone clasts are also reported from a faulted shear zone at Kungälv, 50 km S of Trollhättan (Samuelsson 1967, Martinsson 1968). Where isolated fracture fillings occur remotely from the buried unconformity, the depth below the former unconformity is uncertain and may be several tens of metres (Mattsson 1962).

4.6 Dislocation of the sub-Cambrian unconformity

Summit envelope surfaces and profiles generally support previous interpretations of the basement surface around Trollhättan as a mosaic of fault blocks of km-scale extent that represent the dislocated surface of U2. An additional prominent W-E lineament N of Sjuntorp is also recognised as a fault, the Sjölanda Fault, that separates Fault Blocks D and E. Summit envelope surfaces also support previous

estimates of the inclinations of Blocks A–D (Table 3-1) (Ahlin 1987, Johansson et al. 1999). Vertical fault displacements were generally in the range of 10 to 30 m. Previously unidentified minor faults, with 5–10 m vertical displacements, are identified within fault Blocks B and D. Previous assessments (Ahlin 1987) are supported that Phanerozoic fault displacements of the unconformity in this part of Västergötland were only of small magnitude.

Similar minor block faulting of the sub-Cambrian unconformity has been recognised across much of lowland Sweden. At Billingen, fault displacement across an Early Permian sill is 25–30 m (Andersson et al. 1985). Post-Ordovician displacement of rock blocks in the Bothnian and Åland Seas is a few tens of metres (Flodén 1977). Minor displacement of rock blocks in basement close to the edge of Cambrian and Ordovician sedimentary rocks have been identified from S and SE Sweden (Tirén and Beckholmen 1989, 1992), at Närke (Möller and Dowling 2016, Hall et al. 2019) and in Uppland (Beckholmen and Tirén 2010, Grigull et al. 2019).

The timing of faulting in Västergötland remains uncertain and may include multiple episodes of fault movement during the Palaeozoic and in the Cenozoic (Ahlin 1987, Månsson 1996). The widespread evidence of rounding and indentation of fault scarps by glacial erosion, as found along the edge of the block S of the Sjölanda Fault (Figure 3-19), is consistent with interpretation of the main fault scarps as exhumed, pre-Pleistocene features, rather than as neotectonic fault scarps of Pleistocene age.

4.7 Glacial erosion of the sub-Cambrian unconformity

Glacial erosion in the Trollhättan area has involved the local removal of Early Palaeozoic cover from a hard, variably fractured basement unconformity of very low relief. Subglacial erosion processes have produced a distinctive set of new glacial landforms in the basement.

4.7.1 Timing of re-exposure of the basement unconformity by glacial erosion

At the present day, the Early Palaeozoic outliers in Västergötland are of restricted extent (Figure 3-43). That a more extensive cover of Early Palaeozoic sedimentary rocks persisted here into the Middle Pleistocene (0.781–0.126 Ma) is demonstrated by the clast composition of Middle to Late Pleistocene tills in Denmark and northern Germany. Three indicator rocks sourced from Västergötland are recorded in tills in Jutland, Denmark (Smed 2016) and in north Germany (Smed and Ehlers 2002): Cambrian sandstone (Smed 2016), Ordovician limestone (Weidner et al. 2015) and Kinnekulle dolerite (Smed 1993). The frequent presence of these indicators in till stone counts of 50–100 stones (Smed 1993) implies that debris from the Early Palaeozoic sequence in Västergötland makes up a significant proportion of Middle to Late Pleistocene till volumes in parts of Jutland. The present extent of the dolerite-capped mesas in Västergötland is ~900 km^2 whereas the receiving area in Denmark alone is ~70 000 km^2. The small extent of the present outcrops does not allow the generation of the large volumes of Early Palaeozoic sedimentary and Permian igneous debris from Västergötland as indicated by till erratic contents in Denmark and N Germany. Till clast lithology and simple source to sink comparisons indicate that large volumes of Early Palaeozoic cover rocks and Early Permian dolerite cap rocks were removed from parts of Västergötland by glacial erosion in the Middle and Late Pleistocene. Substantial erosion is consistent with the large numbers of the same erratic suite found in tills of the last ice sheet standing in positions down-ice from the Halleberg-Hunneberg (Hillefors 1979) and Kinnekulle (Gillberg 1970) outliers.

Erosion of substantial volumes of Early Palaeozoic sedimentary rocks and Permian dolerite implies widespread exhumation of the Early Cambrian basement unconformity in Västergötland. This is consistent with evidence for major erosion by the FIS elsewhere in southern Scandinavia (Hjelstuen et al. 2012). Through the Neogene and into the Early Pleistocene, Fennoscandia was drained by the Baltic River system (Overeem et al. 2001) via a network of major rivers that flowed through the Gulfs of Finland and Bothnia (Gibbard and Lewin 2016), perhaps along precursors of the Baltic klints (Tuuling 2017), with a major tributary flowing via the Vänern depression (Lidmar-Bergström et al. 2017). The Baltic River system delivered the distinctive Baltic Gravel Assemblage, in which sedimentary rock types derived from the Early Palaeozoic sequence of southern Scandinavia are strongly represented (Bijlsma 1981), to sedimentary basins in the southern North Sea, Denmark and northern Germany (Gibbard and Lewin 2016). This river system was destroyed by ice sheet advance

after ~1.1 Ma (Bijlsma 1981, Overeem et al. 2001). The onset of over-deepening in the Norwegian Trench (Sejrup et al. 2003, Reinardy et al. 2017), in the Skagerrak and Kattegat (Lykke-Andersen 1987, Houmark-Nielsen 2004) and deep erosion in SW Sweden (Hjelstuen et al. 2012) also date from this phase.

The Menapian cold stage (MIS 36-34) at ~1.1 Ma falls within the Middle Pleistocene Transition, the period when 100 ka cycles began to dominate the build-up and decay of major Northern Hemisphere ice sheets (Clark et al. 2006, Willeit and Ganopolski 2019). Around this time, the FIS developed in full ice sheet mode and extended into Västergötland (Kleman et al. 2008). The FIS subsequently reached its greatest thickness in Denmark and Germany during the Elsterian and later glacial cycles (Mangerud et al. 2011, Batchelor et al. 2019). Advances of the FIS to Pleistocene maximum limits involved major phases of subglacial erosion and deposition in the foreland (Ehlers 1981, Gyldenholm et al. 1993). Deep glacial incisions in the southern Baltic appear to have Elsterian or younger ages (Meyer 1991, Flodén et al. 1997) and to correspond to the period of maximum erosion in the Norwegian Trench after 0.5 Ma (Hjelstuen et al. 2012). It is likely that the highest glacial erosion rates in SW Sweden were associated with the maximum advances of the FIS in the Middle and Late Pleistocene (Ehlers et al. 2018). In Denmark, the Elsterian, Saalian and Weichselian ice sheets standing at or close to maximum limits caused thrusting, deformation and deep erosion of soft sedimentary cover rocks, as indicated by huge rafts of Late Cretaceous chalk and Palaeogene sands and muds found beneath till layers in Denmark (Jakobsen 1996). Although previously largely unrecognised (Lidmar-Bergström 1997, Stroeven et al. 2013), erosion beneath successive large ice sheets since 1.1 Ma likely led to widespread, and deep erosion and local removal of soft Mesozoic cover from Bohuslän southwards to Skåne and from adjacent parts of the Skagerrak and Kattegat. Palaeozoic to Palaeogene sedimentary rocks eroded from southern Sweden represent a substantial portion of the Pleistocene sediment volumes now found in N Poland, N Germany, Denmark and the southern North Sea.

4.7.2 Glacial erosion of cover rocks in Västergötland

Glacial erosion in the Trollhättan region involved separate rock substrates: dolerite cap rock, Early Palaeozoic sedimentary rock, a thin mantle of weathered and densely fractured basement immediately below the sub-Cambrian unconformity and hard, variably fractured basement below (Figure 3-42). Each substrate offered markedly different resistance to glacial erosion. The dolerite cap rock at Halleberg and Hunneberg is hard with orthogonal joint sets at mainly 1–3 m spacing (Figure 3-5). The Early Palaeozoic sequence includes beds of hard Early Cambrian quartz sandstone but also thick sequences of younger, softer mudstone and limestone. Bedding planes and joints are closely spaced (Figure 1-9). Any weathered or highly fractured gneiss immediately below the unconformity would offer only low resistance to glacial erosion. In contrast, the underlying gneiss is very hard and vertical fracture spacing locally can exceed 10 m (Figure 3-25), although spacing of long, open fractures is generally less at 0.5–3 m. The boundaries between the rock substrates and any horizontal discontinuities along bedding planes or fractures within the substrates also represent potential detachment zones for the removal of rock sheets. The rates of glacial erosion across the four substrates were likely very different, with slow removal of cap rocks, rapid stripping of Early Palaeozoic cover and of weathered and fractured rock immediately below the unconformity but much slower erosion of hard, massive basement. It is speculated on the basis of the distribution of inherited planar flats that a hill equivalent in size to the Lugnås outlier (10 km^2 in area and 60 m high) may have been lost to glacial erosion in the Trollhättan area through the Middle Pleistocene.

Contrasts in rock resistance where a hard cap rock overlies soft, fractured sedimentary rock are common on platforms formerly covered by large Northern Hemisphere ice sheets. Examples include Silurian limestones along the Niagara escarpment, Ontario (Straw 1968) and the Carboniferous limestone and sandstone uplands of Northern England (Evans et al. 2018). A close analogue for glacial erosion of the rock sequence in Västergötland is provided by the lowlands of central Scotland. Here, Late Carboniferous to Early Permian dolerite sills were intruded into thick sequences of Carboniferous sandstone, limestone, mudstone and coal (Cameron and Stephenson 1985). In this setting, glacial erosion has progressively thinned and reduced in area the cap rocks, exposing generally softer and more fractured sedimentary rocks developed. Many crag and tail forms in the glacially streamlined terrain of the Central Lowlands are largely erosional features, with crags formed in volcanic plugs, tails formed in sedimentary rock and lunate depressions formed where

ice has deformed around and eroded sedimentary rock from around the volcanic crag (Burke 1969). The difference in elevation of beds on the stoss and lee sides provides a minimum depth of glacial erosion in the sedimentary rocks around the crags of 25–100 m (Hall et al. 2018). Erosion of sedimentary units involved mobilisation of rafts of sedimentary rock (McAdam and Tulloch 1985). Glacial erosion through the Pleistocene led locally to breaching of escarpments, lowering and elimination of interfluves, except in sheltered lee locations, and excavation of 100 m-deep basins and trenches (Hall et al. 2018, Kearsey et al. 2019). In Västergötland, the thinning and reduction of cap rocks and the development of glacial lineations on the Early Palaeozoic sedimentary rocks indicates a similar sequence of degradation and elimination of hill forms (Figure 3-43). Glacitectonic disturbance of Alum Shale and Ordovician limestone beds is recorded at Närke (Thorslund and Jaanusson 1960, Lindskoga et al. 2018) and Motala (Lundqvist 1987) and may have operated beneath the FIS in Västergötland on hills such as Kinnekulle and Lugnås, where the dolerite cap was removed. A key difference between central Scotland and Västergötland is that, in the latter region, the hard gneissic basement has restricted the glacial excavation of deep valleys and depressions.

Till clast composition in Västergötland (Gillberg 1965) and in Denmark (Weidner et al. 2015) indicates that large volumes of Early Palaeozoic sedimentary cover rocks and Permian dolerite cap rocks were removed from Västergötland, but the depth of this erosion is unclear. Small grabens in the archipelago SE of Forsmark, Uppland, have lost thicknesses of more than 30–40 m of Jotnian and Ordovician sedimentary fill (Hall et al. 2019). Greater thicknesses of Mesoproterozoic and Early Palaeozoic cover rocks have been removed from across the Bothnian and Åland Sea basins (Hall et al. 2019). South of the Gulf of Finland, it has been estimated, using pre-Pleistocene epigene planation surfaces as reference surfaces, that ~40 m of mainly Devonian cover was removed in the Pleistocene (Amantov 1995). Pleistocene sediment on the East European Plain, including Baltic and Fennoscandian material but also more locally sourced rock debris, indicate erosion depths from glaciations since ~1.1 Ma sufficient to generate sediment thicknesses of 49–62 m (Gorlach et al. 2015, Kalm and Gorlach 2014). Such comparisons suggest that it is plausible that at least several tens of metres of sedimentary rock have been lost from large parts of Västergötland after erosion by the FIS.

The table mountains of Västergötland have been likely substantially reduced in area by scarp retreat (Figure 3-42). The cluster of planar flats at Trollhättan may suggest that a former Early Palaeozoic outlier has been removed as recently as the Middle Pleistocene in that area. The actual extent of glacial exhumation may be much greater. The exposed basement unconformity in Västergötland seen in DEMs as a smooth surface at the regional and landscape scales (Figure 3-1) remains within 10–20 m of the elevation of the buried unconformity around outliers. Typical total erosion depths in basement derived from cosmogenic nuclide analyses in the Forsmark area are 1.6–3.5 m over the last 100 ka and 13–27 m erosion over the last 1 Ma (Hall et al. 2019). These depths are consistent with re-exposure of the basement from beneath cover in Västergötland in the last 1.1 Ma. The smooth basement surfaces interpreted to represent the geologically-recent exhumation of the sub-Cambrian unconformity cover an extent of up to 2×10^4 km^2 in the Trollhättan area of Västergötland. Whilst the extent of erosion of cover rocks in Västergötland since 1.1 Ma remains unclear, it is potentially very large.

4.7.3 Glacial lowering and roughening of the sub-Cambrian unconformity

Lowering

Available evidence from the buried unconformity and the exposed basement in its surroundings supports the long-held view that glacial erosion has modified but not obliterated an originally smooth and generally flat surface inherited from the sub-Cambrian unconformity (Fredén 1982, Lidmar-Bergström 1997, Johansson et al. 2001b). The depth and pattern of glacial erosion in this part of Västergötland is derived by using summit envelope surfaces as reference surfaces for erosion beneath the former unconformity. The mean depth of erosion below the basement unconformity across the Trollhättan area is 14 m (Figure 3-53). Extensive basement areas with < 5–10 m of glacial erosion occur around the flanks of the Halleberg and Hunneberg Early Palaeozoic outliers at Vargön (Figure 3-14) and Åsaka (Figure 3-17) and at Trollhättan town (Figure 3-18) and southwards towards the Sjölanda Fault (Figure 3-19). Erosion depths in large basins around Sjuntorp reach 40 m (Figure 3-19). The greatest depths of glacial erosion are in basins that reach depths of 40 m

in the high ground W of the Göta Älv and along the Göta Fault in the 80 m-deep Göta trench. The estimated depths of basement erosion are consistent with the preservation of exhumed Phanerozoic fault scarps on block edges with heights of 5–30 m. To each of these figures should be added the loss of rock from basement highs estimated as 2–6 m based on the height difference between the buried unconformity and the exposed basement around Halleberg and Hunneberg.

A potential check on these estimates is provided by previous calculations of erosion depths by the FIS based on the volumes of Quaternary deposits for a sector of the formerly glaciated area of Fennoscandia that includes Sweden, Denmark and adjacent sea areas (Påsse 2004). The average thickness of sediments in the maximum area exposed to glaciation during the Pleistocene is estimated to be equivalent to a depth of 12 m erosion of bedrock. Glacial erosion during a full glacial cycle is estimated as 0.2–4 m, with a mid-range value of 1 m (Påsse 2004). The estimated depths are similar to those derived for the Trollhättan area based on geomorphological evidence. Further work is needed, however, to better constrain sediment sources and sinks and the relative contributions of the glacial erosion of basement and cover rocks around the Baltic basin (Hall et al. 2019).

Roughening

The present basement surface in Västergötland is considerably rougher than the buried unconformity surface. The roughness on a glacially-exhumed basement unconformity has three components that may derive from: (i) its topography prior to burial, (ii) the form of the basal surface of weathering on that topography and (iii) glacial erosion of the variably fractured basement after exhumation of the unconformity and stripping of saprolite from its surface. For example, the sub-Torridonian surface of NW Scotland had an original mountainous to low relief, shallow but variable thicknesses of palaeosols and highly variable fracture densities in the Lewisian gneiss (Williams, 1969). On this Precambrian basement unconformity, the roughness of the present gneiss surface after Pleistocene glacial erosion derives from all three components. In contrast, the former sub-Cambrian unconformity across large parts of Västergötland was flat at the local scale and retained little of no weathering prior to burial in the early Cambrian. Hence the surface roughness in this region derives mainly from Pleistocene glacial erosion of variably fractured basement across U2, with localised removal of shallow regolith.

At the regional scale in Västergötland, the differences in summit elevations between the buried and exposed basement are small and so the increases in bedrock relief and topographic roughness derive mainly from the excavation of trenches and depressions (Table 3-2). At the local scale, initial exploitation of bounding fracture zones by glacial erosion led to isolation of planar flats as slättbergen and other massive gneiss kernels as box hills. In detail, the slättbergen and box hills have been shaped by abrasion and plucking, with smaller roches moutonnées developed on their surface, extensive rounded and striated surfaces on stoss and top surfaces and plucked flank and lee faces. Planar flat and box hill margins, however, have not retreated far from the bounding fractures that determine their shapes. Topographic and surface roughness are highest along the edges of box hills, trenches and basins. Topographic roughness in Västergötland is scale dependent, as in other glaciated crystalline bedrock terrains (Falcini et al. 2018).

Roughness increases with distance from Early Palaeozoic outliers (Figures 3-46 and 3-47). Similar transitions from smooth basement surfaces in proximity to Early Palaeozoic outliers to rougher terrain at more distant locations occur at the landscape scale in Sweden to the W of Kalmar, SE of the Lockne impact structure (Sturkell and Lindström 2004) and southwards across Uppland (Hall et al. 2019). The Motala Cambro-Ordovician outlier on the NE shore of Lake Vättern provides another close analogue (Figure 4-6). Where the basement surface emerges south of the Motala outlier, it is smooth, with narrow trenches standing <20 m below generally accordant hill summits. Over a distance of up to 30 km southwards, the basement surface becomes much rougher, and relative relief increases to >50 m, with the development of large, lake-filled rock basins. At Närke, where basement inliers exist on several fault blocks, differences in the roughness of basement surfaces can be linked to progressive exhumation of the sub-Cambrian unconformity (Hall et al. 2019). These transitions in bedrock morphology along former ice sheet flow lines relate to differences in the total time that the basement surface has been subjected to glacial erosion. Along the present edges of outliers, re-exposure of the unconformity occurred in recent glacial cycles, whereas at greater distances re-exposure was later and consequently the total time available for glacial erosion was longer.

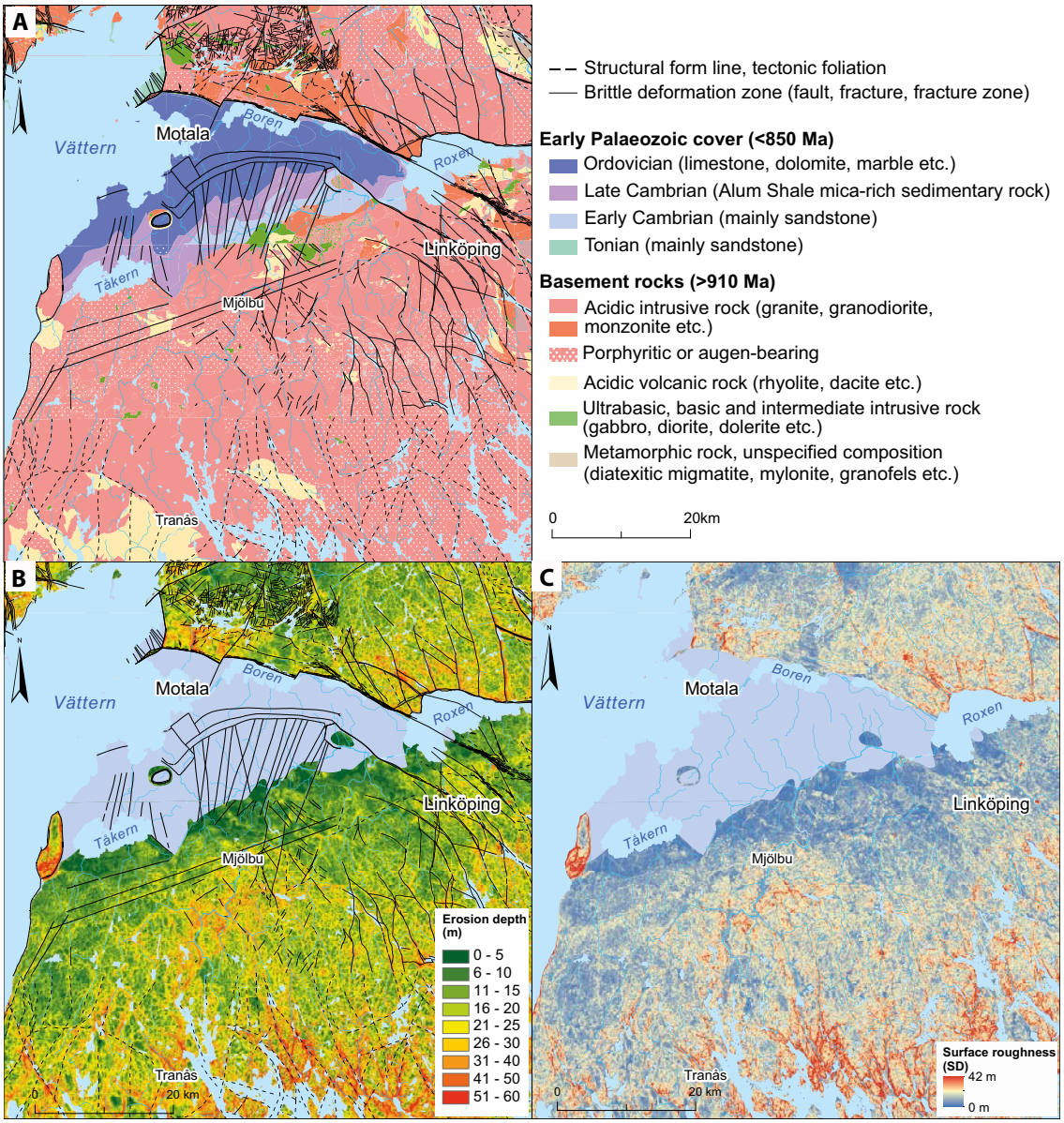

Figure 4-6. *Glacial modification of the exhumed Cambrian unconformity at Motala E of Lake Vättern. A. Geology and fractures. B. Surface roughness (SD). C. Estimated erosion depths below the summit envelope surface. Geological data from SGU; elevation data from Lantmäteriet.*

In other crystalline terrains, zones of low glacial erosion with few, if any well-developed glacial bedforms are seen to pass into landscapes with classic glacial bedforms, such as large roches moutonnées, rock basins and streamlined ridges and furrows (Rudberg 1988, Krabbendam and Bradwell 2013, Ebert 2015, Ebert et al. 2015, Hall et al. 2015). Such transformations are often apparent with descending elevations in mountains (Goodfellow et al. 2008, Kleman et al. 2008) and across pre-Pleistocene planation surfaces in lowlands (Godard 1961, Hall and Sugden 1987). In Fennoscandia, transitions from smooth to glacially-roughened terrain are apparent in parts of Kola (Kleman et al. 1997) and Finnmark (Olsen 1998), around the ice-divide zone in northern Finland (Ebert et al. 2015), in west-central Finland (Punkari 1994) and in southern Sweden (Johansson et al. 2001a). Glacial roughening of cratonic lowlands also has been identified from the Canadian Arctic (Bird 1967, Sugden 1978, Ebert 2015) and parts of Greenland (Sugden 1974). Hence glacial roughening of the sub-Cambrian unconformity around Trollhättan is typical of hard, crystalline bedrock terrains but provides a distinctive example where the initial relief on the basement was near planar before glacial erosion and so closely constrains the depths of rocks removed.

4.7.4 Persistence of planar flats

Planar flats are distinctive, local scale, near-horizontal slope facets set within the much wider, near-planar surface of the re-exposed unconformity. Planar flats stand within elevations 2–6 m of the projected buried unconformity on the flank of Halleberg (Figure 3-9) and Hunneberg (Figure 3-7). Thus, the planar flats are not likely to exactly mirror the unconformity, and a minor amount of glacial erosion must have occurred. However, transitions observed from well-preserved to degraded forms (Figure 3-49) indicate that a depth of only 2–3 metres of erosion is sufficient to significantly modify these features and to form low roches moutonnées. Several factors acted to reduce the effectiveness of glacial erosion on planar flats (i) high rock hardness, (ii) very widely-spaced vertical fractures, (iii) essentially flat upper surfaces that offered low frictional resistance to the flow of overriding ice sheets (Cohen et al. 2005, Krabbendam et al. 2016), (iv) alignment of planar flats parallel to dominant NE-SW fracture sets and subparallel to former ice flow and (v) low profiles and streamlined stoss faces (Krabbendam and Hall 2019). The survival of the planar flats around Trollhättan is interpreted as a result of extreme resistance to glacial erosion. However, whilst the planar flats are persistent features, glacial erosion had led to progressive lowering, modification and isolation. Small planar flats, such as at Kåtene (Figure 3-26), represent, in their vicinity, the last remaining and least-modified parts of the original U2 surface. Planar flats that were re-exposed earlier in other parts of the study area by glacial erosion were likely worn down and reshaped by that erosion to form the roches moutonnees now found at lower elevations (Figure 3-49F)

We see two possible explanations for the extraordinary flatness and smoothness of the tops of the planar flats found around Trollhättan: (1) a process of slow but continuous abrasion (e.g. without plucking), that removed any weathering and asperities from the original unconformity (as seen by micro-roughness on parts of the preserved unconformity at Kinnekulle; see Figure 3-11), or maintained flat rock surfaces (as at Trollhättan; see Figure 3-26) but otherwise acted uniformly across the unconformity surface; the abrasion depth was not sufficient to develop any relief; (2) a process of erosion guided by long and extensive horizontal fractures, with the top few metres removed by plucking, but strongly influenced by horizontal fractures. Extensive horizontal fractures have been observed in places along the Vänern shoreline (Figure 3-9). At Trollhättan, however, planar flats are developed across vertical and inclined fractures, as seen, for example, at Hjortmossen where the development of sub-horizontal fractures is very restricted (Figure 3-38). Also, glacial erosion of hard rocks with horizontal fracture sets and widely spaced vertical fractures forms stepped terrain with long, horizontal treads at different elevations (Krabbendam and Glasser 2011). At Trollhättan, the planar flats are found only at the highest points in the local topography (Figure 3-24); there is no significant local control on rock slopes by HFs or SHFs. On this basis, we regard uniform abrasion was the more likely mechanism. Abrasion without other erosional processes (meltwater erosion, fracturing of the bedrock surface or plucking) in general leads to surface smoothing and rounding of edges, rather than roughening (Boulton 1979, Hubbard et al. 2000). Smooth and flat basement gneiss surfaces elsewhere (e.g. at Georgian Bay, Ontario) may show localised erosional marks produced by focussed meltwater (Kor et al. 1991). In Västergötland, such meltwater evidently did not affect the planar flats, likely because of a well-established network of trenches developed along fractures and fracture zones adjacent to the planar flats.

4.7.5 Relevance to models of the development of landscapes and landforms of glacial erosion

Available evidence indicates that, in the Trollhättan region, the originally near planar, hard and variably fractured surface of U2 has been lowered and roughened by glacial erosion. Summit lowering has been limited in Areas 1–3 (Figures 3-14, 3-16 and 3-17) but significant differential rock removal from summits is evident in the southern part of Area 4, where summit elevation ranges reach 20 m (Figure 3-19). The largest volumes of rock removed are also from this sub-area. A terrain has developed that resembles in its assemblage of landforms the cnoc and lochain topography that is typical after glacial erosion by ice sheets in shield bedrock (Krabbendam and Bradwell 2014). Progressive glacial erosion of U2 in the Trollhättan region has brought about its modification and trends towards its destruction. Whilst maintenance of ice-roughened topography, such as at Sjuntorp, may occur under future glacial erosion, there is little evidence for maintenance of low relief in the early stages of glacial modification of U2 that are represented around Trollhättan. Evidence from this study does not support recent models of glacial landform development that require the formation

or maintenance of extensive low relief surfaces by glacial erosion (Egholm et al. 2017). Moreover, the strong control of fracture spacing over the selective development of glacial landforms in the Trollhättan region, also identified around Forsmark (Hall et al. 2019), requires that mathematical models of glacial erosion include this fundamental control over spatial variations in erosion processes and rates. The progressive modification of U2 identified in this study invites direct comparisons with the modification of non-glacial landscapes by glacial erosion through the Pleistocene (Godard 1961, Hall and Sugden 1987, Briner et al. 2006, Stroeven et al. 2006, Krabbendam and Bradwell 2013), with the development of distinct zones of glacial erosion identified by typical assemblages of non-glacial and glacial landforms (Sugden 1974, 1978).

Our observations on the glacial modification of near planar basement U2 surfaces reveal that the development of glacial landscapes does not require deep erosion. The estimated average depth of glacial erosion below U2 at Sjuntorp is 19.4 m yet the present surface shows an assemblage of box hills and fracture-guided rock basins and trenches that are typical of cnoc and lochain landscapes found on other glaciated shields. Moreover, the formation of roches moutonnées after re-exposure of U2 has required only a few metres of erosion. At the Lake Vänern shoreline at Kinnekulle, 1–2 m high domes on U2 show stoss side smoothing and lee-side cliffs, signs of incipient reshaping (Högbom and Ahlström 1924, Rudberg 1970). Around Halleberg and Hunneberg, summits on the exposed basement at elevations 2–6 m below the projected plane of U2 show well-developed roche moutonnée forms. At Hjortmossen, Trollhättan, the upper surface of a roche moutonnée stands 3 m below the adjacent planar flat (Figure 3-49F). The reshaping of non-glacial surfaces to form roches moutonnées after only limited depths of glacial erosion is consistent with previous observations on other glaciated unconformities (Olvmo et al. 1999), shore platforms (Smith et al. 2019), tor fields (André 2001, Hall and Phillips 2006) and stripped basal surfaces of weathering (Lindström 1988).

4.8 Glacial erosion depths and rates in the last glacial cycle estimated from cosmogenic nuclide inventories

Our cosmogenic nuclide sampling strategy was designed to establish erosion rates through the last glaciation on granite gneiss surfaces at 4 sites in the Trollhättan area. Two sites, Bragnum (2 samples) and Nordkroken (3 samples) stand close to the base of Halleberg and Hunneberg table mountains. The other two sites, Hjortmossen (4 samples) and Sandhem (4 samples) are in Trollhättan town and are remote from the the present edge of the buried unconformity (Figure 3-54). At Bragnum, the sampled surface is on a low roche moutonnée that stands above surrounding Late Quaternary sediment cover. All other rock surfaces sampled are on planar flats.

Simple exposure ages are plotted against sample elevation in Figure 3-55. Erosion rates are derived for a set of scenarios for ^{10}Be (Figure 3-58), ^{26}Al (Figure 3-59) and paired nuclides (Figure 3-60) with different starting dates and durations for erosion. The effects of abrasion (constant erosion rate) versus plucking (constant erosion depth) are also modelled. The most likely scenarios for basement erosion involve starting points after 1.1 Ma based on evidence given earlier (Section 4.7.1) for the timing of exhumation of the sub-Cambrian unconformity in the Trollhättan region. On the surfaces of planar flats, microforms such as planed off phenocrysts, striae and shallow grooves provide evidence of effective abrasion and evidence of plucking is confined to flanking cliffs (Figure 3-49). Assuming that abrasion has occurred throughout all ice cover periods, the constant erosion rate scenario is most likely to apply to these planar flat sites. Scenarios 3 and 5 thus appear to provide the best fits for interpretation of the sample results.

The erosion histories for rock surfaces around the flanks of Halleberg and Hunneberg differ from those around Trollhättan town (Figure 3-61). At Bragnum, Hunneberg, samples TROLL-16-06 and -07 relate to a single rock surface. Exposure ages overlap with the expected exposure age after deglaciation and emergence from water. Erosion over the last 100 ka was > 2–3 m and erosion over the last 1 Ma was > 20 m and may have exceeded 40 m. The sample site stands 6 m below and ~100 m distant from the buried sub-Cambrian unconformity below the flank of Hunneberg. Assuming that the present-day surface is no more than a few metres below the original unconformity, the estimated erosion rates allow re-exposure and erosion of the basement below the unconformity at this site during the last 1 or 2 glacial cycles.

At Nordkroken, Halleberg, the sample results are more difficult to interpret. Two samples (TROLL-16-04 and -17-03) have given simple exposure ages that are 2–3 ka less than the expected age. Former shielding is possible from the migration of the dune system on the southern shore of Lake Vänern. As at Bragnum, under all scenarios, erosion over the last 100 ka was >2–3 m and erosion over the last 1 Ma was >20 m and may have exceeded 40 m. The sample sites at Nordkroken stand ~5 m below and ~600 m distant from the buried sub-Cambrian unconformity below the flank of Hunneberg. Assuming that the present-day surface is no more than a few metres below the original unconformity, the minimum erosion depths at Nordkroken allow re-exposure and erosion of the basement below the sub-Cambrian unconformity at this site during the last 1 or 2 glacial cycles.

At Sandhem, Trollhättan town, the samples come from planar flats at two sites: the Skavsta industrial site (TROLL-16-8 to -10) and a site ~500 m to the NE (MJ-13). Nuclide inheritance is low in the Skavsta sample set (^{10}Be 1.6–3.0 ka; ^{26}Al 2.8–4.0 ka). For the single sample (MJ-13) taken in 2000 from a quartz vein, inheritance is greater (^{10}Be 14.1 ka; ^{26}Al 8.7 ka). Under best fit scenarios for the Skavsta sample set, erosion over the last 100 ka was >2 m and erosion over the last 1 Ma was >20 m. Under best fit scenarios for the MJ-13 sample, erosion over the last 100 ka was <2.1 m and erosion over the last 1 Ma was <18 m. The apparent divergence in erosion rates is noteworthy as the two sample sites stand at 52 and 51 m, respectively, on fragments of a 0.9 km long planar flat. If the planar flat at Sandhem represents a facet of the former unconformity then the divergent erosion rates, combined with the apparent preservation of the planar flat, can be interpreted as a result of recent exhumation.

At Hjortmossen, Trollhättan, the samples come from three sites. Samples MJ-14 and -15 and TROLL-17-01 come from the planar flat top surface. Nuclide inheritance is significant (^{10}Be 21.9–34.3 ka; ^{26}Al 8.5–35.9 ka), a result that is consistent with the removal of 0.5–2.2 mof rock in the last glacial cycle and <19 m of rock over the past 1 Ma (Figure 3-56). TROLL-17-02 comes from the rounded flank of the planar flat, ~2 m below TROLL-17-01, on a smooth, abraded rock surface with thin, curved sheet joints that locally have shed small, thin plates under glacial erosion. Nuclide inheritance is low in this sample (^{10}Be 3.2 ka; ^{26}Al 1.6 ka). Deeper erosion on this sample surface is consistent with faster erosion due to higher ice flow velocities and effective pressures acting on the edges of this bedrock high (Krabbendam and Glasser 2011).

The lowest erosion rates for the planar flat surfaces at Trollhättan town apply to very hard gneiss surfaces, with widely spaced vertical and inclined fractures that display widespread evidence of former abrasion. Long, sub-horizontal fractures that might facilitate glacial plucking are rare or absent (Figure 3-38). Hence erosion derives mainly from abrasion. Simulated glacial erosion rates for scenarios 3 and 5 are ~0.007–0.145 mm/a. Significant differences in erosion depths exist, however, between sample sites on planar flats at Trollhättan town (Figure 3-61). Similar differences in estimated erosion rates derived from cosmogenic nuclides are found between resistant summits, with wide spacing of vertical fractures, standing at similar elevations in the Forsmark area (Hall et al. 2019). These differences are consistent with spatially and temporally variable lowering and modification of basement surfaces under glacial erosion.

Close to the flanks of Hunneberg and Halleberg, the height difference between the projected buried unconformity and the sample sites is 5–6 m. At the erosion rates estimated for Bragnum and Nordkroken, this thickness of basement could be removed through the Late Weichselian glaciation and was likely removed through the last two glacial cycles. For the planar flat tops at Trollhättan, erosion rates are lower, except at the Skavsta site. However, transitions observed from well-preserved to degraded planar flats (Figure 3-49) indicate that a depth of only a few metres of erosion is sufficient to modify these features to produce roche moutonnée forms. Hence even slow erosion of a few decimetres per glaciation would degrade these features over several glacial cycles. The wider, exposed basement surface in Västergötland has summits at elevations <15 m below the unconformity at distances of 11 km from the base of the hills. Erosion depths and rates derived from cosmogenic nuclides are consistent with re-exposure of the sub-Cambrian unconformity since 1.1 Ma.

Our cosmogenic nuclide data provide no constraints on depths of glacial erosion of the less resistant Early Palaeozoic sedimentary rocks that formerly covered the sub-Cambrian unconformity or on the rates of scarp retreat around the table mountains. As erosion depths below U2 are 5–20 m in trenches (Section 4.7.3), erosion rates must have been greater than on the tops of planar flats, but we lack constraints from cosmogenic nuclide measurements for erosion on trench floors.

Modelled glacial erosion depths and rates based on cosmogenic nuclide inventories are available for the comparable lowland basement setting around Forsmark in east central Sweden (Hall et al. 2019). Application of the same scenarios to this dataset gives similar results. Typical total erosion depths in basement derived from cosmogenic nuclide analyses in the Forsmark area are 1.6–3.5 m over the last 100 ka and 13–27 m erosion over the last 1 Ma (Hall et al. 2019). Cosmogenic nuclide inheritance is found in all samples at Forsmark, providing confidence that glacial erosion in the last glacial cycle had a moderate to minor impact on the bedrock highs sampled. Typical erosion depths of 1.0–3.6 m under Scenarios 3 and 5 for the last glacial cycle for the complete sample set at Trollhättan town (Figure 3-61) show a similar range of values. As at Forsmark, more extreme scenarios and constant depth erosion yield higher erosion estimates. Consistency with the larger Forsmark cosmogenic nuclide dataset provides confidence in the smaller set of results from Trollhättan.

4.9 Model of glacial erosion of the sub-Cambrian unconformity in Västergötland

A model of glacial erosion beneath the Fennoscandian Ice Sheet in the Trollhättan area is shown in Figure 4-7.

Glacial erosion of early Palaeozoic cover rocks over Västergötland has been extensive and deep. The summits of the Halleberg and Hunneberg table mountains have been lowered through the erosion of sheets of dolerite cap rock. Removal of dolerite around the hill flanks has exposed soft and fissile Early Palaeozoic sandstone, shale and limestone to glacial erosion and led to headward erosion. The total distance of scarp retreat around these hills is unknown but the position of the Hullsjön depression is suggestive that a former scarp foot position was maintained ~3 km from Hunneberg, forcing ice to flow around the former margin of the hill and to excavate the depression. The numerous, well-preserved planar flats are inherited facets of the unconformity surface that have experienced limited glacial erosion and modification. The planar flats, associated with unweathered Cambrian sandstone dykes, point to geologically recent re-exposure and suggest the former presence of a large Early Palaeozoic outlier around Trollhättan. Successive Fennoscandian ice sheets have re-exposed the near-planar sub-Cambrian basement unconformity to glacial erosion. Those areas around Halleberg and Hunneberg, and at Trollhättan, where the original planar form of U2 persists, likely represent areas of relatively recent re-exposure by glacial erosion compared to areas in which nascent cnoc and lochain topography has developed, such as around Sjuntorp. Based on evidence from other parts of Scandinavia, this re-exposure commenced at or after 1.1 Ma and continued with greatest impact around the hill flanks through the Middle and Late Pleistocene glaciations, when the FIS reached its maximum extent and thickness.

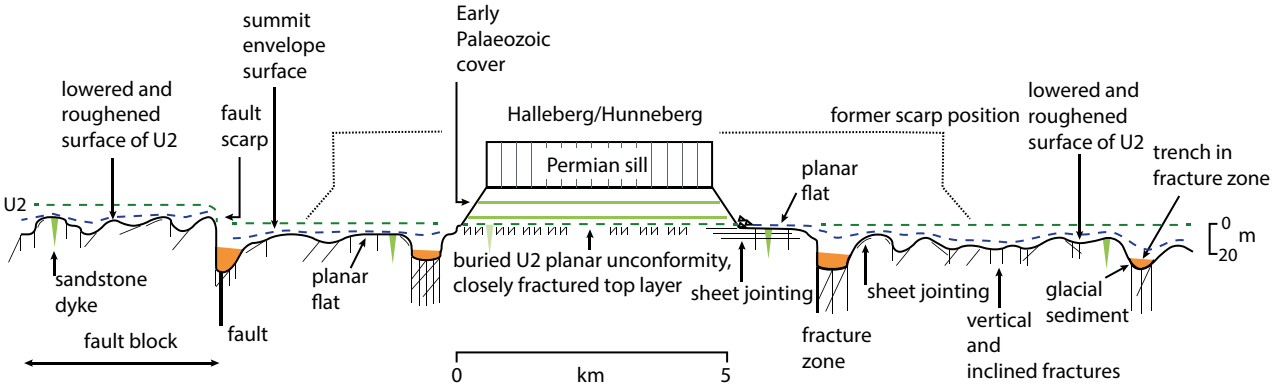

Figure 4-7. *Schematic model of the sub-Cambrian unconformity and its modification by glacial erosion in the Trollhättan area.*

The sub-Cambrian unconformity in the Trollhättan area was exhumed by glacial erosion. The unconformity is of very low relief around Hunneberg and Halleberg, with widely-spaced low (5–15 m) hills separated by extensive areas with relief of < 5 m. There is no evidence for the existence of larger hills on the buried unconformity or for their former existence on the surrounding basement. Evidence is lacking that the surface of the unconformity was extensively or deeply weathered either prior to or subsequent to burial. Any weathering horizon, together with closely fractured rock immediately below the unconformity surface, has been lost to glacial erosion of the exposed basement. Height differences between the buried unconformity and basement risers along its edge indicate that this layer was only 2–6 m thick. U2 provided a smooth, near planar basement surface that after re-exposure was lowered and roughened by glacial erosion.

Lowering of U2 by glacial erosion across summits has been limited. Lowering of basement highs found close to outliers is 2–6 m. Exposed basement summits remain widely accordant in elevation for distances of > 15 km from the edge of Halleberg and Hunneberg and remain at similar elevations to the buried unconformity (Figure 3-28). Steps in the bedrock topography correspond to the edges of basement fault blocks that represent Phanerozoic fault scarps exhumed after glacial erosion of cover rocks. Vertical throw across the Lilleskog Fault is constrained to 24–30 m and remains similar across exposed basement blocks to the west of Halleberg and Hunneberg, indicating very limited lowering by glacial erosion of the southern edge of this fault block. The emergence of slättbergen as low, flat-topped, rectilinear hills and ridges is a result of the excavation of closely-fractured rock to form bounding rectilinear depressions. Increased curvature on the edges of slättbergen and box hills likely led to the formation of curved sheet joints on edges. Much higher erosion depths occurred in trenches and basins now found 10–40 m below the former unconformity. Roughening in this hard gneissic terrain is dominantly a product of the exploitation of fracture zones by glacial erosion.

Glacial forms on the U2 surface in Västergötland have developed since its re-exposure. Cosmogenic nuclide inventories for the sites at Nordkroken and Bragnum, close to the edges of Halleberg and Hunneberg, respectively, indicate that lowering of the unconformity surface was rapid, with glacial erosion capable of removing > 2–3 m of rock over the last 100 ka. Rapid lowering may reflect high fracture density on the former U2 surface. The Bragnum site stands only 6 m below the buried unconformity which is located at 100 m distance, but the site and its surroundings show several low basement highs with asymmetric, roche moutonnée forms. At Hjortmossen, roches moutonnées are found at elevations 3 m below nearby planar flats. The small height differences indicate that typical roches moutonnées can develop at the macro- and local scales after limited glacial erosion. Shallow rock trenches and basins, typical forms of negative relief at the local scale in glacial eroded crystalline terrain, are seen on parts of fault block tops with low roughness (Figure 3-14), indicating the immediate onset of excavation of fractures after re-exposure. At the regional scale, differences in surface roughness relate to progressive glacial erosion, with the highest volumes of rock lost from the sites of trenches and basins (Table 3-2). In the Sjuntorp area, rock trenches and basins > 20 m deep cover 35 % of the total area; this area, with its widely-spaced box hills and roches moutonnées and wide and deep trenches and basins, resembles classic cnoc-and-lochain topography.

4.10 The Trollhättan area as an analogue for NE Uppland

One of the aims of this study is to examine the extent to which basement terrain in Västergötland provides an analogue for the erosion history in Uppland described in a companion report (Hall et al. 2019).

Basement cooling and the onset of brittle deformation in Västergötland occurred during the Sveconorwegian orogeny (1.14–0.96 Ga) and so was much later than at Forsmark where cooling dates from the Svecofennian orogeny (1.97–1.81 Ga). The gneisses in both areas are mainly felsic in composition but the main rock groups at Forsmark include protoliths of more varied granitic, volcanic and sedimentary rock types (Stephens 2010), compared to the rather uniform granite gneisses that are widespread in the Trollhättan area. Around the Bothnian Sea, and across Uppland, deep Mesoproterozoic erosion led to the development of a major basement unconformity (U1) which was later deeply buried beneath Jotnian sandstone. Due to a much later assembly and cooling of basement terranes, no equivalent sub-Jotnian unconformity exists in Västergötland.

Much of Baltica was reduced to low relief and elevation in the late Neoproterozoic prior to burial (U2). In Västergötland and Uppland, there are no reports of Late Neoproterozoic deep weathering residuals on the sub-Cambrian basement surface, in contrast to the Baltic states (Liivamägi et al. 2015). This absence requires either that deep weathering profiles did not develop below the late Neoproterozoic ultiplains in these locations, or that the weathering was removed by erosion before or during later marine transgression. In Västergötland, the basement is covered by Early Cambrian marine quartz sandstones (Nielsen and Schovsbo 2011). In Uppland, Early Cambrian marine sands were also deposited on basement but removed during minor epeirogenic uplift before the basement was later reburied beneath Early Ordovician limestones (Söderberg and Hagenfeldt 1995). The Late Neoproterozoic ultiplains in Västergötland and Uppland were eroded, lowered and probably further graded by the combined action of weathering, wind and wave erosion during marine transgression to produce extensive, near planar Early Palaeozoic unconformities.

Available evidence indicates that the buried sub-Cambrian unconformity around Halleberg, Hunneberg and Kinnekulle in Västergötland has a near planar form. Summit elevations on the neighbouring basement show that low, broad hills, with wavelengths of 0.5–1 km, rise only 5–15 m above surrounding high points. To the NE of Forsmark, a submerged basement fault block has a summit elevation range of < 15 m where it emerges from beneath Ordovician limestone. In Uppland, the exposed basement surfaces on the tops of individual fault blocks retain low relief for ~40 km distance from outliers of Ordovician limestone. Planar flats are numerous on massive kernels of granite gneiss in the Trollhättan area. No planar flats are yet recognised in Uppland, although low relief surfaces are locally extensive on fault block tops (Hall et al. 2019) that are similar to surfaces developed on more fractured gneisses on the unconformity south and south-east of Trollhättan and at Kinnekulle. Cambrian sandstone dykes are widespread in Västergötland, but no Cambrian sandstone dykes are reported from N of Norrtälje in Uppland. The Early Cambrian sandstone mass at Vattholma, NE of Uppsala, is isolated within in a fault zone (Wiman 1918). This absence of sandstone dykes in Uppland may reflect the stripping of Early Cambrian sands from the basement surface in Uppland in the early Middle Cambrian during the Hawke Bay Event (Nielsen and Schovsbo 2015).

The unconformities in both areas were buried by thin, horizontally dipping and laterally continuous beds of Early Palaeozoic marine sandstones, shales and limestone (Nielsen and Schovsbo 2006). Deeper, km-scale burial occurred in the Late Palaeozoic and later due to the accumulation of detritus from the Caledonide orogenic belt (Guenthner et al. 2017). The buried, near-planar unconformities in Västergötland and Uppland were broken by fault movements at intervals during the Phanerozoic, probably mainly in the Permian (Preeden et al. 2009), with dislocation, tilting and jostling of basement fault blocks. The now exhumed fault blocks in both areas have displacements of a few tens of metres, as indicated by displacement of Early Palaeozoic beds and by low fault scarps.

No evidence is known to suggest that the basement in the Trollhättan area or around Forsmark was re-exposed to subaerial weathering and erosion during the Mesozoic and Cenozoic. Instead, the presence of calcite fracture fills in the near surface at Trollhättan (Mattsson 1962) and Forsmark (Sandström et al. 2008) suggest late exhumation. Multiple generations of fracture coatings and fills are present that constrain timings of fracture development, reactivation and opening and changes in groundwater chemistry and circulation through the Phanerozoic (Sandström and Tullborg 2009).

During the Pleistocene, the duration of ice cover may have been similar at Trollhättan and Forsmark due to a similar distance from ice centres (Kleman et al. 2008). Development of the FIS in full ice sheet mode dates from the Middle Pleistocene Transition (Clark and Pollard 1998, Lee et al. 2012). The onset of deep erosion by the FIS, with excavation of deep rock basins in the Ålands basin and in the Skagerrak, likely dates from the Menapian glaciation at 1.1 Ma (Winsemann et al. 2020). Large volumes of Early Palaeozoic cover rocks have been lost to glacial erosion from Västergötland and Uppland since this date and transported towards ice sheet margins in Denmark and Poland, respectively.

Re-exposure of Early Palaeozoic unconformities exposed flat, hard and fractured basement surfaces to erosion by the FIS. Similar assemblages of fracture-controlled glacial bedforms in Västergötland and Uppland with typical glacial bedforms, such as box hills, roches moutonnées, rock trenches, and rock basins. The roughness of the present bedrock surfaces is similar around Trollhättan and Forsmark, and glacial streamlining is only weakly and locally developed in bedrock in both areas.

Similar sets of processes of glacial erosion led to the formation of similar assemblages of glacial bedrock forms in both areas. Evidence for widespread glacial ripping is, however, found only in parts of Uppland.

Glacial erosion depths in the re-exposed basement are low in Västergötland and Uppland. Estimates derived from subtraction of the present basement surface from summit envelope surfaces that conform to the former unconformity indicate losses of < 5 m locally and an average of 14 m in the Trollhättan area and < 10 m locally and averages of 12–18 m in the Forsmark area and NE Uppland (Hall et al. 2019). In both areas, the greatest rock volumes come mainly from the glacial excavation of closely fractured trenches and basins which stand 10–40 m beneath adjacent summits.

Västergötland provides detailed case studies for the development of the Early Palaeozoic basement unconformity, its burial, dislocation and late re-exposure. The Early Palaeozoic outliers at Trollhättan and Kinnekulle are critical for establishing the form of the buried unconformity and its relation to surrounding surfaces in the exposed basement. Important additional evidence comes from around the Early Palaeozoic outliers at Närke and Motala. The near-planar sub-Cambrian unconformity at Trollhättan provides an important reference surface for identifying the pattern and depth of glacial erosion in basement beneath the FIS. The small height differences between summits on the buried and exposed unconformities around Halleberg and Hunneberg provide confidence that the low relief on the presently exposed basement is inherited from the former unconformity. The key elements of the exposed basement surfaces in the Trollhattan and around Forsmark are similar: (i) inheritance of a near-planar form from the sub-Cambrian unconformity, (ii) the presence of low, flat-topped blocks produced by Phanerozoic faulting and (iii) similar assemblages and distribution of glacial erosion forms. Existing models of U2 in Uppland rest on assumptions that U2 was originally a near planar surface, without deep Neoproterozoic weathering at the time of burial, overlain by Ordovician limestone and broken by minor, post-Ordovician faulting (Hall et al. 2019). The evidence presented in his report supports these assumptions, except that in Västergötland the basement unconformity is overlain by older, Early Cambrian cover rocks.

5 Conclusions

The main findings of this study are:

1. Understanding the development of the present basement topography in Västergötland requires distinctions to be made between separate former and existing basement surfaces. Towards the end of a long period of denudation after 900 Ma, Baltica was reduced to low relief. Extensive planation surfaces, with ultiplain and peneplain morphologies, developed by subaerial weathering and erosion that operated over a period of 36–50 Ma on the stable craton of Baltica through the Late Neoproterozoic. The basement surface was further lowered during Cambrian to Ordovician marine transgression when rock shorelines were eroded in multiple short-term transgression-regression cycles, leading to final grading of the rock shelf prior to burial. This near-planar basement surface is now represented by the sub-Cambrian unconformity (U2) in large parts of Fennoscandia. The present basement surface represents the re-exposed unconformity that has been modified and slightly lowered by erosion beneath the Fennoscandian Ice Sheet during the Pleistocene.
2. Previous mapping, SGU datasets and available exposure shows that the relief on the buried sub-Cambrian unconformity is < 5 m over 6–10 km-long stretches of the flanks of Halleberg and Hunneberg and also at Kinnekulle. The preserved unconformity is generally a flat surface in Västergötland.
3. The exposed basement surface in the Trollhättan region is modelled by projection of maximum rock summit elevations across circles of 0.25 and 1 km radius. The summit envelope surfaces revealed are nearly planar. Hills on the exposed basement are low (5–15 m), broad (with wavelengths of 1–2 km), and widely spaced (over several km). Basement summits remain accordant within an elevation range of 5–10 m at distances of > 11 km from the edge of the buried unconformity. Gneiss summits exposed adjacent to Halleberg and Hunneberg stand at elevations only 2 to 6 m below projections of the planar buried unconformity, a height difference that constrains summit erosion since exhumation at these locations. The buried unconformity is inclined at 0.25–0.4 % towards the N. Beds in overlying Early Palaeozoic sedimentary rocks along the flanks of Halleberg and Hunneberg dip N at ~0.3 %. Individual planar flats are inclined N at 0.25–0.4 %. Summit envelope surfaces inclinations of 0.2–0.4 % match these inclinations. Consistent dip orientation and angles between sedimentary beds, the buried unconformity surface and the present basement surface provide strong support for the view that the present basement surface represents the little modified, re-exposed, slightly tilted and near planar sub-Cambrian unconformity.
4. The sub-Cambrian unconformity is not primarily, or widely a structurally controlled surface because it is cut across inclined fractures and variably spaced vertical fractures of Proterozoic age. Planar flats are smooth, bare bedrock surfaces with relief of < 1–2 m over distances of 0.1–0.9 km flanked by steep rock slopes. Planar flats are confined to coarse-grained and porphyritic granite gneisses with up to 10 m wide vertical fracture spacings. Early Cambrian sandstone dykes are common in vertical fractures on planar flat surfaces. Planar flats conform at Nordkroken to near surface horizontal sheet fractures, but at Trollhättan and elsewhere crosscut sub-horizontal fractures or have developed in the absence of long, continuous, horizontal fractures. Planar flats most likely represent inherited facets of the former unconformity surface, modified to a limited degree by later glacial erosion due to high rock resistance.
5. The sub-Cambrian unconformity, its sedimentary cover and Permian sills were dislocated by minor (10–60 m vertical throw) Phanerozoic faulting. Bedrock surface profiles derived from 2 m resolution LiDAR data support patterns identified previously of dislocation and tilting for km-scale fault blocks. Additional small (< 10 m) vertical displacements are recognised within several large fault blocks. Similar patterns of fault block movement are found around Early Palaeozoic outliers at Närke and Motala.
6. The present basement surface lacks remnants of deep weathering and retains unweathered Cambrian sandstone dykes and Palaeozoic calcite fracture coatings. The absence of weathering, together with the widespread persistence of flat basement surfaces inherited from U2, provides evidence for re-exposure of basement in the Pleistocene. Large numbers of Cambrian sandstone, Ordovician

limestone and Kinnekulle dolerite clasts sourced from Västergötland are found in Middle and Late Pleistocene tills in Jutland, Denmark. The source areas for these rocks around outliers in Västergötland are presently small when compared with the large sink area in Denmark. This disparity suggests that Early Palaeozoic cover and Early Permian capping dolerite sills remained more extensive than today into the Middle Pleistocene. Thicknesses of at least a few tens of metres of Early Palaeozoic sedimentary rock likely have been removed from around present day outliers and across wider areas of Västergötland. Re-exposure of the basement unconformity for the first time since the Early Cambrian was likely a result of a step-change in erosion by the Fennoscandian Ice Sheet after 1.1 Ma.

7. Glacial erosion of the re-exposed basement unconformity has lowered and roughened its surface. Less than 5–10 m of basement has been removed from below summit envelope surfaces over wide areas. The summits that pin the summit envelope surfaces to U2 were also lowered. This lowering is limited (2–6 m) close to Halleberg and Hunneberg but may be larger for regions further away from the cover rocks. The limited depths of glacial erosion, together with late re-exposure from beneath Early Palaeozoic cover have allowed the original planar form of the sub-Cambrian unconformity to persist in the present basement landscape at the regional scale. Average depths of erosion below summit envelope surfaces in the Trollhattan region are 14 m. The largest volumes of basement rock removed by glacial erosion are represented by the excavation of 10–40 m deep depressions and valleys, often located in zones with closely fractured gneisses. In the Sjuntorp area, landform assemblages occur that include box hills, large roches moutonnées, and box- and star basins, features that are typical of cnoc and lochain landscapes developed on glaciated shields.
8. Cosmogenic nuclide inventories show little or no nuclide inheritance at two sites close to the flanks of Halleberg and Hunneberg. These results are consistent with removal of > 2 m of rock in the last glaciation and with recent exhumation of basement at the sub-Cambrian unconformity that likely includes scarp retreat around the hill flanks. Erosion depths on planar flats in Trollhättan town, except at the Skavsta site, are 0.5 to 2.2 m for the last 100 ka in best fit scenarios in which basement is re-exposed at 1.0 or 0.5 Ma. The preservation of the planar flats is due to the high resistance of hard, massive granite gneisses to glacial erosion and likely also to late re-exposure of these rock surfaces from beneath cover rocks. Typical estimated depths of glacial erosion over the last 100 ka based on cosmogenic nuclide inventories at Trollhättan (1.0–3.6 m for the last 100 ka under Scenarios 3 and 5 for the complete sample set at Trollhättan town) are similar to that seen in a larger cosmogenic nuclide dataset at Forsmark (1.6–3.5 m over the last 100 ka).
9. Whilst the history of Early Palaeozoic erosion and burial between Västergötland and Uppland shows significant differences, there are many similarities. These include the flatness of the sub-Cambrian unconformity, its minor dislocation as seen in tilted fault blocks and the lack of evidence for re-exposure of the basement to Mesozoic to Cenozoic deep weathering.
10. Similar landforms of glacial erosion are seen at different scales around Trollhättan and Forsmark. This indicates that the processes of glacial erosion operating on low relief, hard, variably-fractured basement surfaces in both areas are directly comparable.
11. It is concluded that modelling of the sub-Cambrian unconformity in the Trollhättan region provides a reference surface for identifying the pattern and estimating the average depth of glacial erosion of basement, a technique that can be applied in other areas of exposed basement in Sweden around Early Palaeozoic outliers. The Trollhättan region provides a valuable analogue for understanding past and future glacial erosion on the sub-Cambrian unconformity at and around the proposed spent nuclear fuel repository site at Forsmark.

References

SKB's (Svensk Kärnbränslehantering AB) publications can be found at www.skb.com/publications.

Abels A, Mannola P, Lehtinen M, Bergman L, Pesonen L, 1998. New observations of the properties of the Lumparn impact structure, Åland Islands, southwestern Finland. Meteoritics and Planetary Science Supplement 33, A7.

Ahlberg A, Olsson I, Simkevicius P, 2003. Triassic-Jurassic weathering and clay mineral dispersal in basement areas and sedimentary basins of southern Sweden. Sedimentary Geology 161, 15–29.

Ahlin S, 1982. NNE–SSW striking Precambrian faults of south-western Sweden. Geologiska Föreningen i Stockholm Förhandlingar, 182–185.

Ahlin S, 1987. Phanerozoic faults in the Västergötland basin area, SW Sweden. GFF 109, 221–227.

Alm E, Sundblad K, 2002. Fluorite-calcite-galena-bearing fractures in the counties of Kalmar and Blekinge, Sweden. SKB R-02-42, Svensk Kärnbränslehantering AB.

Alvarez-Marrón J, Hetzel R, Niedermann S, Menéndez R, Marquínez J, 2008. Origin, structure and exposure history of a wave-cut platform more than 1 Ma in age at the coast of northern Spain: A multiple cosmogenic nuclide approach. Geomorphology 93, 316–334.

Alwmark C, 2009. Shocked quartz grains in the polymict breccia of the Granby structure, Sweden – Verification of an impact. Meteoritics & Planetary Science 44, 1107–1113.

Alwmark C, Ferrière L, Holm-Alwmark S, Ormö J, Leroux H, Sturkell E, 2015. Impact origin for the Hummeln structure (Sweden) and its link to the Ordovician disruption of the L chondrite parent body. Geology 43, 279–282.

Amantov A, 1995. Plio Pleistocene erosion of Fennoscandia and its implications for Baltic area. In Mojski J E (ed) Proceedings of the Third Marine Geological Coonference "The Baltic", 1995. Warszawa. (Prace Panstwowego Instytutu Geologicznego 149)

Ambrose J W, 1964. Exhumed paleoplains of the Precambrian shield of North America. American Journal of Science 262, 817–857.

Andersson A, Dahlman B, Gee D G, Snäll S, 1985. The Scandinavian alum shales. Uppsala: Sveriges geologiska undersökning. (Ser. Ca 56)

André M F, 1996. Rock weathering rates in arctic and subarctic environments (Abisko Mts, Swedish Lappland). Zeitschrift für Geomorphologie 40, 499–517.

André M-F, 2001. Tors et roches moutonnées en Laponie suédoise : antagonisme ou filiation? Géographie physique et Quaternaire 55, 229–242. (In French.)

André M-F, 2002. Rates of Postglacial rock weathering on glacially scoured outcrops (Abisko–Riksgränsen area, 68°N). Geografiska Annaler 84A, 139–150.

Andréasson P-G, Rodhe A, 1990. Geology of the Protogine Zone south of Lake Vättern, southern Sweden: a reinterpretation. Geologiska Föreningen i Stockholm Förhandlingar 112, 107–125.

Andréasson P G, Rodhe A, 1994. Ductile and brittle deformation within the Protogine Zone, southern Sweden: a discussion. GFF 116, 115–116.

Angerer T, Greiling R O, Avigad D, 2011. Fabric development in a weathering profile at a basement–cover interface, the sub-Cambrian peneplain, Israel: Implications for decollement tectonics. Journal of Structural Geology 33, 819–832.

Arnaud E, Halverson G P, Shields-Zhou G (eds), 2011. The geological record of Neoproterozoic glaciations. London: The Geological Society. (Geological Society Memoir3 36)

Artyushkov E A, Lindström M, Popov L E, 2000. Relative sea-level changes in Baltoscandia in the Cambrian and early Ordovician: the predominance of tectonic factors and the absence of large scale eustatic fluctuations. Tectonophysics 320, 375–407.

Avigad D, Sandler A, Kolodner K, Stern R, McWilliams M, Miller N, Beyth M, 2005. Mass-production of Cambro–Ordovician quartz-rich sandstone as a consequence of chemical weathering of Pan-African terranes: Environmental implications. Earth and Planetary Science Letters 240, 818–826.

Balco G, 2017. Production rate calculations for cosmic-ray-muon-produced ^{10}Be and ^{26}Al benchmarked against geological calibration data. Quaternary Geochronology 39, 150–173.

Balco G, Stone J O, Porter S C, Caffee M W, 2002. Cosmogenic-nuclide ages for New England coastal moraines, Martha's Vineyard and Cape Cod, Massachusetts, USA. Quaternary Science Reviews 21, 2127–2135.

Balco G, Stone J O, Lifton N A, Dunai T J, 2008. A complete and easily accessible means of calculating surface exposure ages or erosion rates from ^{10}Be and ^{26}Al measurements. Quaternary Geochronology 3, 174–195.

Batchelor C L, Margold M, Krapp M, Murton D K, Dalton A S, Gibbard P L, Stokes C R, Murton J B, Manica A, 2019. The configuration of Northern Hemisphere ice sheets through the Quaternary. Nature Communications 10, 3713. doi:10.1038/s41467-019-11601-2

Beauvais A, Chardon D, 2013. Modes, tempo, and spatial variability of Cenozoic cratonic denudation: The West African example. Geochemistry, Geophysics, Geosystems 14, 1590–1608.

Beckholmen M, Tirén S A, 2010. Rock-block configuration in Uppland and the Ålands-hav basin, the regional surroundings of the SKB site in Forsmark, Sea and land areas, eastern Sweden. SSM Report 2010:41, Swedish Radiation Safety Authority.

Bergelin I, 2009. Jurassic volcanism in Skåne, southern Sweden, and its relation to coeval regional and global events. GFF 131, 165–175.

Bergsten H, 1994. A high-resolution record of Lateglacial and early Holocene marine sediments from southwestern Sweden; with special emphasis on environmental changes close to the Pleistocene-Holocene transition and the influence of fresh water from the Baltic basin. Journal of Quaternary Science 9, 1–12.

Bergström S M, Bergström J, 1996. The Ordovician–Silurian boundary successions in Östergötland and Västergötland, S. Sweden. GFF 118, 25–42.

Bergström S M, Löfgren A, Maletz J, 2004. The GSSP of the second (upper) stage of the Lower Ordovician Series: Diabasbrottet at Hunneberg, Province of Västergötland, southwestern Sweden. Episodes 27, 265–272.

Bijlsma S, 1981. Fluvial sedimentation from the Fennoscandian area into the north-west European Basin during the Late Cenozoic. Geologie en Mijnbouw 60, 337–345.

Bingen B, Demaiffe D, Breemen O V, 1998. The 616 Ma old Egersund basaltic dike swarm, SW Norway, and late Neoproterozoic opening of the Iapetus Ocean. The Journal of Geology 106, 565–574.

Bingen B, Griffin W L, Torsvik T H, Saeed A, 2005. Timing of Late Neoproterozoic glaciation on Baltica constrained by detrital zircon geochronology in the Hedmark Group, south-east Norway. Terra Nova 17, 250–258.

Bird J B, 1967. The physiography of Arctic Canada: with special reference to the area south of Parry Channel. Baltimore: Johns Hopkins Press.

Björck S, Digerfeldt G, 1991. Allerød–Younger Dryas sea level changes in southwestern Sweden and their relation to the Baltic Ice Lake development. Boreas 20, 115–133.

Bjørlykke A, Cumming G L, Krstic D, 1990. New Isotopic data from davidites and sulfides in the Bidjovagge gold-copper deposit, Finnmark, Northern Norway. Mineralogy and Petrology 43, 1–21.

Bojanowski M J, Goryl M, Kremer B, Marciniak-Maliszewska B, Marynowski L, Środoń J, 2020. Pedogenic siderites fossilizing Ediacaran soil microorganisms on the Baltica paleocontinent. Geology 48, 62–66.

Borchers B, Marrero S, Balco G, Caffee M, Goehring B, Lifton N, Nishiizumi K, Phillips F, Schaefer J, Stone J, 2016. Geological calibration of spallation production rates in the CRONUS-Earth project. Quaternary Geochronology 31, 188–198.

Boulton G S, 1979. Processes of glacier erosion on different substrata. Journal of Glaciology 23, 15–38.

Brandano M, 2017. Unravelling the origin of a Paleogene unconformity in the Latium-Abruzzi carbonate succession: A shaved platform. Palaeogeography, Palaeoclimatology, Palaeoecology 485, 687–696.

Brasier M D, 1980. The Lower Cambrian transgression and glauconite-phosphate facies in western Europe. Journal of the Geological Society 137, 695–703.

Briner J P, Miller G H, Davis P T, Finkel R C, 2006. Cosmogenic radionuclides from fiord landscapes support differential erosion by overriding ice sheets. Geological Society of America Bulletin 118, 406–420.

Brunsden D, 1993. The persistence of landforms. Zeitschrift für Geomorphologie 93, 13–28.

Bruun-Petersen J, 1975. Origin and correlation of the sandstone dykes at Listed, Bornholm (Denmark). Bulletin of the Geological Society of Denmark 24, 33–44.

Burke M J, 1969. The Forth valley: an ice-moulded lowland. Transactions of the Institute of British Geographers 48, 51–59.

Calner M, Ahlberg P, Lehnert O, Erlström M (eds), 2013. The Lower Palaeozoic of southern Sweden and the Oslo region, Norway: field guide for the 3rd Annual Meeting of the IGCP project. Uppsala: Geological Survey of Sweden.

Cameron I B, Stephenson D, 1985. British regional geology. the Midland Valley of Scotland. London: HMSO Books.

Chmeleff J, von Blanckenburg F, Kossert K, Jakob D, 2010. Determination of the ^{10}Be half-life by multicollector ICP-MS and liquid scintillation counting. Nuclear Instruments and Methods in Physics Research Section B: Beam Interactions with Materials and Atoms 268, 192–199.

Clark P U, Pollard D, 1998. Origin of the middle Pleistocene transition by ice sheet erosion of regolith. Palaeoceanography 13, 1–9.

Clark P U, Archer D, Pollard D, Blum J D, Rial J A, Brovkin V, Mix A C, Pisias N G, Roy M, 2006. The middle Pleistocene transition: characteristics, mechanisms, and implications for long-term changes in atmospheric CO_2. Quaternary Science Reviews 25, 3150–3184.

Cooley S W, 2013. GIS4 Geomorphology. http://gis4geomorphology.com/ [09 October 2016]. (Update: information now available at: https://www.skyecooley.com/single-post/2019/10/20/GIS4Geomorphology-Archive)

Cohen D, Iverson N R, Hooyer T, Fischer U, Jackson M, Moore P L, 2005. Debris-bed friction of hard-bedded glaciers. Journal of Geophysical Research: Earth Surface 110. doi:10.1029/2004JF000228|

Cowton T, Nienow P, Bartholomew I, Sole A, Mair D, 2012. Rapid erosion beneath the Greenland ice sheet. Geology 40, 343–346.

Czubla P, Terpiłowski S, Orłowska A, Zieliński P, Zieliński T, Pidek I A, 2017. Petrographic features of tills as a tool in solving stratigraphical and palaeogeographical problems–a case study from Central-Eastern Poland. Quaternary International 501, 45–58.

Dahlke H E, Behrens T, Seibert J, Andersson L, 2009. Test of statistical means for the extrapolation of soil depth point information using overlays of spatial environmental data and bootstrapping techniques. Hydrological Processes 23, 3017–3029.

Dahlqvist P, Bastani M, Persson L, Triumf C, Erlström M, Gustafsson M, Jørgensen F, Gulbrandsen M, Malmberg-Persson K, 2018. SkyTEM-undersökningar på Öland: geologiska tolkningar och hydrogeologisk tillämpning. Uppsala: Sveriges geologiska undersökning. (Rapporter och meddelanden 145) (In Swedish.)

Davis W M, 1902. Baselevel, grade and peneplain. The Journal of Geology 10, 77–111.

Dawes P R, 2009. Precambrian–Palaeozoic geology of Smith Sound, Canada and Greenland: key constraint to palaeogeographic reconstructions of northern Laurentia and the North Atlantic region. Terra Nova 21, 1–13.

DeLucia M, Guenthner W R, Marshak S, Thomson S, Ault A, 2017. Thermochronology links denudation of the Great Unconformity surface to the supercontinent cycle and snowball Earth. Geology 46, 167–170.

Derby J R, Raine R J, Smith M P, Runkel A C, 2012. Paleogeography of the great American carbonate bank of Laurentia in the earliest Ordovician (early Tremadocian): The Stonehenge transgression. AAPG Memoir 98, 5–13.

Digerfeldt G, 1979. The highest shore-line on Hunneberg, southern Sweden. Geologiska Föreningen i Stockholm Förhandlingar 101, 49–64.

Dott Jr R H, 2003. The importance of eolian abrasion in supermature quartz sandstones and the paradox of weathering on vegetation-free landscapes. The Journal of Geology 111, 387–405.

Drake H, Tullborg E-L, Page L, 2009a. Distinguished multiple events of fracture mineralisation related to far-field orogenic effects in Paleoproterozoic crystalline rocks, Simpevarp area, SE Sweden. Lithos 110, 37–49.

Drake H, Tullborg E-L, Page L M, 2009b. Distinguished multiple events of fracture mineralisation related to far-field orogenic effects in Paleoproterozoic crystalline rocks, Simpevarp area, SE Sweden. Lithos 110, 37–49.

Dreyer T, 1988. Late Proterozoic (Vendian) to Early Cambrian sedimentation in the Hedmark Group, southwestern part of the Sparagmite Region, southern Norway. Norges geologiske undersøkelse Bulletin 412, 1–27.

Driese S G, Medaris Jr L G, Kirsimäe K, Somelar P, Stinchcomb G E, 2018. Oxisolic processes and geochemical constraints on duration of weathering for Neoproterozoic Baltic paleosol. Precambrian Research 310, 165–178.

Dronov A, Holmer L, 1999. Depositional sequences in the Ordovician of Baltoscandia. Acta-Universitatis Carolinae Geologica**,** 133–136.

Dunne J, Elmore D, Muzikar P, 1999. Scaling factors for the rates of production of cosmogenic nuclides for geometric shielding and attenuation at depth on sloped surfaces. Geomorphology 27, 3–11.

Duszyński F, Migoń P, Strzelecki M C, 2019. Escarpment retreat in sedimentary tablelands and cuesta landscapes–Landforms, mechanisms and patterns. Earth-Science Reviews 196. doi:10.1016/j.earscirev.2019.102890

Ebert K, 2009. Terminology of long-term geomorphology: a Scandinavian perspective. Progress in Physical Geography 33, 163–182.

Ebert K, 2015. GIS analyses of ice-sheet erosional impacts on the exposed shield of Baffin Island, eastern Canadian Arctic. Canadian Journal of Earth Sciences 52, 966–979.

Ebert K, Hättestrand C, 2010. The impact of Quaternary glaciation on inselbergs in northern Sweden. Geomorphology 115, 56–66.

Ebert K, Hättestrand C, Hall A M, Alm G, 2011. DEM identification of macro-scale stepped relief in arctic northern Sweden. Geomorphology 132, 339–350.

Ebert K, Hall A M, Kleman J, Andersson J, 2015. Unequal ice sheet erosional impacts across low-relief shield terrain in northern Fennoscandia. Geomorphology 233, 64–74.

Egholm D L, Jansen J D, Brædstrup C F, Pedersen V K, Andersen J L, Ugelvig S V, Larsen N K, Knudsen M F, 2017. Formation of plateau landscapes on glaciated continental margins. Nature Geoscience 10, 592–597.

Ehlers J, 1981. Some aspects of glacial erosion and deposition in north Germany. Annals of Glaciology 2, 143–146.

Ehlers J, Gibbard P, Hughes P, 2018. Quaternary glaciations and chronology. In Menzies J, van der Meer J J M (eds). Past glacial environments. 2nd ed. Amsterdam: Elsevier, 77–101.

Ehlers J, Grube A, Stephan H-J, Wansa S, 2011. Pleistocene glaciations of North Germany – New results. In Ehlers J, Gibbard P L, Hughes P D (eds). Quaternary glaciations: extent and chronology: a closer look. Amsterdam: Elsevier, 149–162. (Developments in Quaternary Sciences 15)

Eklund O, Soesoo A, Linna A, 2007. The Precambrian rocks of Southern Finland and Estonia. Tallinn: GEOGuide Baltoscandia.

Eliasson T, Tullborg E, Landström O, 1990. Fracture filling mineralogy and geochemistry at the Swedish HDR research site. Proceedings of Hot Dry Rock: Proceedings Camborne School of Mines International Hot Dry Rock Conference, 1990. Robertson Scientific Publications.

Elvhage C, Lidmar-Bergström K, 1987. Some working hypotheses on the geomorphology of Sweden in the light of a new relief map. Geografiska Annaler Series A, Physical Geography 69, 343–358.

Erlandsson V B, 2017. Mechanism(s) of extreme heavy mineral enrichment in the siltstones of the Cambrian Norretorp member, Southern Sweden. Degree thesis. University of Gothenburg.

Erlström M, Sopher D, 2019. Geophysical well log-motifs, lithology, stratigraphical aspects and correlation of the Ordovician succession in the Swedish part of the Baltic Basin. International Journal of Earth Sciences 108, 1387–1407.

Evans D J, Dinnage M, Roberts D H, 2018. Glacial geomorphology of Teesdale, northern Pennines, England: Implications for upland styles of ice stream operation and deglaciation in the British-Irish Ice Sheet. Proceedings of the Geologists' Association 129, 697–735.

Fabel D, Stroeven A P, Harbor J, Kleman J, Elmore D, Fink D, 2002. Landscape preservation under Fennoscandian ice sheets determined from in situ produced ^{10}Be and ^{26}Al. Earth and Planetary Science Letters 201, 397–406.

Fairbridge R W, Finkl C W, 1980. Cratonic erosional unconformities and peneplains. Journal of Geology 88, 69–86.

Falcini F A M, Rippin D M, Krabbendam M, Selby K A, 2018. Quantifying bed roughness beneath contemporary and palaeo-ice streams. Journal of Glaciology 247, 822–834.

Flesche Kleiven H, Jansen E, Fronval T, Smith T, 2002. Intensification of Northern Hemisphere glaciations in the circum Atlantic region (3.5–2.4 Ma) – ice-rafted detritus evidence. Palaeogeography, Palaeoclimatology, Palaeoecology 184, 213–223.

Flodén T, 1977. Tectonic lineaments in the Baltic from Gävle to Simrishamn. KBS TR 59, Kärnbränslesäkerhet.

Flodén T, 1980. Seismic stratigraphy and bedrock geology of the central Baltic. PhD thesis. Stockholm University. (Stockholm contributions in geology 35)

Flodén T, Bjerkéus M, Sturkell E, Gelumbauskaitė Ž, Grigelis A, Endler R, Lemke W, Flodén T, Bjerkéus M, Sturkell E, 1997. Distribution and seismic stratigraphy of glacially incised valleys in the southern part of the Baltic. Uppsala: Sveriges geologiska undersökning. (Ser. Ca 86)

Forsstrom P-L, Sallasmaa O, Greve R, Zwinger T, 2003. Simulation of fast-flow features of the Fennoscandian ice sheet during the Last Glacial Maximum. Annals of Glaciology 37, 383–389.

Fredén C, 1982. Jordartskartan 8B Vänersborg SO. Uppsala: Sveriges geologiska undersökning. (Ser. Ae 48) (In Swedish.)

Fredén C (ed), 1994. National atlas of Sweden. Geology. Stockholm: SNA Publishing.

Fredin O, Viola G, Zwingmann H, Sørlie R, Brönner M, Lie J-E, Grandal E M, Müller A, Margreth A, Vogt C, 2017. The inheritance of a Mesozoic landscape in western Scandinavia. Nature Communications 8, 14879. doi:10.1038/ncomms14879

Friese N, Vollbrecht A, Leiss B, Jacke O, 2011. Cambrian sedimentary dykes in the Proterozoic basement of the Västervik area (southeast Sweden): episodic formation inferred from macro-and microfabrics. International Journal of Earth Sciences 100, 741–752.

Fu P, Stroeven A P, Harbor J M, Heyman J, Hättestrand C, Caffee M W, 2019. Ice cap erosion patterns from bedrock ^{10}Be and ^{26}Al, southeastern Tibetan Plateau. Earth Surface Processes and Landforms 44, 918–932.

Gabrielsen R H, Nystuen J P, Jarsve E M, Lundmark A M, 2015. The Sub-Cambrian Peneplain in southern Norway: its geological significance and its implications for post-Caledonian faulting, uplift and denudation. Journal of the Geological Society 172, 777–791.

Gavelin A, 1909. Om underkambriska sandstensgångar vid vstra stranden af Vänern. Stockholm: Sveriges geologiska undersökning. (Ser. C 217) (In Swedish.)

Geyer G, Popp A, Weidner T, Förster L, 2004. New Lower Cambrian trilobites from Pleistocene erratic boulders of northern Germany and Denmark and their bearing on the intercontinental correlation. Paläontologische Zeitschrift 78, 127. doi:10.1007/BF03009134

Gibbard P, Lewin J, 2016. Filling the North Sea Basin: Cenozoic sediment sources and river styles. Geologica Belgica 19, 201–217.

Gillberg G, 1955. Den glaciala utvecklingen inom Sydsvenska höglandets västra randzon: I: Glacialerosion och moränackumulation. Geologiska Föreningen i Stockholm Förhandlingar 77, 481–524. (In Swedish.)

Gillberg G, 1965. Till distribution and ice movements on the northern slopes of the South Swedish highlands. Geologiska Föreningen i Stockholm Förhandlingar 86, 433–484.

Gillberg G, 1970. Glacial geology of Kinnekulle, W Sweden. Geologiska Föreningen i Stockholm Förhandlingar 92, 347–381.

Glasser N F, Bennett M R, 2004. Glacial Erosional Landforms: Origins and Significance for Palaeoglaciology. Progress in Physical Geography 28, 43–75.

Godard A, 1961. L'efficacité de l'erosion glaciare en Écosse du Nord. Revue de Géomorphologie Dynamique 12, 32–42. (In French.)

Goehring B M, Vacco D A, Alley R B, Schaefer J M, 2012. Holocene dynamics of the Rhone Glacier, Switzerland, deduced from ice flow models and cosmogenic nuclides. Earth and Planetary Science Letters 351, 27–35.

Goodfellow B, Stroeven A, Fabel D, Fredin O, Derron M, Bintanja R, Caffee M, 2014. Arctic-alpine blockfields in northern Sweden: Quaternary not Neogene. Earth Surface Dynamics Discussions 2, 47–93.

Goodfellow B W, Stroeven A P, Martel S J, Heyman J, Rossi M, Caffee M W, 2019. Exploring alternative models for the formation of conspicuously flat basement surfaces in southern Sweden. SKB TR-19-22, Svensk Kärnbränslehantering AB.

Gorlach A, Kalm V, Hang T, 2015. Thickness distribution of Quaternary deposits in the formerly glaciated part of the East European plain. Journal of Maps 11, 625–635.

Goulty N, 2005. Emplacement mechanism of the Great Whin and Midland Valley dolerite sills. Journal of the Geological Society 162, 1047–1056.

Green P F, Lidmar-Bergström K, Japsen P, Bonow J, Chalmers J A, 2013. Stratigraphic landscape analysis, thermochronology and the episodic development of elevated, passive continental margins. Geological Survey of Denmark and Greenland Bulletin 30, 1–150.

Greiling R O, Samuelsson L, Weinert H, 1988. Sedimentary dykes of Cambrian age in the Baltic Shield of SW Sweden (Lake Vänern to Gullmarn) and their tectonic implications. In Binzer K, Marcussen I, Konradi P (eds). Proceedings of 18th Nordiske Geologiske Vintermøde, København, 1988. Dansk Geologiske Undersøgelse.

Grigull S, Peterson G, Nyberg J, Öhrling C, 2019. Phanerozoic faulting of Precambrian basement in Uppland. SKB R-19-22, Svensk Kärnbränslehantering AB.

Guenthner W R, Reiners P W, Drake H, Tillberg M, 2017. Zircon, titanite, and apatite (U-Th)/He ages and age–eU correlations from the Fennoscandian Shield, southern Sweden. Tectonics 36, 1254–1274.

Gyldenholm K G, Lykke-Andersen H, Lind G, 1993. Seismic stratigraphy of the Quaternary and its substratum in southeastern Kattegat, Scandinavia. Boreas 22, 319–327.

Hadding A R, 1929. The pre-Quaternary sedimentary rocks of Sweden. 3,. The Paleozoic and Mesozoic sandstones of Sweden. Lund: Gleerup.

Hagström J, 1987. Acritarch-based biostratigraphy of the Lower Cambrian deposits in Västergötland, Sweden. Degree thesis. University of Stockholm.

Hall A M, 1986. Deep weathering patterns in north-east Scotland and their geomorphological significance. Zeitschrift für Geomorphologie NF 30, 407–422.

Hall A M, 2011. Storm wave currents, boulder movement and shore platform development: a case study from East Lothian, Scotland. Marine Geology 283, 98–105.

Hall A M, Migoń P, 2010. The first stages of landscape modification by ice sheets: evidence from central Europe. Geomorphology 123, 349–363.

Hall A M, Phillips W M, 2006. Glacial modification of granite tors in the Cairngorms, Scotland. Journal of Quaternary Science 21, 811–830.

Hall A M, Sugden D E, 1987. Limited modification of mid-latitude landscapes by ice sheets: the case of north-east Scotland. Earth Surface Processes and Landforms 12, 531–542.

Hall A M, Ebert K, Hättestrand C, 2013. Pre-glacial landform inheritance in a glaciated shield landscape. Geografiska Annaler Series A, Physical Geography 95, 33–49.

Hall A M, Sarala P, Ebert K, 2015. Late Cenozoic deep weathering patterns on the Fennoscandian shield in northern Finland: a window on ice sheet bed conditions at the onset of Northern Hemisphere glaciation. Geomorphology 246, 472–488.

Hall A M, Merritt J W, Connell E R, Hubbard A, 2018. Early and Middle Pleistocene environments, landforms and sediments in Scotland. Earth and Environmental Science Transactions of the Royal Society of Edinburgh 110, 5–37.

Hall A M, Ebert K, Goodfellow B W, Hättestrand C, Heyman J, Krabbendam M, Moon S, Stroeven A P, 2019. Past and future impact of glacial erosion in Forsmark and Uppland. SKB TR-19-07, Svensk Kärnbränslehantering AB.

Hamberg L, 1991. Tidal and seasonal cycles in a Lower Cambrian shallow marine sandstone (Hardeberga Fm.), Scania, Southern Sweden. In Smith D G, Reinson G E, Zaitlin B A, Rahmani R A (eds). Clastic tidal sedimentology. Canadian Society of Petroleum Geologists, 255–273.

Haq B U, Schutter S R, 2008. A chronology of Paleozoic sea-level changes. Science 322, 64–68.

Harbor J, Stroeven A P, Fabel D, Clarhall A, Kleman J, Li Y, Elmore D, Fink D, 2006. Cosmogenic nuclide evidence for minimal erosion across two subglacial sliding boundaries of the late glacial Fennoscandian ice sheet. Geomorphology 75, 90–99.

Harper D A, Longstaffe F J, Wadleigh M A, McNutt R H, 1995. Secondary K-feldspar at the Precambrian–Paleozoic unconformity, southwestern Ontario. Canadian Journal of Earth Sciences 32, 1432–1450.

Hegardt E A, Cornell D H, Hellström F A, Lundqvist I, 2007. Emplacement ages of the mid-Proterozoic Kungsbacka Bimodal Suite, SW Sweden. GFF 129, 227–234.

Hendriks B, Redfield T, 2005. Apatite fission track and (U-Th)/He data from Fennoscandia: An example of underestimation of fission track annealing in apatite. Earth and Planetary Science Letters 236, 443–458.

Hendriks B, Redfield T, 2006. Reply to: Comment on "Apatite Fission Track and (U–Th)/He data from Fennoscandia: An example of underestimation of fission track annealing in apatite" by BWH Hendriks and TF Redfield. Earth and Planetary Science Letters 248, 569–577.

Heyman J, 2014. Paleoglaciation of the Tibetan Plateau and surrounding mountains based on exposure ages and ELA depression estimates. Quaternary Science Reviews 91, 30–41.

Hillefors Å, 1979. Deglaciation models from the Swedish west coast. Boreas 8, 153–169.

Hjelstuen B O, Nygård A, Sejrup H P, Haflidason H, 2012. Quaternary denudation of southern Fennoscandia–evidence from the marine realm. Boreas 41, 379–390.

Holm G, 1901. Kinnekulles berggrund. Uppsala: Sveriges geologiska undersökning. (Ser. C 172) (In Swedish.)

Houmark-Nielsen M, 2004. The Pleistocene of Denmark: a review of stratigraphy and glaciation history. In Ehlers J, Gibbard P L (eds). Quaternary glaciations: extent and chronology. Amsterdam: Elsevier. (Developments in Quaternary Sciences 2), 35–46.

Houmark-Nielsen M, Kjær K H, 2003. Southwest Scandinavia, 40–15 kyr BP: palaeogeography and environmental change. Journal of Quaternary Science 18, 769–786.

Huang X, Tang G, Zhu T, Ding H, Na J, 2019. Space-for-time substitution in geomorphology. Journal of Geographical Sciences 29, 1670–1680.

Hubbard B, Siegert M J, McCarroll D, 2000. Spectral roughness of glaciated bedrock geomorphic surfaces: implications for glacier sliding. Journal of Geophysical Research: Solid Earth 105, 21295–21303.

Högbom A G, 1910. Precambrian geology of Sweden. Bulletin of the Geological Institutions of Upsala 10.

Högbom A G, Ahlström N G, 1924. Über die subkambrische Landflache am Fusse vom Kinnekulle. Bulletin of the Geological Institution of Uppsala 19, 55–88. (In German.)

Jahns R H, 1943. Sheet structure in granites: its origin and use as a measure of glacial erosion in New England. Journal of Geology 51, 71–98.

Jakobsen P R, 1996. Distribution and intensity of glaciotectonic deformation in Denmark. Bulletin of the Geological Society of Denmark 42, 175–185.

Jansen J D, Knudsen M F, Andersen J L, Heyman J, Egholm D L, 2019. Erosion rates in Fennoscandia during the past million years. Quaternary Science Reviews 207, 37–48.

Japsen P, Green P F, Bonow J M, Erlström M, 2016. Episodic burial and exhumation of the southern Baltic Shield: Epeirogenic uplifts during and after break-up of Pangaea. Gondwana Research 35, 357–377.

Jarsve E M, Krøgli S O, Etzelmüller B, Gabrielsen R H, 2014. Automatic identification of topographic surfaces related to the sub-Cambrian peneplain (SCP) in southern Norway – Surface generation algorithms and implications. Geomorphology 211, 89–99.

Jenness J S, 2004. Calculating landscape surface area from digital elevation models. Wildlife Society Bulletin 32, 829–839.

Jensen S, 1997. Trace fossils from the Lower Cambrian Mickwitzia sandstone, south-central Sweden. Fossils and Strata 42. Oslo, Scandinavian University Press.

Jensen S, Högström A E, Høyberget M, Meinhold G, McIlroy D, Ebbestad J O R, Taylor W L, Agić H, Palacios T, 2018. New occurrences of *Palaeopascichnus* from the Stáhpogieddi Formation, Arctic Norway, and their bearing on the age of the Varanger Ice Age. Canadian Journal of Earth Sciences 55, 1253–1261.

Johansson M, 1999. Analysis of digital elevation data for palaeosurfaces in south-western Sweden. Geomorphology 26, 279–295.

Johansson M, Olvmo M, Söderström M, 1999. Application of digital elevation and geological data in studies of morphotectonics and relief–a case study of the sub-Cambrian peneplain in southwestern Sweden. Zeitschrift für Geomorphologie 43, 505–520.

Johansson M, Migon P, Olvmo M, 2001a. Development of joint-controlled rock basins in Bohus granite, SW Sweden. Geomorphology 40, 145–161.

Johansson M, Olvmo M, Lidmar-Bergström K, 2001b. Inherited landforms and glacial impact of different palaeosurfaces in southwest Sweden. Geografiska Annaler, Series A 83**,** 67–89.

Johansson Å, Meier M, Oberli F, Wikman H, 1993. The early evolution of the Southwest Swedish Gneiss Province: geochronological and isotopic evidence from southernmost Sweden. Precambrian Research 64, 361–388.

Johnson M E, Jia-Yu R, 1989. Middle to Late Ordovician rocky bottoms and rocky shores from the Manitoulin Island area, Ontario. Canadian Journal of Earth Sciences 26, 642–653.

Juhlin C, Sturkell E, Ebbestad J O R, Lehnert O, Högström A E, Meinhold G, 2012. A new interpretation of the sedimentary cover in the western Siljan Ring area, central Sweden, based on seismic data. Tectonophysics 580, 88–99.

Kalm V, Gorlach A, 2014. Impact of bedrock surface topography on spatial distribution of Quaternary sediments and on the flow pattern of late Weichselian glaciers on the East European Craton (Russian Plain). Geomorphology 207, 1–9.

Karis L, Strömberg A G B, 1998. Beskrivning till berggrundskartan över Jämtlands län. Del 2: Fjälldelen. Uppsala: Sveriges geologiska undersökning. (Ser. Ca 53:2) (In Swedish.)

Kearsey T I, Lee J R, Finlayson A, Garcia-Bajo M, Irving A A, 2019. Examining the geometry, age and genesis of buried Quaternary valley systems in the Midland Valley of Scotland, UK. Boreas 48, 658–677.

Keilhau B M, 1838. Gæa Norwegica. Christiania: Johann Dahl.

Keller C B, Husson J M, Mitchell R N, Bottke W F, Gernon T M, Boehnke P, Bell E A, Swanson-Hysell N L, Peters S E, 2019. Neoproterozoic glacial origin of the Great Unconformity. Proceedings of the National Academy of Sciences of the United States of America 116, 1136–1145.

Kirsimae K, Jørgensen P, Kalm V, 1999. Low-temperature diagenetic illite-smectite in Lower Cambrian clays in North Estonia. Clay Minerals 34, 151–163.

Kleman J, 1994. Preservation of landforms under ice sheets and ice caps. Geomorphology 9, 19–32.

Kleman J, Applegate P J, 2014. Durations and propagation patterns of ice sheet instability events. Quaternary Science Reviews 92, 32–39.

Kleman J, Glasser N F, 2007. The subglacial thermal organisation (STO) of ice sheets. Quaternary Science Reviews 26, 585–597.

Kleman J, Borgström I, Robertsson A-M, Lillieskold M, 1992. Morphology and stratigraphy from several deglaciations in the Transtrand Mountains, western Sweden. Journal of Quaternary Science 7, 1–17.

Kleman J, Hättestrand C, Borgström I, Stroeven A, 1997. Fennoscandian palaeoglaciology reconstructed using a glacial geological inversion model. Journal of Glaciology 43, 283–299.

Kleman J, Stroeven A P, Lundqvist J, 2008. Patterns of Quaternary ice sheet erosion and deposition in Fennoscandia and a theoretical framework for explanation. Geomorphology 97, 73–90.

Kohl C, Nishiizumi K, 1992. Chemical isolation of quartz for measurement of in-situ-produced cosmogenic nuclides. Geochimica et Cosmochimica Acta 56, 3583–3587.

Konsa M, Puura V, 1999. Provenance of zircon of the lowermost sedimentary cover, Estonia, East-European Craton. Bulletin-Geological Society of Finland 71, 253–273.

Kor P, Shaw J, Sharpe D, 1991. Erosion of bedrock by subglacial meltwater, Georgian Bay, Ontario: a regional view. Canadian Journal of Earth Sciences 28, 623–642.

Korschinek G, Bergmaier A, Faestermann T, Gerstmann U, Knie K, Rugel G, Wallner A, Dillmann I, Dollinger G, Von Gostomski C L, 2010. A new value for the half-life of ^{10}Be by heavy-ion elastic recoil detection and liquid scintillation counting. Nuclear Instruments and Methods in Physics Research Section B: Beam Interactions with Materials and Atoms 268, 187–191.

Krabbendam M, Bradwell T, 2013. Glacial erosion of gneiss terrains: a re-assessment of the 'landscape of areal scouring' and implications for bed roughness below ice sheets. EGU General Assembly Conference Abstracts, 2013.

Krabbendam M, Bradwell T, 2014. Quaternary evolution of glaciated gneiss terrains: pre-glacial weathering vs. glacial erosion. Quaternary Science Reviews 95, 20–42.

Krabbendam M, Glasser N F, 2011. Glacial erosion and bedrock properties in NW Scotland: abrasion and plucking, hardness and joint spacing. Geomorphology 130, 374–383.

Krabbendam M, Hall A M, 2019. Subglacial block removal – a preliminary analysis of driving and resisting forces under different glaciological scenarios. SKB TR-19-18, Svensk Kärnbränslehantering AB.

Krabbendam M, Eyles N, Putkinen N, Bradwell T, Arbelaez-Moreno L, 2016. Streamlined hard beds formed by palaeo-ice streams: A review. Sedimentary Geology 338, 24–50.

Kresten P, Chyssler J, 1976. The Götemar massif in south-eastern Sweden: a reconnaissance survey. Geologiska Föreningen i Stockholm Förhandlingar 98, 155–161.

Kuhlmann G, de Boer P L, Pedersen R B, Wong T E, 2004. Provenance of Pliocene sediments and paleoenvironmental changes in the southern North Sea region using Samarium–Neodymium (Sm/Nd) provenance ages and clay mineralogy. Sedimentary Geology 171, 205–226.

Kvarnäs H, 2001. Morphometry and hydrology of the four large lakes of Sweden. AMBIO: A Journal of the Human Environment 30, 467–474.

Laajoki K, 2003. The Larajæg'gi outcrop – a large combined Neoproterozoic/Pleistocene roche moutonnée at Karlebotn, Finnmark, North Norway. Norwegian Journal of Geology 84, 107–115.

Lal D, 1991. Cosmic ray labeling of erosion surfaces: in situ nuclide production rates and erosion models. Earth and Planetary Science Letters 104, 424-439.

Lalomov A, Platonov M, Tugarova M, Bochneva A, Chefranova A, 2015. Rare metal–titanium placer metal potential of Cambrian–Ordovician sandstones in the northwestern Russian Plate. Lithology and Mineral Resources 50, 501–511.

Lambeck K, Purcell A, Funder S, Kjær K H, Larsen E, Moller P, 2006. Constraints on the Late Saalian to early Middle Weichselian ice sheet of Eurasia from field data and rebound modelling. Boreas 35, 539–575.

Larson S A, Tullborg E-L, Cederbom C, Stiberg J-P, 1999. Sveconorwegian and Caledonian foreland basins in the Baltic Shield revealed by fission-track thermochronology. Terra Nova 11, 210–215.

Larson S Å, Cederbom C E, Tullborg E-L, Stiberg J-P, 2006. Comment on "Apatite fission track and (U–Th)/He data from Fennoscandia: An example of underestimation of fission track annealing in apatite" by Hendriks and Redfield [Earth Planet. Sci. Lett. 236 (443–458)]. Earth and Planetary Science Letters 248, 561–568.

Larsson I, 1963. Tectonic and morphologic studies in Precambrian rocks at ground water prospecting in south Sweden. Geologiska Föreningen i Stockholm Förhandlingar 85, 320–340.

Lecomte A, Cathelineau M, Michels R, Peiffert C, Brouand M, 2017. Uranium mineralization in the Alum Shale Formation (Sweden): Evolution of a U-rich marine black shale from sedimentation to metamorphism. Ore Geology Reviews 88, 71–98.

Lee J R, Busschers F S, Sejrup H P, 2012. Pre-Weichselian Quaternary glaciations of the British Isles, The Netherlands, Norway and adjacent marine areas south of 68°N: implications for long-term ice sheet development in northern Europe. Quaternary Science Reviews 44, 213–228.

Lehnert O, Meinhold G, Arslan A, Berner U, Calner M, Huff W, Ebbestad J O R, Joachimski M, Juhlin C, Maletz J, 2013. The Siljan impact structure of south-central Sweden: an unique window into the geologic history of western Baltoscandia. Proceedings of Joint IODP/ICDP Colloquium 2013, Freiberg, Germany, 25–27 March 2013.

Li Y, Fabel D, Stroeven A P, Harbor J, 2008. Unraveling complex exposure-burial histories of bedrock surfaces under ice sheets by integrating cosmogenic nuclide concentrations with climate proxy records. Geomorphology 90, 139–149.

Lidmar-Bergström K, 1982. Pre-Quaternary geomorphological evolution in southern Fennoscandia. Stockholm: LiberKartor. (Sveriges geologiska undersökning Ser. C 785)

Lidmar-Bergström K, 1988. Denudation surfaces of a shield area in south Sweden. Geografiska Annaler, Series A. Physical Geography**,** 337–350.

Lidmar-Bergström K, 1991. Phanerozoic tectonics in southern Sweden. Zeitschrift für Geomorphologie, Supplementband 82, 1–16.

Lidmar-Bergström K, 1993. Denudation surfaces and tectonics in the southernmost part of the Baltic Shield. Precambrian Research 64, 337–345.

Lidmar-Bergström K, 1995. Relief and saprolites through time on the Baltic Shield. Geomorphology 12, 45–61.

Lidmar-Bergström K, 1997. A long-term perspective on glacial erosion. Earth Surface Processes and Landforms 22, 297–306.

Lidmar-Bergström K, 1999. Uplift histories revealed by landforms of the Scandinavian domes. In Smith B J, Whalley W B, Warke P A (eds.). Uplift, erosion and stability: perspectives on long-term landscape development. London: Geological Society. (Special publication 162), 85–91.

Lidmar-Bergström K, Olvmo M, 2015. Plains, steps, hilly relief and valleys in northern Sweden – review, interpretations and implications for conclusions on Phanerozoic tectonics. Uppsala: Geological Survey of Sweden. (SGU Research Paper C838)

Lidmar-Bergström K, Olsson S, Olvmo M, 1997. Palaeosurfaces and associated saprolites in southern Sweden. In Widdowson M (ed). Palaeosurfaces: recognition, reconstruction and palaeo-environmental interpretation. London: The Geological Society. (Special publication 120), 95–124.

Lidmar-Bergström K, Näslund J-O, Ebert K, Neubeck T, Bonow J, 2007. Cenozoic landscape development on the passive margin of northern Scandinavia. Norwegian Journal of Geology 87, 181–196.

Lidmar-Bergström K, Bonow J M, Japsen P, 2012. Stratigraphic Landscape Analysis and geo-morphological paradigms: Scandinavia as an example of Phanerozoic uplift and subsidence. Global and Planetary Change 100, 153–171.

Lidmar-Bergström K, Olvmo M, Bonow J M, 2017. The South Swedish Dome: a key structure for identification of peneplains and conclusions on Phanerozoic tectonics of an ancient shield. GFF 139, 244–259.

Lifton N, Sato T, Dunai T J, 2014. Scaling *in situ* cosmogenic nuclide production rates using analytical approximations to atmospheric cosmic-ray fluxes. Earth and Planetary Science Letters 386, 149–160.

Liivamägi S, 2015. Neoproterozoic Baltic paleosol: geology and paleoenvironmental interpretation. PhD thesis. Tartu University, Estonia.

Liivamägi S, Somelar P, Mahaney W C, Kirs J, Vircava I, Kirsimäe K, 2014. Late Neoproterozoic Baltic paleosol: Intense weathering at high latitude? Geology 42, 323–326.

Liivamägi S, Somelar P, Vircava I, Mahaney W C, Kirs J, Kirsimäe K, 2015. Petrology, mineralogy and geochemical climofunctions of the Neoproterozoic Baltic paleosol. Precambrian Research 256, 170–188.

Lindskoga A, Lindskogb A M, Johanssonc J V, Ahlberga P, Erikssona M E, 2018. The Cambrian-Ordovician succession at Lanna, Sweden: stratigraphy and depositional environments. Estonian Journal of Earth Sciences 67, 133–148.

Lindström A F, 1887. Beskrifning till kartbladet Venersborg. Kongl. boktryckeriet, PA Norstedt & söner.

Lindström E, 1988. Are roches moutonnées mainly preglacial forms? Geografiska Annaler, Series A 70, 323–332.

Lindstrom M, Vortisch W, 1978. Sphalerite from transgressive and regressive sediments of the Cambro-Silurian supercycle, Baltic Shield. Bulletin of the Geological Society of Denmark 27, 47–53.

Lindström M, Flodén T, Grahn Y, Kathol B, 1994. Post-impact deposits in Tvären, a marine Middle Ordovician crater south of Stockholm, Sweden. Geological Magazine 131, 91–103.

Lisiecki L E, Raymo M E, 2005. A Pliocene-Pleistocene stack of 57 globally distributed benthic $\delta^{18}O$ records. Paleoceanography 20, PA1003. doi:10.1029/2004PA001071.

Lorentzen S, Augustsson C, Nystuen J P, Berndt J, Jahren J, Schovsbo N H, 2018. Provenance and sedimentary processes controlling the formation of lower Cambrian quartz arenite along the southwestern margin of Baltica. Sedimentary Geology 375, 203–217.

Lorentzen S, Augustsson C, Jahren J, Nystuen J P, Schovsbo N H, 2019. Tectonic, sedimentary and diagenetic controls on sediment maturity of lower Cambrian quartz arenite from southwestern Baltica. Basin Research 31, 1098–1120.

Lundegårdh P, Karis L, Magnusson E, 1973. Beskrivning til berggrundskartan Örebro SO. Uppsala: Sveriges geologiska undersökning. (Ser. Af 104) (In Swedish.)

Lundqvist J, 1987. Glaciodynamics of the Younger Dryas Marginal zone in Scandinavia: implications of a revised glaciation model. Geografiska Annaler, Series A, 69, 305–319.

Lykke-Andersen H, 1987. Thickness of Quaternary deposits and their relation to the pre-Quaternary in the Fennoscandian border zone in Kattegat and Vendsyssel. Boreas 16, 369–371.

Mabbutt J, 1961. A stripped land surface in Western Australia. Transactions and Papers (Institute of British Geographers) 29, 101–114.

MacLean B, Jansa L, Falconer R, Srivastava S, 1977. Ordovician strata on the southeastern Baffin Island shelf revealed by shallow drilling. Canadian Journal of Earth Sciences 14, 1925–1939.

Maletz J, Löfgren A, Bergström S M, 1996. The base of the *Tetragraptus approximatus* Zone at Mt. Hunneberg, SW Sweden: a proposed global stratotype for the base of the second series of the Ordovician System. Newsletters on Stratigraphy 34, 129–160.

Mangerud J, Jansen E, Landvik J Y, 1996. Late Cenozoic history of the Scandinavian and Barents Sea ice sheets. Global and Planetary Change 12, 11–26.

Mangerud J, Gyllencreutz R, Lohne Ö, Svendsen J I, 2011. Glacial history of Norway. In Ehlers J, Gibbard P, Hughes P D (eds.). Quaternary glaciations: extent and chronology: a closer look. Amsterdam: Elsevier, 279–298.

Marrero S M, Phillips F M, Borchers B, Lifton N, Aumer R, Balco G, 2016. Cosmogenic nuclide systematics and the CRONUScalc program. Quaternary Geochronology 31, 160–187.

Martel S J, 2016. Effects of small-amplitude periodic topography on combined stresses due to gravity and tectonics. International Journal of Rock Mechanics and Mining Sciences 89, 1–13.

Martinsson A, 1968. Cambrian palaeontology of Fennoscandian basement fissures. Lethaia 1, 137–155.

Martinsson A, 1974. The Cambrian of Norden. In Holland C H (ed.). Lower Palaeozoic rocks of the world. Vol 2, Cambrian of the British Isles, Norden, and Spitsbergen. Wiley, 185–283.

Mattsson A, 1959. Sandstensgångarna i Västergotlands urberg. In Bergsten K E (ed). Svensk geografisk årsbok 35. Lund: Sydsvenska geografiska sällskapet, 87–101. (In Swedish.)

Mattsson Å, 1962. Morphologische Studien in Südschwedesn und auf Bornholm über die nicht glaciale Formenwelt der Felsenskulptur. Meddelanden Lunds Universitet. Geografiska Institiutionen Avhandlingar 39. (In German.)

McAdam A, Tulloch W, 1985. Geology of the Haddington District. London: Stationery Office Books. (Memoir of the British Geological Survey)

McKie T, 1993. Relative sea-level changes and the development of a Cambrian transgression. Geological Magazine 130, 245–256.

Meidla T, 2017. Ediacaran and Cambrian stratigraphy in Estonia: an updated review. Estonian Journal of Earth Sciences 66, 152–160.

Meyer K-D, 1991. Zur Entstehung der westlichen Ostsee. Geologisches Jahrbuch A 127, 429–446. (In German.)

Moczydłowska M, 2008. New records of late Ediacaran microbiota from Poland. Precambrian Research 167, 71–92.

Moczydłowska M, Pease V, Willman S, Wickström L, Agić H, 2018. A Tonian age for the Visingsö Group in Sweden constrained by detrital zircon dating and biochronology: Implications for evolutionary events. Geological Magazine 155, 1175–1189.

Mossmark F, Ericsson L O, Norin M, Dahlström L-O, 2015. Hydrochemical changes caused by underground constructions – A case study of the Kattleberg rail tunnel. Engineering Geology 191, 86–98.

Mukherji K K, Young G M, 1973. Diagenesis of the black river (middle Ordovician) limestones in Southern Ontario, Canada. Sedimentary Geology 9, 21–51.

Munier R, Talbot C, 1993. Segmentation, fragmentation and jostling of cratonic basement in and near Äspö, southeast Sweden. Tectonics 12, 713–727.

Munthe H, 1915. Nåtgra ord om den plana urbergsytan W om Halleberg i Västergötland. Geologiska Föreningen i Stockholm Förhandlingar 37, 623–625.

Månsson A G M, 1996. Brittle reactivation of ductile basement structures; a tectonic model for the lake Vättern basin, southern Sweden. GFF 118, 19–19.

Möller P, Dowling T P F, 2016. Streamlined subglacial bedforms on the Närke plain, south-central Sweden – Areal distribution, morphometrics, internal architecture and formation. Quaternary Science Reviews 146, 182–215.

Nielsen A T, Schovsbo N H, 2006. Cambrian to basal Ordovician lithostratigraphy in southern Scandinavia. Bulletin of the Geological Society of Denmark 53, 47–92.

Nielsen A T, Schovsbo N H, 2011. The Lower Cambrian of Scandinavia: Depositional environment, sequence stratigraphy and palaeogeography. Earth-Science Reviews 107, 207–310.

Nielsen A T, Schovsbo N H, 2015. The regressive Early-Mid Cambrian 'Hawke Bay Event'in Baltoscandia: epeirogenic uplift in concert with eustasy. Earth-Science Reviews 151, 288–350.

Nikishin A M, Ziegler P A, Stephenson R A, Cloetingh S A P L, Furne A V, Fokin P A, Ershov A V, Bolotov S N, Korotaev M V, Alekseev A S, Gorbachev V I, Shipilov E V, Lankreijer A, Bembinova E Y, Shalimov I V, 1996. Late Precambrian to Triassic history of the East European Craton: dynamics of sedimentary basin evolution. Tectonophysics 268, 23–63.

Nishiizumi K, 2004. Preparation of ^{26}Al AMS standards. Nuclear Instruments and Methods in Physics Research Section B: Beam Interactions with Materials and Atoms 223, 388–392.

Nishiizumi K, Winterer E L, Kohl C P, Klein J, Middleton R, Lal D, Arnold J R, 1989. Cosmic ray production rates of ^{10}Be and ^{26}Al in quartz from glacially polished rocks. Journal of Geophysical Research 94, 17907–17915.

Nishiizumi K, Imamura M, Caffee M W, Southon J R, Finkel R C, McAninch J, 2007. Absolute calibration of ^{10}Be AMS standards. Nuclear Instruments and Methods in Physics Research Section B: Beam Interactions with Materials and Atoms 258, 403–413.

Norling E, Bergström J, 1987. Mesozoic and Cenozoic tectonic evolution of Scania, southern Sweden. Tectonophysics 137, 7–19.

Nystuen J P, Andresen A, Kumpulainen R A, Siedlecka A, 2008. Neoproterozoic basin evolution in Fennoscandia, East Greenland and Svalbard. Episodes 31, 35–43.

Näslund J O, Rodhe L, Fastook J L, Holmlund P, 2003. New ways of studying ice sheet flow directions and glacial erosion by computer modelling--examples from Fennoscandia. Quaternary Science Reviews 22, 245–258.

Olivarius M, Rasmussen E S, Siersma V, Knudsen C, Kokfelt T F, Keulen N, 2014. Provenance signal variations caused by facies and tectonics: Zircon age and heavy mineral evidence from Miocene sand in the north-eastern North Sea Basin. Marine and Petroleum Geology 49, 1–14.

Ollier C, 1991. Ancient landforms. London: Belhaven Press.

Olsen L, 1998. Pleistocene paleosols in Norway: implications for past climate and glacial erosion. Catena 34, 75–103.

Olvmo M, Johansson M, 2002. The significance of rock structure, lithology and pre-glacial deep weathering for the shape of intermediate-scale glacial erosional landforms. Earth Surface Processes and Landforms 27, 251–268.

Olvmo M, Lidmar-Bergström K, Lindberg G, 1999. The glacial impact on an exhumed sub-Mesozoic etchsurface in south-western Sweden. Annals of Glaciology 28, 153–160.

Olvmo M, Lidmar-Bergstrom K, Ericson K, Bonow J M, 2005. Saprolite Remnants as Indicators of Pre-Glacial Landform Genesis in Southeast Sweden. Geografiska Annaler, Series A: Physical Geography 87, 447–460.

Ormö J, Sturkell E, Nõlvak J, Melero-Asensio I, Frisk Å, Wikström T, 2014. The geology of the Målingen structure: A probable doublet to the Lockne marine-target impact crater, central Sweden. Meteoritics & Planetary Science 49, 313–327.

Ormö J, Nielsen A T, Alwmark C, 2017. The Vakkejokk Breccia: An Early Cambrian proximal impact ejecta layer in the North-Swedish Caledonides. Meteoritics & Planetary Science 52, 623–645.

Overeem I, Weltje G, Bishop-Kay C, Kroonenberg S, 2001. The Late Cenozoic Eridanos delta system in the Southern North Sea Basin: a climate signal in sediment supply? Basin Research 13, 293–312.

Parnell J, Mark D F, Frei R, Fallick A E, Ellam R M, 2014. $^{40}Ar/^{39}Ar$ dating of exceptional concentration of metals by weathering of Precambrian rocks at the Precambrian–Cambrian boundary. Precambrian Research 246, 54–63.

Paszkowski M, Budzyń B, Mazur S, Sláma J, Shumlyanskyy L, Środoń J, Dhuime B, Kędzior A, Liivamägi S, Pisarzowska A, 2019. Detrital zircon U-Pb and Hf constraints on provenance and timing of deposition of the Mesoproterozoic to Cambrian sedimentary cover of the East European Craton, Belarus. Precambrian Research**,** 105352. doi:10.1016/j.precamres.2019.105352

Patton H, Hubbard A, Andreassen K, Winsborrow M, Stroeven A P, 2016. The build-up, configuration, and dynamical sensitivity of the Eurasian ice-sheet complex to Late Weichselian climatic and oceanic forcing. Quaternary Science Reviews 153, 97–121.

Pedoja K, Jara-Muñoz J, De Gelder G, Robertson J, Meschis M, Fernandez-Blanco D, Nexer M, Poprawski Y, Dugué O, Delcaillau B, Bessin P, Benabdelouahed M, Authemayou C, Husson L, Regard V, Menier D, Pinel B, 2018. Neogene-Quaternary slow coastal uplift of Western Europe through the perspective of sequences of strandlines from the Cotentin Peninsula (Normandy, France). Geomorphology 303, 338–356.

Peters S E, Gaines R R, 2012. Formation of the `Great Unconformity' as a trigger for the Cambrian explosion. Nature 484, 363–366.

Phillips F M, Argento D C, Balco G, Caffee M W, Clem J, Dunai T J, Finkel R, Goehring B, Gosse J C, Hudson A M, 2016. The CRONUS-Earth project: a synthesis. Quaternary Geochronology 31, 119–154.

Pipping F, Lehtinen M, 1992. Geology, stratigraphy and structure of the Lappajärvi meteorite crater, western Finland: preliminary results of deep drilling. Tectonophysics 216, 91–97.

Pokki J, Kohonen J, Rämö O T, Andersen T, 2013. The Suursaari conglomerate (SE Fennoscandian shield; Russia) – Indication of cratonic conditions and rapid reworking of quartz arenitic cover at the outset of the emplacement of the rapakivi granites at ca. 1.65 Ga. Precambrian Research 233, 132–143.

Porter S C, 1989. Some geological implications of average Quaternary conditions. Quaternary Research 32, 245–261.

Preeden U, Mertanen S, Elminen T, Plado J, 2009. Secondary magnetizations in shear and fault zones in southern Finland. Tectonophysics 479, 203–213.

Priem H, Mulder F, Boelrijk N, Hebeda E, Verschure R, Verdurmen E T, 1968. Geochronological and palaeomagnetic reconnaissance survey in parts of central and southern Sweden. Physics of the Earth and Planetary Interiors 1, 373–380.

Principato S M, Moyer A N, Hampsch A G, Ipsen H A, 2016. Using GIS and streamlined landforms to interpret palaeo-ice flow in northern Iceland. Boreas 45, 470–482.

Pulsipher M A, Dehler C M, 2019. U-Pb detrital zircon geochronology, petrography, and synthesis of the middle Neoproterozoic Visingsö Group, Southern Sweden. Precambrian Research 320, 323–333.

Punkari M, 1994. Function of the ice streams in the Scandinavian ice sheet: analyses of glacial geological data from southwestern Finland. Transactions of the Royal Society of Edinburgh: Earth Sciences 85, 283–302.

Puura V, Suuroja K, 1992. Ordovician impact crater at Kärdla, Hiiumaa Island, Estonia. Tectonophysics 216, 143–156.

Puura V, Amantov A, Tikhomirov S, Laitakari I, 1996. Latest events affecting the Precambrian basement, Gulf of Finland and surrounding areas. In Koistinen T (ed). Explanation to the map of Precambrian basement of the Gulf of Finland and surrounding areas. Espoo: Geological Survey of Finland. (Special paper 21), 115–125.

Påsse T, 2004. The amount of glacial erosion of the bedrock. SKB TR-04-25, Svensk Kärnbränslehantering AB.

Påsse T, Daniels J, 2015. Past shore-level and sea-level displacements. Uppsala: Sveriges geologiska undersökning. (Rapporter och meddelanden 137)

Raine R J, Smith M P, 2012. Sequence stratigraphy of the Scottish Laurentian margin and recognition of the Sauk Megasequence. In Derby J R, Fritz R D, Longacre S A, Morgan W A, Sternbach C A (eds). The great American carbonate bank: the geology and economic resources of the Cambrian–Ordovician Sauk megasequence of Laurentia: AAPG Memoir 98, 575–596,

Rasmussen E S, 2018. Discussion of "Eocene to mid-Pliocene landscape evolution in Scandinavia inferred from offshore sediment volumes and pre-glacial topography using inverse modelling" (Pedersen et al. 2018. Geomorphology, 303: 467–485). Geomorphology 328, 222–224.

Rasmussen E S, Dybkjær K, Piasecki S, 2010. Lithostratigraphy of the upper Oligocene–Miocene succession of Denmark. Geological Survey of Denmark and Greenland Bulletin 22, 1–92.

Reinardy B T I, Hjelstuen B O, Sejrup H P, Augedal H, Jørstad A, 2017. Late Pliocene-Pleistocene environments and glacial history of the northern North Sea. Quaternary Science Reviews 158, 107–126.

Rice A H N, Edwards M B, Hansen T A, Arnaud E, Halverson G P, 2011. Glaciogenic rocks of the Neoproterozoic Smalfjord and Mortensnes formations, Vestertana Group, E. Finnmark, Norway. In Arnaud E, Halverson G P, Shields-Zhou G (eds). The geological record of Neoproterozoic glaciations. London: The Geological Society. (Geological Society Memoir3 36), 593–602.

Roberts D H, Long A J, 2005. Streamlined bedrock terrain and fast ice flow, Jakobshavns Isbrae, West Greenland: implications for ice stream and ice sheet dynamics. Boreas 34, 25–42.

Rudberg S, 1954. Västerbottens berggrundsmorfologi: ett försök till rekonstruktion av preglaciala erosionsgenerationer i Sverige. Uppsala. (Geographica 25) (In Swedish.)

Rudberg S, 1970. The sub-Cambrian peneplain in Sweden and its slope gradient. Zeitschrift für Geomorphologie 9, 157–167.

Rudberg S, 1988. Gross morphology of Fennoscandia – six complementary ways of explanation. Geografiska Annaler, Series A 70**,** 135–167.

Rudberg S, 1992. Multiple glaciation in Scandinavia – Seen in gross geomorphology or not? Geografiska Annaler, Series A 74**,** 231–243.

Rudberg S, Eriksson H, Krathmann R, Sandqvist A, Wejeoal J, 1976. Halle- och Hunneberg; geoinventering med en geomorfologisk karta [Halle and Hunneberg; inventory of geo-objects with a geomorphological map]. University of Gothenburg: (GUNI rapport 9) (In Swedish.)

Röshoff K, 1988. Characterization of the morphology, basement rock and tectonics in Sweden. SKB TR 89-03, Svensk Kärnbränslehantering AB.

Samuelsson A L, 1967. Breccia av Paleozoiska Bergarter 1,5 km Väster om Bohus Fästning, Kungälv. Geologiska Föreningen i Stockholm Förhandlingar 89, 448–459.

Samuelsson J, Middleton M F, 1998. The Caledonian foreland basin in Scandinavia: constrained by the thermal maturation of the Alum Shale. GFF 120, 307–314.

Samuelsson L, Lundqvist I, 1988. Berggrundskartan 8B Vänersborg SO. Uppsala: Sveriges geologiska undersökning. (Ser. Af 160) (In Swedish.)

Sandiford M, 2007. The tilting continent: a new constraint on the dynamic topographic field from Australia. Earth and Planetary Science Letters 261, 152–163.

Sandström B, Tullborg E-L, 2009. Episodic fluid migration in the Fennoscandian Shield recorded by stable isotopes, rare earth elements and fluid inclusions in fracture minerals at Forsmark, Sweden. Chemical Geology 266, 126–142.

Sandström B, Tullborg E-L, Smellie J, MacKenzie A B, Suksi J, 2008. Fracture mineralogy of the Forsmark Site: SDM-Site Forsmark. SKB R-08-102, Svensk kärnbränslehantering AB.

Schmieder M, Jourdan F, 2013. The Lappajärvi impact structure (Finland): Age, duration of crater cooling, and implications for early life. Geochimica et Cosmochimica Acta 112, 321–339.

Scholz H, Frieling D, Obst K, 2009. Funnel structures and clastic dykes in Cambrian sandstones of southern Sweden–indications for tensional tectonics and seismic events in a shallow marine environment. Neues Jahrbuch für Geologie und Paläontologie-Abhandlungen 251, 355–380.

Schovsbo N H, 2002. Uranium enrichment shorewards in black shales: A case study from the Scandinavian Alum Shale. GFF 124, 107–115.

Sears J W, Price R A, 2003. Tightening the Siberian connection to western Laurentia. Geological Society of America Bulletin 115, 943–953.

Sejrup H P, Larsen E, Landvik J, King E L, Haflidason H, Nesje A, 2000. Quaternary glaciations in southern Fennoscandia: evidence from southwestern Norway and the northern North Sea region. Quaternary Science Reviews 19, 667–685.

Sejrup H-P, Larsen E, Haflidason H, Berstad I M, Hjelstuen B O, Jonsdottir H E, King E L, Landvik J, Longva O, Nygård A, Ottesen D, Raunholm S, Rise L, Stalsberg K, 2003. Configuration, history and impact of the Norwegian Channel Ice Stream. Boreas 32, 18–36.

Sejrup H P, Hjelstuen B O, Dahlgren K T, Haflidason H, Kuijpers A, Nygård A, Praeg D, Stoker M S, Vorren T O, 2005. Pleistocene glacial history of the NW European continental margin. Marine and Petroleum Geology 22, 1111–1129.

Sidenbladh E, 1870. Nagra ord till upplysning om bladet "Wenersborg". Uppsala: Sveriges geologiska undersokning. (Ser. Aa 40), 45–49 (In Swedish).

SKB, 2010. Climate and climate-related issues for the safety assessment SR-Site. SKB TR-10-49, Svensk Kärnbränslehantering AB.

Slater B J, Willman S, 2019. Early Cambrian small carbonaceous fossils (SCFs) from an impact crater in western Finland. Lethaia 52, 570–582.

Slater B J, Harvey T H, Butterfield N J, 2018. Small carbonaceous fossils (SCFs) from the Terreneuvian (lower Cambrian) of Baltica. Palaeontology 61, 417–439.

Šliaupa S, Hoth P, 2011. Geological evolution and resources of the Baltic Sea area from the Precambrian to the Quaternary. In Harff J, Björck S, Hoth P (eds). The Baltic Sea basin. Berlin: Springer, 13–51.

Smed P, 1993. Indicator studies: a critical review and a new data-presentation method. Bulletin of the Geological Society of Denmark 40, 332–344.

Smed P, 2016. Sten i det danske landskab. 4th ed. Højers Forlag. (In Danish.)

Smed P, Ehlers J, 2002. Steine aus dem Norden: geschiebe als zeugen der eiszeit in Norddeutschland. Berlin: Borntraeger. (In German.)

Smith D E, Barlow N, Bradley S, Firth C, Hall A M, Jordan J, Long D, 2019. Quaternary sea level change in Scotland. Earth and Environmental Science Transactions of the Royal Society of Edinburgh 110, 219–256.

Stephansson O, 1971. Gravity tectonics on Öland. Bulletin of the Geological Institute of the University of Uppsala NS3, 37–78.

Stephens M B, 2010. Forsmark site investigation. Bedrock geology – overview and excursion guide. SKB R-10-04, Svensk Kärnbränslehantering AB.

Straw A, 1968. Late Pleistocene glacial erosion along the Niagara escarpment of southern Ontario. Geological Society of America Bulletin 79, 889–910.

Stroeven A P, Fabel D, Harbor J, Hättestrand C, Kleman J, 2002a. Reconstructing the erosion history of glaciated passive margins: applications of *in situ* produced cosmogenic nuclide techniques. Geological Society, London, Special Publications 196, 153–168.

Stroeven A P, Fabel D, Hättestrand C, Harbor J, 2002b. A relict landscape in the centre of Fennoscandian glaciation: cosmogenic radionuclide evidence of tors preserved through multiple glacial cycles. Geomorphology 44, 145–154.

Stroeven A P, Harbor J, Fabel D, Kleman J, Hättestrand C, Elmore D, Fink D, Fredin O, 2006. Slow, patchy landscape evolution in northern Sweden despite repeated ice-sheet glaciation. Geological Society of America Special Papers 398, 387–396.

Stroeven A P, Harbor J, Heyman J, 2013. Erosional landscapes. In Shroder J, Giardino R, Harbor J (eds). Treatise on geomorphology. San Diego, CA: Academic Press, Vol 8, 100–112.

Stroeven A P, Heyman J, Fabel D, Björck S, Caffee M W, Fredin O, Harbor J M, 2015. A new Scandinavian reference ^{10}Be production rate. Quaternary Geochronology 29, 104–115.

Stroeven A P, Hättestrand C, Kleman J, Heyman J, Fabel D, Fredin O, Goodfellow B W, Harbor J M, Jansen J D, Olsen L, 2016. Deglaciation of Fennoscandia. Quaternary Science Reviews 147, 91–121.

Sturkell E, Lindström M, 2004. The target peneplain of the Lockne impact. Meteoritics & Planetary Science 39, 1721–1731.

Sugden D E, 1974. Landscapes of glacial erosion in Greenland and their relationship to ice, topographic and bedrock conditions. Institute of British Geographers Special Publication 7, 177–195.

Sugden D E, 1978. Glacial erosion by the Laurentide ice sheet. Journal of Glaciology 20, 367–391.

Sugden D E, Glasser N, Clapperton C M, 1992. Evolution of large roches moutonnées. Geografiska Annaler, Series A 74**,** 253–264.

Sugden D E, Hall A M, Phillips W M, Stewart M, 2019. Plucking enhanced beneath ice sheet margins: evidence from the Grampian Mountains, Scotland. Geografiska Annaler, Series A 101, 34–44.

Suuroja S, Suuroja K, 2006. Kärdla impact (Hiiumaa Island, Estonia) – Ejecta blanket and environmental disturbances. In Cockell C, Gilmour I, Koeberl C (eds). Biological processes associated with impact events. Berlin: Springer, 309–333.

Swett K, Klein G D, Smit D E, 1971. A Cambrian tidal sand body: the Eriboll Sandstone of Northwest Scotland: an ancient-recent analog. The Journal of Geology 79, 400–415.

Söderberg P, Hagenfeldt S E, 1995. Upper Proterozoic and Ordovician submarine outliers in the archipelago northeast of Stockholm, Sweden. GFF 117, 153–161.

Söderlund P, Juez-Larré J, Page L M, Dunai T J, 2005a. Extending the time range of apatite (U-Th)/He thermochronometry in slowly cooled terranes: Palaeozoic to Cenozoic exhumation history of southeast Sweden. Earth and Planetary Science Letters 239, 266–275.

Söderlund U, Isachsen C E, Bylund G, Heaman L M, Jonathan Patchett P, Vervoort J D, Andersson U B, 2005b. U–Pb baddeleyite ages and Hf, Nd isotope chemistry constraining repeated mafic magmatism in the Fennoscandian Shield from 1.6 to 0.9 Ga. Contributions to Mineralogy and Petrology 150, 174. doi:10.1007/s00410-005-0011-1.

Söderman G, 1985. Planation and weathering in eastern Fennoscandia. Fennia 163, 347–352.

Söderman G, Kejonen A, Kujansuu R, 1983. The riddle of the tors at Lauhavuori, western Finland. Fennia 161, 91–144.

Sømme T O, Skogseid J, Løseth H, Embry P, 2019. Manifestation of tectonic and climatic perturbations in deep-time stratigraphy–an example from the Paleocene succession offshore western Norway. Frontiers in Earth Science 7. doi:10.3389/feart.2019.00303

Tanner W F, 1967. Ripple mark indices and their uses. Sedimentology 9, 89–104.

Thom B G, Keene J B, Cowell P J, Daley M, 2010. East Australian marine abrasion surface. Geological Society, London, Special Publications 346, 57–69.

Thomas M F, 1989. The role of etch processes in landform development. II. Etching and the formation of relief. Zeitschrift für Geomorphologie 33, 257–274.

Thornes J B, Brunsden D, 1977. Geomorphology and time. London: Methuen.

Thornton L E, Stephenson W J, 2006. Rock strength: a control of shore platform elevation. Journal of Coastal Research 22, 224–231.

Thorslund P, Jaanusson V, 1960. The Cambrian, Ordovician, and Silurian in Västergötland, Närke, Dalarna, and Jämtland, central Sweden. Guide to excursions Nos A 23 and C 18. Stockholm: Geological Survey of Sweden.

Timmerman M J, Heeremans M, Kirstein L A, Larsen B T, Spencer-Dunworth E-A, Sundvoll B, 2009. Linking changes in tectonic style with magmatism in northern Europe during the late Carboniferous to latest Permian. Tectonophysics 473, 375–390.

Tirén S A, Beckholmen M, 1989. Block faulting in southeastern Sweden interpreted from digital terrain models. GFF 111, 171–179.

Tirén S A, Beckholmen M, 1992. Rock block map analysis of southern Sweden. Geologiska Föreningen i Stockholm Förhandlingar 114, 253–269.

Torsvik T H, Cocks L R M, 2013. New global palaeogeographical reconstructions for the Early Palaeozoic and their generation. Geological Society, London, Memoirs 38, 5–24.

Trenhaile A S, 1987. The geomorphology of rock coasts. Oxford: Oxford University Press.

Trenhaile A S, 2004. Modeling the accumulation and dynamics of beaches on shore platforms. Marine Geology 206, 55–72.

Tuke M, Dineley D, Rust B, 1966. The basal sedimentary rocks in Somerset Island, NWT. Canadian Journal of Earth Sciences 3, 697–711.

Tullborg E-L, Larson S A, Björklund L, Samuelsson L, Stigh J, 1995. Thermal evidence of Caledonide foreland, molasse sedimentation in Fennoscandia. SKB TR 95-18, Svensk Kärnbränslehantering AB.

Tuuling I, 2017. Paleozoic rocks structure versus Cenozoic cuesta relief along the Baltic Shield–East European Platform transect. Geological Quarterly 61, 396–412.

Tuuling I, Flodén T, Sjöberg J, 1997. Seismic correlation of the Cambrian sequence between Gotland and Hiiumaa in the Baltic Sea. GFF 119, 45–54.

Twidale C R, 1982. Granite landforms. Amsterdam: Elsevier.

Twidale C R, 1983. Pediments, peneplains and ultiplains. Revue de Géomorphologie dynamique 32, 1–35.

Twidale C, 2009. Differentiating etch, epigene, and subaerial landforms. Zeitschrift für Geomorphologie 53, 1–21.

Uutela A, 2001. Proterozoic and early Palaeozoic microfossils in the Karikkoselkä impact crater, central Finland. Bulletin of the Geological Society of Finland 73, 75–85.

van Boeckel M, 2018. Identifying the controlling factors on variable glacial modification of bedrock dominated areas in Kongsfjorden, Svalbard. MSc thesis. Department of Geosciences, UiT the Arctic University of Tromsø.

Van der Wateren F M, Dunai T J, 2001. Late Neogene passive margin denudation history–cosmogenic isotope measurements from the central Namib desert. Global and Planetary Change 30, 271–307.

Vasconcelos P M, Carmo I d O, 2018. Calibrating denudation chronology through $^{40}Ar/^{39}Ar$ weathering geochronology. Earth-Science Reviews 179, 411–435.

Vidal Romaní J R, 2008. Forms and structural fabric in granite rocks. Cadernos Lab. Xeolóxico de Laxe Coruña 33, 175–198.

Viola G, Henderson I, Bingen B, Hendriks B, 2011. The Grenvillian–Sveconorwegian orogeny in Fennoscandia: back-thrusting and extensional shearing along the "Mylonite Zone". Precambrian Research 189, 368–388.

Weidner T R, Ahlberg P, Axheimer N, Clarkson E N, 2004. The middle Cambrian *Ptychagnostus punctuosus* and *Goniagnostus nathorsti* zones in Västergötland, Sweden. Bulletin of the Geological Society of Denmark 50, 39–45.

Weidner T, Geyer G, Ebbestad J, Von Seckendorff V, 2015. Glacial erratic boulders from Jutland, Denmark, feature an uppermost lower Cambrian fauna of the Lingulid Sandstone Member of Västergötland, Sweden. Bulletin of the Geological Society of Denmark 63, 59–86.

Westergård A, 1943. Den kambro-siluriska lagerserien. Beskrivning till kartbladet Lidköping. Uppsala: Sveriges geologiska undersökning. (Ser. Aa 182), 22–89.

Wickström L M, Stephens M B, 2020. Tonian–Cryogenian rifting and Cambrian–Early Devonian platformal to foreland basin development outside the Caledonide orogen. Geological Society, London, Memoirs 50, 451–477.

Wikström A, Karis L, 1993. Note on the basement-cover relationship of the Visingsö group in the northern part of the Lake Vättern basin, south Sweden. Geologiska Föreningen i Stockholm Förhandlingar 115, 311–313.

Willeit M, Ganopolski A, 2019. Modeling perspectives on the mid-Pleistocene transition. PAGES Magazine 27, 64–65.

Williams G E, 1969. Characteristics and origin of a Precambrian pediment. Journal of Geology 77, 183–207.

Wiman C, 1918. Kambrisk sandsten anstående i trakten af Upsalas. Geologiska Föreningen i Stockholm Förhandlingar 40, 726–730 (In Swedish).

Wiman E, 1942. Studies of the morpho-tectonics of the Mälar depression, Sweden. Bulletin of the Geological Institute of the University of Uppsala 29, 287–303.

Winsemann J, Koopmann H, Tanner D C, Lutz R, Lang J, Brandes C, Gaedicke C, 2020. Seismic interpretation and structural restoration of the Heligoland glaciotectonic thrust-fault complex: Implications for multiple deformation during (pre-) Elsterian to Warthian ice advances into the southern North Sea Basin. Quaternary Science Reviews 227, 106068. doi:10.1016/j.quascirev.2019.106068

Winterhalter B, Flodén T, Ignatius H, Axberg S, Niemistö L, 1981. Geology of the Baltic Sea. In Voipio A (ed). The Baltic Sea. Amsterdam: Elsevier. (Elsevier Oceanography Series 30), 1–121.

Wotte T, Skovsted C B, Whitehouse M J, Kouchinsky A, 2019. Isotopic evidence for temperate oceans during the Cambrian Explosion. Scientific Reports 9, 6330. doi:10.1038/s41598-019-42719-4

Zeck H P, Andriessen P A M, Hansen K, Jensen P K, Rasmussen B L, 1988. Paleozoic paleo-cover of the southern part of the Fennoscandian Shield – fission track constraints. Tectonophysics 149, 61–66.

Zumberge J H, 1955. Glacial erosion in tilted rock layers. The Journal of Geology 63, 149–158.

Öhman T, 2007. The origin and tectonic modification of the Saarijärvi impact structure, Northern Finland. Bridging the gap II: Effect of target properties on the impact cratering process, September 22–26, 2007, Saint-Hubert, Canada (abstract). LPI Contribution 1360. Houston, Texas: Lunar and Planetary Institute. pp. 85–86.

Øvretveit K, 2016. Depositional and structural relationships along the basement-Cambrian contact in the Hardangervidda area. Master thesis. The University of Bergen. http://hdl.handle.net/1956/12616

Arkitektkopia AB, Bromma, 2020

SKB is responsible for managing spent nuclear fuel and radioactive waste produced by the Swedish nuclear power plants such that man and the environment are protected in the near and distant future.

skb.se